



UNIVERSITAT DE
BARCELONA

Antigens and mechanisms of immune-mediated encephalitis

Mar Petit Pedrol

ADVERTIMENT. La consulta d'aquesta tesi queda condicionada a l'acceptació de les següents condicions d'ús: La difusió d'aquesta tesi per mitjà del servei TDX (www.tdx.cat) i a través del Dipòsit Digital de la UB (diposit.ub.edu) ha estat autoritzada pels titulars dels drets de propietat intel·lectual únicament per a usos privats emmarcats en activitats d'investigació i docència. No s'autoritza la seva reproducció amb finalitats de lucre ni la seva difusió i posada a disposició des d'un lloc aliè al servei TDX ni al Dipòsit Digital de la UB. No s'autoritza la presentació del seu contingut en una finestra o marc aliè a TDX o al Dipòsit Digital de la UB (framing). Aquesta reserva de drets afecta tant al resum de presentació de la tesi com als seus continguts. En la utilització o cita de parts de la tesi és obligat indicar el nom de la persona autora.

ADVERTENCIA. La consulta de esta tesis queda condicionada a la aceptación de las siguientes condiciones de uso: La difusión de esta tesis por medio del servicio TDR (www.tdx.cat) y a través del Repositorio Digital de la UB (diposit.ub.edu) ha sido autorizada por los titulares de los derechos de propiedad intelectual únicamente para usos privados enmarcados en actividades de investigación y docencia. No se autoriza su reproducción con finalidades de lucro ni su difusión y puesta a disposición desde un sitio ajeno al servicio TDR o al Repositorio Digital de la UB. No se autoriza la presentación de su contenido en una ventana o marco ajeno a TDR o al Repositorio Digital de la UB (framing). Esta reserva de derechos afecta tanto al resumen de presentación de la tesis como a sus contenidos. En la utilización o cita de partes de la tesis es obligado indicar el nombre de la persona autora.

WARNING. On having consulted this thesis you're accepting the following use conditions: Spreading this thesis by the TDX (www.tdx.cat) service and by the UB Digital Repository (diposit.ub.edu) has been authorized by the titular of the intellectual property rights only for private uses placed in investigation and teaching activities. Reproduction with lucrative aims is not authorized nor its spreading and availability from a site foreign to the TDX service or to the UB Digital Repository. Introducing its content in a window or frame foreign to the TDX service or to the UB Digital Repository is not authorized (framing). Those rights affect to the presentation summary of the thesis as well as to its contents. In the using or citation of parts of the thesis it's obliged to indicate the name of the author.

A fluorescence microscopy image of brain tissue. The image shows a dense network of cells and fibers. The nuclei are stained blue, while other cellular components and structures are stained in green and red. The overall appearance is a complex, textured pattern of colors representing different biological structures.

**Antigens and mechanisms of
immune-mediated encephalitis**

**Doctoral thesis
Mar Petit Pedrol**

Antigens and mechanisms of immune-mediated encephalitis

Doctoral thesis presented by

Mar Petit Pedrol

Barcelona, June 2018

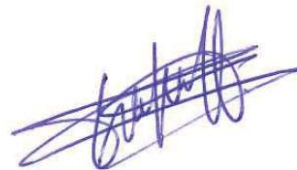
Doctoral Programme in Biomedicine, Research area of Neuroscience

Director of thesis



Josep Dalmau, MD, PhD

Tutor of thesis



Francesc Graus, MD, PhD



Cover and back cover: Detail of mouse cerebellum stained with kv1.1 (green), Bassoon (red) and Dapi (blue) scanned with a confocal microscopy (Zeiss LSM710) with Plan APOCHROMAT x 40/1.3 NA oil objective.

All rights reserved. No part of this publication may be reproduced by any means including electronic, mechanical, photocopying, recording or otherwise, without permission of the author, or when appropriate, of the scientific journal in which parts of this thesis have been published.

Report for the contribution of Mar Petit-Pedrol to the publications that form part of this thesis

Below please find my comments on the publications of Mar Petit-Pedrol as part of the group of reports that comprise her doctoral thesis entitled "Antigens and mechanisms of immune-mediated encephalitis". The comments include my assessment on her level of participation as well as the journal impact factor.

Publications:

I. Title: Encephalitis with refractory seizures, status epilepticus, and antibodies to the GABAA receptor: a case series, characterisation of the antigen, and analysis of the effects of antibodies

Authors: **Mar Petit-Pedrol***, Thaís Armangue*, Xiaoyu Peng*, Luis Bataller, Tania Cellucci, Rebecca Davis, Lindsey McCracken, Eugenia Martinez-Hernandez, Warren P. Mason, Michael C. Kruer, David G. Ritacco, Wolfgang Grisold, Brandon F. Meaney, Carmen Alcalá, Peter Sillevs-Smitt, Maarten J Titulaer, Rita Balice-Gordon, Francesc Graus, and Josep Dalmau *These authors contributed equally

Journal: Lancet Neurol. 2014;13(3):276-86 (Highlighted with an editorial)

Impact factor JCR 2014 (percentile): 21.896 (D1)

PhD candidate contribution: The PhD candidate participated in the conceptual and experimental design of this study, and performed the experiments including, the detection and immunoprecipitation of the new target antigen and mass spectrometry data analysis, development of a CBA as a diagnostic test, and screening of patients' samples for the detection of GABA_AR antibodies. She drafted the manuscript, including tables, figures, and supplemental material, and participated to write the revised version of the manuscript.

This article was included in the PhD thesis of Dr. Thaís Armangué.

II. Title: Investigations in GABA_A receptor antibody-associated encephalitis

Authors: Marianna Spatola, **Mar Petit-Pedrol**, Mateus Mistieri Simabukuro, Thaís Armangue, Fernanda J. Castro, Maria I. Barcelo Artigues, Maria R. Julià Benique, Leslie Benson, Mark Gorman, Ana Felipe, Ruben L. Caparó Oblitas, Myrna R. Rosenfeld, Francesc Graus, and Josep Dalmau

Journal: Neurology. 2017 Mar 14;88(11):1012-1020

Impact factor JCR 2017 (percentile): The available IF from 2016 is 8.32 (D1)

PhD candidate contribution: The PhD candidate participated in the conceptual and experimental design of the study, and developed a CBA as a diagnostic test. She participated in the initial drafting of the manuscript, including the tables, development of the figures, and in the writing of the revised version of the manuscript.

This article is expected to be included in the PhD thesis of Marianna Spatola.

III. Title: Human neurexin-3 α antibodies associate with encephalitis and alter synapse development

Authors: Núria Gresa-Arribas, Jesús Planagumà, **Mar Petit-Pedrol**, Izumi Kawachi, Shinichi Katada, Carol A. Glaser, Mateus M. Simabukuro, Thaís Armangué, Eugenia Martinez-Hernandez, Francesc Graus, and Josep Dalmau

Journal: Neurology. 2016;86(24):2235-42

Impact factor JCR 2016 (percentile): 8.32 (D1)

PhD candidate contribution: The PhD candidate participated in the experimental design of the study and in carrying some of the experiments including the detection and immunoprecipitation of the new target antigen, and mass spectrometry data analysis, development of a CBA as a diagnostic test, and screening of patients' samples for the presence of neurexin-3 α antibodies. She also participated in the study of the effect of patients' antibodies in cultures of neurons, and helped drafting the manuscript, including tables, figures, and supplemental material, and writing the revised version of the manuscript.

This article is not expected to be included in any other doctoral thesis.

IV. Title: Human N-methyl D-aspartate receptor antibodies alter memory and behaviour in mice

Authors: Jesús Planagumà*, Frank Leypoldt*, Francesco Mannara*, Javier Gutiérrez-Cuesta, Elena Martín-García, Esther Aguilar, Maarten J. Titulaer, **Mar Petit-Pedrol**, Ankit Jain, Rita Balice-Gordon, Melike Lakadamyali, Francesc Graus, Rafael Maldonado and Josep Dalmau * These authors contributed equally

Journal: Brain. 2015;138(Pt 1):94-109

Impact factor JCR 2015 (percentile): 10.103 (D1)

PhD candidate contribution: The PhD candidate participated in the design and development of the following experiments: removal of mouse brains, tissue processing for extraction of human IgG bound to mouse brain, GluN1 CBA analysis of antibodies extracted from brain, and immunoblot analysis for quantification of NMDAR. She provided figures and supplemental material, and participated in the initial drafting of the manuscript.

This article was included in the PhD thesis of Dr. Francesco Mannara.

V. Title: Ephrin-B2 prevents N-methyl-D-aspartate receptor antibody effects on memory and neuroplasticity

Authors: Jesús Planagumà*, Holger Haselmann*, Francesco Mannara*, **Mar Petit-Pedrol**, Benedikt Grünewald, Esther Aguilar, Louis Röpke, Elena Martín-García, Marteen J. Titulaer, Pablo Jercog, Francesc Graus, Rafael Maldonado, Christian Geis, Josep Dalmau * These authors contributed equally

Journal: Ann Neurol. 2016; 80(3):388-400

Impact factor JCR 2016 (percentile): 9.89 (D1)

PhD candidate contribution: The PhD candidate participated in the experimental design of the study and participated in the following experiments: CSF preparation and immunoabsorption of

patients' samples, provided assistance in the surgery of mice for the implantation of intraventricular osmotic pumps, removed the brains, processed the tissue for IgG extraction, and characterized the human IgG bound to mouse brain using immunoprecipitation. She participated in the drafting of tables and figures and participated in writing the revised version of the manuscript.

This article was included in the PhD thesis of Dr. Francesco Mannara.

VI. Title: LGI1 antibodies alter Kv1.1 and AMPA receptors changing synaptic excitability, plasticity and memory

Authors: Mar Petit-Pedrol*, Josefine Sell*, Jesús Planagumà, Francesco Mannara, Marija Radosevic, Holger Haselmann, Mihai Ceanga, Lidia Sabater, Marianna Spatola, David Soto, Xavier Gasull, Josep Dalmau, and Christian Geis * These authors contributed equally

Journal: A revised version of the manuscript will be re-submitted in the next 4 weeks (journal: Brain)

Impact factor JCR 2018 (percentile): Paper not yet accepted, potential impact factor in Brain (2016) is 10.292 (D1)

PhD candidate contribution: The PhD candidate participated in the experimental design of the study and in most of the experiments including, analysis of the effects of patients' antibodies on LGI1-ADAM in cell cultures, epitope mapping of LGI1 antibodies, mice brain surgery, behavioral tests and development of the molecular analysis of the pathogenic effect of patients' LGI1 antibodies in a mouse model. She performed the statistics, drafted the manuscript, including tables, figures, and supplemental material and is writing the revised version of the manuscript. This article is expected to be used for the PhD thesis of Josefine Sell.

A handwritten signature in black ink, appearing to read 'Josep Dalmau', with a long horizontal stroke extending to the right.

Josep Dalmau MD, PhD

*Somos nuestra memoria, somos ese quimérico museo
de formas inconstantes, ese montón de espejos rotos*

Jorge Luis Borges (1899 - 1986, Escritor Argentí)

Poema Cambridge del libro Elogio de la sombra

Abbreviations

AChR	Acetylcholine Receptor
ADEM	Acute Disseminated Encephalomyelitis
ADLTE	Autosomal Dominant Lateral Temporal Epilepsy
ADAM	A Disintegrin And Metalloproteinase
AMPA	α -amino-3-hydroxy-5-methyl-4-isoxazolepropionic acid receptor
BBB	Blood-Brain Barrier
CASPR2	Contactin-Associated Protein 2
CBA	Cell-Based Assay
CSF	Cerebrospinal Fluid
CNS	Central Nervous System
DPPX	Dipeptidyl-Peptidase-like Protein 6
EEG	Electroencephalogram
EPTP domain	Epitempin domain
GABA	Gamma-aminobutyric acid
GABAAr	Gamma-aminobutyric acid type a Receptor
GABAbR	Gamma-aminobutyric acid type b Receptor
GAD	Glutamic Acid Decarboxylase
GluN	Glutamate NMDAR subunit
GlyR	Glycine Receptor
HEK293	Human Embryonic Kidney 293
HSE	Herpes Simplex Encephalitis
LE	Limbic Encephalitis
LEMS	Lambert-Eaton Myasthenic Syndrome
LGI1	Leucine-rich Glioma Inactivated 1
LTD	Long-Term Depression
LTP	Long-Term Potentiation
LRR domain	Leucine Rich Repeat domain
MG	Myasthenia Gravis
mGluR1	metabotropic Glutamate Receptor 1
mGluR5	metabotropic Glutamate Receptor 5
MRI	Magnetic Resonance Image
NMDAR	N-methyl-D-aspartate receptor
PCD	Paraneoplastic Cerebellar Degeneration
PEM	Paraneoplastic Encephalomyelitis
PERM	Progressive Encephalomyelitis with Myoclonus
PNS	Paraneoplastic Neurological Syndromes
SCLC	Small Cell Lung Cancer
VGCC	Voltage-Gated Calcium Channels
VGKC	Voltage-Gated Potassium Channels

Table of Contents

ABSTRACT	13
1. INTRODUCTION	17
1.1. Encephalitis.....	19
1.1.1. Definition	19
1.1.2. Incidence and Classification.....	19
1.1.3. The importance of the clinical and etiological characterization of encephalitis.....	21
1.1.4. General diagnostic approach to encephalitis	22
1.2. Paraneoplastic neurological syndromes, and the discovery of the antibody-mediated encephalitis	23
1.2.1. Paraneoplastic neurologic syndromes (PNS).....	23
1.2.2. Myasthenic syndromes.....	26
1.2.3. GAD autoimmunity, a non-paraneoplastic disorder with antibodies against intracellular antigens	26
1.2.4. Discovery of antibody-mediated encephalitis.....	27
1.3. Syndromes related to antibody-mediated encephalitis	29
1.3.1. Anti-NMDAR encephalitis	32
1.3.2. Anti-LGI1 encephalitis.....	38
1.3.3. Anti-AMPA encephalitis.....	43
1.3.4. Anti-Caspr2 encephalitis.....	45
1.3.5. Other autoimmune encephalitis with antigenic targets located on glial cells.....	48
2. HYPOTHESIS.....	49
3. OBJECTIVES.....	53
4. GENERAL METHODS.....	57
4.1. Immunohistochemical methods using brain tissue	59
4.2. Immunohistochemical methods using primary cultures of rodent dissociated hippocampal neurons.....	59
4.3. Immunoprecipitation techniques to identify novel target antigens.....	60
4.4. Development of diagnostic tests.....	60
4.5. Determination of the effect of patients' antibodies in cultured neurons	60
4.6. Cerebroventricular infusion patients' antibodies to mice	61

4.7. Determination of the pathogenic effects of the antibodies in mice.....	61
5. PUBLICATIONS.....	63
5.1. Paper I.....	65
5.2. Paper II.....	87
5.3. Paper III.....	105
5.5. Paper V	153
5.6. Paper VI (unpublished paper).....	171
6. DISCUSSION	231
7. CONCLUSIONS	241
8. REFERENCES	245
9. ANNEX	259
9.1. Other publications.....	261
9.2. Acknowledgments / Agraïments	263

ABSTRACT

Background: The autoimmune encephalitis represents a new category of immune-mediated diseases of the brain that are mediated by antibodies against neurotransmitter receptors, ion channels or neuronal cell-surface proteins. Among the many encephalitis considered idiopathic, there are subtypes that are probably immune-mediated and are pending to be discovered. In the last 11 years, 16 subtypes of idiopathic encephalitis have been found to be immune-mediated. The recognition of these disorders is important because despite being potentially lethal, they are curable if promptly recognized and treated. On a more basic level, the study of these diseases has uncovered novel antibody-mediated mechanisms of synaptic dysfunction that lead to changes in memory and behavior, epilepsy, abnormal movements, or decreased level of consciousness.

Objectives: 1) Identify patients with encephalitis of unclear etiology but whose clinical features and initial investigations strongly suggest an antibody-mediated cause; 2) characterize the new autoantibodies associated with these disorders along with the neuronal target antigens, and develop unambiguous diagnostic tests, and 3) determine in animal models how autoantibodies alter the level and function of neuronal synaptic antigens (NMDAR and LGI1) potentially resulting in an impairment of memory and behavior.

Methods: Rat brain sections and primary cultures of dissociated rat hippocampal neurons served to identify patients whose serum and CSF samples contained novel neuronal antibodies. Techniques of tissue immunohistochemistry, neuronal immunocytochemistry and cell-based assays were used to identify the antibodies. Cell-surface neuronal protein immunoprecipitation with patients' antibodies was used to isolate the target antigen, which was subsequently characterized by mass spectrometry. Cerebroventricular transfer of patients' antibodies to mice through subcutaneously implanted mini-osmotic pumps was used to determine the pathogenic effect of patients' antibodies on the corresponding synaptic targets and how these changes altered memory and behavior. An extensive combination of techniques was used for these studies, including quantitative confocal microscopy analysis of the levels of synaptic targets, immunoprecipitation of brain-bound antibodies, immunoblot of precipitated proteins, electrophysiology on acute sections of mice hippocampus, and a comprehensive panel of standard behavioral tests. All studies were conducted with sets of mice at different time points during the antibody infusion (disease phase) and after the infusion was stopped (recovery phase).

Results: (1) Two novel autoimmune encephalitis were identified: anti-GABA_AR encephalitis and anti-neurexin-3 α encephalitis. Anti-GABA_AR encephalitis can affect children and adults, associates with prominent seizures and highly suggestive MRI abnormalities, and is treatable with immunotherapy. In some patients the immune response is triggered by the presence of a tumor. Anti-neurexin-3 α encephalitis manifests with a less distinctive syndrome, often

associates with seizures and is also treatable with immunotherapy. No tumor association has been identified.

(2) Immunoprecipitation of the target antigen of anti-GABA_AR encephalitis demonstrated that the epitopes are mainly located in the α 1 and β 3 subunits, and less frequently in the γ 2 subunit. Whereas the antibodies against α 1 and β 3 subunits are disease relevant, the presence of additional antibodies to γ 2 does not modify the disease phenotype. Patients' GABA_AR antibodies cause a decrease in the total and synaptic levels of GABA_AR clusters, supporting their pathogenicity.

(3) Immunoprecipitation of the target antigen of patients with anti-neurexin-3 α encephalitis demonstrated that the epitopes are specifically located in neurexin-3 α , but not in its post-synaptic ligand LRRTM2. Patients' antibodies cause a reduction of the total number of synapses as well as the levels of the presynaptic protein Bassoon and the post-synaptic protein Homer1, supporting the pathogenicity of the antibodies.

(4) Recombinant expression of the indicated subunits of the GABA_AR and neurexin-3 α in HEK293 cells can be used as a test to diagnose patients with these autoimmune encephalitis.

(5) The infusion of patients' NMDAR antibodies into the cerebroventricular system of mice, cause memory deficits, anhedonia, and depressive-like behavior. The infused antibodies specifically bind to brain NMDAR resulting in a highly specific reduction of the density of these receptors at synaptic and extrasynaptic levels. The behavioral and molecular effects caused by patients' antibodies are reversible upon stopping the infusion of antibodies.

(6) The administration of ephrin-B2 antagonizes the pathogenic effects of patients' NMDAR antibodies in all the investigated paradigms, including memory, depressive-like behavior, density of cell-surface and synaptic NMDAR and EphB2, and long-term synaptic plasticity. These findings reveal a strategy beyond immunotherapy to antagonize patients' antibody effects.

(7) The antibodies of patients with anti-LGI1 encephalitis abrogate the binding of the neuronal secreted LGI1 with the presynaptic ADAM23 and with the postsynaptic ADAM22.

(8) The infusion of patients' LGI1 antibodies into the cerebroventricular system of mice cause protracted memory deficits, together with a decrease of presynaptic Kv1.1 potassium channels and post-synaptic AMPAR. These structural effects associate with impairment of synaptic plasticity and increase of neuronal excitability, which are in line with the models of genetic depletion of LGI1.

Conclusions: (1) Anti-GABA_AR and anti-neurexin-3 α encephalitis are two new forms of antibody-mediated encephalitis for which there is evidence of antibody-mediated pathogenicity. These findings support the concept that among the many types of encephalitis of unclear etiology, there are some that are immune mediated but are still pending to characterize. (2) Direct neuronal antigen precipitation using patients' antibodies is an excellent strategy to isolate and characterize disease-relevant antigens, and subsequently develop diagnostic screening tests. (3) My studies have contributed to develop two animal models of

antibody-mediated symptoms (NMDAR, LGI1) and uncover the underlying antibody-mediated changes in synaptic function and plasticity. Both models fulfill the Witebsky's criteria for antibody-mediated disease, and provide the basis for modeling other antibody-mediated neurological disorders.

1. INTRODUCTION

1.1. Encephalitis

1.1.1. Definition

Encephalitis is an inflammatory disorder of the brain that can affect people of all ages and occurs with prominent neuropsychiatric symptoms.¹ The disease develops as a rapidly progressive encephalopathy, usually in less than 6 weeks.² Symptoms may include fever, headache, irritability, confusion, memory problems, behavioral changes, seizures, and abnormal movements.³ When severe, patients can have decreased level of consciousness or coma. Encephalitis associates with high morbidity and mortality;¹ nearly 6% of encephalitis-associated hospitalizations end with patient's dead.³ Prompt diagnosis of encephalitis is important, because depending on the etiology, treatment can improve outcomes.⁴

1.1.2. Incidence and Classification

Overall, the frequency of encephalitis in Western countries is estimated 8-10/100.000 inhabitants per year. There are many different disorders that can result in encephalitis (**Figure 1**).

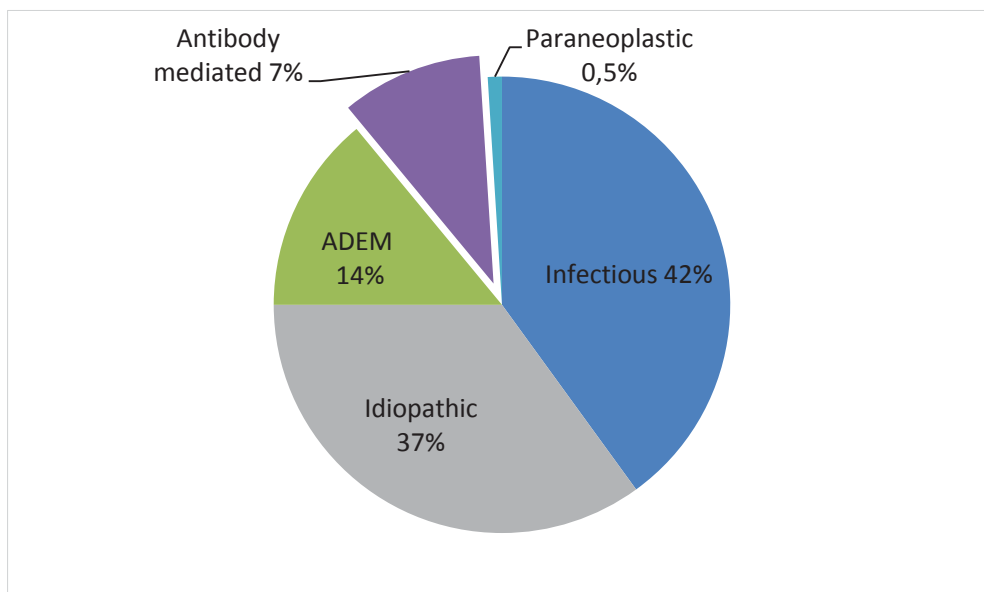


Figure 1. Causes of encephalitis. Adapted from ^{1,5-7}

The most predominant etiology is infectious and it is estimated that represents approximately 40% of all cases of encephalitis.¹ Herpes simplex virus, varicella zoster virus and less often enterovirus are in our environment the most frequent causes of sporadic viral encephalitis. New viral causes of encephalitis are constantly emerging and bacterial, fungal or parasitic infections can also cause encephalitis.⁸

In about 20% of patients with encephalitis the etiology is autoimmune.¹ In some of these patients the encephalitis forms part of a systemic autoimmune disease that in addition to involving systemic organs also affects the brain (e.g., systemic lupus erythematosus, connective tissue diseases).^{9,10} However, in other patients the autoimmune disorder affects exclusively the brain and other parts of the nervous system, and therefore it can be considered a primary form of autoimmune encephalitis. The target antigens may be expressed by neurons, glial cells, or myelin and patients may have specific autoantibodies against one or several of these antigens. These antibody-associated encephalitis can be further subdivided according to whether the antigens are intracellular or located on the cell-surface which as it will be discussed later, has important implications for pathogenicity, treatment, and prognosis.

There is still a large group of patients whose disorders fulfill criteria of definite or possible autoimmune encephalitis, but the antigens are unknown. For example, the target antigens in acute disseminated encephalomyelitis (ADEM), one of the most frequent immune-mediated encephalitis that affects the white matter, are largely unknown. Similarly, there are patients with other inflammatory, possibly immune-mediated encephalitis predominantly affecting the grey matter, in which the target and mechanisms are unknown (**Figure 2**).

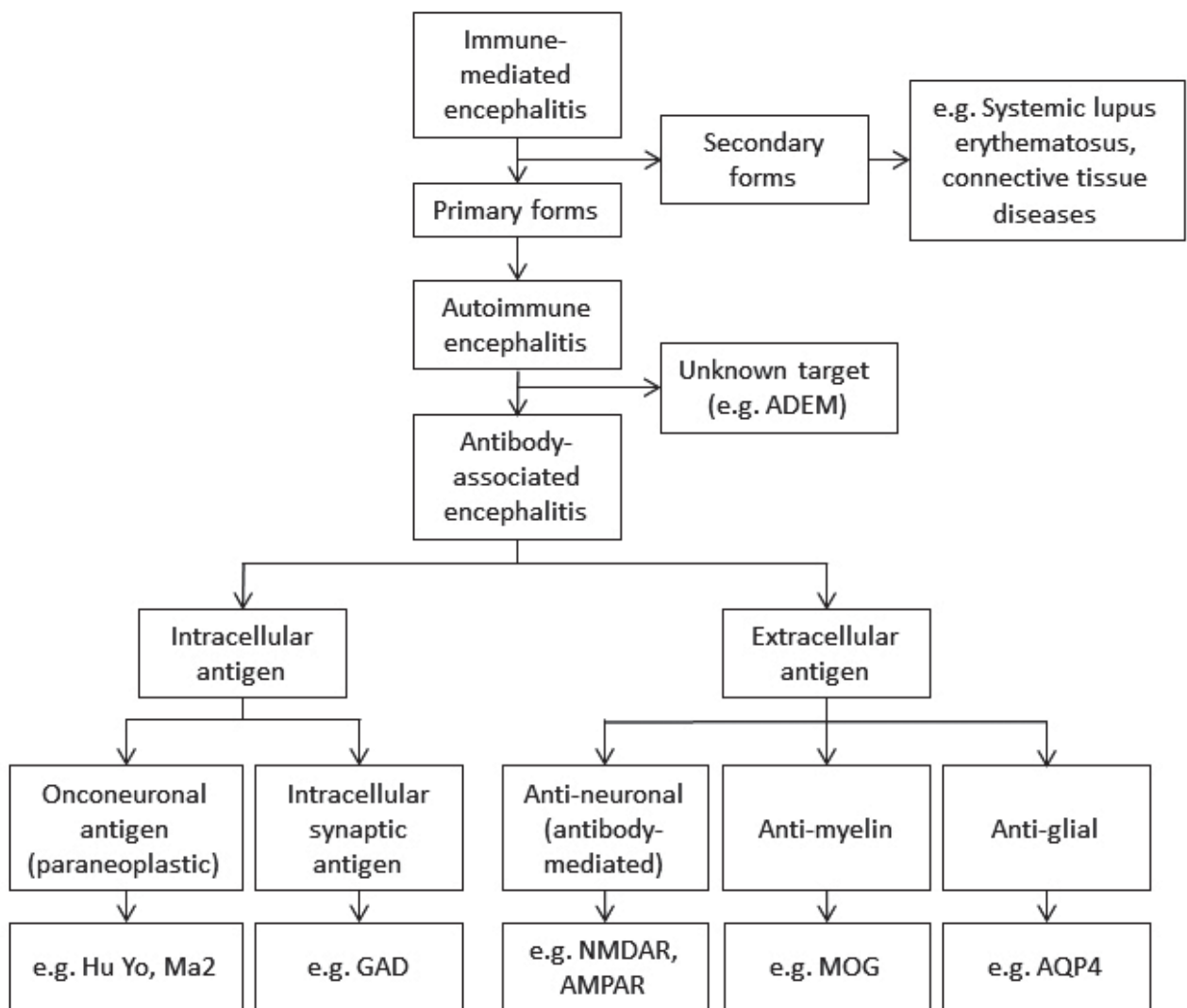


Figure 2. Classification of immune-mediated encephalitis

In addition to the infectious and immune-mediated encephalitis, genetic background contributes significantly to the variation in infectious disease susceptibility and severity.^{2,11} Mutations of genes related to interferon and other molecules of inflammatory pathways can predispose to infections or degenerative processes accompanied by inflammation of the brain. For example, mutations in RANBP2 gene predispose to infection-induced acute encephalopathy 3 (IAE3) or familial acute necrotizing encephalopathy;^{12,13} toll-like receptor 3 (TLR3) deficiency has been identified as a genetic etiology of childhood herpes simplex virus 1 (HSV-1) encephalitis (HSE);^{14–16} and mutations in interferon regulatory factor 3 (IRF3) are associated to symptomatic West Nile virus Encephalitis.¹⁷

For the remaining patients with encephalitis (about 40% of all cases) the cause of the disorder is unknown.^{1,18} The etiology of the encephalitis of these patients may include unidentified infectious etiologies and immune-mediated mechanisms that are pending to be characterized. The possibility that some forms of idiopathic encephalitis are likely immune-mediated gains strong support from the recent experience with a group of encephalitis associated with antibodies against neuronal cell-surface proteins. The first of these diseases, defined as “antibody-mediated” encephalitis, was reported in 2007,¹⁹ but there are currently 16 additional diseases that form part of the same group and were previously unknown or considered idiopathic.²⁰ Therefore, it is reasonable to postulate that some types of encephalitis that remain of unknown etiology may be immune-mediated.

1.1.3. The importance of the clinical and etiological characterization of encephalitis

Most types of encephalitis, regardless of their etiology, have similar clinical manifestations including headache, fever, change of memory and behavior, confusion, focal motor or sensory deficits, seizures, and decreased level of consciousness.² Because the treatment is different according to the etiology of the encephalitis, it is important to recognize the cause in order to implement the appropriate treatment (e.g., specific anti-infectious treatments for viral or bacterial encephalitis, or immunotherapy for immune-mediated encephalitis). Moreover, just as each infectious agent may have a specific treatment, the type of immunotherapy can also vary according to the immune trigger and type of immune response.⁸ For example, some types of autoimmune encephalitis are triggered by the presence of an underlying cancer. These syndromes, known as classical paraneoplastic encephalitis, often occur in association with antibodies against intracellular neuronal antigens. These antibodies are not directly pathogenic but their presence is diagnostic of the paraneoplastic etiology of the syndrome.^{21,22} For these syndromes the autoimmune response is mediated by cytotoxic T-cell mechanisms against the neurons, and the treatment should include immunotherapy to abrogate the abnormal immune response, and oncologic therapy in order to control the tumor which is the trigger of the immune response. However, since the cytotoxic T-cells cause neuronal death, the response to treatment is suboptimal (more detailed information on paraneoplastic syndromes is provided later in another section). In contrast, in the antibody-mediated encephalitis, the antibodies target cell-surface antigens which function is directly affected by the antibodies, and

treatments aimed at removing or reducing the production of the antibodies, are often effective. Therefore, the type of immune response determines the appropriate treatment, predicts the likelihood of responding to treatment, and can, for some syndromes, suggest the trigger of the immune response.²³ For example, patients with autoimmune limbic encephalitis (LE, a form of encephalitis that affects the limbic system and associates with memory loss and seizures) may have antibodies against Hu, GABA_B receptor (GABA_BR), or leucine-rich glioma inactivated 1 (LGI1) among others. Those with Hu and GABA_BR antibodies usually have small cell lung cancer (SCLC), but the LE encephalitis of patients with Hu is poorly responsive to immunotherapy (Hu is an intracellular antigen, and symptoms are mediated by T-cells). In contrast, the LE encephalitis of patients with GABA_BR antibodies is more often responsive to immunotherapy (GABA_BR is on the neuronal cell-surface/synapse, and symptoms are mediated by the antibodies). On the other hand, the LE of patients with LGI1 antibodies almost never associates with cancer and the symptoms are usually responsive to immunotherapy (LGI1 is a secreted protein that forms a trans-synaptic complex, and the disease is mediated by antibodies).

Keeping these considerations in mind, the current approach to the diagnosis of any patient with encephalitis is to identify the cause with a careful clinical assessment and paraclinical tests (brain MRI, EEG, study of CSF). If the cause is suspected to be autoimmune, it is important to establish the type of immune response (cytotoxic T-cell versus antibody-mediated).

1.1.4. General diagnostic approach to encephalitis

Although all types of encephalitis may present with similar symptoms, there are some demographic and clinical features that may help in the differential diagnosis. These include geographical location of the patient (with certain viruses predominating in different regions), recent history of traveling to those regions, age and sex of the patient (some autoimmune encephalitis have different age and sex distribution), and prodromal symptoms or co-morbidities.²⁴ In clinical practice all of these features are routinely considered at the initial evaluation of patients with encephalitis. The next step includes a careful assessment of the clinical syndrome, which can vary according to the type of encephalitis (described later in detail), and the results of paraclinical tests. These include brain MRI to demonstrate inflammatory changes and exclude other diseases such as stroke or tumor; EEG to assess the presence of epileptic activity and other alterations of brain function; and CSF examination. This is important for three reasons, 1) the presence of inflammation, characterized by increased number of white blood cells, elevated protein concentration, and/or presence of oligoclonal bands, helps to differentiate the neurologic syndrome from other non-inflammatory conditions (e.g., metabolic or neurodegenerative diseases), 2) it may demonstrate the presence of an infectious agent with appropriate tests (such as PCR for viruses, bacterial culture, specific tests for fungal infections), confirming the diagnosis of an infectious encephalitis, or 3) it may show the presence of specific autoantibodies directed to glial or neuronal antigens, confirming the diagnosis of autoimmune encephalitis. Although most of these autoantibodies are usually

present in serum, about 10-15% of patients with several types of autoimmune encephalitis (e.g., anti-NMDA receptor encephalitis) only have antibodies detectable in CSF.²⁵

1.2. Paraneoplastic neurological syndromes, and the discovery of the antibody-mediated encephalitis

Our current understanding of the antibody-mediated encephalitis comes from an idea proposed about 15 years ago that suggested that some diseases of the central nervous system (CNS) were directly mediated by neuronal autoantibodies.⁴ This concept was initially influenced by studies on two groups of disorders: the classic paraneoplastic neurologic syndromes affecting the CNS (including the paraneoplastic encephalitis) that led to the investigations that facilitated the discovery of the antibody-mediated encephalitis,^{4,21} and the myasthenic syndromes which demonstrated that autoantibodies can alter neurologic function.^{26–29}

1.2.1. Paraneoplastic neurologic syndromes (PNS)

PNS are remote effects of cancer that in many instances are mediated by the immunological system (see Darnell et al²¹; and Dalmau et al³⁰ for reviews on these disorders). They include many different disorders that can affect any part of the nervous system, from retina to muscle, and are associated with immune responses against neuronal proteins that are also expressed by the associated cancer (onconeurological antigens). Many onconeurological antigens are intracellular (**Table 1**).

Table 1: Overview of the intracellular antigens in paraneoplastic syndromes, and their associated syndrome and tumor

Antigen	Associated syndrome	Tumor type
Hu (ANNA1)	PEM, paraneoplastic sensory neuronopathy, PCD, LE	SCLC, neuroblastoma, prostate cancer
Yo (PCA1)	PCD	Ovarian, breast and lung cancer
CV2/CRMP5	LE, PCD, chorea, uveitis, optic neuritis, retinopathy, sensorimotor neuropathy	SCLC, thymoma
Ri (ANNA2)	Ataxia, opsoclonus-myoclonus, brainstem encephalitis	Breast, gynecologic, SCLC
Ma2	Limbic, hypothalamic, brainstem encephalitis	Testicular, lung, breast
Amphiphysin	Stiff-person syndrome, PEM, LE, PCD	Breast, SCLC
DNER (Tr)	Cerebellitis, PCD	Hodgkin's lymphoma
PCA-2	Encephalomyelitis, cerebellar degeneration, LEMS	SCLC

PEM: Paraneoplastic encephalomyelitis, PCD: paraneoplastic cerebellar degeneration, SCLC: Small-cell lung cancer, LE: limbic encephalitis, LEMS: Lambert-Eaton myasthenic syndrome. Table adapted from²³

It is believed that the ectopic expression of these neuronal proteins by the tumor triggers an immune response that is misdirected against the nervous system. As indicated, these patients develop antibodies against onconeural antigens but also prominent cytotoxic T-cell responses against the nervous system. In studies using cultures of live neurons, patients' antibodies cannot reach the intracellular antigen and do not have pathogenic effects.³¹ Moreover, autopsy studies of patients with these disorders show extensive inflammatory infiltrates, including perivascular B- and T-cells, and cytotoxic T-cells surrounding neurons and causing degeneration via perforin or granzyme B mechanisms (**Figure 3**).³²⁻³⁴ These pathological findings likely explain why patients with these syndromes rarely respond to immunotherapies directed to removing the antibodies or antibody-producing cells.³⁵⁻³⁷

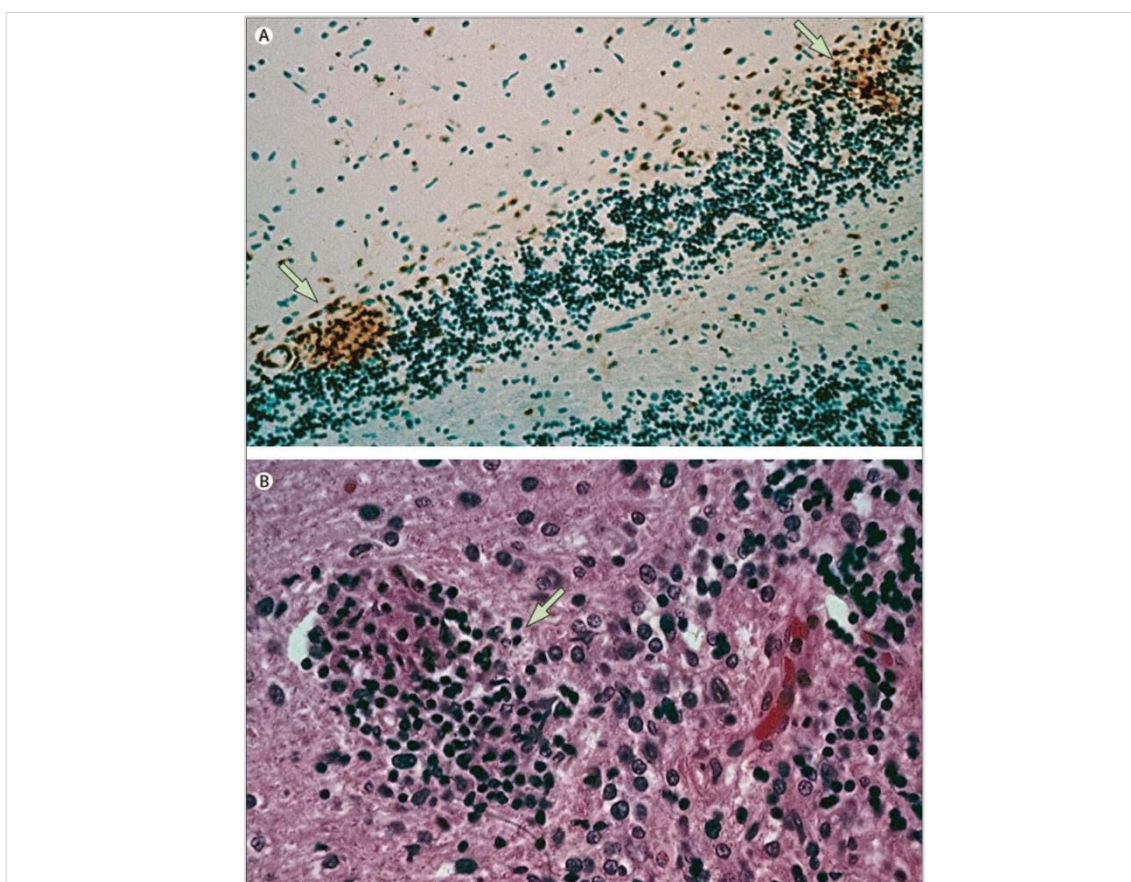


Figure 3. Inflammatory infiltrates in subacute cerebellar degeneration in a patient with encephalomyelitis and anti-Hu antibodies

(A) CD3 T-cells, which helps to activate both the cytotoxic T-cell (CD8+ naive T-cells) and also T helper cells (CD4+ naive T-cells), form clusters (arrows) at the level of the Purkinje cell layer. No remaining Purkinje cells are visible. Higher magnification (B) shows a neuronophagic nodule of T lymphocytes that are probably destroying a Purkinje cell. A: $\times 100$, immunostained for CD3 and counterstained with hematoxylin. B: $\times 400$ hematoxylin-eosin". From³⁰

The exact mechanisms underlying the pathogenesis of the neuronal dysfunction in PNS are not well understood. As noted above, in the classical paraneoplastic syndromes, the antibodies are not pathogenic, and the disorders are not responsive to antibody depleting strategies. Evidence

for T-cell mediated mechanisms is stronger but remains circumstantial. This includes the detection of antigen-specific T-cells in the serum and CSF of patients with Hu antibodies,^{38,39} autopsy studies demonstrating the presence of extensive T-cell infiltrates in the brain parenchyma of patients,^{32,34} and the presence of oligoclonal cytotoxic T-cell infiltrates in the brains and tumors of patients with anti-Hu-associated encephalomyelitis, suggesting a specific antigen-driven clonal expansion of T-cells. In one study, adoptive transfer of T-cells specific for autologous Ma1 in rats, produced perivascular and meningeal lymphocytic infiltrates, indistinguishable from those induced by CD4+ T-cells against myelin proteins. However the mice did not develop the symptoms or pathological features typical of the paraneoplastic syndrome, such as predominant parenchymal inflammatory infiltrates.⁴⁰ Based on these findings a model for the pathogenesis of PND has been proposed (Figure 4).

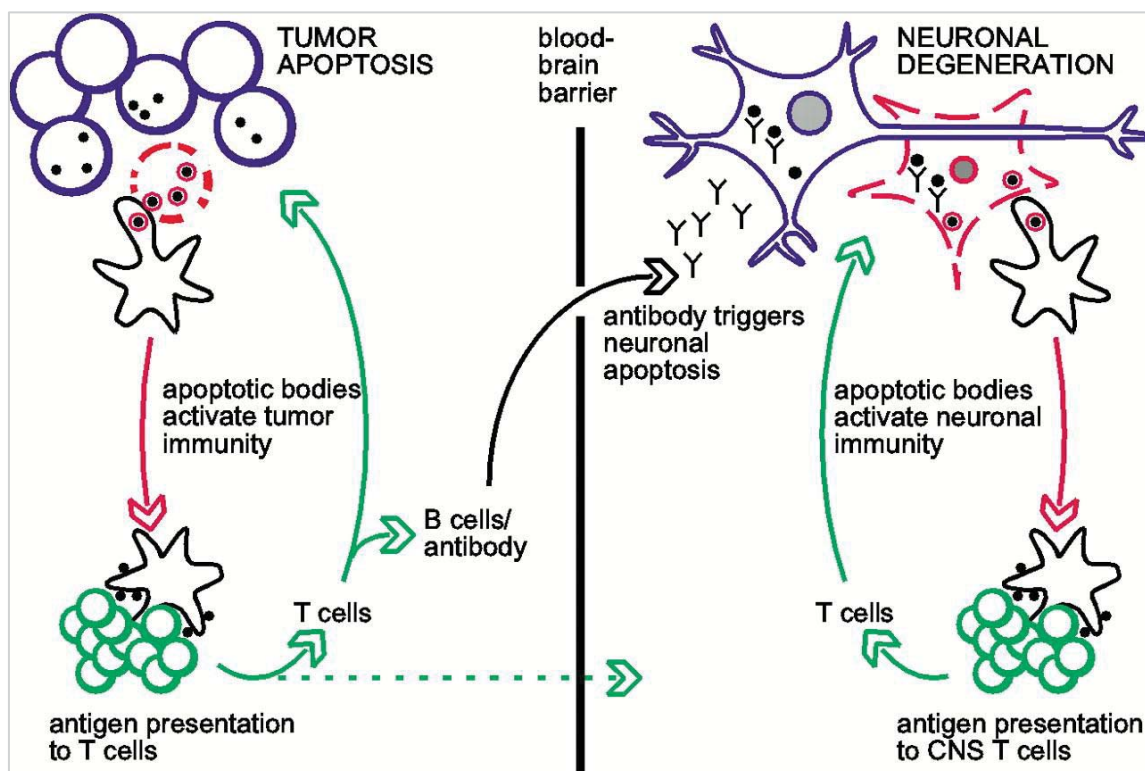


Figure 4. Model of pathogenesis of PND

Tumor cells (blue) aberrantly express an onconeural antigen, represented as a black spot. As tumor cells undergo apoptosis (red), dendritic cells (DCs) take up apoptotic fragments containing the onconeural antigen. DCs present the onconeural antigen on MHC class I, along with costimulatory signals, to T cells (green), thereby activating antigen-specific CD8+ T-cells. These T-cells are competent to mediate effective tumor immunity but not to induce neurologic disease. DCs also activate CD4+ T-cells, which in turn help activate B-cells that produce onconeural antibodies (represented as symbol Y). Some of these antibodies cross the blood-brain barrier by passive diffusion. Neurons (blue) expressing the onconeural antigen take up the antibody (inefficiently), which binds to the antigen and thereby impairs onconeural activities essential for neuronal survival and triggers rare events of neuronal apoptosis. Apoptosis of even a small number of neurons will generate apoptotic material (red) that is very efficiently scavenged by DCs. DCs resident in the CNS stimulate extant antigen-specific T-cells (green). From⁴¹

In this model, tumor cells expressing the onconeural antigen undergo apoptosis. Apoptotic fragments of the tumor cells are then loaded in dendritic cells that present the antigen via MHC class I to T-cells which leads to activation of antigen-specific CD8+ and CD4+ T-cells. These CD4+ T-cells activate B-cells that produce the onconeural autoantibodies. Some of these antibodies will passively cross the blood-brain-barrier where they will be taken up by neurons, bind to the antigenic target and impair neuronal function that in some cases will result in neuronal apoptosis. Any apoptotic neuronal material will be loaded by dendritic cells that will stimulate antigen-specific T-cells that are able to cross the blood-brain-barrier, perpetuating the neuronal killing. This theory, however, while interesting remains unproven.

1.2.2. Myasthenic syndromes

In contrast to the paraneoplastic antibodies against intracellular antigens discussed above, the antibodies associated with **myasthenic syndromes** such as myasthenia gravis (MG) and the Lambert-Eaton myasthenic syndrome (LEMS) can reach the cell-surface targets (acetylcholine receptor [AChR] for MG, and voltage-gated calcium channels [VGCC] for LEMS) and alter their structure and function. In these two diseases several pathogenic effects of the antibodies have been described: 1) cross-linking and internalization of the receptors, 2) blocking receptor function (e.g., AChR), and/or 3) complement-mediated injury of the cell-membrane at the neuromuscular junction.^{26–29} Moreover, the characterization of these antibody effects led to effective treatment approaches beyond immunotherapy (e.g., anticholinesterase drugs that increase the levels of acetylcholine, or 3-4 diaminopyridine that enhances acetylcholine release) which compensate or antagonize the antibody effects.^{42,43}

1.2.3. GAD autoimmunity, a non-paraneoplastic disorder with antibodies against intracellular antigens

GAD autoimmunity is characterized by antibodies predominantly targeting the GAD65 isoform of GAD, a cytoplasmic protein involved in the synthesis of GABA. There are 3 syndromes associated with GAD65 autoantibodies, 1) stiff-person syndrome, 2) cerebellar ataxia, and 3) encephalitis associated with seizures and frequent limbic involvement. Of all 3, only the latter can result in a syndrome similar to the paraneoplastic or antibody-mediated encephalitis. Although the encephalitis associated with GAD65 antibodies infrequently associates with cancer (and therefore it is rarely paraneoplastic),⁴⁴ the underlying mechanism is probably mediated by T-cell mechanisms similar to those of the paraneoplastic syndromes. Studies using rat cerebellar extracts or cerebellar slices showed that GAD65 antibodies from patients with stiff-person syndrome and cerebellar ataxia inhibited GAD enzymatic activity resulting in a reduction of GABA^{45,46} and suppressed GABA-mediated transmission without affecting glutamate-mediated transmission.⁴⁷ However, *in vitro* studies examining whether antibodies have pathogenic effects on rat hippocampal neurons in culture, showed that the antibodies cannot reach the intracellular antigen and therefore it is unlikely that they are pathogenic.⁴⁸

Accordingly, the encephalitis of patients with GAD65 antibodies is less responsive to immunotherapy than the encephalitis of patients with antibodies against cell-surface proteins.

1.2.4. Discovery of antibody-mediated encephalitis

In recent years, the identification of patients with syndromes similar to those with classical paraneoplastic encephalitis or anti-GAD associated encephalitis but without cancer or without antibodies against intracellular antigens, and who frequently responded to immunotherapy, suggested their disease could be directly mediated by autoantibodies against cell-surface or synaptic proteins (**Figure 5**). The mechanisms for antibodies in antibody-mediated encephalitis are somewhat similar to the mechanisms described for the myasthenic syndromes.⁴

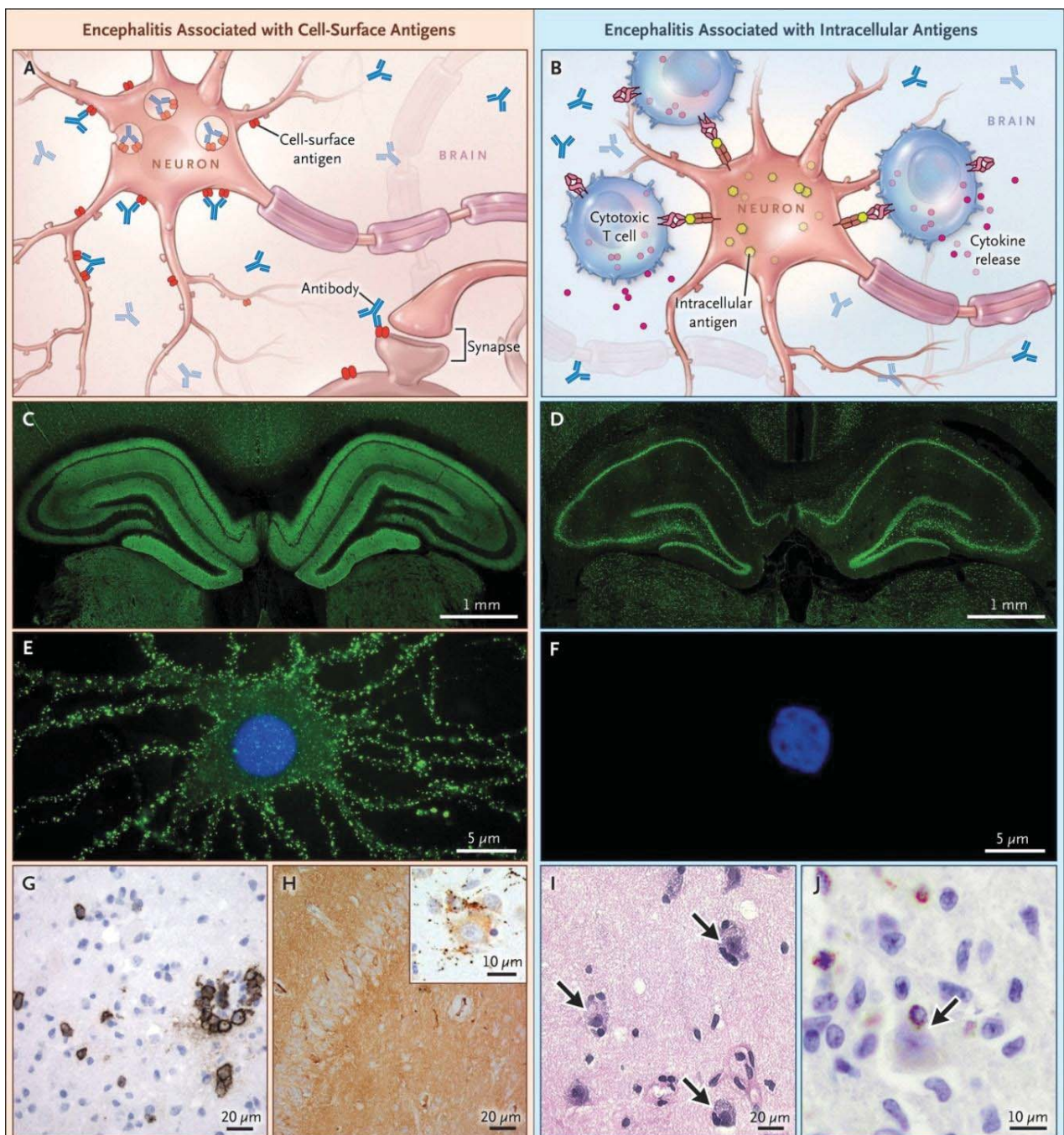


Figure 5. Antibody reactivity and pathological features of encephalitis associated with antibodies against neuronal cell-surface antigens as compared with encephalitis associated with antibodies against intracellular antigens

In encephalitis associated with antibodies against cell-surface antigens, the antibodies have access to the epitopes (A), whereas in encephalitis associated with antibodies against intracellular antigens, the antibodies cannot reach the intracellular epitopes, and cytotoxic T-cell mechanisms are predominantly involved (B). As examples, NMDAR antibodies are directed against cell-surface antigens react with rat brain hippocampus (C) and non permeabilized hippocampal neurons (E). In contrast, Hu antibodies are directed against intracellular antigens, which react with permeabilized rat brain sections (D) but cannot reach the intracellular antigen in non-permeabilized hippocampal neurons (F). Autopsy studies have shown that anti-NMDAR encephalitis patients have moderate brain inflammatory infiltrates along with plasma cells (G, cells stained brown with a CD138 antibody), deposits of IgG (H, diffuse brown staining with an antihuman IgG antibody), and microglial proliferation (H inset, microglial cells stained red with a CD68 antibody), without evidence of T-cell-mediated neuronal loss (not shown). In contrast, patients with anti-Hu paraneoplastic encephalitis have extensive neuronal loss and inflammatory infiltrates (not shown); the T cells are in direct contact with neurons (I, arrows; hematoxylin and eosin), probably contributing to neuronal degeneration through perforin and granzyme mechanisms (J, arrow; granzyme B staining). All human tissue sections (G through J) were obtained from the hippocampus. From ⁴⁹

One of the initial studies that led to the discovery of one of these novel antibodies described two patients who developed symptoms similar to paraneoplastic LE and had antibodies against surface proteins interacting with the voltage-gated potassium channels (VGKC). None of the two patients had cancer and both improved after immunotherapy.^{50,51} Another study identified four young women with neuropsychiatric symptoms hypoventilation and coma, who harbored neuronal antibodies that produced a characteristic pattern of immunostaining of the neuropil of rodent brain and intense immunolabeling of the surface of live neurons ⁵² (**Figure 6**). All four patients had an ovarian teratoma, and 3 substantially recovered with immunotherapy. The neuronal antigen was eventually characterized as the GluN1 subunit of the NMDA receptor, and the disease is now known as anti-NMDA receptor encephalitis.¹⁹

The approach used for the discovery of these two syndromes and the corresponding antibodies was subsequently adapted to identify a large number of neuronal antigens in several types of encephalitis suspected to be immune-mediated. These studies are based on 1) the identification of homogeneous groups of patients with similar symptoms or comorbidities, and 2) the demonstration that all patients have the same type of neuronal antibody (defined by the pattern of brain immunostaining and presence of cell-surface immunolabeling.^{19,53–56} The antibodies are then used to precipitate the target antigen the identity of which is eventually established by mass spectrometry.

Once the target antigen is characterized, a diagnostic test is developed using human embryonic kidney (HEK)293 cells transfected to express the antigen of interest. This cell-based diagnostic test is called cell-based assay (CBA), which can be applied to detect by immunofluorescence the reactivity of patients' serum or CSF antibodies. This antibody detection strategy is important because the epitope targets of many of the antibody-mediated encephalitis are

conformational, and therefore most techniques that use denatured or recombinant proteins are inadequate for antibody detection.

Overall, these studies set in motion the field of antibody-mediated encephalitis leading to a better definition of the syndromes and investigations on the antibody pathogenicity at the cellular, synaptic, and circuitry levels.

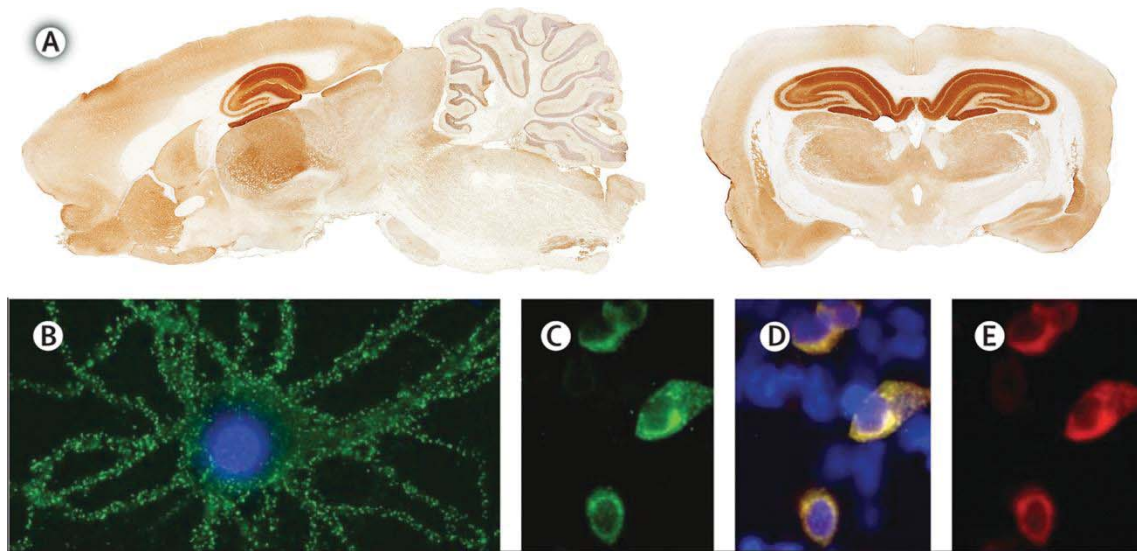


Figure 6. Patients' NMDAR react with neuronal cell-surface proteins

Immunoreactivity of patients' NMDAR antibodies with (A) sagittal and coronal section of rat brain predominantly involving the hippocampus, (B) cultures of non-permeabilised live rat hippocampal neurons and (C) with HEK293 cells transfected with GluN1 and GluN2B (forming GluN1–GluN2B heteromers of the NMDAR) with patients' antibodies (in green), which colocalizes with a monoclonal antibody against GluN1 subunit (E, in red). Merged reactivities are shown in D. Adapted from^{20,57}

1.3. Syndromes related to antibody-mediated encephalitis

There are currently 16 known disorders that occur in association with antibodies against neuronal surface antigens, 10 of which manifesting as encephalitis (**Table 2**). The other 6 usually present as cerebellar ataxia or symptoms of spinal cord dysfunction such as stiff-person syndrome.

Table 2. Extracellular neuronal antigens in autoimmune encephalitis

Target antigen	Clinical features	Associated symptoms and tumor	Main IgG isotype	Effects
NMDAR	80% female, median age 21 yrs (2mo – 85yrs)	Encephalitis, psychosis, dystonia, chorea, status epilepticus Ovarian teratoma	IgG1	Displacement from synapse and Internalization of NMDAR receptor ^{58,59}
LGI1	65% male, median age 60yrs (30-80 yrs)	LE, fasciobrachial dystonic seizures, memory loss No tumor associated	IgG4	Disruption of LGI1-Adam binding, and decrease GluR1 of AMPAR ⁶⁰
Caspr2	85% male, median age 60 yrs (46-77 yrs)	Neuromyotonia, muscle spasms, fasciculations, LE, memory loss Thymoma	IgG4	Decrease Gephyrin clusters at inhibitory synaptic contacts ⁶¹
GlyR	60% male, median age 47 yrs (1-75 yrs)	Hyperekplexia, muscle spasms and cramps, stiff-person syndrome and/or exaggerated startle, PERM No tumor associated	IgG1	Internalization of GlyR ⁶²
GABABR	60% male, median age 61yrs (16-77 yrs)	LE with severe seizures, memory loss SCLC	IgG1	Block activation of GABABR by baclofen ⁵⁶
IgLON5	50 % male, median age 64 yrs (46–83 yrs)	Sleep movements and parasomnia with sleep breathing problems No tumor associated	IgG4	Decrease of surface IgLon5 ⁶³
AMPA	70% female, median age 56yrs (23-81 yrs)	LE with memory loss, psychiatric features SCLC, thymoma, breast	IgG1	Decrease in the total surface and synaptic GluA1 and GluA2, and decrease of AMPAR-mEPSC ⁶⁴

DPPX	70% male, median age 57 yrs (36-69 yrs)	CNS (myoclonus, startle, delirium) and gastrointestinal hyper-excitability No tumor associated	IgG4/IgG1	Decrease of surface DPPX clusters and Kv4.2 ⁶⁵
Dopamine-2 Receptor	50% female, median age 5,5 yrs (1,6-15 yrs)	Dystonia, chorea No tumor associated	Unknown	Internalization of D2R in HEK293 cells ⁶⁶
mGluR5	60% male, median age 29 yrs (6-75yrs)	LE Hodgkin lymphoma	IgG1	Decrease density of mGluR5 ⁶⁷
GABAaR*	50% female, median age 40 yrs (2.5mo-88yrs)	Status epilepticus No tumor associated	IgG1	Decrease synaptic GABAaR ⁶⁸
Neurexin-3 α *	80% female, median age 44 yrs (23-50 yrs)	Not characterized No tumor associated	IgG1	Decrease of neurexin-3 α and number of synapses in developing neurons ⁶⁹
P/Q-type VGCC	52% female, median age 57 years (9-87 years)	LEMS CPCP, Hodgkin lymphoma	Unknown	Reduction of VGCC, and inhibit Ca ²⁺ influx ⁷⁰ Intrathecal injection in mice cause transient ataxia ^{71,72}
mGluR1	50% male, median age 58 yrs (33-81 yrs)	PCD Hodgkin's lymphoma	Unknown	Reduction of basal activity of Purkinje cells ⁷³ <i>In vivo</i> , transient ataxia ⁷⁴
Amphiphysin	100% female, median age 58yrs (39-73 yrs)	Stiff person syndrome Encephalomyelitis SCLC, breast cancer	IgG1	Disrupt vesicle endocytosis in cultures of neurons ⁷⁵ <i>In vivo</i> cause motor hyperactivity, stiffness, and muscle spasms ⁷⁶
DNER (Tr)	78% male, median age 61 yrs (14 - 75 yrs)	paraneoplastic cerebellar degeneration Hodgkin's lymphoma	IgG1	Unknown

* Newly identified in this thesis

Table adapted from^{9,20}

1.3.1. Anti-NMDAR encephalitis

History and frequency

In 2005, four young women were identified with a syndrome characterized by acute psychiatric symptoms, seizures, memory deficits, decreased level of consciousness, and central hypoventilation, with CSF inflammatory abnormalities, and all had an ovarian teratoma. Moreover, all 4 patients had antibodies in CSF and serum that reacted with a neuronal cell-surface protein.^{4,52} At that time the identity of the cell-surface antigen was unknown, and in 2007 it was identified as the NMDAR.¹⁹ Since then, this disorder has become the most frequent antibody-mediated encephalitis; it represented 4% of all types of encephalitis in the study of Granerod and colleagues.¹ A study from a center that is specifically concerned with the epidemiology of encephalitis showed that the frequency of anti-NMDAR encephalitis surpassed that of any individual viral cause of encephalitis in young persons,⁷⁷ and in one retrospective study, anti-NMDAR encephalitis accounted for 1% of all admissions of young adults to an intensive care unit.⁷⁸

Clinical features

Anti-NMDAR encephalitis predominantly affects young women and children (40% <18 years, median age 21 years old [range, 2 months old – 85 years old]; 80% women). The initial clinical presentation usually includes prodromal headache or fever, which occur in 70% of the patients, followed by psychiatric manifestations that may include anxiety, insomnia, delusional thinking (e.g., grandiose delusions, hyper-religiosity), hallucinations, paranoid thoughts, pressured speech, mood disorder (predominantly manic), or aggressive behavior, with alternating episodes of extreme agitation and catatonia.⁷⁹ At this stage, these symptoms may suggest drug abuse or the manifestation of an acute psychotic break and a psychiatric consultation is often considered. However, the clinical picture usually progresses with other symptoms such as seizures, reduced verbal output, decreased level of consciousness, highly characteristic orofacial and limb dyskinesias, choreoathetosis, dystonic postures, rigidity, and autonomic dysfunction (including tachycardia, high blood pressure, hyperthermia, profuse salivation, and hypoventilation) suggesting that the disorder is not a primary psychiatric disease (**Figure 7**). The initial symptom presentation in children is mildly different; while adults usually present with psychiatric and cognitive alterations, children more frequently present with seizures, insomnia, abnormal movements, and change of behavior (irritability, disintegration of language).⁸⁰

Diagnosis can be established after demonstrating that serum and/or CSF contain antibodies against NMDAR. Study of the CSF, and alterations in MRI and EEG might help in the diagnosis. Patients' CSF often shows inflammatory changes including pleocytosis, elevated IgG index, or oligoclonal bands.^{81,82} The EEG is usually abnormal (>90% of patients),^{77,83} showing general slow activity in the theta or delta range, often with superimposed epileptic activity.⁸⁴ Conventional clinical MRI is normal in 65% of the patients, and the other 35% show mild or transient cortical or subcortical brain, cerebellar, or brain stem abnormalities.⁷⁹

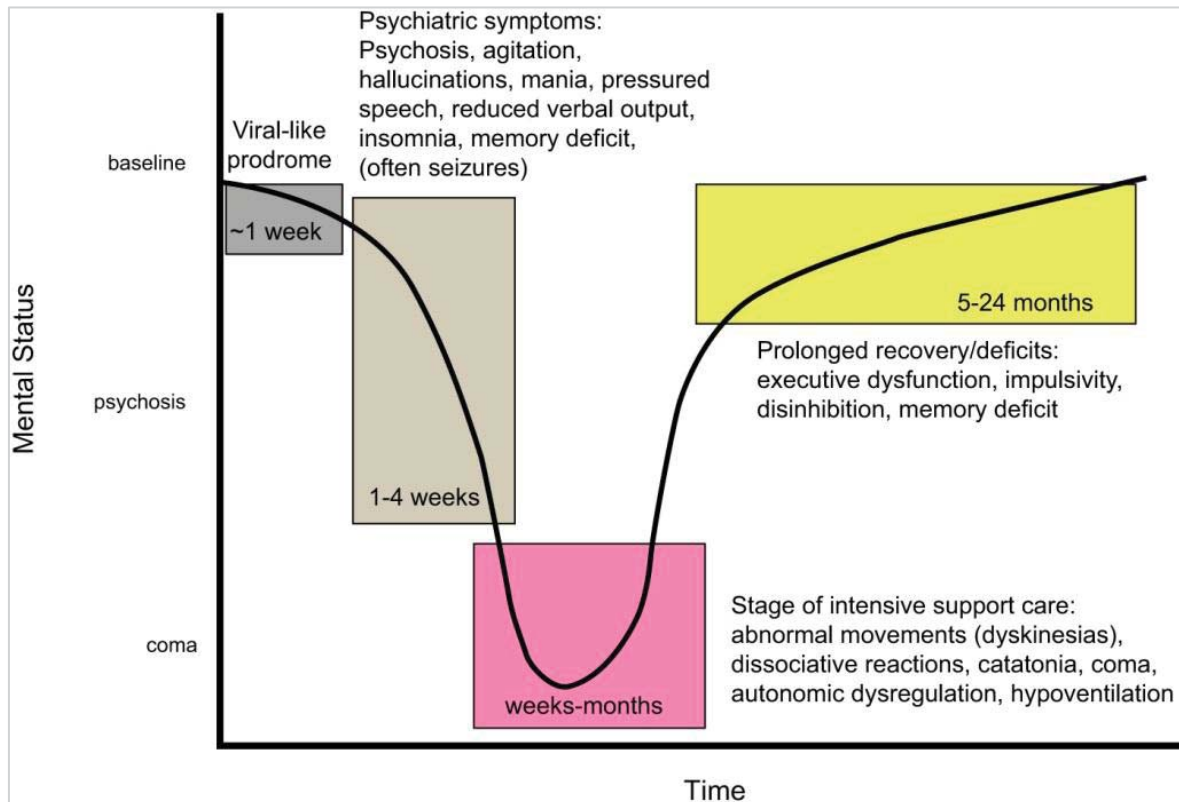


Figure 7. Development of anti-NMDAR encephalitis symptoms

Symptom development and time course of anti-NMDA receptor encephalitis. The graph shows the typical course of symptoms in a young adult with full-blown anti-NMDA receptor encephalitis. In children and young males, the symptom onset can be seizures, abnormal movements, or psychiatric symptoms. Otherwise, the progression of symptoms is remarkably similar in most patients. Milder forms of the disorder, without symptoms requiring intensive support care, are becoming more frequent as the disease is better known and diagnosed and treated earlier. From ²⁰

Triggers

The triggers of this disorder include tumors, viral infections, and yet unknown factors (**Figure 8**). Up to 58% of young women have an ovarian teratoma, which contains mature and immature nervous tissue that expresses NMDAR which react with patients' antibodies,⁷⁹ suggesting that the ectopic expression of these proteins may play a role in initiating the autoimmune response. Furthermore, samples of teratomas from patients with anti-NMDAR encephalitis, show extensive inflammatory cell infiltrates, including macrophages, T-cells, B-cells, and plasma cells, whereas these are less evident in teratomas from patients without anti-NMDAR encephalitis.⁸⁵

The frequency of tumors in children and men is lower and the histology different (e.g., older men and women have carcinomas instead of teratomas).^{81,86} Twenty-three percent of patients older than 45 years have underlying tumors, which are usually carcinomas rather than teratomas.⁷⁹ Moreover, African-American female patients are more likely to have an ovarian teratoma than patients from other ethnic groups.⁸⁷

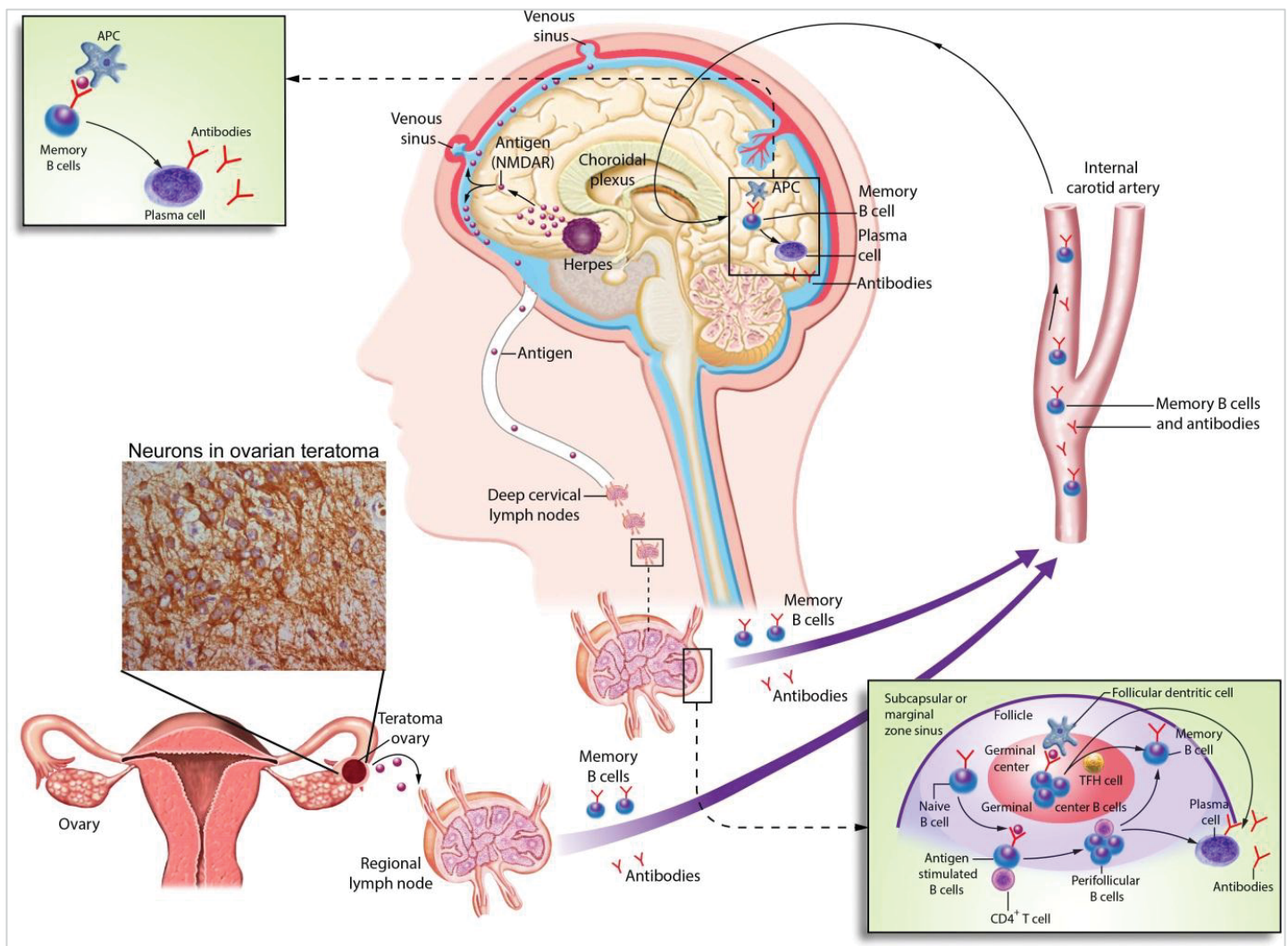


Figure 8. Triggers of anti-NMDA receptor encephalitis and a proposed model of B-cell activation. The figure shows two identified triggers of the disorder: a tumor (usually ovarian teratoma) and much less frequently HSE. In ovarian teratoma, the nervous tissue present in the tumor contains neurons and NMDARs that are likely released by tumor-related necrotic changes, reaching the local, pelvic-abdominal lymph nodes. In cases of HSE, the prominent viral-induced inflammation, tissue necrosis, and neuronal degeneration may release the antigen which is transported to the local brain-draining deep cervical lymph nodes (an alternative route is through the venous sinuses). In the lymph nodes (pelvic-abdominal or deep cervical), the antigen is presented to naive B-cells by antigen-presenting cells in cooperation with CD4+ T-cells leading to generation of memory B-cells and antibody-producing plasma cells. Activated memory B-cells reach the brain through the bloodstream, crossing the choroidal plexus; in the brain the activated B-cells undergo restimulation, antigen-driven affinity maturation, and differentiation into plasma cells. A smaller contribution would be the crossing of a leaky or disrupted BBB by autoantibodies. From ²⁰

In a small subset of patients (less than 5%), the trigger of the disease is herpes simplex encephalitis (HSE). About 25% of patients HSE develop antibodies to neuronal cell-surface antigens (mainly NMDAR). It has been proposed that the release of neuronal cell-surface proteins caused by the viral infection, in the context of extensive inflammatory infiltrates, may

trigger the immune response against the NMDAR.

The anti-NMDAR encephalitis that occurs post-HSE is more frequent in children than adults, and while children present with predominant choreoathetoid movements, adults more frequently show psychiatric and cognitive alterations.⁸⁸

In 55-60% of the patients with anti-NMDAR encephalitis the trigger of the autoimmune response is unknown. A genetic predisposition has been suggested for Maori and Pacific Islands' population,⁸⁹ and a recent study found a mild association with HLA.⁹⁰

Treatment and prognosis

The current approach to the treatment of anti-NMDAR encephalitis is immunotherapy and removal of the tumor, when it applies. The immunotherapy is directed to remove the autoantibodies (steroids, intravenous immunoglobulins [IVIg], plasma exchange) and the antibody-producing B-cells (rituximab, cyclophosphamide).⁷⁹ Despite the severity of the disease, 80% of patients recover or substantially improve after intensive care support, immunotherapy, and prolonged hospitalizations. In a series of 577 patients with anti-NMDAR, 53% showed clinical improvement within four weeks, and 81% showed substantial recovery (normal or mild residual symptoms) at 24 months. The treatment and outcome are similar in patients of different ages and gender. The recovery is usually slow (>6 months), gradually improving from autonomic dysfunction, seizures, and abnormal movements to recovering the deficits of memory, attention, and behavior. It has been demonstrated that prompt initiation of immunotherapy and tumor removal, are predictors of good outcome. Relapses occur in about 20-25% of cases, sometimes triggered by discontinuation of medication or tumor recurrence. As the first episodes, relapses usually improve with immunotherapy and tumor removal, when needed.⁷⁹ Not all appropriately treated patients with anti-NMDAR encephalitis experience full recovery, thus the investigation on the mechanisms is of high importance.

When the disease follows HSE, the response to immunotherapy is less optimal, particularly in children. The cause of this limited response to treatment is currently unknown but co-existent immune mechanisms against the NMDAR or other neuronal proteins may play a role.⁸⁸

The antigen

The NMDA receptor is a glutamatergic ion channel receptor composed of 4 subunits, two GluN1 (the obligatory subunit) and two GluN2 or GluN3.⁹¹ They require multiple events for activation, including the binding of glutamate to the GluN2 subunits, and glycine to the GluN1 or GluN3 subunits along with opening the channel (which is normally blocked by magnesium). With maturity many GluN1/GluN2B receptors become largely extrasynaptic in hippocampal neurons and GluN1/GluN2A/GluN2B become the major synaptic receptors in hippocampus and forebrain. The subunit composition can affect Ca²⁺ affinity, channel activity, and downstream signaling. For example, GluN1-GluN2B complexes *in vitro* have longer excitatory postsynaptic potentials than GluN1-GluN2A.⁹²

NMDARs have critical roles in synaptic transmission and plasticity, memory formation, learning and cognition. The activation of postsynaptic NMDAR in the hippocampus determines the

mechanism of long-term potentiation (LTP), considered to be involved in memory by promoting the mobilization of AMPAR to the postsynaptic membrane.

Pharmacological blockade of NMDAR with phencyclidine or ketamine causes symptoms similar to those associated with schizophrenia^{93–97} along with repetitive orofacial and limb movements, autonomic instability, and seizures.^{98–102} Interestingly, this phenotype closely resembles that of patients with encephalitis associated with antibodies against the NMDAR.

NMDAR knock outs have also been useful for the study of NMDAR function. Although GluN1 knock-out mice die a few hours after birth,¹⁰³ specific hippocampal GluN1 knock-down mice are viable into adulthood, and show impaired spatial and temporal learning with severe impairment of LTP in the Schaffer collateral-CA1 synapse, demonstrating the role of the NMDA receptor in establishing synaptic plasticity and memory formation.¹⁰⁴ Interestingly, mice with reduced expression of NMDAR show repetitive orofacial movements, autonomic instability and seizures that also resemble the symptoms of patients with anti-NMDAR encephalitis.¹⁰⁵

Pathogenesis

In vitro studies have demonstrated that application of CSF or purified IgG from patients with antibodies to GluN1 in cultured hippocampal neurons caused a progressive decrease of GluN1 but also GluN2A and GluN2B clusters in a titer-dependent manner. Although the effect was noted after 2 hours, the maximal effect was at 12 hours, with no further reduction with longer treatment. This effect was reversed 4 days after the removal of antibodies, supporting the reversibility of the symptoms of patients treated with immunotherapy. The effect of patients' NMDAR antibodies was specific, and did not alter the number of synapses, the cluster density of synaptic markers such as PSD95 or Bassoon, other synaptic receptors such as AMPAR, GABA_AR, or dendritic branching and dendritic spine density indicating a specific effect on the NMDAR. The antibody-mediated decrease of NMDAR clusters affected both inhibitory (GAD positive) and excitatory neurons (GAD negative).^{58,106} Whole-cell patch recordings of neurons treated with patients antibodies showed that these caused a decrease of NMDAR-specific mEPSC.⁵⁸

Application of Fab fragments (one antigen-specific arm of the antibodies) derived from patients' antibodies did not cause any of the indicated effects. However, when the Fab fragments were linked with an antibody anti-Fab (reconstituting a two-arm molecule similar to the original NMDAR antibody), they caused the same pathogenic effect as the original antibody, suggesting that the antibody effects are mediated by crosslinking of the receptors followed by internalization.

Subsequent studies by other investigators confirmed these findings and showed that patients antibodies disrupt the interaction of NMDAR with ephrin-B2 receptor at synapses, before removing the NMDAR from synapses and internalizing them (**Figure 9**).⁵⁹

Additional findings related to the pathogenic effects of patients' antibodies are summarized in **Table 3**. All these *in vitro* studies suggest that patients' antibodies are pathogenic; however, definitive evidence of pathogenicity can only be established with an animal model of NMDAR-specific antibody-mediated memory and behavioral deficits^{107,108} and this is one of the goals of

my thesis.

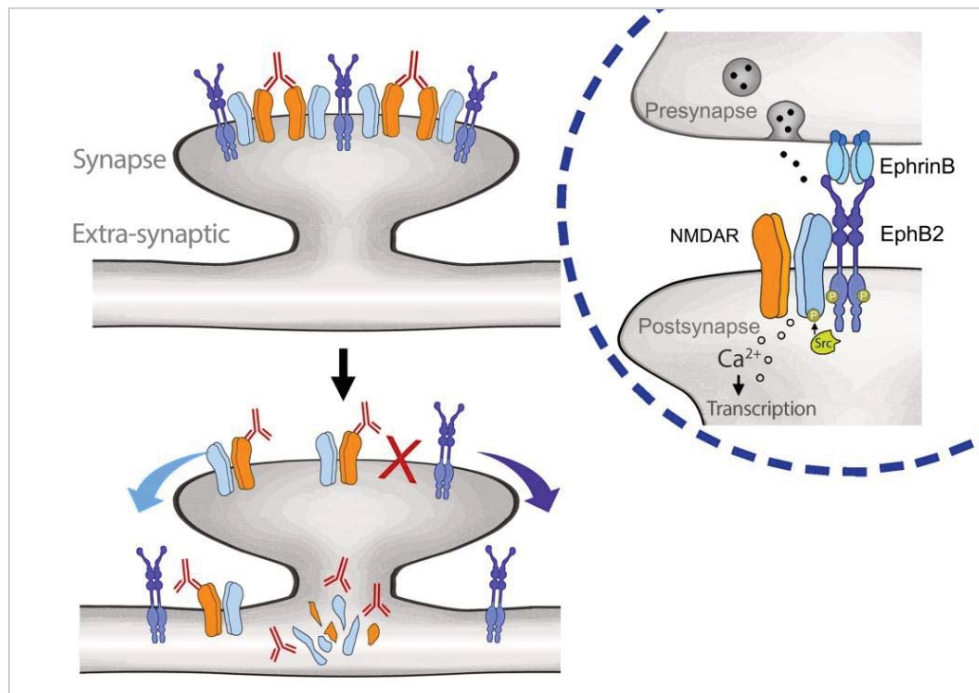


Figure 9. Proposed model of antibody-mediated disruption of NMDARs leading to neuropsychiatric disease

Specific binding of patients' antibodies to the GluN1 subunit of the NMDAR alters the normal interaction between NMDAR and EphB2 displacing them from synaptic to extrasynaptic sites before the NMDARs are internalized. The inset shows the normal cross-talk between EphB2 and the NMDAR at the extracellular and intracellular levels (the latter via kinase signaling; phosphorylation sites in both receptors shown with green circles). From ²⁰

Table 3. Effects of patients' CSF NMDAR antibodies on cultures of hippocampal neurons for 24 hours from Mikasova et al ¹⁰⁶

Observed Effects of patients' NMDAR antibodies
Decrease of cell-surface NMDARs in excitatory and inhibitory hippocampal neurons
Internalization of NMDAR in a time-dependent manner (maximum effect at 12 hours)
F(ab) fragments do not cause effects. Crosslinking mediated by the two arms of the antibody is required for pathogenicity
Decrease of NMDAR is not mitigated by the presence of APV (a specific antagonist of NMDAR). Antibody-mediated internalization is independent of NMDAR activity
NMDAR antibodies do not affect the postendocytic trafficking through recycling endosomes and lysosomes
The antibodies cause a reduction in NMDAR-mediated mEPSC amplitude (whole cell patch clamp recordings)
To compensate the antibody effects, there is homeostatic plasticity of inhibitory synapse density (decrease in inhibitory synapse density). However, no changes in gene expression of NMDAR were identified

1.3.2. Anti-LGI1 encephalitis

History and frequency

In 2001, a treatment-responsive form of LE with antibodies considered directed against VGKC was described.⁵¹ The antibody detection was done by radioimmunoassay (RIA) which consisted in the immunoprecipitation of 125I-dendrotoxin labeled VGKCs, a method that can co-immunoprecipitate other proteins associated with the VGKC complex. Although patients' serum was positive on this test, all attempts to show direct reactivity with VGKC-transfected cells failed. It was not until 2010 that Lai and colleagues⁵⁴ and subsequently Irani and colleagues¹⁰⁹ demonstrated that the previously named VGKC-antibodies were in fact directed against two different proteins of the VGKC complex, named leucine rich glioma inactivated 1 (LGI1), and contactin-associated protein-like 2 (Caspr2). Whereas antibodies against LGI1 predominantly associated with limbic encephalitis, those against Caspr2 associated with encephalitis, neuromyotonia and the Morvan syndrome, a disorder characterized by encephalopathy, hallucinations, sleep dysfunction, autonomic alterations and peripheral nervous system hyperexcitability or neuromyotonia.^{55,109}

In a study performed in 2015 in the Netherlands, the incidence of anti-LGI1 encephalitis was estimated to be 0.83 per million people. It is the most common cause of autoimmune LE and the second most common cause of auto immune encephalitis after anti-NMDAR encephalitis.¹¹⁰ The incidence is rising, probably owing to improved recognition.

Clinical features

Patients with LGI1 antibodies are predominantly male (65% male, median age 60 years old [range 30-80 years old]) who develop rapidly progressive confusion, agitation, spatial disorientation, seizures and difficulty forming new memories, resulting in a dramatic picture of short-term memory loss (a feature typical of LE). These symptoms are often preceded by faciobrachial dystonic seizures, a form of focal epilepsy characterized by short lasting dystonic movements with face, arm and sometimes the leg. It can be uni- or bilateral and may occur hundreds of times every day. Patients may have a brief, transient confusion after these episodes, but there is no loss of consciousness. About 60% of patients with anti-LGI1 associated LE have hyponatremia, and REM sleep behavior disorder is also common.¹¹¹ These problems are likely caused by a disturbance of monoaminergic diencephalic and brainstem nuclei involved in arousal and autonomic homeostasis.¹¹⁰

Brain MRI shows unilateral or bilateral fluid-attenuated inversion recovery (FLAIR) signal hyperintensity in the medial temporal lobes, but it can be initially normal in 10–25% of the cases.^{110,112} Hippocampal atrophy has been reported in 40–95% of patients.^{110,113} Approximately 10-15% of patients with LGI1 antibodies have a slowly progressive encephalopathy without evidence of CSF inflammation. This atypical presentation is important to recognize because, different from many untreatable rapidly progressive dementias, patients with LGI1 antibodies are often responsive to immunotherapy.¹¹²

Triggers

Different from other forms of paraneoplastic or autoimmune LE, most patients with LGI1 antibodies do not have cancer (only 5% of cases have thymoma). A significant genetic predisposition has been associated with HLA haplotypes DRB1*07, DQB1*02, and DRB4 in 75–91% of LGI1 patients. Interestingly, this haplotype association did not appear to apply to patients who developed the disorder in the context of a systemic tumor, suggesting that the absence of those haplotypes could raise suspicion for an underlying tumor or paraneoplastic mechanism.^{90,114,115}

Treatment and prognosis

In patients with this disorder, antiepileptic drugs to treat the seizures have limited effect, while immunotherapy shows impressive results. About 70% of the patients show substantial neurological improvement after immunotherapy, but at the follow-up of ≥ 2 years only 35% have fully returned to their baseline cognitive function. The most frequent residual symptoms included memory deficits, apathy and difficulties with spatial orientation. Clinical relapses occur in 24–35% of the patients after >2 years follow-up; overall, the fatality rate is 6–19%.^{110,112}

The antigen

The target antigen, LGI1, is a glycoprotein that is secreted at the pre- and post-synaptic sites. It is widely expressed in inhibitory and excitatory neurons of the brain, mainly in the hippocampus, where it appears to have a role in synaptic transmission, dendritic pruning, neuronal excitability, and maturation of excitatory neurons.^{116,117} LGI1 interacts with the presynaptic proteins ADAM23 (a disintegrin and metalloproteinase 23) and ADAM11, and the postsynaptic ADAM22. These are catalytically active metalloproteases that control cell signaling by activating membrane-bound growth factors or by shedding the ectodomain of cell-surface receptors. In the presynapsis, ADAM11 and ADAM23 interact with the Kv1 subunit of the VGKC, and are essential for localizing the Kv1.1 and Kv1.2 subunit complexes to synaptic terminals. In the post-synapsis, the LGI1 trans-synaptic protein complex organizes the AMPA receptors through ADAM22, which contains a carboxyl terminal motif that binds to a PDZ domain of PSD-95 and regulates their function.^{117–119}

VGKCs are present on the membrane of neurons in the CNS and at the juxtaparadonal region of peripheral myelinated nerves, where they mediate repolarization after an action potential allowing the entrance of positively charged ions to repolarize the neuron. In the CNS, the inactivation of presynaptic Kv1.1 VGKC enhances release probability resulting in increased and prolonged depolarization, Ca²⁺ influx, and subsequent potentiation of excitatory transmission.¹²⁰

In normal conditions, LGI1 reduces the probability of glutamate release (presynaptic release probability) by antagonizing the rapid inactivation of the Kv1.1 potassium channel mediated by the Kv1 β subunit.¹¹⁷ Several mutations of LGI1 reverse this effect, thus leading to rapid inactivation possibly contributing to an increase of action potential broadening and glutamate

release.¹²¹ Indeed, studies with acute hippocampal slices of LGI1 knockout mice showed evidence for enhanced neuronal excitability, increased release of presynaptic glutamate, and enlarged excitatory synaptic drive.^{122,123}

There is data suggesting that LGI1 modulates the function of post-synaptic AMPAR. The AMPARs mediate most of the fast excitatory synaptic transmission in the brain, and are necessary for hippocampal long-term synaptic plasticity, with a well-established role in learning and memory formation. AMPAR undergo a highly controlled trafficking and turnover, which is very important for memory formation and storage.^{124–126}

Structurally, LGI1 is composed of two domains, the Leucine-Rich Repeat domain (LRR) and the β -propeller structural domain of epitempin (EPTP) (**Figure 10**). Both domains mediate protein-protein interactions and the EPTP is sufficient for binding to the ectodomain (ECD) of the postsynaptic ADAM22 and the presynaptic ADAM23.^{127,128}

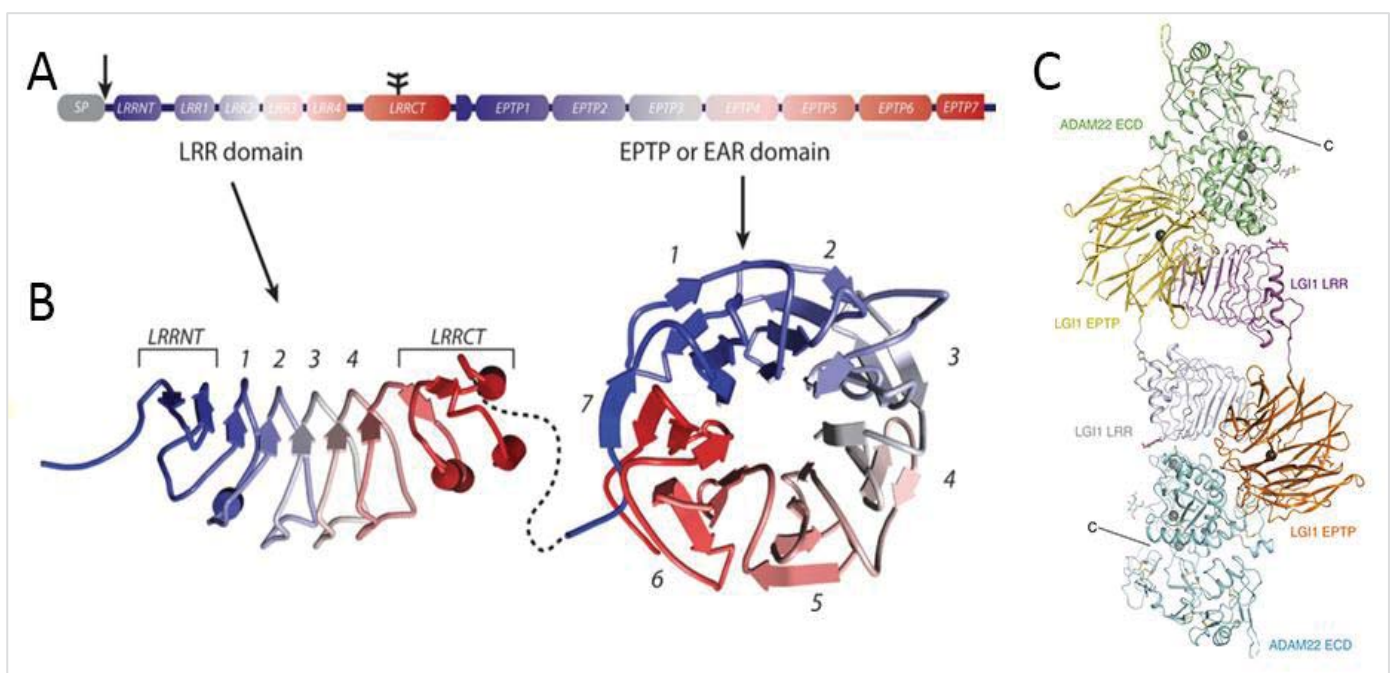


Figure 10. Structural characteristics the LGI1 protein

In (A), domain structure of the LGI1 protein. The LGI1 has an SP (signal peptide) that is cleaved off (arrow in A) and is not included in the putative protein structure shown in (B). The glycosylation site is indicated in (A) with a branched line structure. The structure is color-coded from N-terminus (blue) to C-terminus (red) and corresponds with the color code in (A). The color-code graphically reveals the Velcro β -strand (blue) interacting with the last β -strand (red) of the seventh EPTP module to zip up the EPTP domain structure. (C) Overall structure of the dimerized LGI1–ADAM22 complex. LGI1 LRR, LGI1 EPTP, and ADAM22 ectodomain (ECD) ADAM22 ECD (or alternatively ADAM23 ECD) bind to LGI1 EPTP domain and LGI1 dimerizes through the LRR domain from of LGI1 with the EPTP domain of the other LGI1 forming a transynaptic complex of two LGI1 and two ADAM. Adapted from^{129,130}

The study of crystal structures of ADAM and LGI1 with single mutations of LGI1 suggests that LRR domain of one LGI1 molecule interacts with the EPTP domain of the other LGI1 molecule,

thereby bridging two distant ADAM molecules in the complex. This study was focused on the binding of ADAM22 with LGI1, and theoretically this could be applied to ADAM23, due to the molecular similarity between both metalloproteases. The resulting structure of two LGI1 each binding to an ADAM forms a complex, and the length along the longest axis is about 190 Å, which matches the height of the synaptic cleft.¹³⁰

In humans, mutations in LGI1 cause a disorder named autosomal dominant lateral temporal lobe epilepsy (ADLTE), a genetic alteration characterized by partial seizures with acoustic or visual hallucinations.¹²¹ Some of the mutations causing ADLTE prevent the secretion of LGI1 and others result in a secreted LGI1 that is not functional. Described mutations causing epilepsy include truncated forms that lack the EPTP domain, which is needed for its secretion and correct function.

In mice, LGI1 heterozygous knockouts show increased susceptibility to seizure-inducing stimuli, whereas homozygous knockouts die within the third postnatal week of seizures. This is explained by the fact that the expression of LGI1 increases in the brain in the third postnatal week, when glutamatergic synapses are pruned and matured. Transgenic mice with a mutant LGI1 that causes ADLTE, have decreased dendritic pruning and increased spine density, resulting in increased excitatory synaptic transmission. The normal postnatal Kv1 channel-dependent down-regulation of presynaptic release probability is arrested in the LGI1 mutant of ADLTE.^{117,118}

Interestingly, ADAM22 and ADAM23 knock outs present similar phenotype as LGI1 knock out suggesting that LGI1 function depends on these two metalloproteases.¹³¹ The constitutional inactivation of ADAM22 in mice leads to seizures that are very similar to those seen in the LGI1 null mice. In addition, ADAM22 null animals also showed reduced body weight, ataxia, and hypomyelination in the peripheral nervous system.¹³² ADAM23^{-/-} mice exhibit spontaneous seizures, and ADAM23^{+/-} mice have a decreased seizure threshold. Morphologically, CA1 pyramidal neurons of ADAM23^{-/-} hippocampi have reduced dendritic arborization, thus the ability of LGI1 to stimulate neurite outgrowth from either cell type is significantly reduced in the absence of ADAM23. This suggests that LGI1 binding to ADAM23 is necessary to correctly pattern neuronal morphology and altered anatomical patterning contributes to epileptic activity.¹¹⁹

Pathogenesis

Little is known about the role of the patients' LGI1 antibodies in the pathogenesis of the autoimmune LE. In contrast to most autoimmune encephalitides in which the antibody subclass is predominantly IgG1, LGI1 antibodies are predominantly IgG4,^{112,133} which do not fix complement and due to their unique feature of being bispecific (IgG4 antibodies are continuously undergoing half-antibody exchange), they predominantly interfere with protein-protein interactions.¹³⁴ Indeed, a proposed mechanism for most IgG4-mediated autoimmune disorders is that the antibodies mechanically interfere with the extracellular protein-protein

interactions disrupting the normal function of the target (similar to MusK antibodies in a subtype of MG which blocks the clustering of AChR).¹³⁵

In vitro studies using HEK293 cells expressing LGI1 and soluble forms of ADAM22 and ADAM23 showed that patients' LGI1 antibodies prevented the interaction of LGI1 with its ligands.⁶⁰ Application of patients' LGI1 IgG in cultured rat hippocampal neurons for 3 days decreased synaptic GluA1-containing AMPAR demonstrating a postsynaptic effect of patients LGI1 antibodies. Importantly, these antibody-mediated effects reversed upon removal of the antibodies from the media (**Figure 11**). These findings are in line with those observed with LGI1 knockout mice, which also showed a selective decrease of AMPA receptor-mediated synaptic transmission in the hippocampus.^{127,136} It was postulated that a decrease of AMPAR in inhibitory interneurons resulted in an increased of synaptic excitability resulting in seizures.

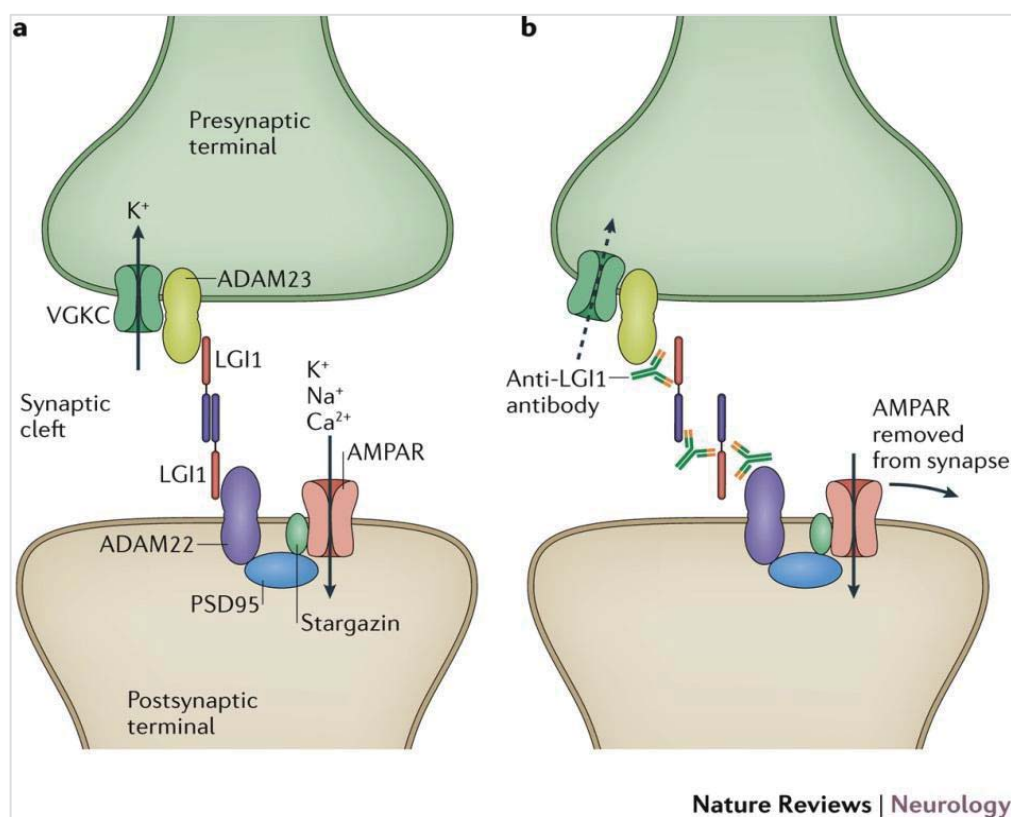


Figure 11. The transsynaptic complex formed by LGI1 is likely disrupted by patients' LGI1 antibodies. Graphic representing LGI1 in normal conditions (a), and the postulated effect of patients LGI1 autoantibodies (b). The antibodies may bind to LGI1 preventing its interaction with ADAM23 and ADAM22, and possibly preventing the dimerization of LGI1. From¹³⁷

It is currently unclear whether the antibodies of patients with anti-LGI1 encephalitis may also cause effects at the pre-synaptic level altering the expression of Kv1.1 potassium channels. It is also unknown whether these synaptic alterations would result in memory deficits. To answer these questions, we would need an animal model of the disease which is one of the goals of this thesis.

1.3.3. Anti-AMPA encephalitis

History

The encephalitis with antibodies against the α -amino-3-hydroxy-5-methyl-4-isoxazolepropionic acid receptor (AMPA) was identified in 2009.¹³⁸ The first study included 10 patients, all with LE who had CSF and serum antibodies that reacted with the neuropil of rat brain and the cell-surface of cultures of rat hippocampal neurons, leading to precipitate and characterize the target antigens as the GluA1 or GluA2 subunits of the AMPA. Together with LGI1 and GABA_B receptor antibodies, AMPA antibodies belong to a group of disorders that manifest as LE.

Clinical features

About 2/3 of the patients with anti-AMPA encephalitis are female (median age 62 years old, [range 23-81 years old]). The clinical presentation usually includes severe short-term memory loss, together with confusion, agitation and seizures.¹³⁸ Less frequently patients with AMPA antibodies can present with symptoms of psychosis. The clinical picture associated to GluA1 antibodies is similar to patients with GluA2 or both antibodies.

Triggers

About 70% of patients have an underlying tumor, usually SCLC or thymoma, and less frequently ovarian, breast cancer or teratoma.¹³⁹

In about 32% of patients AMPA antibodies coexist with other antibodies to cell-surface antigens or with onconeural antigens in which case patients usually present with symptoms or tumors that reflect the concurrent autoimmunity. The association with onconeural antibodies such as CRMP5 or amphiphysin antibodies, which usually associate with cytotoxic T-cell responses, carries a poorer prognosis.

Treatment and prognosis

In a recent study, about 70% of the patients responded to immunotherapy and treatment of the tumor (if present), but only 24% had full recovery.¹³⁹ Relapses are frequent, mostly in those who do not receive aggressive treatments like rituximab or cyclophosphamide.¹³⁸ The association with cancer and additional paraneoplastic mechanisms such as onconeural antibodies and T-cell responses against intracellular antigens result in lower rate of response to immunotherapy.

The antigen

AMPA receptors are ionotropic glutamate receptors that mediate most of the fast excitatory synaptic transmission in the brain.¹⁴⁰ AMPA receptors are heterotetramers composed of a combination of subunits, GluA1–4, that are expressed in a region-specific manner. Although AMPA receptors are widely expressed throughout the central nervous system, GluA1/2 and GluA2/3 levels are exceptionally high in the hippocampus and other limbic regions, similar to the distribution of immunoreactivity with patient antibodies. AMPA receptors interact with multiple accessory proteins (e.g., TARPs and cornichons) and are localized in the postsynaptic density. The C-

terminal tails of the GluA2/3 subunits can selectively interact with a number of intracellular proteins (e.g., GRIP1, ABP, NSF, and PICK1) and these interactions are important for targeting and accumulating GluA2-containing AMPARs at specific subcellular sites, either at the postsynaptic membrane or inside the cell.^{141–143}

The receptor is permeable to Na⁺ and K⁺, and is activated by the pre-synaptic release of glutamate leading to a brief depolarization of the postsynaptic neuron. Subunit composition determines properties and functions of the receptor. For example, GluA1 AMPA receptor subunit is required for activity-dependent trafficking and contributes to basal synaptic transmission, while the GluA2 subunit regulates Ca²⁺ permeability, homeostasis and trafficking to the synapse under basal conditions.⁹¹ Postsynaptic insertion and internalization of AMPAR play a critical role in the regulation of LTP. Therefore, the alteration of AMPAR trafficking disrupts the process of memory formation.¹⁴⁴

The role of GluA2 in AMPAR trafficking has attracted special attention because it provides a key mechanism for regulating the number of synaptic receptors and plasticity. In GluA2 mutants, LTP in the CA1 region of hippocampal slices is enhanced whereas neuronal excitability is not altered.¹⁴⁵

GluA2 and GluA3 are thought to be important for synaptic targeting/stabilization of AMPARs and the expression of hippocampal long-term depression (LTD). Double GluA2 and GluA3 knock mice, but not GluA2 or GluA3 knock out, are severely impaired in basal synaptic transmission indicating that GluA2/3 are essential to maintain high levels of synaptic transmission *in vivo*.¹⁴⁴ However, genetic manipulations eliminating individual AMPAR subunit expression result in only limited deficits in memory tasks, inconsistent with the complete loss of short-term memory seen in patients who have antibodies against AMPARs.

Pathogenesis

Patients with anti-AMPA encephalitis have antibodies in serum and/or CSF that are mainly IgG1, directed to extracellular epitopes of the GluA1 and/or GluA2 subunits of the AMPAR.¹⁴⁶ The effects of antibodies have been studied in cultures of neurons where it was demonstrated that application of patients' antibodies to GluA2 decreased total and synaptic GluA2 without affecting NMDAR clusters. The effects were reversed after the removal of antibodies.¹³⁸ A later publication demonstrated that both autoantibodies to GluA1 and GluA2 cause a selective decrease of total surface amount of GluA1 and GluA2/3 in cultured hippocampal neurons.⁶⁴ Patients' antibodies caused the internalization and degradation of surface AMPAR clusters regardless of receptor subunit binding specificity, without altering the density of excitatory synapses, NMDAR clusters, or cell viability. A short exposure (15-30 minutes) of rat hippocampal neurons to patients' antibodies did not change synaptic transmission mediated by AMPARs, but an important effect was seen at 12 hours of treatment suggesting that the reduction of glutamatergic signaling at the synapse is due to an antibody-mediated, reversible loss of receptors from synapses. In neurons treated with patients' antibodies, whole-cell patch clamp recordings showed a reduction of AMPAR-mediated miniature excitatory postsynaptic

currents, without affecting NMDAR-mediated currents.⁶⁴ Interestingly, loss of AMPAR-mediated synaptic transmission resulted in a compensatory decrease of inhibitory synaptic transmission and an increase in intrinsic excitability.

Further studies are needed to better understand the exact mechanism that leads to this increase of intrinsic excitability, possibly as a result of a compensatory synaptic homeostatic mechanism. Nevertheless, the described effects support the memory loss and seizures, among other symptoms related to hyperexcitability that are hallmarks of this disorder in patients.

1.3.4. Anti-Caspr2 encephalitis

History

Contactin-Associated Protein-like 2 (Caspr2) was identified by immunoprecipitation with samples of patients previously considered to have antibodies against VGKC. These patients usually had encephalitis and seizures but also presented with involvement of the PNS with Morvan's syndrome and neuromyotonia.¹⁰⁹ The finding that patients' antibodies precipitated Caspr2 was confirmed with CBA with HEK293 cells specifically expressing Caspr2. Subsequent studies demonstrated that, although patients with Caspr2 or LGI1 antibodies had been previously considered to have antibodies against VGKC, the molecular differentiation of the targets was important because each associated with a different syndrome.¹³⁷

Clinical features

The largest series of patients with Caspr2 antibody-associated encephalitis, showed a predominance of men (85%) with a median age of 60 years old (range 46-77 years old). About 75% had three or more of the following symptoms: encephalopathy, cerebellar symptoms, peripheral nerve hyperexcitability (PNH, or acquired neuromyotonia), autonomic dysregulation, insomnia, neuropathic pain, or weight loss. Half of the patients developed seizures and 80% showed cognitive deficits.¹⁴⁷

Therefore, patients with antibodies to Caspr2 present with a substantial overlap of CNS and PNS symptoms including, encephalitis (42%), peripheral nerve dysfunction (29%), or a combination of both (Morvan's syndrome). Morvan's syndrome, which may also occur without Caspr2 antibodies, is characterized by the combination of neuromyotonia, neuropathic pain, autonomic dysfunction, encephalopathy with hallucinations, and a characteristic sleep disorder, described as agrypnia excitata. Patients with agrypnia excitata have severe insomnia, dreamlike stupor (hallucinations and enacted dreams), sympathetic hyperactivity (hyperthermia, perspiration, tachypnea, tachycardia, and hypertension), and motor agitation. Key neurophysiological features include the loss of slow-wave sleep, which represents the transitional process of falling asleep, and the presence of abnormal REM sleep without atonia in the antigravity muscles

The syndrome presentation of encephalitis associated with Caspr2 antibodies can take a few

months to develop, but progression over 1 year is not uncommon (~30% of cases).

Triggers

Approximately 20% of patients with Caspr2-antibodies have an underlying thymoma, which probably has a role in trigger the autoimmune response.¹⁴⁷ For unknown reasons, patients who develop Morvan's syndrome have a higher tumor association (20–50%) than patients with any other syndrome associated with Caspr2 antibodies.¹³³

Treatment and prognosis

Immunotherapy together with treatment of the tumor (when appropriate) result in improvement of 90% of the patients.¹⁴⁷ The largest reported series indicated a favorable outcome (modified Rankin Scale score ≤ 2) in 73% of patients with Caspr2 antibodies, and the 2-year fatality rate was 10%. Relapses occurred in about 25% of the patients, without differences between patients with or without tumors, sometimes up to 6 years after the initial disease episode.¹⁴⁷

The antigen

The target antigen of patients' autoantibodies, Caspr2, is a cell adhesion molecule member of the neurexin IV superfamily.¹⁴⁸ It is expressed in the juxtaparanodal regions of nodes of Ranvier of myelinated nerves and also in the CNS. Unlike most neurexin proteins, the Caspr2 extracellular region contains a discoidin/neuropilin homology domain and a fibrinogen-like region which mediate cell-cell adhesions and extracellular matrix interactions.

Caspr2 forms a transmembrane axonal complex with contactin2 (or TAG1), a cell adhesion protein expressed on the axon and adjacent myelinating cells, and the protein 4.1b, which stabilize the function of the nodes of Ranvier and regulate axonal excitability (**Figure 12**). This protein complex is responsible for the organization and concentration of the VGKCs Kv1.1 and Kv1.2 at the juxtaparanode regions of myelinated nerves.^{148,149} The clustering of potassium channels is required for the proper stabilization of the electrical conduction at the nodes of Ranvier, which avoid repetitive firing and help to maintain the internodal resting potential. In the absence of TAG1, Caspr2 does not accumulate at the juxtaparanodal regions and the VGKC channels distribution is also altered.¹⁴⁹

Additionally, Caspr2 is widely expressed by inhibitory neurons in the CNS, where it interacts presynaptically with contactin-2 and postsynaptically with gephyrin, and probably acts as a cell recognition molecule that is essential for synaptic network formation.

In humans, mutations in CNTNAP2, the gene that encodes Caspr2, are associated with intellectual disability, seizures, increased risk of autism spectrum disorder, and impaired language.¹⁵⁰ As for some mutations of LGI1, heterozygous deletion spanning exons 2–3 of CNTNAP2 also associate with ADLTE.¹⁵¹

Caspr2-deficient mice have a mislocalization of the VGKC Kv1.1 and Kv1.2, alteration in the migration of cortical neurons, and a reduction of GABAergic interneurons, which is related to

epileptic phenotypes and autism-related behaviors.¹⁵²

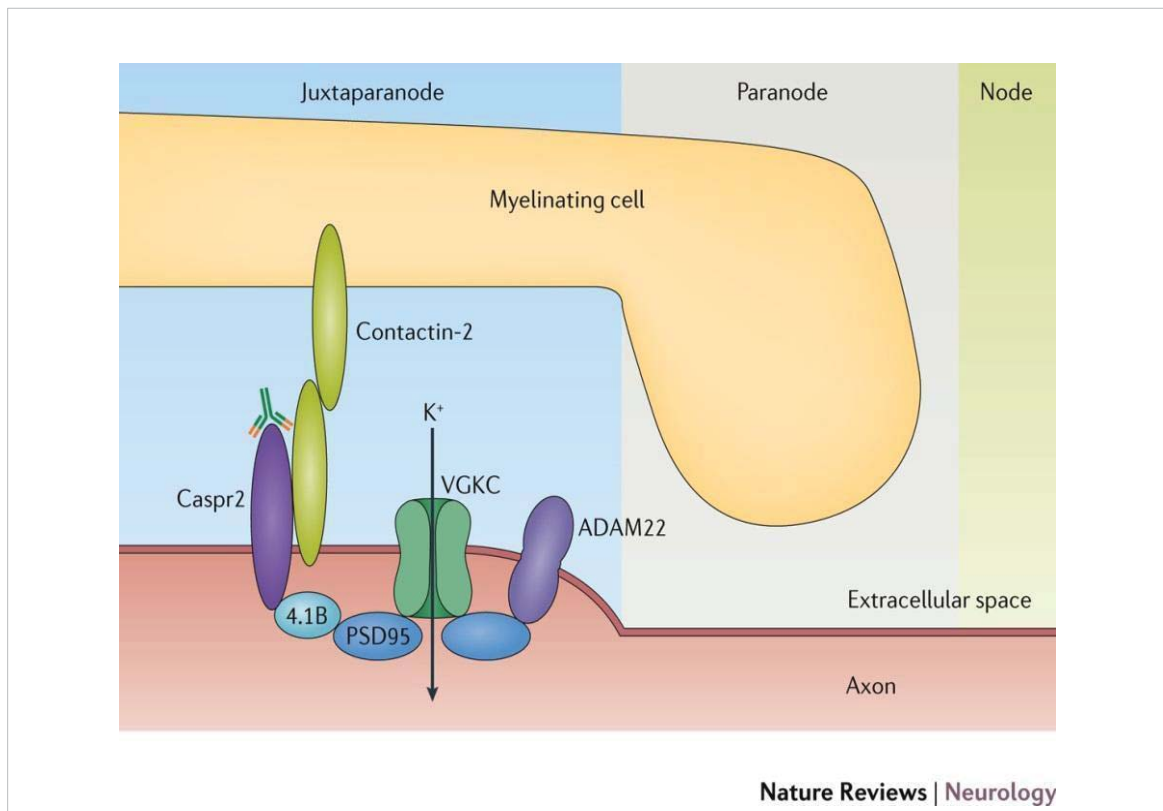


Figure 12. Schematic overview of the Caspr2 protein in the juxtapanodal region of myelinated axons. Caspr2 interacts with the dimerized contactin-2 (also known as TAG-1) located in the axon and myelinating cell, and also interacts via protein 4.1B with PSD95. This complex organizes the Kv1 potassium channels. Patients' antibodies bind to the extracellular region of Caspr2, possibly abrogating the Caspr2–contactin-2 interaction. From¹³⁷.

Pathogenesis

The antibodies of patients with anti-Caspr2 related syndromes react as expected with the two main regions where this protein is expressed, the juxtapanodal region of myelinated peripheral nerves and the CNS. The antibodies target several epitopes of the N-terminal domain, specifically the discoidin and laminin γ 1 modules; no glycosylation is required for immunoreactivity.^{61,153}

The main IgG subclass of Caspr2 antibodies is IgG4, and approximately 60% of the patients also have IgG1 antibodies.¹⁴⁷ As other IgG4-mediated diseases, Caspr2 antibodies might exert their pathogenicity by inhibiting protein-protein interactions. The effects of Caspr2 antibodies on the CNS have been examined with IgG from patients with symptoms limited to the limbic system.⁶¹ Using cultures of dissociated rat hippocampal neurons, patients' antibodies predominantly reacted with inhibitory interneurons (GAD65 and VGAT-positive in inhibitory presynaptic contacts). A Caspr2-Fc chimera revealed that Caspr2 receptors were localized at the

postsynaptic region and somatodendritic compartment, and the binding was strongly increased on TAG-1 transfected neurons. Taken together, these findings suggest that within the CNS Caspr2 operates as a cell recognition molecule in inhibitory networks, and therefore, the Caspr2 autoantibodies may potentially impair inhibitory interneuron activity.⁶¹

A more recent study showed that patients' Caspr2 antibodies interfered with the interaction Caspr2-contactin2, but did not cause a decrease of the levels of Caspr2 further confirming that the pathogenic mechanism of these antibodies is based on disrupting the interaction of Caspr2 with other normally interacting proteins, such as contactin2.¹⁵⁴

1.3.5. Other autoimmune encephalitis with antigenic targets located on glial cells

Other autoimmune encephalitis with antibodies against neuronal surface antigens are summarized in **Table 2**. In contrast to these disorders in which the antigens are on the neuronal cell-surface, there are several disorders in which the epitopes are expressed on the surface of astrocytes (i.e., aquaporin4 [AQP4]) or oligodendrocytes (i.e., myelin oligodendrocyte glycoprotein [MOG]) and may present with syndromes indistinguishable from some neuronal-antibody mediated encephalitis.¹⁵⁵ The syndromes typically associated with AQP4 antibodies are enclosed within the term neuromyelitis optica spectrum disorders. In these AQP4 antibody-related disorders there is an antibody attack, mediated by complement, against AQP4, which is mainly expressed in the end-feet of astrocytes.^{156,157} The most common symptoms related to AQP4 antibodies are optic neuritis and myelitis, although some patients develop brainstem dysfunction and encephalopathy.¹⁵⁸ On the other hand, antibodies against MOG can associate with optic neuritis and myelitis, but they usually occur with a wider spectrum of clinical manifestations.¹⁵⁹ In children, MOG antibodies frequently associate with acute disseminated encephalomyelitis (ADEM), but only 50% of all patients with ADEM have MOG antibodies.^{160,161} The pathogenicity of AQP4 antibodies has been demonstrated *in vitro* and *in vivo* studies using passive transfer of antibodies and complement to rodents.¹⁶²⁻¹⁶⁵ On the other hand, the pathogenicity of MOG antibodies is suspected but not proven.^{166,167}

2. HYPOTHESIS

Based on the concepts previously described, the antibody-mediated encephalitis represents a rapidly expanding group of neurologic disorders for which the cause and treatment were unknown until recently. Considering that at the beginning of my thesis approximately 50% of patients with encephalitis remained without an etiologic diagnosis, it was reasonable to postulate that there were subgroups of patients with syndromes that were likely mediated by autoantibodies. Moreover, given that the target antigens that had been discovered for some of these disorders are relevant cell-surface or synaptic proteins with critical roles in synaptic transmission and plasticity (NMDAR, AMPAR,...), I postulated that the study of these disorders and autoantibodies could shed light on how autoimmunity can affect brain function leading to alterations of memory, behavior, cognition, and other neuropsychiatric symptoms such as seizures, abnormal movements or psychosis. To show these effects I would need to develop *in vitro* and *in vivo* models fulfilling the modified Witebsky's criteria for antibody-mediated disease, including, 1) the development of symptoms in animals infused with patients' CSF, but not control CSF, 2) the demonstration that the infused antibodies reacted predominantly with brain regions with high density of the target antigen (e.g., NMDAR in hippocampus) and specifically recognized these receptors, 3) the identification of a selective involvement (e.g., decrease density or blocking of function) of the target antigen, and that these effects correlated with the concentration of brain-bound antibodies, and 4) show a the correlation between the intensity of the above-mentioned findings and time-course of the antibody administration, as well as between the reversibility of symptoms and restoration of the antigenic target after stopping the infusion of CSF antibodies.

Therefore, considering all the above I hypothesized that:

- 1) Patients with encephalitis manifesting with neurologic syndromes of unclear etiology but suspected to have an autoimmune cause (because of the symptoms, paraclinical findings, or response to empiric immunotherapy) are likely to have an antibody-mediated disease.
- 2) The autoantibodies of these patients are likely directed against unknown self-antigens that need identification to better understand the disease and find the appropriate treatments and develop fast and reliable diagnostic tests for patients with similar disorders.
- 3) Once the novel syndromes and autoantigens are identified, the effect of the autoantibodies will need to be demonstrated in studies using cultured neurons. The effects of each antibody are likely related to the specific antigen but also to the IgG isotype, for example, IgG1 or IgG3 are monospecific (each arm has the same epitope specificity) and are able to activate complement, in contrast IgG4 is bispecific (each arm has different epitope specificity) and does not activate complement.
- 4) Passive transfer of patients' autoantibodies to the cerebroventricular system of rodents should model the molecular, synaptic and behavioral effects of the human disease fulfilling the modified Witebsky's criteria for antibody-mediated disease.¹⁰⁷

3. OBJECTIVES

The **objectives** of this thesis are:

- 3.1. Identify new diseases: Select patients with encephalitis of unclear etiology but whose symptoms or paraclinical findings strongly suggest to have a disorder mediated by autoantibodies to yet unknown neuronal cell-surface or synaptic antigens.
- 3.2. Characterize the neuronal antigenic targets: Immunoprecipitate the antigenic targets of these disorders and develop diagnostic tests based on the recombinant expression of the antigens in HEK293 cells in order to facilitate the diagnosis of the same disorder in other patients.
- 3.3. Develop models of the discovered diseases: Select the most relevant newly identified autoantibodies to determine their pathogenic effect (a) on cultured rodent hippocampal neurons, focusing in structural changes of the target antigen and other synaptic proteins, and (b) on mice infused with patients' autoantibodies in the cerebroventricular system, focusing on alterations in behavior, synaptic function, and plasticity, as well as the process of recovery from all these alterations

4. GENERAL METHODS

There are 5 sets of methods that have been used in the enclosed publications, each of them adapted to the specific goals of the project. Learning each of these techniques has been crucial for the accomplishment of the goals. They are briefly summarized below and can be found described in more detail in the corresponding manuscripts included in this thesis. In addition, each of the publications have additional methods and techniques that are particularly relevant for the individual project and are only described in the published manuscripts.

- 1) Immunohistochemical methods using rodent brain tissue
- 2) Immunohistochemical methods using primary cultures of rodent dissociated hippocampal neurons
- 3) Immunoprecipitation techniques to identify novel target antigens
- 4) Development of diagnostic tests
- 5) Determination of effects of antibodies in cultured neurons
- 6) Cerebroventricular infusion of patients' CSF or IgG isolated from serum
- 7) Determination of the effects of antibodies in mice, including
 - a. memory and behavior
 - b. structural changes in the target
 - c. functional alterations

4.1. Immunohistochemical methods using brain tissue

These studies are particularly relevant to first identify a novel autoantibody in the serum or CSF of patients afflicted by a specific set of symptoms of unknown etiology. Patients were selected according to criteria developed by Drs. Graus and Dalmau, published in the *Lancet Neurol* 2016.²⁴ Clinical information was provided by the treating physicians and collaborators who sent serum and CSF of patients to the laboratory of Dr. Dalmau. For tissue immunohistochemistry, we used non-perfused rat brain that after being removed from the animal is split sagittally, fixed by immersion in 4% paraformaldehyde for 1 hour at 4°C, and cryoprotected by immersion with 40% sucrose for 48 hours. The tissue is then embedded in freezing compound, snap frozen in isopentane chilled with liquid nitrogen, and cut into 7 µm sections using a cryostat. Sections of tissue are then incubated overnight with serum or CSF of the patients using the indicated dilutions, and the reactivity developed with a standard immunoperoxidase technique (avidin-biotin peroxidase) and diaminobenzidine.

4.2. Immunohistochemical methods using primary cultures of rodent dissociated hippocampal neurons

To determine whether any reactivity identified with tissue immunostaining is directed against neuronal surface antigens, we used immunolabeling of cultured live neurons. In brief hippocampus are isolated from rat embryos at embryonic development day 18 (E18), homogenized with trypsin and seeded in P35 plates with poly-L-lysine coated coverslips. Neurons are cultured in neurobasal medium for 15-21 DIV at 37°C, 5% CO₂, 95% humidity,

incubated with serum or CSF for 1 hour, fixed with 4% paraformaldehyd, developed with a fluorescent secondary antibody and observed under a fluorescent microscope.

4.3. Immunoprecipitation techniques to identify novel target antigens

Once we have identified in the serum or CSF of patients a novel autoantibody reacting with the cell-surface of neurons, the next step is to characterize the target antigen with immunoprecipitation techniques. For this we use live cultured neurons exposed to patients' serum or CSF for 2 hours. After washing the neurons to remove non-relevant proteins or IgG, the neurons are lysed with lysis buffer for 1 hour, collected and mechanically homogenized and centrifugated. Supernatants are then exposed to A/G protein beads in order to capture human IgG bound to neuronal proteins. After 2 hours, beads are washed, diluted in rotload® loading buffer and boiled to dissolve disulfide protein bonds. Proteins are separated using 10-12% polyacrylamide gel. Gels are then stained with Coomassie blue, and protein bands seen in the study sample that are not present in the immunoprecipitation of a control serum are sequenced with mass spectrometry in the proteomics facility.

4.4. Development of diagnostic tests

After the identity of the neuronal cell-surface antigen is revealed by mass spectrometry, we commercially purchase the corresponding plasmid and develop a diagnostic test to facilitate the diagnosis of the disease in other patients with similar symptoms. The test is based on HEK293 cells transfected with the plasmid and used to immunocytochemically detect the reactivity of patients' antibodies (CBA). Depending on the type of antigen identified, the CBA may require auxiliary proteins or subunits to better express it on the cell-surface, keeping the appropriate conformation for patients' antibody reactivity (e.g., co-transfection of GluN1 and GluN2B of the NMDAR for determination of antibodies against GluN1; or co-transfection of LGI1 and ADAM23 for determination of LGI1 autoantibodies). In brief, HEK293 cells are seeded in plates containing poly-D-lysine coated coverslips, and 24 hours later, when the confluency is approximately 80%, cells are transfected with lipofectamine with the appropriate plasmid. Twenty-four hours after transfection, cells are incubated with patients' serum or CSF either before (live CBA) or after (fixed CBA) fixation with 4% paraformaldehyde. A commercial antibody against a different epitope of the antigen is used as control for the transfection. The reactivity of patients' and commercial antibodies is then developed with the appropriate secondary antibodies (e.g., fluorescein labeled anti-human IgG, or rhodamine labeled anti-mouse [commercial] IgG) and observed under a fluorescent microscope.

4.5. Determination of the effect of patients' antibodies in cultured neurons

For the current project, the potential effect of patients' antibodies on cultured neurons was assessed measuring the alteration of the levels of the target antigen at synaptic and extrasynaptic sites, using confocal microscopy. In brief, neurons were isolated and cultured as described above. Depending on the type of study, neurons at different stage of maturation

were exposed to patients' CSF, serum or purified IgG for several hours to days. The effect of patients' antibodies on specific receptors or synaptic proteins was then assessed with commercially available biomarkers against the receptor or protein of interest and quantified with confocal microscopy (Zeiss LSM710) using software Imaris (Bitplane).

4.6. Cerebroventricular infusion patients' antibodies to mice

To determine the behavioral and synaptic effects of patients' antibodies, we have developed a model of passive transfer of patients CSF or IgG to the cerebroventricular system of mice (**Figure 13**). In brief, intraventricular bilateral catheters connected to two osmotic minipumps each containing 100 μ l of patients' CSF or purified IgG are used to infuse patients' antibodies for 14 days at a constant flow rate of 0.25 ml/h.

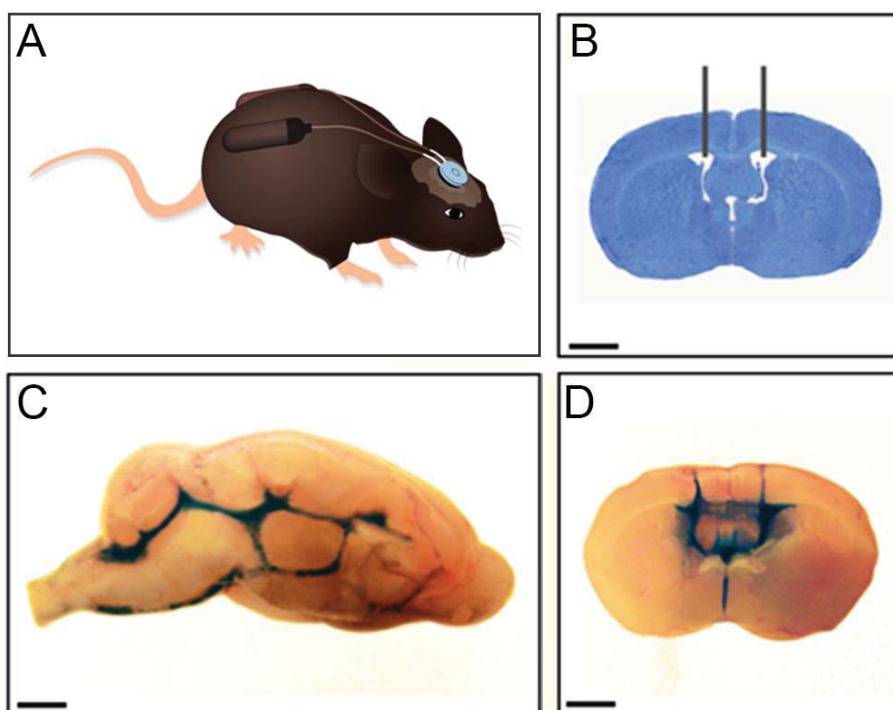


Figure 13. Cerebroventricular infusion patients' antibodies to mice

(A) Schematic representation of mice implanted with intraventricular catheters connected to osmotic minipumps subcutaneously placed on the back of the mice. (B) Representative coronal mouse brain section with catheter placement. (C and D) Coronal and sagittal mouse brain sections demonstrating cerebroventricular diffusion of methylene blue after ventricular infusion. Scale bar in B, C and D =2mm. Adapted from ¹⁶⁸

4.7. Determination of the pathogenic effects of the antibodies in mice

During and after the cerebroventricular infusion of patients' antibodies into mice, these were subjected to a battery of memory and behavioral tests, summarized in **table 4** (described in detail in ¹⁶⁸).

Table 4. Behavioral tests used for the study of the pathogenicity of antibodies

Test	Assessment	Basis
Novel object recognition open field (NOR Open field)	Memory	Animals tend to spend more time exploring a novel than a familiar object
Novel object recognition V-maze (NOR V-maze)		
Tail suspension test (TST)	Depressive-like behaviors	The animal will try to escape from an aversive stimulus such as an inescapable situation
Forced swimming tests (FST)		
Anhedonia (sucrose preference test)		Healthy animals have preference for a sucrose solution
Black and white test (BW)	Anxiety	Conflict between escaping from a potentially dangerous situation and the natural tendency to explore
Elevated plus maze test (EPM)		
Resident-intruder test (RI)	Aggressiveness	When placed in a new environment, two unfamiliar mice explore each other
Horizontal and vertical activity assessment	Locomotor activity	Ability to move in all the planes

At different time points, representative sets of mice were sacrificed, and the presence of antibodies bound to tissue was assessed by experiments of elution and immunoprecipitation. In addition, the effects of antibodies were assessed with confocal microscopy including quantification of the levels of the target antigens (e.g., NMDAR, neurexin-3 α , LGI1-related proteins such as AMPAR and Kv1.1) using specific antigen and synaptic markers (e.g., VGLUT or VGAT as pre-synaptic markers, or PSD95 as post-synaptic marker). Assessment of functional effects, such as impairment of hippocampal long-term potentiation and long-term plasticity was performed in collaboration with electrophysiologists.

5. PUBLICATIONS

5.1. Paper I

Encephalitis with refractory seizures, status epilepticus, and antibodies to the GABA_A receptor: a case series, characterization of the antigen, and analysis of the effects of the antibodies

Mar Petit-Pedrol*, Thaís Armangue*, Xiaoyu Peng*, Luis Bataller, Tania Cellucci, Rebecca Davis, Lindsey McCracken, Eugenia Martinez-Hernandez, Warren P. Mason, Michael C. Kruer, David G. Ritacco, Wolfgang Grisold, Brandon F. Meaney, Carmen Alcalá, Peter Sillevs-Smitt, Maarten J Titulaer, Rita Balice-Gordon, Francesc Graus, and Josep Dalmau

*These authors contributed equally

Lancet Neurol. 2014;13(3):276-86

Impact Factor JCR 2014 (percentile): 21.896 (D1)

Highlighted with an editorial



Encephalitis with refractory seizures, status epilepticus, and antibodies to the GABA_A receptor: a case series, characterisation of the antigen, and analysis of the effects of antibodies

Mar Petit-Pedrol*, Thaïs Armangue*, Xiaoyu Peng*, Luis Bataller, Tania Cellucci, Rebecca Davis, Lindsey McCracken, Eugenia Martinez-Hernandez, Warren P Mason, Michael C Krueer, David G Ritacco, Wolfgang Grisold, Brandon F Meaney, Carmen Alcalá, Peter Sillevs-Smitt, Maarten J Titulaer, Rita Balice-Gordon, Francesc Graus, Josep Dalmau

Summary

Background Increasing evidence suggests that seizures and status epilepticus can be immune-mediated. We aimed to describe the clinical features of a new epileptic disorder, and to establish the target antigen and the effects of patients' antibodies on neuronal cultures.

Methods In this observational study, we selected serum and CSF samples for antigen characterisation from 140 patients with encephalitis, seizures or status epilepticus, and antibodies to unknown neuropil antigens. The samples were obtained from worldwide referrals of patients with disorders suspected to be autoimmune between April 28, 2006, and April 25, 2013. We used samples from 75 healthy individuals and 416 patients with a range of neurological diseases as controls. We assessed the samples using immunoprecipitation, mass spectrometry, cell-based assay, and analysis of antibody effects in cultured rat hippocampal neurons with confocal microscopy.

Findings Neuronal cell-membrane immunoprecipitation with serum of two index patients revealed GABA_A receptor sequences. Cell-based assay with HEK293 expressing $\alpha 1/\beta 3$ subunits of the GABA_A receptor showed high titre serum antibodies (>1:160) and CSF antibodies in six patients. All six patients (age 3–63 years, median 22 years; five male patients) developed refractory status epilepticus or epilepsy partialis continua along with extensive cortical-subcortical MRI abnormalities; four patients needed pharmacologically induced coma. 12 of 416 control patients with other diseases, but none of the healthy controls, had low-titre GABA_A receptor antibodies detectable in only serum samples, five of them also had GAD-65 antibodies. These 12 patients (age 2–74 years, median 26.5 years; seven male patients) developed a broader spectrum of symptoms probably indicative of coexisting autoimmune disorders: six had encephalitis with seizures (one with status epilepticus needing pharmacologically induced coma; one with epilepsy partialis continua), four had stiff-person syndrome (one with seizures and limbic involvement), and two had opsoclonus-myoclonus. Overall, 12 of 15 patients for whom treatment and outcome were assessable had full (three patients) or partial (nine patients) response to immunotherapy or symptomatic treatment, and three died. Patients' antibodies caused a selective reduction of GABA_A receptor clusters at synapses, but not along dendrites, without altering NMDA receptors and gephyrin (a protein that anchors the GABA_A receptor).

Interpretation High titres of serum and CSF GABA_A receptor antibodies are associated with a severe form of encephalitis with seizures, refractory status epilepticus, or both. The antibodies cause a selective reduction of synaptic GABA_A receptors. The disorder often occurs with GABAergic and other coexisting autoimmune disorders and is potentially treatable.

Funding The National Institutes of Health, the McKnight Neuroscience of Brain Disorders, the Fondo de Investigaciones Sanitarias, Fundació la Marató de TV3, the Netherlands Organisation for Scientific Research (Veni-incentive), the Dutch Epilepsy Foundation.

Introduction

Seizures and status epilepticus can result from immunological responses to excitatory or inhibitory synaptic receptors or associated cell-surface proteins.^{1–3} These include the N-methyl-D-aspartate receptor (NMDAR),⁴ the alpha-amino-3-hydroxy-5-methyl-4-isoxazolepropionic acid receptor (AMPA),⁵ the gamma-aminobutyric acid-B receptor (GABA_BR),⁶ leucine-rich glioma inactivated protein 1 (LGI1),⁷ contactin-associated protein-like 2 (Caspr2),^{8,9} dipeptidyl-peptidase-like protein-6 (DPPX),¹⁰ and the metabotropic glutamate receptor 5 (mGluR5).¹¹

The seizures that accompany any of these disorders are often refractory to antiepileptic treatment unless the immune mechanism is identified and treated.^{6,12,13} In some patients, generalised seizures or status epilepticus can be the first manifestation of the disease, with patients needing heavy sedation or induced pharmacological coma.^{6,14–16} These treatments might conceal other symptoms such as dyskinesias or psychiatric alterations, delaying the recognition of the syndrome. Hitherto, the main epilepsy-related inhibitory receptor known to be a target of autoimmunity was the GABA_AR.^{9,16,17} Most

Lancet Neurol 2014

Published Online
January 22, 2014
[http://dx.doi.org/10.1016/S1474-4422\(13\)70299-0](http://dx.doi.org/10.1016/S1474-4422(13)70299-0)

See Online/Comment
[http://dx.doi.org/10.1016/S1474-4422\(14\)70013-4](http://dx.doi.org/10.1016/S1474-4422(14)70013-4)

*These authors contributed equally

August Pi i Sunyer Biomedical Research Institute (IDIBAPS), Barcelona, Spain (M Petit-Pedrol BS, T Armangue MD, E Martinez-Hernandez MD, Prof F Graus MD, Prof J Dalmau MD); Department of Pediatric Neurology, Hospital Materno-Infantil Vall d'Hebron, Universitat Autònoma de Barcelona, Barcelona, Spain (T Armangue); Department of Neuroscience, Perelman School of Medicine, University of Pennsylvania, Philadelphia, PA, USA (X Peng PhD, Prof R Balice-Gordon PhD); Service of Neurology, University Hospital Politècnic La Fe, Valencia, Spain (L Bataller MD, C Alcalá MD); Division of Rheumatology, Department of Pediatrics, McMaster University, Hamilton, Ontario, Canada (T Cellucci MD); Department of Neurology, University of Pennsylvania, Philadelphia, PA, USA (R Davis BA, L McCracken MPH, Prof J Dalmau); Department of Medicine, Princess Margaret Cancer Center and University of Toronto, Toronto, Canada (W P Mason MD); Sanford Children's Health Research Center, Sanford Children's Specialty Clinic, Sioux Falls, SD, USA (M C Krueer MD); Division of Pediatric Neurology, Lurie Children's Hospital, Chicago, USA (D G Ritacco MD); Service of

Neurology, Ludwig Boltzmann Institute of Neurooncology, Vienna, Austria (Prof W Grisold MD); Division of Neurology, Department of Pediatrics, McMaster University, Hamilton, Ontario, Canada (B F Meaney MD); Department of Neurology, Erasmus Medical Center, Rotterdam, Netherlands (Prof P Sillevius-Smitt MD, M J Titulaer MD); Hospital Clinic, University of Barcelona, Barcelona, Spain (M Petit-Pedrol, T Armangué, Prof F Graus, Prof J Dalmau); and Catalan Institution for Research and Advanced Studies (ICREA), Barcelona, Spain (Prof J Dalmau)

Correspondence to: Prof Josep Dalmau, IDIBAPS-Hospital Clínic, Universitat de Barcelona, Department of Neurology, c/ Villarroel 170, Barcelona, 08036, Spain jdalmau@clinic.ub.es

patients with GABA_BR antibodies develop early seizures or status epilepticus as a component of limbic encephalitis. About 50% of these patients have an underlying small-cell lung cancer, and the neurological symptoms usually respond to immunotherapy and treatment of the cancer.^{9,16,17} Although the GABA_BR belongs to the category of metabotropic G protein-coupled receptors, the GABA_A receptor (GABA_AR) is a ligand-gated ion channel that modulates most of the fast inhibitory synaptic transmission in the brain and has not been previously recognised as a target of autoimmunity.

The identification of the above-mentioned disorders, all potentially treatable with immunotherapy,¹⁻¹¹ has enhanced awareness of autoimmune mechanisms in patients with encephalitis associated with refractory seizures or status epilepticus, leading to an increased recognition of cases in which the antigens are unknown. Some patients might have several autoantibodies, suggesting that they have a propensity to autoimmunity, but also leading investigators to attribute the disorder to intracellular antigens that are not accessible to circulating antibodies, such as thyroid peroxidase or glutamic acid decarboxylase 65 (GAD65),^{5,6} and therefore of questionable pathogenic significance. In such patients, other more relevant, yet unknown cell-surface antigens can be overlooked, as occurred in previously reported patients who were eventually shown to have AMPAR or GABA_BR antibodies.^{5,6} We aimed to establish the identity of a novel synaptic antigen in a subset of patients with encephalitis and refractory seizures or status epilepticus. We report the clinical features of this new syndrome, the identity of the antigen, and the effects of patients' antibodies on neuronal cultures.

Methods

Study design and participants

Between Aug 20, 2012, and Dec 10, 2012, we identified two patients with encephalitis, refractory seizures, and serum and CSF antibodies with a similar pattern of reactivity against the neuropil of rat brain (appendix). The severity of the symptoms and unknown identity of the antigen prompted us to immunoprecipitate the antigen and to retrospectively review clinical and immunological information from patients with similar symptoms. We assessed serum and CSF samples, collected worldwide between April 28, 2006, and April 25, 2013, from 1134 patients with encephalitis and seizures that were suspected to be autoimmune. The samples had been sent to two referral centres (Department of Neurology, Hospital of the University of Pennsylvania, PA, USA, and Center of Neuroimmunology, Institut d'Investigacions Biomediques August Pi i Sunyer [IDIBAPS], Hospital Clínic, University of Barcelona, Barcelona, Spain) for confirmation of the presence of cell-surface antibodies or investigation for novel antibodies after standard laboratory studies were negative. Serum and CSF samples were kept frozen at -80° C. For all patients, we obtained clinical information using a questionnaire completed by

the treating physicians when the samples were sent to our centres. The treating physician also did subsequent clinical follow-up via email or phone.

Of these 1134 patients, 356 (44%) had antibodies that reacted with known cell-surface or synaptic antigens such as NMDAR, AMPAR, and LGI1, and 140 (including the two index patients) had the triad of encephalitis, seizures, and antibodies against unknown rat brain neuropil antigens. In all instances, the assessment of antibodies to brain neuropil antigens was done independently by two investigators (FG and JD), with results kept in a database. We then re-examined serum and CSF samples from these 140 patients with immunohistochemistry of rat brain, cultured live neurons, and a cell-based assay to establish whether they had similar antibodies to the two index patients. We also examined serum samples from 75 otherwise healthy individuals (blood donors) and serum or CSF samples from 416 patients with a range of neurological disorders (worldwide referrals). These 416 patients with diverse disorders were re-examined for neuropil antibodies and antibodies to α 1/ β 3 subunits of the GABA_AR. They included 41 seronegative patients with encephalitis and seizures or status epilepticus, 59 with opsoclonus-myoclonus, 20 with non-inflammatory degenerative ataxia, nine with herpes-simplex-virus encephalitis, 30 with multiple sclerosis, 101 with antibodies against GAD65 (16 limbic encephalitis, 33 epilepsy, 13 ataxia, 39 stiff-person syndrome), 90 with stiff-person syndrome without GAD65 antibodies, 30 with NMDAR antibodies, 19 with GABA_BR antibodies, and 17 with LGI1 antibodies. Only serum samples were available from 238 patients, and only CSF samples were available from 35 patients, with both types of samples available from 143 patients.

Partial clinical information about two patients with coexisting GABA_BR antibodies (patients 4 and 6) has been reported elsewhere.^{9,18} Our final protocol was approved by the institutional review boards of the University of Pennsylvania and the Hospital Clínic, and written informed consent was obtained from all patients or representatives.

Laboratory procedures

All laboratory techniques are described in the appendix and elsewhere.^{5,19-22} Briefly, we did immunohistochemistry on rodent brain, immunocytochemistry of rodent neuronal cultures, immunoprecipitation, mass spectrometry, immunoabsorption and immune-competition studies, immunocytochemistry on live or fixed HEK293 cells (cell-based assays), quantitative analysis of neuronal GABA_AR immunoreactivity of patients' antibodies, and analysis of the effects of these antibodies on GABA_AR using confocal microscopy.

Role of the funding source

The study sponsors had no role in the study design, data collection, data analysis, data interpretation, or writing of

See Online for appendix

the report. The corresponding author had full access to all the data in the study and had final responsibility for the decision to submit for publication.

Results

On immunohistochemistry with rat brain, the serum and CSF samples of the two index patients produced a similar and intense pattern of neuropil reactivity (figure 1, appendix). This neuropil reactivity resembled that reported for GABA_BR antibodies (figure 1, appendix),⁶ but specific testing for these antibodies with a cell-based assay was negative in both index patients (data not shown). Findings from a subsequent assessment with cultured live rodent hippocampal neurons showed that the novel antigen was on the cell surface (figure 1). Immunoprecipitation of neuronal proteins reacting with antibodies from the two index patients, followed by electrophoretic protein separation and EZBlue gel staining, did not produce any specific band compared with serum samples from individuals in the healthy control group (data not shown). Mass spectrometry of all separated proteins showed that serum samples from the two index patients but not from otherwise healthy control individuals had precipitated protein fragments containing sequences of the $\beta 3$ subunit of the GABA_AR (sequences shown in appendix).

Because the $\beta 3$ subunit of the GABA_AR forms complexes with the $\alpha 1$ subunit, we tested the reactivity of patients' antibodies with HEK293 cells transfected with the human $\alpha 1$ or $\beta 3$ subunits or both. This cell-based assay identified GABA_AR antibodies in six patients, including four of the 140 patients with encephalitis, seizures or status epilepticus, and antibodies to unknown neuropil antigens, and two of the 19 patients with GABA_BR antibodies. All six patients' serum and CSF samples reacted with cells coexpressing $\alpha 1$ and $\beta 3$ subunits, but when the subunits were individually assessed, four patients' samples reacted with both the $\alpha 1$ and $\beta 3$ subunit, one patient's sample reacted with only the $\alpha 1$ subunit, and another patient's sample reacted with only the coexpression of $\alpha 1$ and $\beta 3$ subunits. For this reason, we subsequently used $\alpha 1$ and $\beta 3$ heteromers to assess antibody titres. To optimise the cell-based assay, we compared the sensitivity of the assay with live or fixed and permeabilised $\alpha 1/\beta 3$ receptor-expressing HEK293 cells (live cell-based assay vs fixed cell-based assay). These studies showed that all patients' CSF antibodies were detectable with either live or fixed cell-based assay, but serum antibodies were mostly visible with live cell-based assay (figure 2).

Immunocompetition assays with serum antibodies of the six patients showed that all recognised the same epitopes of the GABA_AR (appendix). Immunoabsorption of a representative serum sample with HEK293 cells expressing the $\alpha 1/\beta 3$ subunits resulted in abrogation of reactivity in rat brain and culture neurons, further confirming the reactivity with the GABA_AR (figure 3).

Using live cell-based assay in cells coexpressing $\alpha 1/\beta 3$, we identified two clinical-immunological groups of patients: the first comprised the six patients with GABA_AR antibodies identified from the cohort of 140 patients with encephalitis and unknown neuropil antigens and from the group of 19 patients with GABA_BR antibodies; all six patients had a high titre (>1:160) of serum (when available) and CSF GABA_AR antibodies (patients 1–6; table. The second group consisted of 12 patients from the disease control groups, but not from the group of healthy individuals. In these 12 patients, the serum antibody titre was always 1:160 or lower; CSF samples were available from three individuals (patients 7, 12, and 18) and all three were negative. Moreover, whereas in patients in the first group the antibodies were detectable with three techniques (immunohistochemistry with rat brain, cultured neurons, and live or fixed cell-based assay), in patients of the second group the antibodies were detectable only with live cell-based assay

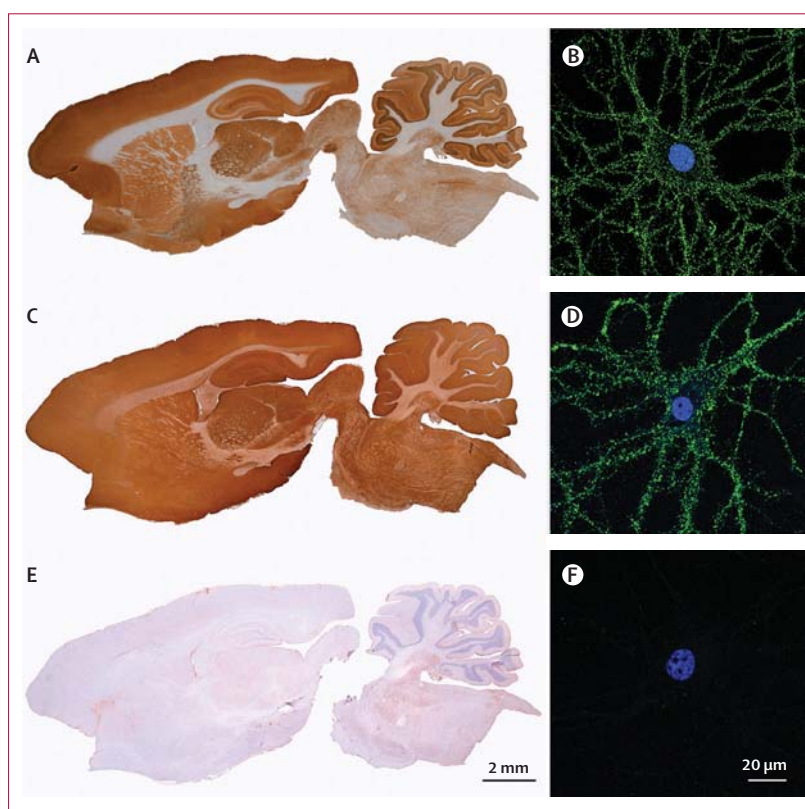


Figure 1: Reactivity with brain tissue and neuron cultures of the CSF of patients with GABA_AR or GABA_BR antibodies

The CSF of patient 2 showed extensive and diffuse immunostaining of the neuropil of cortical and cerebellar regions (A; see the appendix for higher magnifications of selected brain regions). This pattern of brain and cerebellar staining is similar to that produced by the CSF of a patient with GABA_BR antibodies (C). However, patient 2 was negative for GABA_BR antibodies in a specific cell-based assay (data not shown). These findings suggested the presence of antibodies against a novel neuronal cell-surface antigen, which was confirmed in cultures of live rat hippocampal neurons (B). The CSF of the patient with GABA_BR antibodies also reacted with the neuronal cell surface, as expected (D). E and F show a similar study using CSF of a control patient without neuronal cell-surface antibodies. In B, D, and F the nucleus of the neurons was counterstained with DAPI. In A, C, and E the tissue was counterstained with haematoxylin.

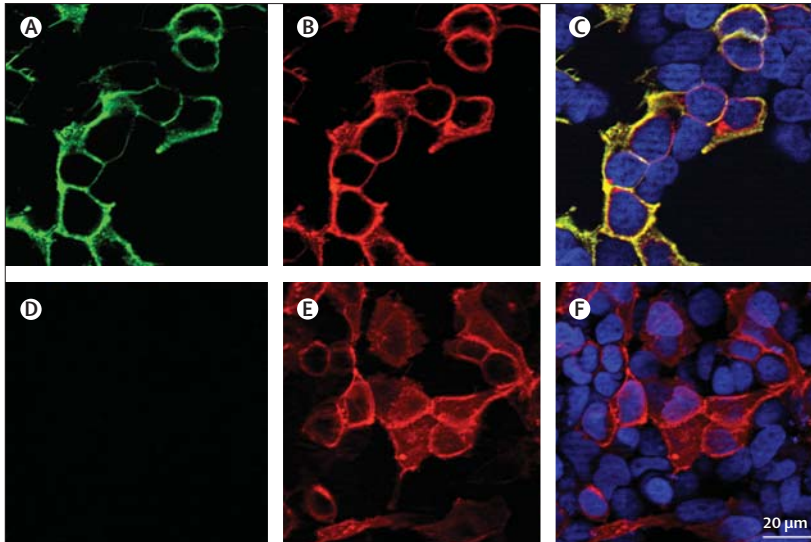


Figure 2: Reactivity of a patient's serum with live HEK293 cells expressing GABA_AR
 Reactivity of live HEK293 cells expressing human $\alpha 1/\beta 3$ subunits of the GABA_AR with a patient's serum (A) and a monoclonal antibody against the $\alpha 1$ subunit (B). Merged reactivities (C). A similar assay with serum from a control individual is shown in (D–F). The nuclei of the cells are shown with DAPI in C and F. Note the specific reactivity of patient's antibodies with cells expressing GABA_AR and the co-localisation with the reactivity of the commercial antibody.

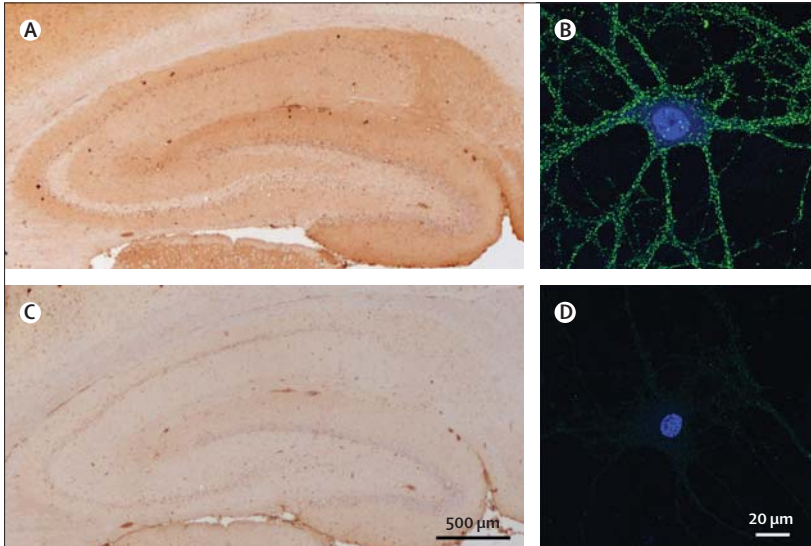


Figure 3: Abrogation of serum antibody reactivity with brain and cultures of neurons after GABA_AR immunoabsorption
 Panels A and B show the reactivity of a patient's serum after immunoabsorption with non-transfected HEK293 cells. C and D show that this reactivity is abolished after the serum has been immunoabsorbed with HEK293 cells expressing the $\alpha 1/\beta 3$ subunits of the GABA_AR.

(all individuals) and cultured live neurons (patients 7–13).

Five of the six patients with high concentrations of GABA_AR antibodies in serum and CSF samples were male; three were children and three were adults (age range 3–63 years). All developed a rapidly progressive encephalopathy that eventually resulted in refractory seizures, five of the six had status epilepticus and one of them (patient 2) also had epilepsy partialis continua

(table). In all six patients, epileptic symptoms were preceded or associated with a change in behaviour or level of cognition. A 3-year-old child (patient 4), who also had GABA_AR antibodies, developed seizures along with confusion, opsoclonus, ataxia, and chorea. Another patient (patient 5) developed a progressive hemiparesis before seizures. One patient had normal CSF white-cell count and protein concentration and the other five had at least one abnormality, including pleocytosis in four of six patients, increased protein concentration in four of six patients, and oligoclonal bands in two of six patients (patients 2 and 6 in the table). All six patients had abnormal brain MRI, often showing extensive abnormalities on FLAIR and T2 imaging, with multifocal or diffuse cortical involvement without contrast enhancement (figures 4 and 5); one patient had involvement of the basal ganglia. The EEG showed seizures in all patients, two of whom had periodic generalised discharges (appendix). In addition to GABA_AR antibodies, three patients had thyroid peroxidase antibodies, one had GAD65 antibodies, and two had GABA_BR antibodies. Other findings suggestive of a propensity to autoimmunity or immune dysregulation included a past history of Hodgkin's lymphoma in one patient, and idiopathic thrombocytopenic purpura in another.

Treatment and follow-up were assessable in all six patients: one child received levetiracetam without immunotherapy and had substantial recovery, although 3 years after symptom onset he still requires antiepileptic treatment to avoid seizure recurrence. The other five received immunotherapy and multiple antiepileptic drugs, and four patients needed a pharmacologically induced coma. Three of these patients had total or partial recovery and two died as a result of sepsis during status epilepticus. One death was a child (patient 4) with concomitant GABA_BR antibodies indicated above (clinical and autopsy findings have been reported in detail elsewhere;¹⁸ the GABA_AR antibodies were identified in archived serum and CSF samples). The oldest of the six patients (age 63 years) also had GABA_BR antibodies; the GABA_AR antibodies were identified in samples that had been archived for 7 years. This patient fully recovered from the encephalopathy associated with antibodies against both GABA_AR, but 7 years later developed diplopia and hemiataxia with GAD65 antibodies (without antibodies to GABA_AR) from which he fully recovered.

12 patients (age 2–74 years, median 26.5 years; seven male patients) had low serum concentrations of GABA_AR antibodies (table). Briefly, all six patients with encephalitis had seizures; one of them (patient 7; a 2-year-old boy) with refractory status epilepticus that needed a pharmacologically induced coma, and another patient (patient 8; a 41-year-old man) with epilepsy partialis continua. In the other six patients, four had stiff-person syndrome (one of them associated with seizures), and two had opsoclonus-myoclonus.

Six of the 12 patients had other neuronal antibodies in addition to GABA_AR antibodies: five had GAD65 and one had NMDAR antibodies. Additional findings suggestive of a propensity to autoimmunity or immunological dysfunction included: Hashimoto's thyroiditis with thyroid peroxidase antibodies in one patient, and type 1 diabetes mellitus in two patients. None of the patients with stiff-person syndrome had amphiphysin or glycine receptor (GlyR) antibodies. Treatment and follow-up were assessable in nine patients. Immunotherapy was used in seven patients: one had full recovery, five had partial recovery, and one died. The two patients who did not receive immunotherapy had stiff-

person syndrome that was controlled symptomatically with clonazepam or baclofen.

We did the following studies with CSF of a representative patient (index patient 1) with high titre serum and CSF antibodies reacting with only GABA_AR. The reactivity was abrogated by pre-absorption with HEK293 cells expressing GABA_AR (figure 3), and by immunocompetition assays with antibodies from the other five patients with high antibody titres, indicating that all patients' antibodies targeted the same GABA_AR epitopes (appendix). To examine the extent of recognition of GABA_AR by patients' CSF antibodies, we quantified GABA_AR immunolabelling by confocal microscopy

	Sex, age in years	Presentation and main symptoms	CSF	MRI	EEG	History of autoimmunity or cancer	Treatment	Outcome	Sample: subunit target (α1/β3 titres)
Patients with high titres of serum GABA_AR antibodies and with antibodies detectable in CSF									
1 (index patient 1)	F, 16	Memory, cognitive, and affective problems for several months. Developed headache and 9 days later tonic-clonic seizures progressing to status epilepticus	23 WBC/μL; protein 60 mg/dL	Multifocal increased T2/FLAIR signal with cortical-subcortical involvement	Generalised slowing, bilateral temporal seizures. Generalised periodic discharges	Hodgkin's lymphoma 10 months before onset of encephalitis	Anticonvulsants: LEV, TPM, MDZ, barbiturate coma. Immunosuppressants: MTP, IVIG, PEX, RTX, CPH	Progressive neurological recovery after 12 weeks in hospital. At 15-month follow-up she had returned to school with mild cognitive deficit that is improving	Serum: α1, β3 (>1/1280) CSF: α1 (>1/320)
2 (index patient 2)	M, 51	Behavioural change, depression, psychosis, and mutism for several weeks. Developed partial clonic seizures and epilepsy partialis progressing in 48 h to status epilepticus	Normal WBC and protein concentration; OCB-positive	Multifocal increased T2/FLAIR signal with extensive cortical-subcortical involvement	Right temporal ictal activity, secondary generalisation. Generalised periodic discharges	Idiopathic thrombocytopenic purpura; TPO and thyroglobulin antibodies	Anticonvulsants: LEV, DZP, LCM, PHT, MDZ, PPF, barbiturate coma. Immunosuppressants: MTP, IVIG, PEX, CPH, RTX.	After 10 weeks, status epilepticus persisted and the patient died of sepsis	Serum: α1, β3 (1/1280) CSF: α1 (1/320)
3	M, 28	Subacute presentation of behavioural and cognitive deficits followed 5 days later by complex partial seizures and status epilepticus	Normal WBC and protein concentration	Bilateral mesiotemporal high T2/FLAIR signal	Ictal activity	TPO antibodies	Anticonvulsants: PPF, MDZ, LEV, PHT, TPM, CLB, barbiturate coma. Immunosuppressants: MTP with PDN taper.	After 8 weeks in the intensive care unit he gradually returned to baseline function. At last follow-up (18 months) he was seizure free and back to work	Serum: α1, β3 (1/640) CSF: α1, β3 (1/160)
4	M, 3	Acute development of confusion, lethargy, dystonic tongue movements, chorea of limbs and trunk, opsochonus, ataxia, evolving in 24 h to complex partial seizures and status epilepticus	154 WBC/μL; protein 59 mg/dL	Multifocal high T2/FLAIR signal in brainstem and cerebellum with involvement of basal ganglia and hippocampi	Generalised slowing and bioccipital ictal activity	GABA _A R antibodies in serum and CSF	Anticonvulsants: multiple, barbiturate coma. Decompressive posterior craniectomy due to cerebral oedema. Immunosuppressants: MTP, IVIG	After 4 weeks, status epilepticus persisted and the patient died of sepsis	Serum: NA CSF: α1, β3 (1/320)
5	M, 4	Progressive right hemiparesis; 2 months later, partial seizures progressing to status epilepticus	Increased WBC and protein concentration	Abnormal FLAIR changes suggesting encephalitis	Generalised slowing and ictal activity	No	Anticonvulsants: LEV. Immunosuppressants: No	Substantial recovery but, 2.5 years after symptom onset, still requires antiepileptics to prevent seizures.	Serum: α1 (1/320) CSF: α1/β3 (1/40)
6	M, 63	Subacute memory problems, gustatory and olfactory hallucinations, facial cramps, psychomotor agitation, tinnitus	75 WBC/μL; increased protein concentration; OCB-positive	Right temporal cortex high T2/FLAIR signal	Frontotemporal ictal activity	GABA _A R, GAD65, TPO and thyroglobulin antibodies	Anticonvulsants: VPA, LEV, barbiturate. Immunosuppressants: PDN	Full recovery. 7 years later: diplopia and hemiataxia that spontaneously resolved (positive GAD65 but negative GABA _A R and GABA _B R antibodies)	Serum: NA CSF: α1/β3 (1/20)

(Table continues on next page)

(Continued from previous page)

Patients with low titres of serum GABA_AR antibodies and without antibodies detectable in CSF

	Sex, age in years	Presentation and main symptoms	CSF	MRI	EEG	History of autoimmunity or cancer	Treatment	Outcome	Sample: subunit target (α1/β3 titres)
7	M, 2	Subacute onset partial seizures; 4 months later, choreathetoid movements and status epilepticus.	Normal WBC and protein concentration	Cortical atrophy	Generalised slowing and right parietal ictal activity	No	Anticonvulsants: CBZ, VPA, MDZ, LEV, ketogenic diet, barbiturate coma. Immunosuppressants: MTP with PDN taper	Partial response, cognitive and motor skills improved. At last follow-up (2 years), partial seizures persist	Serum: β3 (1/160) CSF: negative
8	M, 41	Subacute onset generalised seizures with fever, epilepsia partialis continua, aphasia. 2 years later, status epilepticus	Normal WBC and protein concentration	Multifocal cortical-subcortical high T2/FLAIR signal in both hemispheres	Bifrontal ictal activity	GAD65 antibodies	Anticonvulsants: VPA, OXC, LEV. Immunosuppressants: MTP with PDN taper	Partial response at initial presentation. Status epilepticus responded to anticonvulsants	Serum: α1 (1/160) CSF: NA
9	F, 15	Reduced verbal output and seizures	8 WBC/μL; normal protein concentration	Bilateral fronto-temporal increased T2/FLAIR signal, leptomeningeal enhancement	Multifocal ictal activity	GAD65 antibodies	NA	NA	Serum: α1, β3 (1/160) CSF: NA
10	F, 32	Multifocal refractory seizures	Normal WBC and protein concentration	Normal	Bilateral temporal ictal activity and multifocal interictal epileptiform discharges	Type 1 diabetes mellitus, Hashimoto's thyroiditis. GAD65, TPO and thyroglobulin antibodies	Anticonvulsants: OXC, CBZ, LCM, LEV, ZNS, TPM, CLB, PHT, LTG. Immunosuppressants: IVIG, PDN, ciclosporin	After 7 years she still has uncontrolled seizures	Serum: α1/β3 (1/40) CSF: NA
11	F, 74	Subacute onset of lethargy and alternating changes in level of consciousness. Suspected temporal lobe seizures	Normal WBC and protein concentration	Normal	NA	Previous history of ovarian cancer	NA	NA	Serum: α1/β3 (1/40) CSF: NA
12	F, 16	Behavioural changes, insomnia, orofacial dyskinesia, decreased level of consciousness, brief seizure, dysautonomia	17 WBC/μL; normal protein concentration	Left temporal cortical-subcortical high T2/FLAIR signal	Generalised slowing	NMDAR antibodies in serum and CSF samples	Anticonvulsants: VPA. Immunosuppressants: MTP, IVIG, PEX, RTX	Full recovery, gradual improvement over many months	Serum: α1/β3 (1/20) CSF: negative
13	M, 19	Stiff-person syndrome since age 14 years	Normal WBC; protein 85 mg/dL	Not done	Not done	Type 1 diabetes mellitus. GAD65 antibodies	Clonazepam, baclofen. Immunosuppressants: No	Marked improvement. At last follow-up (16 years) he is independent for all daily life activities	Serum: α1/β3 (1/40) CSF: NA
14	M, 12	Stiff-person syndrome since age 5 years; brief episodes of seizures	NA	Hippocampal high T2/FLAIR signal	Right temporal seizures, bifrontal sharp waves	GAD65 antibodies	Anticonvulsants: LEV. Immunosuppressants: IVIG, RTX	Partial improvement of stiff-person symptoms, free of seizures	Serum: α1/β3 (1/20) CSF: NA
15	M, 21	Stiff-person syndrome since age 16 years	Normal WBC and protein concentration	Normal	Normal	Antinuclear antibodies; anti-endomysial immunoglobulin A	Anticonvulsants: CBZ, OXC. Immunosuppressants: IVIG	Partial improvement	Serum: α1/β3 (1/20) CSF: NA
16	M, 46	Stiff-limb syndrome	Not done	Not done	Not done	No	Baclofen. Immunosuppressants: No	Substantial improvement	Serum: α1/β3 (1/20) CSF: NA
17	F, 34	Opsoclonus-myoclonus syndrome	NA	Normal	Not done	No	NA	NA	Serum: α1/β3 (1/40) CSF: NA
18	M, 65	Opsoclonus-myoclonus syndrome	Normal WBC and protein concentration	Normal	Not done	Antinuclear antibodies	Immunosuppressants: MTP	No response, died few months after onset	Serum: α1/β3 (1/20) CSF: negative

CBZ=carbamazepine. CLB=clobazam. CPH=cyclophosphamide. DZP=diazepam. F=female. GABA_AR=gamma-aminobutyric acid receptor. GAD65=glutamic acid decarboxylase 65. IVIG=intravenous immunoglobulin. LCM=lacosamide. LEV=levetiracetam. LTG=lamotrigine. M=male. MDZ=midazolam. MTP=intravenous methylprednisolone. NA=not available. NMDAR=N-methyl-D-aspartate receptor. OCB=oligoclonal bands. OXC=oxcarbazepine. PDN=oral prednisone. PEX=plasma exchange. PHT=phenytoin. PPF=propofol. RTX=rituximab. TPM=topiramate. TPO=thyroid peroxidase. VPA=valproate. WBC=white blood cell count. ZNS=zonisamide.

Table: Clinical characteristics of patients with GABA_AR antibodies in serum and CSF samples

(figure 6). These results showed that 89% of patient's antibodies labelled GABA_AR-containing clusters (figure 6). To examine the effects of the antibodies on inhibitory synapses containing GABA_AR, neurons were treated with patient's CSF antibodies or a control CSF for 48 h. These studies showed that the density of GABA_AR clusters along dendrites was not affected (figure 6), but the clusters of GABA_AR at synapses, measured as cluster density co-labelled by the presynaptic marker vGAT (vesicular GABA transporter), were substantially reduced (figure 6). This finding suggests that the antibodies in the patient's CSF, but not control CSF, removed GABA_AR from synapses. The effect was specific for GABA_AR because the cluster density of other synaptic markers such as gephyrin (figure 6) and the GluN1 subunit of the NMDAR (data not shown) were not affected.

Discussion

We report the identification of high titre serum and CSF antibodies against the GABA_AR in a subset of patients with encephalitis and refractory seizures or status epilepticus, who often needed pharmacologically induced coma. This finding is important because the disorder is potentially treatable. However, because of the rapid development of seizures and frequent presence of coexisting autoimmune disorders, recognition of the disorder might be difficult. Findings from the four following sets of experiments establish GABA_AR as a relevant autoantigen: direct immunoprecipitation of the receptor by patients' antibodies, specific immunostaining of HEK293 cells expressing $\alpha 1/\beta 3$ subunits of the receptor, competition of patients' antibodies for the same GABA_AR epitopes, and demonstration that patients' antibodies selectively remove GABA_AR from synapses without affecting NMDAR or gephyrin (a scaffold protein that anchors the receptor at post-synaptic sites).

Most fast inhibitory neurotransmission in the adult brain is mediated by ligand-gated GABA_AR.²³ These receptors are regulated by many positive (barbiturates, benzodiazepines) and negative (picrotoxin, bicuculline) allosteric modulators, providing several models of GABA_AR-antagonist induced seizures.^{24,25} The GABA_ARs are pentamers, the five subunits of which originate from eight gene families that encode different isoforms ($\alpha 1-6$, $\beta 1-3$, $\gamma 1-3$, δ , ϵ , θ , π , and $\rho 1-3$). The subunit composition of the receptor governs the intrinsic properties of the channel, such as affinity for GABA, receptor conductance, kinetics, and modulation.²⁶ These 19 subunits combine in different ways to form functional receptors, but at synaptic sites most receptors contain two α subunits ($\alpha 1-3$ isoforms), two β subunits, and a γ subunit arranged in the order $\gamma\text{-}\beta\text{-}\alpha\text{-}\beta\text{-}\alpha$. By contrast with receptors at synaptic sites, those at perisynaptic or extrasynaptic sites are mainly composed of $\alpha 4$ or $\alpha 6$ subunits combined with β and δ subunits.²⁷ The antibodies of our patients reacted with the $\alpha 1$, $\beta 3$, or both subunits (we did not assess other subunits), and when the reactivity with each subunit was

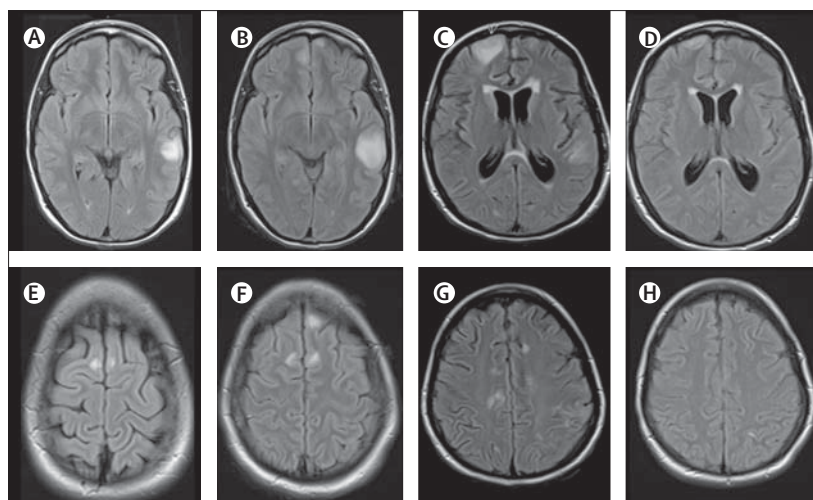


Figure 4: MRI findings in index patient 1

On day 3 of admission, the MRI of this 16-year-old girl showed multiple cortical-subcortical abnormalities with increased FLAIR and T2 signal involving the left temporal lobe and frontal parasagittal regions (A, E). On day 10, a repeat MRI showed an increase of the size of the temporal lesion and a new cortical lesion in the left frontal lobe (B, F). Repeat MRIs on days 22 and 48 did not show substantial changes (data not shown). Another MRI done 4 months after disease onset showed many new multifocal abnormalities and diffuse atrophy and increase of the size of the ventricles (C, G). A repeat MRI 2 months later, 6 months after symptom onset, showed substantial improvement and resolution of the abnormalities as well as improvement of the ventricular dilatation (D, H).

individually assessed, the $\alpha 1$ subunit was always recognised by patients' CSF. Therefore, that the main effects of patients' antibodies occurred at synaptic sites, where the $\alpha 1$ receptors are enriched, is not surprising. Indeed, using cultures of rat hippocampal neurons, patients' antibodies caused a decrease in the density of GABA_AR at synaptic sites. The total density of GABA_ARs, including synaptic and extrasynaptic receptors, was not affected, suggesting a relocation of receptors from synaptic to extrasynaptic sites. This finding contrasts with the effects of antibodies identified in other autoimmune encephalitis, such as anti-NMDAR or anti-AMPA, in which the decrease of the corresponding receptors occurs at both synaptic and extrasynaptic sites.^{5,22,28}

At least four mutations in the $\alpha 1$ subunit of the GABA_AR are associated with generalised epilepsy.²⁷ Findings from in-vitro studies have shown that each of these mutations results in a substantial loss of $\alpha 1$ -subunit function or level of expression.²⁷ Additionally, mutations of the $\beta 3$ subunit have been reported in children with absence epilepsy.²⁹ In line with these findings, in our study, all patients with high titres of serum and CSF $\alpha 1/\beta 3$ receptor antibodies developed seizures, status epilepticus, or epilepsy partialis continua. Most of these patients had an abnormal EEG with multifocal seizures and, in two cases, generalised periodic discharges. These findings were associated with extensive cortical and subcortical brain MRI abnormalities in all six patients with high serum antibody titres (all with CSF antibodies) and in three (25%) of 12 patients with low serum titres. We do not know if the MRI findings were caused by the immune

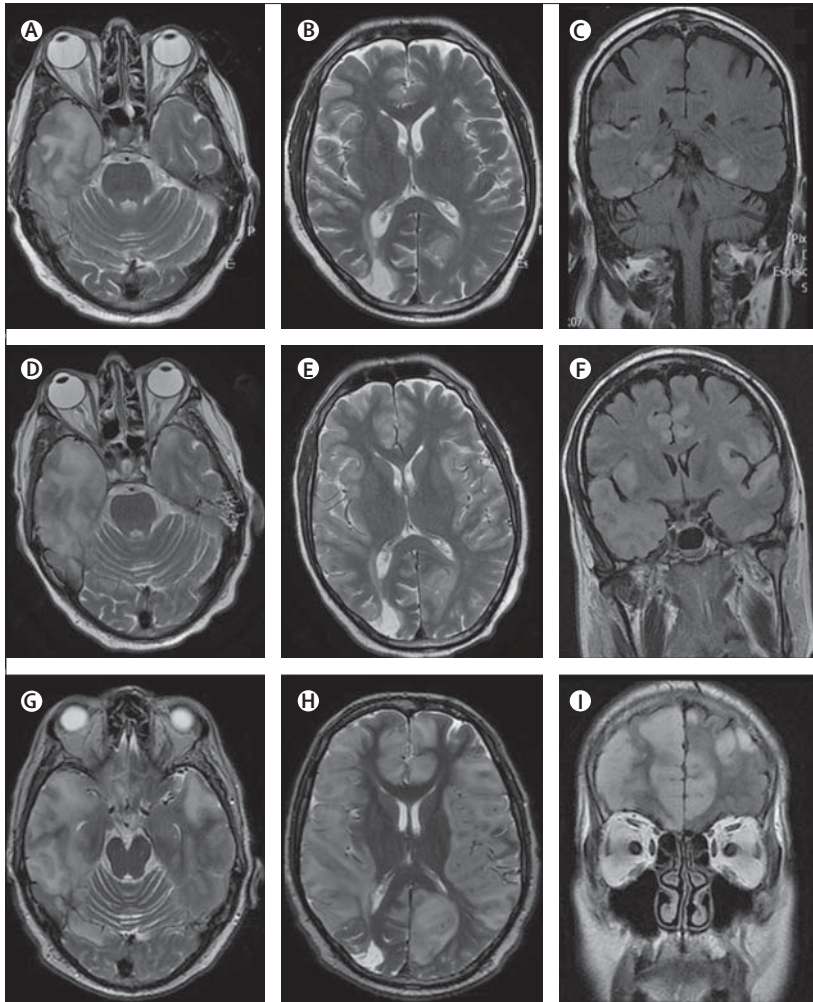


Figure 5: MRI findings in index patient

On day 2 of admission, the MRI of this patient showed multiple areas of FLAIR and T2 signal abnormality predominantly involving cortical regions (A–C), without oedema, mass effect, or contrast enhancement (data not shown), but with blurring of the grey-white matter junction. On day 14, repeated MRI showed interval increase of the cortical-subcortical involvement, with oedema in the right temporal lobe (D–F). Subsequent MRIs showed a pronounced worsening of these abnormalities now extensively involving cortical and subcortical regions (G–I).

response or resulted from the lengthy seizures. However, the multifocal and extensive brain MRI abnormalities were different from those seen in other autoimmune encephalitis, in which the MRI is often normal (NMDAR)³⁰ or shows predominant involvement of the hippocampus (AMPA, GABA_BR, LGI1).^{5,7,16} The comparison with other autoimmune encephalitis shows other differences: 39% of patients with GABA_AR antibodies are younger than 18 years, whereas most patients with other encephalitis (except anti-NMDAR) are adults.³¹ Patients with GABA_AR antibodies do not seem to frequently have an underlying tumour (similar to LGI1 autoimmunity), whereas about 30–60% of patients with other antibodies (Caspr2, GABA_BR, or AMPAR) have a tumour³² and, for patients with NMDAR antibodies, the frequency of tumours varies with age,

sex, and ethnicity.³⁰ Since the end of this study, we have identified a patient with a malignant thymoma and encephalitis, seizures, multifocal cortical FLAIR MRI abnormalities, and LGI1 and GABA_AR antibodies, suggesting that patients with thymoma and seizures should be tested for GABA_AR antibodies (data not shown).

In the group with low serum titres of antibodies and absent CSF antibodies, all patients with encephalitis developed seizures; the youngest patient, a 2-year-old child, also required pharmacologically induced coma for status epilepticus. The frequent presence of other relevant autoimmunities could explain the broader spectrum of symptoms in this group. Indeed, two of the four patients with stiff-person syndrome had coexisting GAD65 antibodies, and another patient with GABA_AR antibodies only detected in serum had high titres of NMDAR antibodies in serum and CSF samples that were responsible for most of the clinical features (anti-NMDAR encephalitis).

Findings from this and previous studies suggest that patients with encephalitis or seizures attributed to GAD65 antibodies should be examined for other relevant antibodies against cell-surface antigens, such as GABA_AR and other synaptic receptors (panel).^{6,33–35} Additionally, the increasing recognition of autoimmune encephalitis with neuronal cell-surface antibodies and concurrent thyroid peroxidase antibodies (as in four of 18 patients in this study) suggests that Hashimoto's encephalitis should be a diagnosis of exclusion—that is, the detection of thyroid peroxidase antibodies and symptom response to steroids are not sufficient criteria to establish the diagnosis of Hashimoto's encephalitis.^{9,35,36}

Evidence suggests that status epilepticus can lead to chronic epilepsy. The development of epilepsy is usually preceded by a silent period during which there is increasing hyperexcitability and a progressive decrease of synaptic GABA_AR.²⁶ This effect has been attributed in part to a disruption of the GABA_AR-anchoring protein, gephyrin.^{26,37} Additionally, lengthy seizures reduce GABA_AR inhibition, which might lead to the development of status epilepticus.³⁸ These findings and the antibody-mediated decrease of synaptic GABA_AR seen in neuronal cultures exposed to patients' antibodies suggest a model whereby the GABA_ARs are removed from synapses leading to status epilepticus, which in turn causes a further decrease of receptors along with reduced GABA_AR inhibition, resulting in a pathogenic reinforcement. This would explain the severity and refractory nature of the seizures associated with high concentrations of GABA_AR antibodies, and why this disorder seems to be more difficult to treat than the syndromes associated with NMDAR, GABA_BR, AMPAR, or LGI1 antibodies, emphasising the importance of prompt diagnosis and treatment. Despite the difficulties in treatment, 12 of 15 patients had partial or complete response to immunotherapy

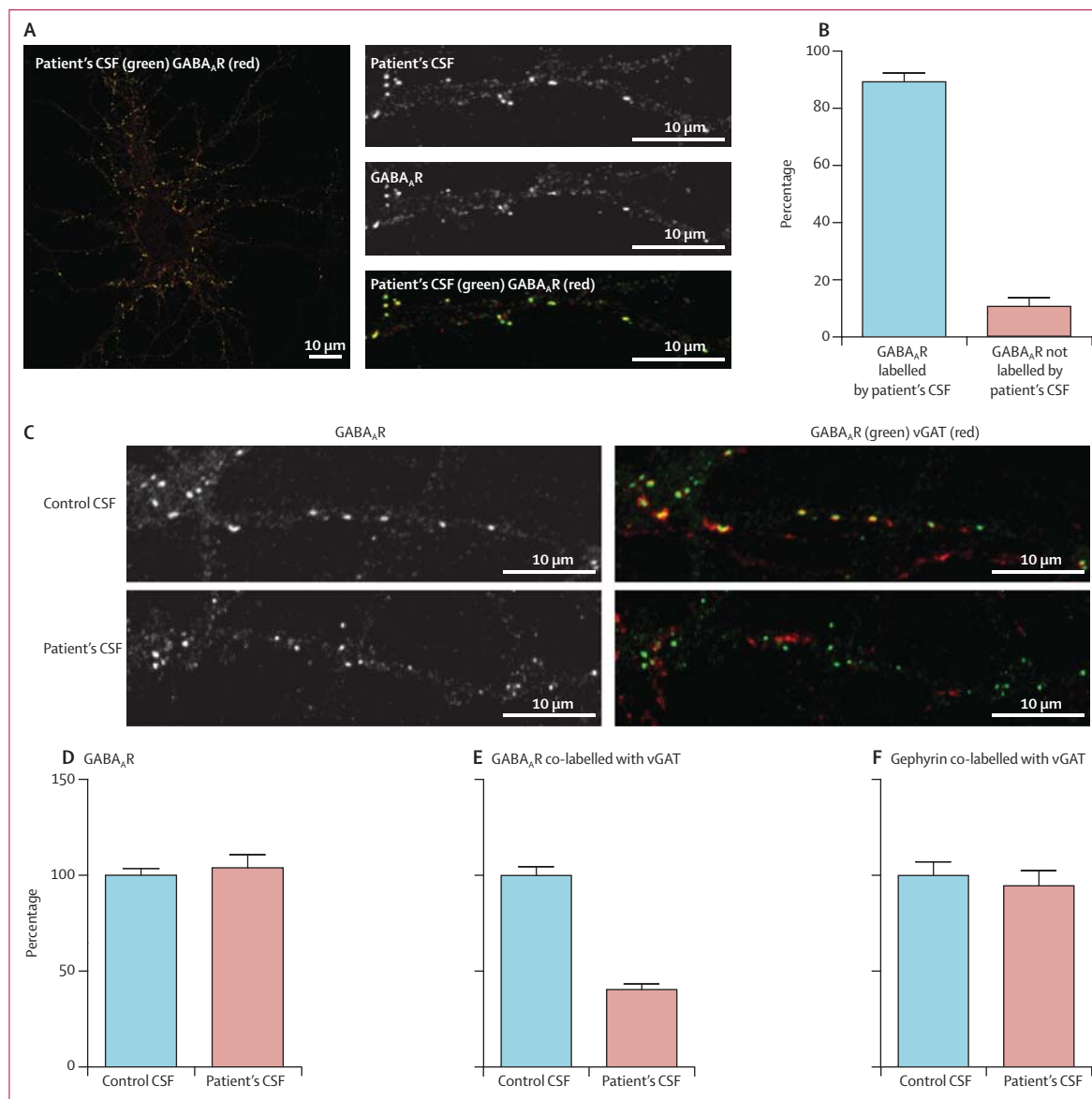


Figure 6: Effect of patient's antibodies on the density of GABA_AR clusters in cultures of hippocampal neurons

Live 14-day-in-vitro cultures of dissociated rat hippocampal neurons were stained with patient's CSF containing GABA_AR antibodies (green), then fixed and stained with commercial GABA_AR antibodies (red; A). Quantification of colocalisation between patient's CSF antibodies and the commercial GABA_AR antibody shows that 89% (SE 3%) of receptors labelled by patient's antibodies were colabelled with the commercial antibody against GABA_AR (B). In a similar assay, neurons were incubated with patient's CSF for 48 h and subsequently stained for postsynaptic GABA_AR (green) and presynaptic vesicular GABA transporter (vGAT) (red; C). The synaptic GABA_ARs (shown as yellow clusters in control conditions) were greatly reduced after treatment with patient's CSF (C). The number of GABA_AR clusters along dendrites of neurons treated with patient's CSF is not different from neurons treated with control CSF (Mann-Whitney test $p=0.6$; D). The number of GABA_ARs localised in synapses, however, decreased significantly in neurons treated with a patient's CSF compared with neurons treated with control CSF (40% [3%] compared with control as 100%; $p<0.0001$; E). Patients' CSF did not affect the clusters of post-synaptic gephyrin colabelled with presynaptic vGAT when compared with the effects of control CSF ($p=0.5$; F).

(nine patients), symptomatic therapy (three patients), and extended intensive care support (all patients with encephalitis).

Our study has several limitations, including the retrospective assessment of most patients (except the two index patients), and the absence of CSF samples from nine of the 12 patients with low serum titres of GABA_AR

antibodies. Therefore, the clinical implications of low serum antibody titres should be interpreted with caution, especially because in some patients (eg, the patients with NMDAR antibodies) other coexisting immunological mechanisms could have contributed to the patients' symptoms. Future studies should establish, in a prospective manner, the incidence of serum and CSF

Panel: Research in context**Systematic review**

We searched Medline and Embase up to Nov 1, 2013, for articles published in English with the search terms "gamma-aminobutyric acid-A receptor", "GABA_A", "GABA_B", "GABA", "receptors", "antibodies" and "encephalitis" [MeSH terms]. We restricted searches to studies in human beings. We also reviewed the reference lists of the papers identified by this search. We identified 36 papers, of which none was related to encephalitis associated with GABA_AR antibodies; of the papers identified, three were series of patients with GABA_BR antibodies, 18 were reviews of autoimmune encephalitis, 12 were original research articles, two were editorials, and one was a letter.

Interpretation

Our findings suggest that the GABA_A receptor is a novel target antigen of autoimmune encephalitis, and provides an unambiguous test for the detection of patients' antibodies in serum and CSF samples. Although we found high titres of serum and CSF GABA_AR antibodies in patients with seizures, refractory status epilepticus, or *epilepsia partialis continua*, low titre serum antibodies were associated with a wider spectrum of symptoms, probably due to the high prevalence of coexisting autoimmunities. We also show that patients' GABA_AR antibodies cause a selective decrease of the clusters of GABA_AR at synapses, but not along dendrites, without altering other post-synaptic proteins such as the NMDAR or gephyrin. These findings are important for three reasons: they define a novel form of autoimmune epileptic disorder, usually non-paraneoplastic, that affects children and adults and is severe but potentially treatable; that the severity of the seizures (often needing pharmacologically induced coma) and frequent presence of other less relevant antibodies against intracellular antigens (eg, thyroid peroxidase, GAD65) can mislead diagnosis (eg, Hashimoto's encephalitis, anti-GAD65 encephalitis or seizures); and that patients' antibodies have a direct effect on the GABA_AR receptors, which provides a useful reagent (purified patients' antibodies) to understand how selective disruption of GABA_AR leads to neuronal hyperexcitability, seizures, or status epilepticus.

GABA_AR antibodies in patients with seizures or status epilepticus, opsoclonus-myoclonus, and stiff-person syndrome with or without GAD65 autoimmunity, and whether the presence of antibodies in CSF always associates with seizures or status epilepticus.

Findings from this study have several clinical implications. The presence of GABA_AR antibodies should be tested in patients with severe seizures or status epilepticus in the context of encephalitis of unclear cause with MRI and CSF abnormalities suggestive of an inflammatory process, patients with opsoclonus-myoclonus or stiff-person syndrome, and any patients with GAD65 or thyroid peroxidase antibodies and other clinical features suggesting a propensity to autoimmunity.

In addition to the clinical implications, the identification of a disorder in which patients' antibodies specifically eliminate GABA_ARs from synapses provides a useful reagent (purified patients' antibodies) to understand how selective disruption of these receptors leads to neuronal hyperexcitability, seizures, or status epilepticus.

Contributors

M-PP, TA, and XP did the literature search, study design, data collection, data analysis, writing, and critical approval of the final paper. LB, TC, RD, LM, WM, MK, DR, WG, BM, CA, PSS, and MJT did the data collection and critical approval of the final paper. EM-H did the data collection, data analysis, interpretation, and critical approval of the paper. RBG did the data interpretation, critical approval of the final paper, and

obtained funding. FG did the data collection, data analysis, data interpretation, critical approval of the final manuscript, and obtained funding. JD did the figures, study design, data collection, data analysis, data interpretation, writing, critical approval of the final paper, and obtained funding.

Conflicts of interest

JD holds patents for the use of Ma2 and NMDAR as autoantibody tests, and has filed patents for the use of DPPX, GABA_AR, and GABA_BR as diagnostic tests. JD and PS-S receive research grant support from Euroimmun. PS-S has filed a patent for the use of DNER as diagnostic test. MJT received a travel grant for Lecturing in India from Sun Pharma, India. The rest of the authors have no conflicts of interest.

Acknowledgments

This study was supported by Instituto Carlos III (TA, FI12/00366; EMH, CM12/00055, JD, FIS PI11/01780; and FG, PI12/00611), the National Institutes of Health (JD, ROINS077851; and RB-G and JD, MH094741), Fundació la Marató TV3 (JD, 101530), the Netherlands Organisation for Scientific Research (MT), the Dutch Epilepsy Foundations (MT, project 14-19), and a ErasmusMC fellowship (MT). We thank Maria Rodés, Mercè Alba, Eva Caballero, and Esther Aguilar for excellent technical support and the patients and their families for volunteering to participate in this study. We thank Miquel Raspall-Chaure, Marcelo Malakooti, Mark Wainwright, Adam Kirton, Michael Esser, Albert Quilez-Martínez, Verónica González-Álvarez, Federico Ramos, Francesc Xavier Sanmartí, Jordi Bruna, Jong Woo Lee, Stacy A Rudnicki, and Alma R Bicknese for providing patients' samples and clinical information.

References

- Dalmau J. Status epilepticus due to paraneoplastic and nonparaneoplastic encephalitis. *Epilepsia* 2009; **50** (suppl 12): 58–60.
- Wong-Kisiel LC, McKeon A, Wirrell EC. Autoimmune encephalopathies and epilepsies in children and teenagers. *Can J Neurol Sci* 2012; **39**: 134–44.
- Quek AM, Britton JW, McKeon A, et al. Autoimmune epilepsy: clinical characteristics and response to immunotherapy. *Arch Neurol* 2012; **69**: 582–93.
- Dalmau J, Tuzun E, Wu HY, et al. Paraneoplastic anti-N-methyl-D-aspartate receptor encephalitis associated with ovarian teratoma. *Ann Neurol* 2007; **61**: 25–36.
- Lai M, Hughes EG, Peng X, et al. AMPA receptor antibodies in limbic encephalitis alter synaptic receptor location. *Ann Neurol* 2009; **65**: 424–34.
- Lancaster E, Lai M, Peng X, et al. Antibodies to the GABA(B) receptor in limbic encephalitis with seizures: case series and characterisation of the antigen. *Lancet Neurol* 2010; **9**: 67–76.
- Lai M, Huijbers MG, Lancaster E, et al. Investigation of LGI1 as the antigen in limbic encephalitis previously attributed to potassium channels: a case series. *Lancet Neurol* 2010; **9**: 776–85.
- Irani SR, Alexander S, Waters P, et al. Antibodies to Kv1 potassium channel-complex proteins leucine-rich, glioma inactivated 1 protein and contactin-associated protein-2 in limbic encephalitis, Morvan's syndrome and acquired neuromyotonia. *Brain* 2010; **133**: 2734–48.
- Lancaster E, Huijbers MG, Bar V, et al. Investigations of caspr2, an autoantigen of encephalitis and neuromyotonia. *Ann Neurol* 2011; **69**: 303–11.
- Boronat A, Gelfand JM, Gresa-Arribas N, et al. Encephalitis and antibodies to dipeptidyl-peptidase-like protein-6, a subunit of Kv4.2 potassium channels. *Ann Neurol* 2013; **73**: 120–28.
- Lancaster E, Martínez-Hernández E, Titulaer MJ, et al. Antibodies to metabotropic glutamate receptor 5 in the Ophelia syndrome. *Neurology* 2011; **77**: 1698–701.
- Andrade DM, Tai P, Dalmau J, Wennberg R. Tonic seizures: a diagnostic clue of anti-LGI1 encephalitis? *Neurology* 2011; **76**: 1355–57.
- Irani SR, Michell AW, Lang B, et al. Faciobrachial dystonic seizures precede Lgi1 antibody limbic encephalitis. *Ann Neurol* 2011; **69**: 892–900.
- Johnson N, Henry C, Fessler AJ, Dalmau J. Anti-NMDA receptor encephalitis causing prolonged nonconvulsive status epilepticus. *Neurology* 2010; **75**: 1480–82.

- 15 Bayreuther C, Bourg V, Dellamonica J, Borg M, Bernardin G, Thomas P. Complex partial status epilepticus revealing anti-NMDA receptor encephalitis. *Epileptic Disord* 2009; **11**: 261–65.
- 16 Höftberger R, Titulaer MJ, Sabater L, et al. Encephalitis and GABA(B) receptor antibodies: Novel findings in a new case series of 20 patients. *Neurology* 2013; **81**: 1500–06.
- 17 Jeffery OJ, Lennon VA, Pittock SJ, Gregory JK, Britton JW, McKeon A. GABAB receptor autoantibody frequency in service serologic evaluation. *Neurology* 2013; **81**: 882–87.
- 18 Krüer MC, Lim KY, Hoffberger R, Svoboda MD, Woltjer RL, Dalmau J. Aggressive course in encephalitis with opsoclonus, ataxia, chorea, and seizures. *JAMA Neurol* (in press).
- 19 Ances BM, Vitaliani R, Taylor RA, et al. Treatment-responsive limbic encephalitis identified by neuropil antibodies: MRI and PET correlates. *Brain* 2005; **128**: 1764–77.
- 20 Buchhalter JR, Dichter MA. Electrophysiological comparison of pyramidal and stellate nonpyramidal neurons in dissociated cell culture of rat hippocampus. *Brain Res Bull* 1991; **26**: 333–38.
- 21 Dalmau J, Gleichman AJ, Hughes EG, et al. Anti-NMDA-receptor encephalitis: case series and analysis of the effects of antibodies. *Lancet Neurol* 2008; **7**: 1091–8.
- 22 Hughes EG, Peng X, Gleichman AJ, et al. Cellular and synaptic mechanisms of anti-NMDA receptor encephalitis. *J Neurosci* 2010; **30**: 5866–75.
- 23 Tretter V, Moss SJ. GABA(A) Receptor Dynamics and Constructing GABAergic Synapses. *Front Mol Neurosci* 2008; **1**: 1–13.
- 24 Kapur J, Macdonald RL. Rapid seizure-induced reduction of benzodiazepine and Zn²⁺ sensitivity of hippocampal dentate granule cell GABA_A receptors. *J Neurosci* 1997; **17**: 7532–40.
- 25 Vazquez-Lopez A, Sierra-Paredes G, Sierra-Marcuno G. Anticonvulsant effect of the calcineurin inhibitor ascomycin on seizures induced by picrotoxin microperfusion in the rat hippocampus. *Pharmacol Biochem Behav* 2006; **84**: 511–16.
- 26 Gonzalez MI. The possible role of GABA_A receptors and gephyrin in epileptogenesis. *Front Cell Neurosci* 2013; **7**: 1–7.
- 27 Zhou C, Huang Z, Ding L, et al. Altered cortical GABA_A receptor composition, physiology, and endocytosis in a mouse model of a human genetic absence epilepsy syndrome. *J Biol Chem* 2013; **288**: 21458–72.
- 28 Mikasova L, De Rossi P, Bouchet D, et al. Disrupted surface cross-talk between NMDA and Ephrin-B2 receptors in anti-NMDA encephalitis. *Brain* 2012; **135**: 1606–21.
- 29 Tanaka M, Olsen RW, Medina MT, et al. Hyperglycosylation and reduced GABA currents of mutated GABRB3 polypeptide in remitting childhood absence epilepsy. *Am J Hum Genet* 2008; **82**: 1249–61.
- 30 Titulaer MJ, McCracken L, Gabilondo I, et al. Treatment and prognostic factors for long-term outcome in patients with anti-NMDA receptor encephalitis: an observational cohort study. *Lancet Neurol* 2013; **12**: 157–65.
- 31 Lancaster E, Dalmau J. Neuronal autoantigens-pathogenesis, associated disorders and antibody testing. *Nat Rev Neurol* 2012; **8**: 380–90.
- 32 Lancaster E, Martinez-Hernandez E, Dalmau J. Encephalitis and antibodies to synaptic and neuronal cell surface proteins. *Neurology* 2011; **77**: 179–89.
- 33 Malter MP, Helmstaedter C, Urbach H, Vincent A, Bien CG. Antibodies to glutamic acid decarboxylase define a form of limbic encephalitis. *Ann Neurol* 2010; **67**: 470–78.
- 34 Blanc F, Ruppert E, Kleitz C, et al. Acute limbic encephalitis and glutamic acid decarboxylase antibodies: a reality? *J Neurol Sci* 2009; **287**: 69–71.
- 35 Florance NR, Davis RL, Lam C. Anti-N-methyl-D-aspartate receptor (NMDAR) encephalitis in children and adolescents. *Ann Neurol* 2009; **66**: 11–18.
- 36 Tuzun E, Erdag E, Durmus H, et al. Autoantibodies to neuronal surface antigens in thyroid antibody-positive and -negative limbic encephalitis. *Neurol India* 2011; **59**: 47–50.
- 37 Mukherjee J, Kretschmannova K, Gouzer G, et al. The residence time of GABA(A)Rs at inhibitory synapses is determined by direct binding of the receptor alpha1 subunit to gephyrin. *J Neurosci* 2011; **31**: 14677–87.
- 38 Kapur J, Lothman EW, DeLorenzo RJ. Loss of GABA_A receptors during partial status epilepticus. *Neurology* 1994; **44**: 2407–08.

Supplementary webappendix

This webappendix formed part of the original submission and has been peer reviewed. We post it as supplied by the authors.

Supplement to: Petit-Pedrol M, Armangue T, Peng X, et al. Encephalitis with refractory seizures, status epilepticus, and antibodies to the GABA_A receptor: a case series, characterisation of the antigen, and analysis of the effects of antibodies. *Lancet Neurol* 2014; published online Jan 22. [http://dx.doi.org/10.1016/S1474-4422\(13\)70299-0](http://dx.doi.org/10.1016/S1474-4422(13)70299-0).

APPENDIX

Supplemental information

Index case 1

This 16 year-old girl presented to the hospital with a four-day history of severe fatigue and headache, accompanied by vertigo, nausea, and scintillating scotomas. She complained of several months of memory difficulties, cognitive dysfunction, anxiety, depressed mood and fatigue. Her past medical history was significant for Hodgkin's lymphoma which was in remission since completing chemotherapy and radiation 10 months earlier. On the fifth day of admission, she had a generalized tonic-clonic seizure and rapidly progressed to having frequent seizures. Complete blood cell count, C-reactive protein and erythrocyte sedimentation rate were normal. Testing for anti-thyroid peroxidase, anti-thyroglobulin, anti-nuclear antibodies, anti-neutrophil cytoplasmic antibodies, and paraneoplastic antibodies (Hu, Ri, Yo, CRMP5, amphiphysin) were negative. Brain MRI on day 3 demonstrated multiple foci of increased T2/FLAIR signal in both hemispheres (Figure 4A, E). CSF analysis showed normal opening pressure, 23 white blood cells (WBC)/ mm³ (69% lymphocytes), protein concentration 60 mg/dL, normal glucose concentration and negative cytology. Gram stain, routine cultures and PCR testing for Herpes simplex virus, Enterovirus and *Mycoplasma pneumoniae* were negative. Serology for Cytomegalovirus, Epstein-Barr virus, Arbovirus, *Bartonella henselae*, and Lyme disease were negative. Treatment with high-dose methylprednisolone was initiated on day 7. Very high doses of phenobarbital were required to suppress electrographic seizures. A subsequent course of plasma exchange on alternating days for one week failed to improve the seizure pattern. On day 10, repeat brain MRI showed increase of the size of the FLAIR/T2 abnormalities, mainly in the left temporal lobe, and multifocal new cortical and subcortical lesions in both cerebral hemispheres (Figure 4B, F). Brain biopsy on day 14 demonstrated intense diffuse reactive astrocytic gliosis throughout the cortex associated with microglial activation and a population of reactive T lymphocytes. Several days later, antibodies against unknown neuronal cell-surface antigens were identified in her CSF. She received high-dose corticosteroids, intravenous immunoglobulin, rituximab and cyclophosphamide. Phenobarbital coma was continued for four months; during this time breakthrough clinical and electrographic seizures occurred if the phenobarbital level was allowed to decrease. EEG recordings demonstrated generalized periodic discharges late in the first month of admission (Supplemental Figure 3 A).

After three months, the EEG showed more focal left-sided ictal activity. The phenobarbital dose was weaned and she began a slow neurological recovery with gradual resolution of the encephalopathic EEG pattern. Four months after admission a repeat lumbar puncture showed resolution of the leukocytosis; however, repeat MRI showed numerous new multifocal lesions throughout the brain with diffuse atrophy and moderate ex-vacuo ventricular dilatation (Figure 4 C, G). Six months after her initial presentation, she began to show more rapid neurological recovery. Repeat MRI demonstrated no new lesions, improvement or resolution of all previous lesions, and reduction of the previous seen diffuse atrophy (Figure 4 D, H). She was transferred to an inpatient rehabilitation facility seven months after presentation and over the subsequent three months made significant gains to the point that she was able to communicate, eat, dress and groom herself. She could walk short distances with minimal assistance. Ten months after symptom onset, she was discharged home able to carry out most activities of daily living independently. At the last follow-up, 15 months after symptom onset, she walks with no assistance and is able to perform all daily

activities independently. She has returned to school with a modified course load due to mild cognitive deficits that continue to improve.

Index case 2

A 51 year-old man was admitted to the hospital for rapidly progressive symptoms of change of behavior and new-onset psychosis. Prior to admission the patient was seen several times in the emergency department of another hospital where he was diagnosed with new onset depression and treated with sertraline and alprazolam. In addition, he had complained of generalized pruritis and developed worsening high blood pressure. On several occasions the family heard the patient saying he was going to kill other people and himself. A few days prior to admission, he refused to get out of bed, and became apathetic with almost total reduction of verbal output. His past medical history was relevant for high blood pressure, diabetes mellitus, hypercholesterolemia, stroke (from which he had fully recovered), and thrombotic thrombocytopenic purpura treated a few years earlier with splenectomy and steroids.

At admission, the clinical picture resembled akinetic mutism, with brief periods in which the patient spontaneously uttered a few incoherent sentences. The day of admission, he was noted to have clonic seizures involving the left side of the face and left arm that resolved with intravenous diazepam and levetiracetam. Over the next 24 hours he developed acute respiratory failure due to pneumonia, requiring intubation and admission to intensive care unit. Two days later he developed status epilepticus characterized by clonic movements of the left side of the face and left arm, associated with continuous saccadic eye movements to the left that were refractory to all treatments, including levetiracetam, lacosamide, and phenytoin. The patient was maintained in a pharmacological coma, sequentially using midazolam, propofol, and thiopental. The seizures persisted until the patients' death 10 weeks after presentation.

The initial EEG showed seizures in the right temporal lobe with a tendency to generalization that in subsequent recordings progressed to a pattern of generalized periodic discharges (Supplemental Figure 3 B). The MRI showed multiple increased FLAIR/T2 signal abnormalities, extensively involving cortex without mass effect or contrast enhancement, blurring the grey-white matter junction (Figure 5). The initial CSF study was normal, but a repeat CSF analysis several days later showed IgG and IgM oligoclonal bands without matching serum bands. The following tests were negative: 1) Blood studies for syphilis, hepatitis virus B and C, *Brucella melitensis*, *Borrelia burgdorferi*, *Toxoplasma gondii*, *Streptococcus pneumoniae*, and *Legionella pneumophila*; 2) CSF studies for bacterial and fungal infections, Herpes simplex virus 1 and 2; Human herpesvirus 6, Cytomegalovirus, Varicella zoster virus, JC virus and Enterovirus, 3) panel for paraneoplastic antibodies, and connective tissue disorders (antibodies to GAD65, Hu, Ri, Yo, CRMP5, amphiphysin, DNAdc, Sm, Rib-P, PCNA, U1-RNP, SS-A/Ro, SS-B/La, Scl-70, CENP-B, RNA Pol III, Jo-1, Mi-2, PM-Scl, and ANCA), complement levels, 4) serum protein electrophoresis, 5) tumor markers: CEA, AFP, Ca 19.9, PSA, and B-2-microglobulina. The patient was found to have low levels of thyroid peroxidase antibodies (156 IU/ml) and thyroglobulin antibodies (158 IU/ml).

After excluding an infectious etiology, the patient was started on corticosteroids and IVIG without significant effect. One week later, he received 5 plasma exchange treatments without clinical effect and no change in the MRI (Figure 5 D-F). By this time laboratory studies revealed serum and CSF antibodies against unknown neuronal cell-surface antigens, and he was started on cyclophosphamide (1 g per m²/ month) and

rituximab (1 g every 2 weeks). Despite these treatments the patient showed no clinical or radiological improvement and continued with electrographic status epilepticus. Repeat MRIs showed new FLAIR/T2 abnormalities diffusely involving cortex (Figure 5 G-I), and the patient died two months after admission.

Supplemental methods

Immunohistochemistry of rat brain

Adult female Wistar rats were sacrificed without perfusion, and the brain was removed and fixed by immersion in 4% paraformaldehyde for 1 hour at 4°C, cryoprotected in 40% sucrose for 48 hours, embedded in freezing compound media, and snap frozen in isopentane chilled with liquid nitrogen. Seven-micrometer-thick tissue sections were then sequentially incubated with 0.3% H₂O₂ for 15 minutes, 5% goat serum for 1 hour, and patient or control serum (1:200), or CSF (1:5) at 4°C overnight. After using a secondary biotinylated antibody goat anti-human IgG (diluted 1:2000, Vector, BA-3000), the reactivity was developed with the avidin-biotin-peroxidase method, as reported.¹

Immunocytochemistry on neuronal cultures

Rat hippocampal neuronal cultures were prepared as reported.² Live neurons grown on coverslips were incubated for 1 hour at 37°C with patient or control serum (final dilution 1:200) or CSF (1:10). After removing the media and extensive washing with phosphate-buffered saline (PBS), neurons were fixed with 4% paraformaldehyde, permeabilized with 0.3% Triton X-100, and immunolabeled with Alexa Fluor 488 goat anti-human IgG (diluted 1:1000, Invitrogen, A11013). Results were photographed under a fluorescence microscope using Zeiss Axiovision software (Zeiss, Thornwood, NY).

Immunocytochemistry on HEK293 cells

Fixed cells:

HEK293 cells were transfected with plasmids containing the human $\alpha 1$ subunit of the GABA_AR (accession number: NM_000806.3; Origene catalog number: SC119668) or the human $\beta 3$ subunit of the receptor (accession number: NM_000814.3; Origene catalog number: SC125324); cells transfected with a plasmid without insert was used as control. Cells were grown for 24 hours after transfection before assessment. Transfected cells were fixed in 4% paraformaldehyde, permeabilized with 0.3% Triton X-100 and then incubated with patients' serum (1:20 and higher serial dilutions) or CSF (1:5 and higher serial dilutions) along with a commercial mouse antibody against the $\alpha 1$ subunit of the GABA_AR (dilution 1:5000, Millipore, MAB339) or the $\beta 3$ subunit (dilution 1:5000, Abcam, AB4046) for 2 hours at room temperature, and the corresponding fluorescent secondary antibodies (Alexa Fluor 488 goat anti-human IgG, diluted 1:1000, A11013; and Alexa Fluor 594 goat anti-mouse IgG, diluted 1:1000, A11032, both from Invitrogen). Results were photographed under a fluorescence microscope using Zeiss Axiovision software.

Live cells:

Live HEK cells were incubated with serum (1:20 and higher serial dilutions) or CSF (1:5 and higher serial dilutions) of the patient together with the same commercial antibody against GABA_AR indicated above for 1 hour at 37°C, washed, and fixed with 4% paraformaldehyde for 5 minutes. After washing cells were then incubated with the corresponding Alexa Fluor secondary antibodies indicated above.

Immunoprecipitation and immunoblot

Live neurons obtained as above, were grown in 100 mm plates (density 1.5×10^6 neurons/plate), and incubated at 37°C with filtered patient serum (diluted 1:200) for 1 hour. Neurons were then washed with PBS, lysed with buffer (NaCl 150mM, EDTA 1mM, tris (hydroxymethyl) aminomethane [Tris]-HCl 100mM, deoxycholate acid 0.5%, 1% Triton X-100, pH 7.5) containing protease inhibitors (P8340; Sigma Labs), and centrifuged at 16.1×10^3 g for 20 minutes at 4°C. The supernatant was retained and incubated with protein A/G agarose beads (20423; Pierce, Rockford, IL) overnight at 4°C, centrifuged, and the pellet containing the beads with patients' antibodies bound to the target cell-surface antigen was then washed with lysis buffer, aliquoted, and kept at -80°C. An aliquot of this pellet was resuspended in Laemmli buffer, boiled for 5 minutes, separated in a 4 to 15% sodium dodecyl sulfate polyacrylamide gel electrophoresis, and the proteins visualized with EZBlue gel staining (G1041; Sigma Labs). Due to the lack of differences between the EZBlue-visible bands between patient's and control samples, all precipitated proteins run along the gel were analyzed using mass spectrometry.

Mass spectrometry

Mass spectrometry was performed at the Proteomics Facility at the Abramson Cancer Center of the University of Pennsylvania. Protein bands were trypsin digested and analyzed with a nano liquid chromatography (nano LC)/nanospray/linear ion trap (LTQ) mass spectrometer (Thermo Electron Corporation, San Jose, CA) as reported.³ Briefly, 3 ml trypsin digested sample was injected with autosampler from Eksigent (Dublin, CA). The digested samples were separated on a 10 cm C18 column, using nano LC from Eksigent with 200 ml/minute flow rate, 45 minute gradient. Online nanospray was used to spray the separated peptides into LTQ, and Xcalibur software (Thermo Scientific, Waltham, MA) was utilized to acquire the raw data. The raw data files were searched using Mascot (Matrix Science, Boston, MA) against the NCBI and Swissprot databases (Swiss Institute of Bioinformatics (Basel, Switzerland)).

Immunoabsorption and immunocompetition studies

In order to determine whether the brain reactivity of patient's antibodies was specifically due to GABA_AR binding, six 60 mm plates of HEK 293 cells expressing GABA_AR were sequentially incubated with patient's serum (1:200), each plate for 1 hour at 37°C. After incubation with the six plates, the immunoabsorbed serum was incubated with sections of rat hippocampus, as above. Patient's serum absorbed with non-transfected HEK 293 cells served as control.

To determine whether patients' antibodies were directed against similar antigens and epitopes of GABA_AR, immunocompetition studies were performed. IgG was isolated from a patient whose serum contained high levels of IgG antibodies against GABA_AR using protein A and G sepharose beads, and subsequently eluted and labeled with biotin (Vector, SP1200), as reported.⁴ Then, sections of rat brain were incubated with other patients' or control sera (diluted 1:5) overnight at 4°C, washed in PBS, and subsequently incubated with the indicated human biotinylated IgG containing GABA_AR antibodies (diluted 1:40) for 1 hour at room temperature, and the reactivity was developed using the avidin-biotin-peroxidase method. Two sera were considered to compete for the same GABA_AR epitopes, when pre-incubation of the tissue with one serum abrogated the reactivity of the other patient's IgG.

Quantitative analysis of neuronal GABA_AR immunolabeling by patient's antibodies

To determine the degree of immunolabeling of GABA_ARs by patient's antibodies, 14-day *in vitro* (*div*) rat hippocampal neurons were incubated with a representative patient's CSF (diluted 1:20) for 30 minutes, then washed, fixed, and incubated with a commercial mouse monoclonal antibody (Millipore 05-474; 1:500) against a sequence contained in the β 2/3 subunit (which is a component of most GABA_AR⁵) followed by appropriate fluorescent-conjugated secondary antibodies, Alexa Fluor 488 goat anti-human IgG (1:200, Invitrogen, A11013) and Alexa Fluor 594 donkey anti-mouse IgG (1:200, A21203, both from Invitrogen). Images were obtained with a laser-scanning confocal microscope (Leica TCS SP5). Laser light levels and detector gain and offset were adjusted in every experiment so that no pixel values were saturated in any treatment conditions. Images were thresholded, and the number of individual clusters along neuronal dendrites was determined using interactive software (ImageJ).

Analysis of the structural effects of patient's antibodies on GABA_AR clusters

To determine the effects of patient's antibodies on the number and localization of GABA_AR clusters, 14 *div* rat hippocampal neurons were treated with patient's or control CSF (1:20 dilution in Neuro-Basal supplemented with B27 medium; GIBCO, Carlsbad, CA) for 2 days. Every day, 20 of the 300 μ l medium in each culture well were removed and replaced with 20 μ l fresh patient or control CSF. On 16 *div*, neurons were fixed in freshly made paraformaldehyde (4% paraformaldehyde, 4% sucrose in phosphate-buffered saline) for 5 minutes, permeabilized in 0.25% Triton X-100 for 10 minutes, and blocked in 5% normal goat serum for 1 hour. Neurons were then incubated with the indicated monoclonal antibody against the GABA_AR β 2/3 (1:500), or a mouse monoclonal antibody against Gephyrin (1:200, Synaptic Systems, 147011), or a guinea pig polyclonal antibody against vesicular-GABA transporter (VGAT, 1:1000; Synaptic Systems, 131004) or a rabbit antibody against GluN1 (anti-NMDAR1, 1:100; Millipore AB9864R) for 2 hours, followed by the appropriate fluorescent-conjugated secondary antibodies (Alexa Fluor 488 goat anti mouse IgG, 1:200, A-11001; Alexa Fluor 594 goat anti-guinea pig IgG, A-11076, 1:200; Cy5 donkey anti-rabbit IgG, 1:200, Jackson ImmunoResearch 711-175-152). Images were obtained and analyzed as above.

Supplemental Table 1: Sequences isolated by immunoprecipitation with patient's serum

Sequence	β 3 subunit of the GABA _A R, peptide identification probability	Sequest XCorr	Sequest deltaCn
(R)LHPDGTVLYGLR(I) (+3H)	95%	2.97	0.21
R)NVVFATGAYPR(L) (+2H)	95%	3.21	0.55
(R)VADqLWVPDITYFLnDKK(S) (+3H)	95%	2.98	0.42

Mass spectral data was analyzed using the search engine Sequest. Peptide confidence was determined by the cross-correlation scoring which represent sensitivity, comparing the experimental fragmentation spectrum of the peptides against the theoretical predicted fragmentation spectrum; and by the DeltaCn, which represents specificity for the peptide identification. Xcorr > 2 (+2 H), 2.5 (+3 H) and deltaCn > 0.2) indicate a good spectrum.

Legends to Supplemental figures

Supplemental Figure 1: Comparison of reactivity of CSF of a patient with GABA_AR antibodies with that of a patient with GABA_BR antibodies using rat brain immunohistochemistry (high magnification of figure 1)

Panel A shows the reactivity of the CSF (dilution 1:4) of patient #2 with hippocampus; the asterisk indicates the area shown at higher magnification in panel B. Panel C shows the reactivity with cerebellum. Panels D-F correspond to the same brain regions immunostained with CSF of a patient with GABA_BR antibodies, and panels G-I with CSF of a control subject (without GABA_AR or GABA_BR antibodies). Note that the pattern of reactivity of GABA_AR antibodies is very similar to that of the GABA_BR antibodies which makes difficult to distinguish one from the other by plain immunohistochemistry. Scale bar for G = 100 μ m, Scale bar for H and I = 200 μ m

Supplemental Figure 2: Immunocompetition studies demonstrating that patients' antibodies compete for the same epitopes of the GABA_AR

Reactivity with rat brain of biotinylated IgG from a patient with GABA_AR antibodies in which the tissue has been pre-incubated with serum from a control individual (A and B), the serum from the same patient whose IgG has been biotinylated (C, D), and the serum of another patient with GABA_AR antibodies. Note the dramatic decrease of reactivity (competition for the same GABA_AR epitopes) in panels E and F compared with A and B. Panels C and D (competition with same patient's serum serves to demonstrate the background reactivity). Scale bar for A, C, E = 1 mm; Scale bar for B, DD and E = 200 μ m

Supplemental Figure 3: Generalized periodic discharges in patients with encephalitis and antibodies to GABA_AR

The recording in A corresponds to the EEG of patient #1 obtained one month after admission; note the presence of generalized epileptiform discharges. Settings: gain (sensitivity): 5 $\mu\text{V}/\text{mm}$; low frequency filter: 1 Hz, high frequency filter: 70 Hz. The recording in B corresponds to patient #2; this patient initially showed epileptiform activity in the right temporal lobe with tendency to generalization in posterior recordings, as shown in B. Settings: gain (sensitivity): 15 $\mu\text{V}/\text{mm}$; low frequency filter: 0.5 Hz, high frequency filter: 35 Hz.

Supplemental Reference List

1. Ances BM, Vitaliani R, Taylor RA, et al. Treatment-responsive limbic encephalitis identified by neuropil antibodies: MRI and PET correlates. *Brain* 2005; **128**: 1764-77.
2. Buchhalter JR, Dichter MA. Electrophysiological comparison of pyramidal and stellate nonpyramidal neurons in dissociated cell culture of rat hippocampus. *Brain Res Bull* 1991; **26**: 333-8.
3. Strader MB, Tabb DL, Hervey WJ, Pan C, Hurst GB. Efficient and specific trypsin digestion of microgram to nanogram quantities of proteins in organic-aqueous solvent systems. *Anal Chem* 2006; **78**: 125-34.
4. Dalmau J, Furneaux HM, Cordon-Cardo C, Posner JB. The expression of the Hu (paraneoplastic encephalomyelitis/sensory neuronopathy) antigen in human normal and tumor tissues. *Am J Pathol* 1992; **141**: 881-6.
5. Vithlani M, Terunuma M, Moss SJ. The dynamic modulation of GABA(A) receptor trafficking and its role in regulating the plasticity of inhibitory synapses. *Physiol Rev* 2011; **91**: 1009- 22.

5.2. Paper II

Investigations in GABAA receptor antibody-associated encephalitis

Marianna Spatola, **Mar Petit-Pedrol**, Mateus Mistieri Simabukuro, Thaís Armangue, Fernanda J. Castro, Maria I. Barcelo Artigues, Maria R. Julià Benique, Leslie Benson, Mark Gorman, Ana Felipe, Ruben L. Caparó Oblitas, Myrna R. Rosenfeld, Francesc Graus, and Josep Dalmau

Neurology. 2017 Mar 14;88(11):1012-1020.

Impact factor JCR 2016: The available IF from 2016 is 8.32 (D1)

Investigations in GABA_A receptor antibody-associated encephalitis



Marianna Spatola, MD
 Mar Petit-Pedrol, BS
 Mateus Mistieri
 Simabukuro, MD
 Thaís Armangué, MD,
 PhD
 Fernanda J. Castro, MD
 Maria I. Barcelo Artigues,
 MD
 Maria R. Julià Benique,
 MD
 Leslie Benson, MD
 Mark Goran, MD
 Ana Felipe, MD
 Ruben L. Caparó Oblitas,
 MD
 Myrna R. Rosenfeld, MD,
 PhD
 Francesc Graus, MD,
 PhD
 Josep Dalmau, MD, PhD

Correspondence to
 Dr. Dalmau:
 jdalmau@clinic.ub.es

ABSTRACT

Objective: To report the clinical features, comorbidities, receptor subunit targets, and outcome in patients with anti-GABA_A receptor (GABA_AR) encephalitis.

Methods: Clinical study of 26 patients, including 17 new (April 2013–January 2016) and 9 previously reported patients. Antibodies to α 1, β 3, and γ 2 subunits of the GABA_AR were determined using reported techniques.

Results: Patients' median age was 40.5 years (interquartile range 48.5 [13.75–62.35] years; the youngest 2.5 months old; 13 female). Symptoms included seizures (88%), alteration of cognition (67%), behavior (46%), consciousness (42%), or abnormal movements (35%). Comorbidities were identified in 11 (42%) patients, including 7 tumors (mostly thymomas), 2 herpesvirus encephalitis (herpes simplex virus 1, human herpesvirus 6; coexisting with NMDAR antibodies), and 2 myasthenia without thymoma. Brain MRI was abnormal in 23 (88%) patients, showing in 20 (77%) multifocal, asynchronous, cortical-subcortical T2/fluid-attenuated inversion recovery abnormalities predominantly involving temporal (95%) and frontal (65%) lobes, but also basal ganglia and other regions. Immunologic or tumor therapy resulted in substantial improvement in 18/21 (86%) assessable patients; the other 3 (14%) died (2 status epilepticus, 1 sepsis). Compared with adults, children were more likely to have generalized seizures ($p = 0.007$) and movement disorders ($p = 0.01$) and less likely to have a tumor ($p = 0.01$). The main epitope targets were in the α 1/ β 3 subunits of the GABA_AR.

Conclusions: Anti-GABA_AR encephalitis is characterized by frequent seizures and distinctive multifocal cortical-subcortical MRI abnormalities that provide an important clue to the diagnosis. The frequency of symptoms and comorbidities differ between children (more viral-related) and adults (more tumor-related). The disorder is severe but most patients respond to treatment.

Neurology® 2017;88:1012–1020

GLOSSARY

CBA = cell-based assay; **FLAIR** = fluid-attenuated inversion recovery; **GABA_AR** = GABA_A receptor; **HHV6** = human herpesvirus 6; **HSV1** = herpes simplex 1; **PSCT** = peripheral stem cell transplantation.

The GABA_A receptor (GABA_AR) is a ligand-gated chloride channel that mediates fast inhibitory synaptic transmission in the CNS. At the synapse, most GABA_ARs contain 2 α subunits, 2 β subunits, and 1 γ subunit, arranged as γ - β - α - β - α . Pharmacologic or genetic alteration of this receptor causes seizures,^{1–7} and we recently reported that human autoantibodies to the α 1 and β 3 subunits associate with seizures and status epilepticus in the context of autoimmune encephalitis.⁸ Since then, the γ 2 subunit was also found to be a target of autoantibodies in one patient,⁹ and subsequently confirmed in other cases.¹⁰ Recognition of anti-GABA_AR encephalitis is important because the seizures may be refractory to antiepileptic drugs unless the autoimmune response is treated. It is unclear whether the clinical features associated with antibodies against

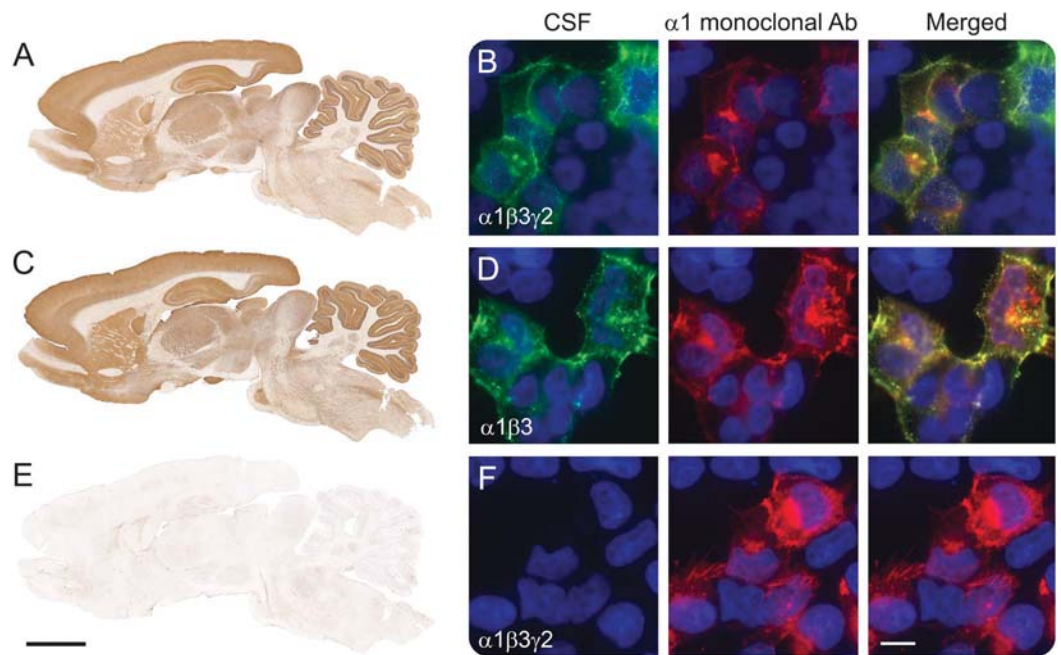
Editorial, page 1010

Supplemental data
 at Neurology.org

From the Institut d'Investigacions Biomèdiques August Pi i Sunyer (IDIBAPS) (M.S., M.P.-P., T.A., M.R.R., F.G., J.D.), University of Barcelona, Spain; University of Lausanne (UNIL) (M.S.), Switzerland; Centro de Investigación Biomédica en Red de Enfermedades Raras (CIBERER) (M.P.-P., T.A., M.R.R., J.D., F.G.), Madrid, Spain; Neurology Service (T.A., J.D.), Hospital Sant Joan de Déu, Barcelona, Spain; Neurology Division, Hospital das Clínicas (M.M.S.), São Paulo University, Brazil; Hospital de Base (F.J.C.), Brasília, Brazil; Service of Neurology (M.I.B.A.) and Service of Immunology (M.R.J.B.), University Hospital of Son Espases, Mallorca, Spain; Department of Neurology (L.B., M.G.), Children's Hospital, Boston, MA; Pediatric Neurology Section (A.F.), Vall d'Hebron University Hospital, Barcelona, Spain; Hospital Nacional Edgardo Rebagliati Martins (R.L.C.O.), Lima, Peru; Department of Neurology (M.R.R., J.D.), University of Pennsylvania, Philadelphia; Service of Neurology (F.G., J.D.), Hospital Clínic; and Catalan Institution for Research and Advanced Studies (ICREA) (J.D.), Barcelona, Spain.

Go to Neurology.org for full disclosures. Funding information and disclosures deemed relevant by the authors, if any, are provided at the end of the article.

Figure 1 Reactivity of patient's antibodies with the GABA_A receptor (GABA_AR)



Rat brain immunostaining with CSF of a patient with antibodies against the $\alpha 1$, $\beta 3$, and $\gamma 2$ subunits of the GABA_AR (A), compared with that of another CSF sample containing antibodies against $\alpha 1$ and $\beta 3$ subunits (C). Note the remarkable similarity of immunostaining of the samples of both patients. (B, D) Reactivity of the same patients' CSF samples with the corresponding HEK cells expressing the $\alpha 1\beta 3\gamma 2$ subunits (B), and HEK cells expressing the $\alpha 1\beta 3$ subunits (D). For patients with antibodies against $\alpha 1\beta 3$ subunits, adding the $\gamma 2$ subunit did not increase the intensity of reactivity with $\alpha 1\beta 3$ (data not shown). The CSF of a patient without these antibodies serves as control (E, F). Scale bar rat brain = 2 mm, scale bar HEK cells = 10 μ m.

the $\gamma 2$ subunit are different from those associated with antibodies against the $\alpha 1$ and $\beta 3$ subunits. Moreover, since anti-GABA_AR encephalitis was described recently, the spectrum of symptoms has not been fully defined. We describe the clinical, MRI, and immunologic features of 17 newly identified patients and 9 previously reported but not investigated for antibodies against the $\gamma 2$ subunit of the receptor.

METHODS **Patients, controls, clinical definitions, and sample collection.** Between April 2013 and January 2016, we investigated the sera or CSF of 2,914 patients with suspected autoimmune neurologic disorders. We included in the current study only those patients who fulfilled the following 3 criteria (figure e-1 at Neurology.org): (1) syndrome compatible with possible autoimmune encephalitis,¹¹ (2) serum or CSF reactivity with neuropil of rat brain suggesting a cell surface or synaptic target antigen, and (3) reactivity in a specific GABA_AR cell-based assay (CBA) using live HEK cells expressing $\alpha 1\beta 3$ or $\alpha 1\beta 3\gamma 2$ subunits. In addition, we included 9 patients (1–6, 9, 11, and 12 from our original report describing the GABA_AR antibodies) whose serum or CSF fulfilled the above criteria; the other 9 patients from that study were excluded because the antibodies did not show brain reactivity.⁸

Clinical information was obtained from questionnaires completed by physicians. The severity of symptoms was evaluated by

the modified Rankin Scale.¹² The outcome at the last follow-up was defined as complete recovery (able to return to all previous activities), partial recovery (objective improvement but unable to return to all activities), no improvement, or death. Controls (total 461) for tissue immunohistochemistry and CBA antibody studies included serum or CSF of 169 patients with autoimmune encephalitis (paraneoplastic or nonparaneoplastic), 114 with opsoclonus-myoclonus, 117 with stiff-person syndrome, 20 with neurodegenerative disorders, and 41 healthy blood donors.

Immunohistochemical studies. All samples were screened for reactivity with rat brain sections using previously reported immunohistochemical methods.^{8,13} Specific neuronal surface targets were investigated with CBA that included 13 autoantigens (NMDAR, AMPAR, GABA_BR, GABA_AR, LGI1, CASPR2, DPPX, GlyR, GAD65, IgLON5, mGluR5, Dopamine2R, neurexin-3 α), as reported.^{13–18} The CBA for GABA_AR antibodies is described in the supplemental material.

Standard protocol approvals, registrations, and patient consents. All patients gave written informed consent for use of samples and clinical information. This study was approved by the Institutional Review Board of the Hospital Clinic in Barcelona, Spain.

Statistical analysis. Comparisons between adults and children, and between patients with and without tumor, were assessed with the 2-tailed Fisher exact test and Mann-Whitney *U* test. Results <0.05 were regarded as statistically significant.

RESULTS Seventeen newly identified and 9 previously reported patients fulfilled the indicated criteria

for anti-GABA_AR encephalitis. These 26 patients, but none of the 461 controls, had antibodies identified with rat brain immunostaining and live HEK CBA expressing $\alpha 1\beta 3$ subunits of the GABA_AR (figures 1 and e-2). Among the 16 patients with paired serum and CSF samples, 14 had antibodies in both and 2 only in serum. The samples of all 26 patients reacted with live neurons (data not shown) similarly to those previously reported. Parallel studies in all 461 controls with live HEK cells expressing $\alpha 1\beta 3\gamma 2$ subunits of the GABA_AR (expression of individual subunits confirmed with commercial antibodies) did not reveal additional patients, indicating the absence of patients with isolated $\gamma 2$ antibodies in our study. Indeed, all patients with $\gamma 2$ antibodies (8/26, 31%) also had antibodies against the $\alpha 1$ or $\beta 3$ subunits (see supplemental material and figure e-3).

Detailed clinical features of the 17 newly identified patients are described in table 1, and of the 26 pooled cases in tables 2 and e-1. The median age of all patients was 40.5 years (interquartile range 48.5 [13.75–62.35] years), including 15 adults and 11 children; 13 were (50%) female. The median follow-up was 9 months (range 2 weeks–7 years), and the median duration of symptoms by the time of diagnosis was 2 months (range 1 week–5 years).

Tumor, viral, and other autoimmune associations occurred in 11 patients (table 1). Seven of these patients had an underlying tumor: 4 thymoma (1 with LGI1 antibodies, 1 with myasthenia), 1 small-cell lung cancer, 1 rectal cancer in association with HIV, and 1 multiple myeloma treated with autologous peripheral stem cell transplantation (PSCT) and lenalidomide (the autoimmune encephalitis developed 10 months after PSCT). Another 2 patients developed the autoimmune encephalitis a few weeks after viral encephalitis, one post herpes simplex 1 (HSV1) encephalitis and the other post human herpesvirus 6 (HHV6) encephalitis. By the time of the autoimmune encephalitis, both patients had GABA_AR and NMDAR antibodies that were not present during the viral infection. Another 2 patients had myasthenia without thymoma. One of the patients with coexisting GABA_AR and NMDAR antibodies is described in the supplemental material; the patient with thymoma and LGI1 antibodies has been reported previously.¹⁹

The most frequent (core) symptoms included seizures (23/26, 88%), cognitive impairment (n = 16/24, 67%, 2 babies excluded from analysis), altered behavior (12/26, 46%), decreased level of consciousness (11/26, 42%), and movement disorders (9/26, 35%). Status epilepticus occurred in 11 (48%) of the 23 patients with seizures, and 7 (64%) of them required pharmacologic coma. Seizures accompanied by at least another core symptom occurred in 23/26 (88%) patients and by at least 2 core symptoms in 14/26 (54%). Nine

(35%) patients developed abnormal movements, including 7/11 (64%) children who showed orofacial dyskinesias, dystonic postures, or generalized choreoathetosis, and 2/15 (13%) adults, both showing facial twitches and cramps. Two of the 11 children developed the symptoms as part of a postviral encephalitis (coexisting with NMDAR antibodies) and 1 after vaccination for yellow fever (without NMDAR antibodies). The latter was a 10-month-old baby girl (patient 8, video) who developed a clinical picture that initially suggested anti-NMDAR encephalitis, including dysautonomia and orofacial and limb dyskinesias without NMDAR antibodies in serum and CSF.

CSF was abnormal in 15 of 26 (58%) patients including pleocytosis (6–154 leukocytes/mm³), increased protein concentration (0.52–0.85 g/L), or oligoclonal bands (table 2). EEG was available for 21 patients: 16 (76%) had epileptiform activity, mostly unilateral or bilateral periodic epileptiform discharges involving the temporal lobes (9 associated with focal or diffuse slow activity) and 5 (24%) had slow activity. Brain biopsy, performed in patient 15, demonstrated mild parenchymal and perivascular lymphocytic infiltrates without vessel wall involvement, and microglial activation (data not shown).

T2/fluid-attenuated inversion recovery (FLAIR) brain MRI abnormalities were identified in 23/26 (88%) patients. In 20 (77%), the abnormalities were multifocal, involving both gray and white matter in 2 or more of the following regions: temporal (95%, 16 bilateral, 3 unilateral), frontal (65%, 10 bilateral, 3 unilateral), parietal (25%, 3 bilateral, 2 unilateral), occipital (15%, 2 bilateral, 1 unilateral), basal ganglia (15%), cerebellum (10%), or brainstem (5%). Only 2 patients had isolated unilateral involvement of the temporal lobe, another patient had isolated unilateral parietal involvement, and 3 had normal MRI. The multifocal abnormalities involved cortical and subcortical regions (figure 2), without diffusion restriction (except for patient 7) and without gadolinium enhancement (except for patient 14, who had focal gyriform leptomeningeal enhancement, and 16, who had mild hippocampal enhancement). The multifocal T2/FLAIR changes were asynchronous, with some appearing while others were disappearing during the course of the disease. In one of the patients (case 17), the MRI abnormalities persisted during short periods (4–6 weeks) in which the patient was remarkably free of seizures or other symptoms.

Treatment information was available for 23 patients: 13 (56%) received first-line immunotherapy (corticosteroids, plasma exchange, IV immunoglobulin), 8 (35%) first- and second-line immunotherapy (rituximab, azathioprine, cyclosporine, or cyclophosphamide), and 2 (9%) were only treated with anti-epileptics. At the last follow-up, 18 of 21 (86%)

Table 1 Main clinical features and antibody specificity in 17 new patients with anti-GABA_A receptor (GABA_AR) encephalitis

Patient, sex, age, y	Prodromal features	Tumor; other autoimmune disorders	Main clinical features; mRS at the peak of disease	CSF	EEG	MRI (increased T2/FLAIR signal)	Immunotherapy and tumor treatment	Last follow-up, mo; recovery; mRS	GABA _A R subunit; additional Ab
1, F, 58	Fatigue, fever	Thymoma (identified at diagnosis)	Memory loss; 2	Normal	Intermittent slowing	Bilateral insula and basal ganglia	Steroids, thymectomy	9; partial; mRS 1	S: 1/640; CSF: 1/20; α1, β3
2, F, 88	None	Thymoma (identified at diagnosis)	dLOC, cognitive decline, L hemiplegia; 5	Normal	NA	R temporal, bilateral frontal lobes	PE, thymectomy	10; partial; mRS 3	S: NA; CSF: 1/20; α1
3, F, 74	Headache	None	Personality change, apathy, anxiety, memory loss, speech disorder, dLOC, focal seizures, SE; 5	Normal	Bilateral temporal PED	L temporal lobe, mild hippocampal Gd ⁺	Steroids, AZA	2; partial; mRS 2; died 6 months later of sepsis	S: NA; CSF: 1/20; α1, β3
4, M, 60	None	None	Focal auditory seizures; R facial twitches, R hemibody paresthesia, dysarthria and aphasia; 5	Normal	NA	L temporal and bilateral frontal lobes	Steroids	12; partial; mRS 2	S: 1/160; CSF: 1/40; α1, β3, γ2
5, F, 66	Skin rash, vomiting	Thymoma (preceded encephalitis)	Right arm paresthesia; 1	Normal	NA	Bilateral frontal, temporal, parietal lobes	Steroids, thymectomy	3; partial; mRS 1	S: 1/40; CSF: 1/20; α1, γ2
6, M, 36	HIV	Rectal cancer (preceded encephalitis)	Seizures, confusion, dLOC; 2 months later hearing difficulty, slurred speech; 4	Normal	Intermittent diffuse slowing	L operculum and bilateral temporal lobes	Steroids, cancer treatment	12; partial; mRS 2	S: 1/160; CSF: 1/20; β3, γ2
7, M, 62	None	10 months posttransplant for multiple myeloma	Seizures, cognitive deterioration, altered mental status, dLOC, coma; 5	Normal	Diffuse slowing	Frontal, temporal, and occipital lobes with diffusion restriction	Steroids, PE	2; complete; mRS 0	S: >1/1280; CSF: NA; β3
8, F, 10 mo	Yellow fever vaccine	None	Focal motor seizures, involuntary movements, dLOC, coma, SE, autonomic instability; 5	Normal	Diffuse slowing, epileptiform activity	Normal CT and MRI	Steroids, IVIg	8; partial; mRS 4	S: >1/640; CSF: 1/40; β3
9, M, 15 mo	HSV1 encephalitis	None	8 weeks after HSE: irritability, focal motor refractory seizures, SE, choreoathetosis, ataxia, dysphagia; 5	53 WBC, EP (0.83)	Generalized bilateral epileptiform activity	New increased T2/FLAIR signal in bilateral frontal and temporal lobes	Steroids, PE, RTX	14; partial; mRS 4	S: 1/80; CSF: 1/20; α1, β3, γ2; NMDAR
10, F, 45	Headache, flushing	Myasthenia gravis, metastatic thymoma	Focal motor seizures, mood and behavioral change, memory loss, dysautonomia; new pleural metastasis; 3	EP	R temporal PED and L epileptiform activity	Bilateral temporal lobes	Steroids, PE, surgical removal of metastasis	3; complete; mRS 0	S: >1/640; CSF: 1/40; α1, β3; LGI1
11, F, 14	Headache, malaise	None	Seizures, abnormal movements; NA	51 WBC	NA	Normal (1 week from disease onset)	NA	NA	S: 1/40; CSF: NA; α1, β3, γ2
12, F, 63	None	Small cell lung cancer (identified at diagnosis)	Focal motor seizures, memory loss, personality change, ataxia, gait problems; 6 months later: hallucinations, choreiform movements; 3	44 WBC, EP (0.52), OCB	Diffuse slowing, L hemisphere PED	Bilateral temporal lobes and basal ganglia	NA	NA	S: 1/40; CSF: negative; α1, β3, γ2
13, M, 53	Headache, vomiting	Myasthenia gravis; no tumor	Focal motor seizures with secondary generalization, cognitive decline; 4	52 WBC	Diffuse slowing, L PED	Bilateral temporal lobes, L frontal lobe and R occipital lobe	No immunotherapy (only AED)	1.5; partial; mRS 1	S: NA; CSF: 1/40; α1, β3
14, M, 16	Headache, weight loss, vomiting	None	Seizures, personality change, memory loss, insomnia, L dysmetria and weakness, dysautonomia; 3	10 WBC, OCB	Diffuse and focal slowing, bilateral PED	Bilateral temporal, frontal and occipital lobes, focal leptomeningeal Gd ⁺	Steroids, IVIg, PE, RTX	3; complete; mRS 0	S: 1/320; CSF: 1/80; β3, γ2

Continued

Table 1 Continued

Patient, sex, age, y	Prodromal features	Tumor; other autoimmune disorders	Main clinical features; mRS at the peak of disease	CSF	EEG	MRI (increased T2/FLAIR signal)	Immunotherapy and tumor treatment	Last follow-up, mo; recovery; mRS	GABA _A R subunit; additional Ab
15, F, 2.5 mo	HHV-6 encephalitis	None	5 weeks after HHV6 encephalitis: seizures, hypoactivity, orofacial and generalized dyskinesias, dLOC; 5	40 WBC, EP (0.85)	Asymmetric slowing, bilateral epileptiform activity	No new abnormalities	Steroids, IVIg	6; partial (only seizures and dyskinesias improved); mRS 4	S: 1/160; CSF: >1/320; β3, γ2; NMDAR
16, F, 57	None	Myasthenia gravis, uterine tumor (remote history)	Generalized and focal seizures, mood disorder, hallucinations, aphasia, dysphagia requiring nasogastric feeding; 4	Normal WBC and protein, OCB	Bilateral frontotemporal epileptiform activity	Bilateral frontal and temporal lobes, mild hippocampal Gd+	Steroids, PE	1.5; partial; mRS 3	S: > 1/1280; CSF: >1/320; α1, β3; NMDAR
17, M, 13	None	None	History of focal seizures successfully treated with phenytoin; 1 year later: episodes of focal motor seizures, secondary generalization, epilepsy partialis continua, psychomotor agitation; 2	Normal	Asymmetric slowing R > L, no epileptiform activity	Bilateral parietal and occipital lobes, R frontal lobe; some abnormalities persisted during periods free of symptoms	Steroids, IVIg, RTX	8; complete; mRS 0	S: > 1/1280; CSF: >1/320; α1, β3

Abbreviations: Ab = antibodies; AED = antiepileptic drugs; AZA = azathioprine; dLOC = decreased level of consciousness; EP = elevated CSF protein concentration (>0.45 g/L); FLAIR = fluid-attenuated inversion recovery; Gd+ = gadolinium enhancement; HHV6 = human herpesvirus 6; HSE = herpes simplex encephalitis; HSV1 = herpes simplex 1; IVIg = IV immunoglobulins; mRS = modified Rankin Scale; NA = not available; OCB = CSF oligoclonal bands; PE = plasma exchange; PED = periodic epileptiform discharges in EEG; RTX = rituximab; SE = status epilepticus; WBC = white blood cells. Antibody titers were defined as the highest dilution for which the reactivity with HEK cells expressing α1β3γ2 was no longer detectable.

patients treated with immunotherapy (and tumor removal when appropriate) had partial (n = 13, 72%) or complete (n = 5, 28%) recovery, and the other 3 (14%) patients died of sepsis, which in 2 was associated with status epilepticus; none of the patients who died had a tumor. One of the 2 patients who did not receive immunotherapy showed partial improvement (case 13), and the other was lost to follow-up (unknown outcome). At the last follow-up, none of the 26 patients has had a relapse. One patient (case 17) developed anti-GABA_AR encephalitis 1 year after a first episode of seizures successfully treated with antiepileptic drugs. However, it is unclear whether the first episode was related to anti-GABA_AR encephalitis given that no CSF, MRI, or antibody studies were obtained.

Compared to adults (table 2), children were more likely to develop generalized seizures (11/11, 100% vs 7/15, 47%, *p* = 0.007), movement disorders (7/11, 64% vs 2/15, 13%, *p* = 0.01), and CSF abnormalities (10/11, 91% vs 5/15, 33%, *p* = 0.005), and less likely to have a tumor (1/10, 10% vs 9/15, 60%, *p* = 0.01). Despite these findings, the outcome was not significantly different between the age groups (*p* = 0.06).

Compared to patients without tumor (table e-1), those with tumor were older (median 56.5 vs 16 years in patients without tumor, *p* = 0.006) and less frequently had generalized seizures (4/10, 40% vs 13/15, 87%, *p* = 0.02); the outcome, however, was similar (*p* = 0.14).

Detection of antibodies against the γ2 subunit, which in all cases occurred in association with antibodies against the α1 or β3 subunits, did not segregate with symptoms or paraclinical findings different from those in patients without γ2 subunit antibodies (data not shown).

DISCUSSION We report 17 new patients with anti-GABA_AR encephalitis and review 9 previously reported cases providing the main clinical and radiologic clues that assist in the differential diagnosis of this disorder in children and adults, tumor and viral associations, and the main subunit targets of the antibodies, the α1 and β3 subunits of the GABA_AR.

Our current findings confirm that seizures are the most frequent clinical manifestation of this disorder. Combined with data from our previous study, up to 88% of the patients had seizures, usually at symptom presentation, and frequently accompanied by status epilepticus that often required pharmacologically induced coma. Status epilepticus (along with sepsis) may have contributed to the death of 2 patients. In all patients, the seizures were accompanied by at least one of the following core symptoms: cognitive impairment, decreased level of consciousness, altered behavior, or movement disorders. Interestingly, children were more

Table 2 Clinical features in children and adults with anti-GABA_A receptor (GABA_AR) encephalitis (26 patients)

	Total (26)	Children (11)	Adults (15)	P Value
Demographics				
Median age (range), y	40.5	13 (2.5 mo–16 y)	59 (28–88)	
Female	13/26	6/11 (55%)	7/15 (47%)	1
Clinical association				
Tumor	10/25	1/10	9/15	0.01 ^a
Other autoimmune diseases	5/26	0/11	5/15	0.05
Clinical manifestations				
Prodrome	9/25	4/10	5/15	1
Generalized seizures	18/26	11/11	7/15	0.007 ^a
Focal seizures	21/26	8/11	13/15	0.61
Status epilepticus/seizures (any type)	11/23	6/11	5/12	0.68
Decreased level of consciousness	11/26	4/11	7/15	0.7
Behavioral changes	12/26	5/11	7/15	1
Cognitive decline	16/24	6/9	10/15	1
Movement disorders	9/26	7/11	2/15	0.01 ^a
Dysautonomia	4/25	3/10	1/15	0.26
Clinical severity				
mRS ≥4 at the peak of disease	15/22	7/10	8/12	0.24
Admission to ICU	12/26	7/11	5/15	0.23
Complementary studies				
MRI multifocal abnormalities	20/26	8/11	12/15	1
EEG epileptiform discharges	16/21	8/10	8/11	1
EEG focal/diffuse slowing	12/21	7/10	5/11	0.38
CSF abnormal (cell count, proteins, or OCB)	15/26	10/11	5/15	0.005 ^a
Additional antineuronal antibodies	7/26	4/11	3/15	0.4
Immunotherapy				
First-line alone (steroids, PE, IVIg)	13/23	4/10	9/13	
First- and second-line (AZA, CTX, CyA, RTX)	8/23	5/10	3/13	
No immunotherapy	2/23	1/10	1/13	
Outcome				
Partial recovery	14/22	8/10	6/12	0.06
Complete recovery	5/22	1/10	4/12	
Death	3/22	1/10	2/12	

Abbreviations: AZA = azathioprine; CTX = cyclophosphamide; CyA = cyclosporine; ICU = intensive care unit; IVIg = IV immunoglobulins; mRS = modified Rankin Scale; OCB = oligoclonal bands; PE = plasma exchange; RTX = rituximab.

^aSignificant.

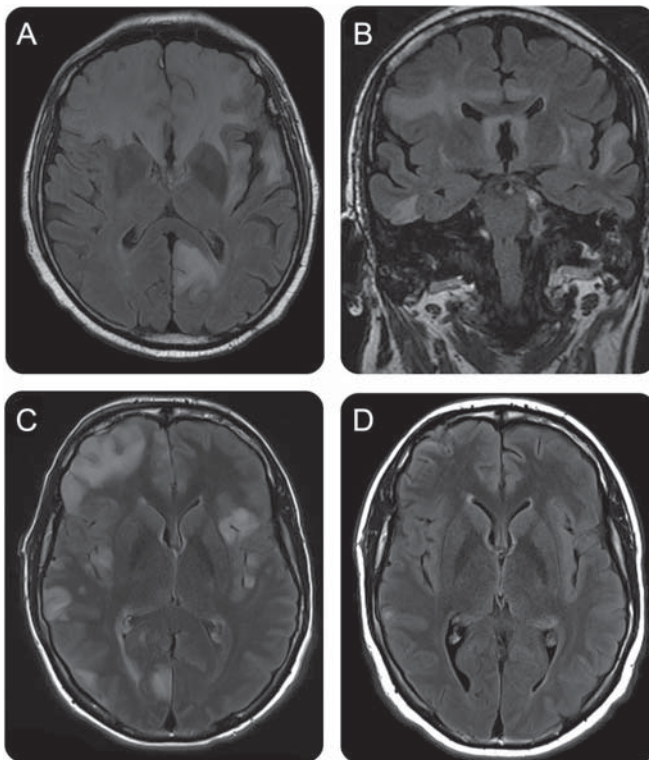
likely to have generalized seizures and movement disorders and less likely to have an underlying tumor than adults. These age-related symptoms may result from the combination of specific antibody effects on synaptic circuits (e.g., antibody-mediated decrease of receptors) and increased vulnerability of some areas of the

developing brain (hippocampus, basal ganglia) to inflammatory disorders. For example, other inflammation-related epileptic conditions (e.g., febrile infection-related epilepsy syndromes²⁰) and movement disorders (e.g., postinfectious Sydenham chorea²¹) occur almost exclusively in children. In addition, in children, GABA_AR antibodies may develop as postviral encephalitis and coexist with NMDAR antibodies, in which case the resulting symptoms (seizures, dyskinesias, choreoathetosis) are likely a manifestation of the combined presence of NMDAR antibody-mediated mechanisms.

Considering the clinical similarities among many forms of autoimmune encephalitis, an important finding of our study is the association of anti-GABA_AR encephalitis with multifocal unilateral or bilateral cortical-subcortical T2/FLAIR MRI abnormalities. These T2/FLAIR abnormalities can manifest asynchronously during the course of the disease (some appear while others disappear), sometimes with limited correlation with the patient's symptoms, and rarely enhance with contrast. These MRI findings are important not only because they are frequent (77% of the patients) but also because they rarely occur in other autoimmune encephalitis, providing a valuable clue to the clinical recognition of GABA_AR autoimmunity.

The experience gained from this and our previous study suggests that 40% of patients with anti-GABA_AR encephalitis have tumors, mostly thymomas, and less commonly, other neoplasms (e.g., Hodgkin lymphoma, multiple myeloma) that may cause alterations of the immunologic system, perhaps leading to autoimmunity. Patients with a tumor were older (only 1 of 11 pediatric patients had a tumor; Hodgkin lymphoma in a 16-year-old patient) and less likely to have seizures than those without tumor, probably due to the general predisposition of children with inflammatory brain disorders to have seizures. Four adult patients had thymoma: 1 of them, previously reported,¹⁹ had a history of several tumor relapses without development of encephalitis until the last relapse, which also associated with LGI1 antibodies. Interestingly, the thymoma of this patient expressed both LGI1 and GABA_AR proteins, and the clinical picture appeared to be driven by the GABA_AR immune response showing widespread multifocal (not hippocampal limited) T2/FLAIR abnormalities, which are highly unusual in anti-LGI1 encephalitis. This clinical case resembled 2 reported patients with anti-GABA_AR encephalitis in association with invasive thymoma, coexisting antibodies (LGI1 or Caspr2), myasthenia gravis (in one), and multifocal T2/FLAIR MRI abnormalities.⁹ We did not find another predominant tumor type among our patients with malignancies, as reported in previous studies.^{9,10} It is unclear whether the history of HIV,

Figure 2 MRI findings in 2 patients with anti-GABA_A receptor (GABA_AR) encephalitis



(A, B) MRI from patient 7, obtained on day 30 after symptom onset, shows extensive, confluent fluid-attenuated inversion recovery (FLAIR) abnormalities involving the left occipital lobe and the frontal and temporal regions, bilaterally, with moderate diffusion restriction (not shown). (C) MRI from patient 14, obtained on day 45 after symptom onset, shows extensive multiple cortical-subcortical FLAIR abnormalities involving bilateral frontal, temporal, and parietal-occipital lobes, without diffusion restriction, but mild gyriform leptomeningeal enhancement in the right temporal pole (not shown). Biopsy was performed in the right frontal region. (D) Follow-up MRI obtained 2.5 months later (4 months after symptom onset) shows substantial improvement and resolution of most abnormalities.

vaccination against yellow fever, or a peripheral stem cell transplant for multiple myeloma in 3 of our patients played a role in triggering the GABA_AR immune response. However, it is interesting to note that post-transplant immunosuppressed patients can develop autoimmune encephalitis, as has been shown in patients with anti-NMDAR and anti-LGI1 encephalitis.^{22,23}

The development of anti-GABA_AR encephalitis as postviral encephalitis (HSV1 and HHV6) expands the number of receptors that can be involved as targets of postviral brain autoimmunity. This and previous findings²⁴ support the concept of autoimmunity triggered by extensive antigen release by infected neurons undergoing degeneration. A mechanism of viral mimicry is less likely because the 2 patients with this complication developed de novo synthesis of antibodies against 2 different targets (GABA_AR and NMDAR) during the weeks following the viral encephalitis.

All patients' serum or CSF antibodies recognized the $\alpha 1$ or $\beta 3$ subunits of the GABA_AR, with 31% of

the cases showing coexisting antibodies against the $\gamma 2$ subunit. None of the patients had isolated antibodies against the $\gamma 2$ subunit, and the presence of these antibodies along with antibodies to $\alpha 1$ or $\beta 3$ subunits did not reveal a specific subphenotype (data not shown), suggesting that CBA expressing $\alpha 1\beta 3$ or $\alpha 1\beta 3\gamma 2$ can be used for comprehensive antibody testing. In a previous study in which the clinical and paraclinical information (CSF, MRI, or EEG) were limited or not available for many patients, antibodies directed only against the $\gamma 2$ subunit were identified in 5 cases.¹⁰ Each of these patients had a different syndrome or suspected etiology (celiac disease, psychological disorder, mild cognitive impairment, pathologically confirmed Huntington disease, focal epilepsy) and only 1 received immunotherapy, suggesting a low index of conviction among the treating physicians for an autoimmune cause. In contrast, our current clinical findings associated with brain tissue reacting antibodies and $\alpha 1\beta 3$ subunit specificity (irrespective of $\gamma 2$ subunit antibodies) show a more homogeneous clinical and radiologic syndrome, and 21 of 23 patients received immunotherapy.

It is premature to indicate whether serum or CSF should preferentially be tested. We have identified GABA_AR antibodies in serum, but not CSF, of patients with other disorders such as stiff-person syndrome or opsoclonus-myoclonus.⁸ Interestingly, the samples of those patients do not react with brain tissue or cultured neurons, suggesting other epitope targets of unclear clinical relevance. This finding and the possible coexistence of CSF or serum antibodies against other synaptic or cell surface proteins⁸⁻¹⁰ suggests caution in selecting only serum or CSF for antibody testing, and for these reasons we prefer determining antibodies in both samples. A comprehensive approach to antibody testing using CBA with both serum and CSF or if only serum is available confirming the results with brain tissue immunohistochemistry has been recommended for most antibodies against cell surface or synaptic proteins.¹¹ In our experience with this and other autoantibodies, the parallel demonstration of antibody reactivity using brain tissue and CBA has more clinical value than CBA alone (irrespective of the titers of this assay), as shown here in some cases.

Despite the limitations of being a retrospective study and that the disease is infrequent, the findings of this study are important in helping to recognize this potentially lethal disorder. Current experience suggests that anti-GABA_AR encephalitis should be suspected in patients with encephalitis predominantly manifesting with seizures and multifocal cortical-subcortical T2/FLAIR MRI abnormalities that usually involve the temporal lobes (95% of cases). The disorder can affect very young children (the youngest

in this study was 2.5 months) and adults. In younger patients, the disorder may be confused with anti-NMDAR encephalitis due to the common presence of dyskinesias, although it is important to keep in mind that both disorders may overlap in the context of postviral autoimmune encephalitis. Compared with other autoimmune encephalitis, anti-GABA_AR encephalitis seems to be less responsive to treatment than NMDAR encephalitis. Although 86% of the patients showed responses to treatment (first- and second-line therapies and tumor treatment if needed), only 28% had full recovery (and only one of them was a child), and the other 14% died, emphasizing the need for prompt recognition and treatment of the disorder. Future studies should focus on clarifying the frequency of GABA_AR antibodies in patients with postviral autoimmune encephalitis, the preferential occurrence of these antibodies in serum or CSF, and whether prompt treatment improves the degree of neurologic recovery.

AUTHOR CONTRIBUTIONS

Design/conceptualization of the study, analysis and interpretation of the data: M.S., M.P.P., and J.D. Data collection: M.S., M.P.P., M.M.S., T.A., C.F.J., M.I.B.A., M.R.J.B., L.B., M.G., A.F., R.L.C.O., M.R.R., F.G., J.D. Statistical analysis: M.S., T.A., J.D. Figure/video development: M.S., M.P.P., M.M.S., L.B., J.D. Drafting of the manuscript: M.S., M.R.R., F.G., and J.D.

ACKNOWLEDGMENT

The authors thank the physicians who provided clinical information, the patients and families for their contribution to research, and E. Aguilar and J. Planagumà for technical support.

STUDY FUNDING

This study was supported in part by Instituto Carlos III/FEDER (CM14/00081, T.A.; FIS PI15/00377, F.G.; FIS PI14/00203, J.D.), CIBERER (CB15/00010, J.D.), NIH RO1NS077851 (J.D.), Agaur SGR93 (J.D.), Fédération pour la Recherche sur le Cerveau, FCR-2013-01 (J.D.), Fundación Mutua Madrileña (T.A.), Fondation Pierre Mercier pour la Science and Société Académique Vaudoise (Lausanne, Switzerland) (M.S.), Dodot Procter & Gamble (DN040579, T.A.), and Fundació CELLEX (J.D.).

DISCLOSURE

M. Spatola, M. Petit-Pedrol, M.M. Simabukuro, T. Armangue, F.J. Castro, M.I. Barcelo Artigues, M.R. Julià Benique, L. Benson, M. Gorman, A. Felipe, and R.L. Caparó Oblitas report no disclosures relevant to the manuscript. M.R. Rosenfeld receives royalties from Athena Diagnostics for the use of Ma2 as an autoantibody test and from Euroimmun for the use of NMDA receptor as an autoantibody test. F. Graus received a licensing fee from Euroimmun for the use of IgLON5 as an autoantibody test. J. Dalmau receives royalties from Athena Diagnostics for the use of Ma2 as an autoantibody test and from Euroimmun for the use of NMDA, GABA_B receptor, GABA_A receptor, DPPX, and IgLON5 as autoantibody tests; he has received an unrestricted research grant from Euroimmun. Go to Neurology.org for full disclosures.

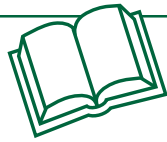
Received June 24, 2016. Accepted in final form October 18, 2016.

REFERENCES

1. Baulac S, Huberfeld G, Gourfinkel-An I, et al. First genetic evidence of GABA(A) receptor dysfunction in epilepsy: a mutation in the gamma2-subunit gene. *Nat Genet* 2001;28:46–48.

2. Wallace RH, Marini C, Petrou S, et al. Mutant GABA_A receptor γ 2-subunit in childhood absence epilepsy and febrile seizures. *Nat Genet* 2001;28:49–52.
3. Maljevic S, Krampfl K, Cobilanschi J, et al. A mutation in the GABA(A) receptor alpha(1)-subunit is associated with absence epilepsy. *Ann Neurol* 2006;59:983–987.
4. Lachance-Touchette P, Martin C, Poulin C, Gravel M, Carmant L, Cossette P. Screening of GABRB3 in French-Canadian families with idiopathic generalized epilepsy. *Epilepsia* 2010;51:1894–1897.
5. González MI, Grabenstatter HL, Cea-Del Rio CA, et al. Seizure-related regulation of GABA_A receptors in spontaneously epileptic rats. *Neurobiol Dis* 2015;77:246–256.
6. Greenfield LJ. Molecular mechanisms of antiseizure drug activity at GABA_A receptors. *Seizure* 2013;22:589–600.
7. Sun Y, Wu Z, Kong S, et al. Regulation of epileptiform activity by two distinct subtypes of extrasynaptic GABA_A receptors. *Mol Brain* 2013;6:21.
8. Petit-Pedrol M, Armangue T, Peng X, et al. Encephalitis with refractory seizures, status epilepticus, and antibodies to the GABA_A receptor: a case series, characterisation of the antigen, and analysis of the effects of antibodies. *Lancet Neurol* 2014;13:276–286.
9. Ohkawa T, Satake S, Yokoi N, et al. Identification and characterization of GABA(A) receptor autoantibodies in autoimmune encephalitis. *J Neurosci* 2014;34:8151–8163.
10. Pettingill P, Kramer HB, Coebergh JA, et al. Antibodies to GABA_A receptor α 1 and γ 2 subunits: clinical and serologic characterization. *Neurology* 2015;84:1233–1241.
11. Graus F, Titulaer MJ, Balu R, et al. A clinical approach to diagnosis of autoimmune encephalitis. *Lancet Neurol* 2016;15:391–404.
12. Sulter G, Steen C. Use of the Barthel Index and modified Rankin Scale in acute stroke trials. *Stroke* 1999;30:1538–1541.
13. Lai M, Hughes EG, Peng X, et al. AMPA receptor antibodies in limbic encephalitis alter synaptic receptor location. *Ann Neurol* 2009;65:424–434.
14. Gresa-Arribas N, Planagumà J, Petit-Pedrol M, et al. Human neurexin-3 α antibodies associate with encephalitis and alter synapse development. *Neurology* 2016;86:2235–2242.
15. Dalmau J, Gleichman AJ, Hughes EG, et al. Anti-NMDA-receptor encephalitis: case series and analysis of the effects of antibodies. *Lancet Neurol* 2008;7:1091–1098.
16. Lai M, Huijbers MG, Lancaster E, et al. Investigation of LGI1 as the antigen in limbic encephalitis previously attributed to potassium channels: a case series. *Lancet Neurol* 2010;9:776–785.
17. Lancaster E, Huijbers MGM, Bar V, et al. Investigations of caspr2, an autoantigen of encephalitis and neuromyotonia. *Ann Neurol* 2011;69:303–311.
18. Lancaster E, Lai M, Peng X, et al. Antibodies to the GABA (B) receptor in limbic encephalitis with seizures: case series and characterisation of the antigen. *Lancet Neurol* 2010;9:67–76.
19. Simabukuro MM, Petit-Pedrol M, Castro LH, et al. GABA_A receptor and LGI1 antibody encephalitis in a patient with thymoma. *Neurol Neuroimmunol Neuroinflammation* 2015;2:e73.
20. Kramer U, Chi C-S, Lin K-L, et al. Febrile infection-related epilepsy syndrome (FIRES): pathogenesis, treatment, and outcome: a multicenter study on 77 children. *Epilepsia* 2011;52:1956–1965.

21. Williams KA, Swedo SE. Post-infectious autoimmune disorders: Sydenham's chorea, PANDAS and beyond. *Brain Res* 2015;1617:144–154.
22. Rathore GS, Leung KS, Muscal E. Autoimmune encephalitis following bone marrow transplantation. *Pediatr Neurol* 2015;53:253–256.
23. Zhao CZ, Erickson J, Dalmau J. Clinical reasoning: agitation and psychosis in a patient after renal transplantation. *Neurology* 2012;79:e41–e44.
24. Armangue T, Leypoldt F, Málaga I, et al. Herpes simplex virus encephalitis is a trigger of brain autoimmunity. *Ann Neurol* 2014;75:317–323.



Neurology® Online CME Program

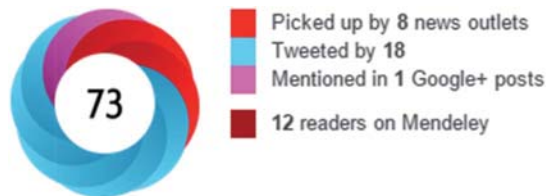
Earn CME while reading *Neurology*. This program is available only to online *Neurology* subscribers. Simply read the articles marked CME, go to Neurology.org, and click on CME. This will provide all of the information necessary to get started. The American Academy of Neurology (AAN) is accredited by the Accreditation Council for Continuing Medical Education (ACCME) to sponsor continuing medical education for physicians. *Neurology* is planned and produced in accordance with the ACCME Essentials. For more information, contact AAN Member Services at 800-879-1960.

Registration Now Open for 2017 AAN Annual Meeting in Boston

Discover the Annual Meeting everyone's talking about. We changed the entire format and feel of the AAN Annual Meeting for 2016—and people took notice! We're doing it again in 2017, and adding even more changes to the docket. Register today to experience the value, choice, customization, and innovation that only an AAN Annual Meeting can offer. We look forward to seeing you April 22-28 in Boston. Register today at AAN.com/view/AM17.

Discover Altmetrics

See real-time downloads and online activity for articles!



[See more details](#)

Authors and readers alike can view real-time data on articles including downloads and online activity across multiple sources. Click on the “Article Metrics” link in the right column of an article for details. To learn more about article metrics visit http://www.neurology.org/site/misc/article_usage.xhtml.

Supplemental Online Content

- GABA_AR cell based assay
- Clinical vignettes (patients 8 and 15)
- Legend to Videoclip
- Table e-1
- Table e-2

GABA_AR cell based assay

To identify antibodies to GABA_AR we used HEK293 cells transfected with human cDNA plasmids containing the $\alpha 1$ (accession number: NM_000806.3; Origene catalog number: SC119668), $\beta 3$ (accession number: NM_000814.3; Origene catalog number: SC125324) or $\gamma 2$ (Uniprot accession number: P18507; Euroimmun M150108RA) subunits of the GABA_AR, alone or in combination ($\alpha 1\beta 3$ or $\alpha 1\beta 3\gamma 2$), using previously reported techniques. Live HEK293 cells were incubated with patient's serum (1:20) or CSF (1:10) for 1 hour at 37°C, then fixed with 4% paraformaldehyde for 5 minutes and permeabilized with 0.3% Triton X-100 for 5 minutes. Cells were then incubated for 1 hour at room temperature with a commercial antibody against the $\alpha 1$ (mouse, dilution 1:10000, Millipore, MAB339), $\beta 3$ (rabbit, dilution 1:3000, Abcam, AB4046) or $\gamma 2$ (goat, dilution 1:2000, Santa Cruz Biotechnology, SC131935) subunits, and then 1 hour with the corresponding fluorescent secondary antibodies (Alexa Fluor 488 goat anti-human IgG, Invitrogen A11013; Dylight 488 donkey anti-human IgG, Abcam AB102424; Alexa Fluor 594: goat anti-mouse IgG, Invitrogen A11032, goat anti-rabbit IgG, Life Technologies A11012, donkey anti-goat IgG, Invitrogen A11058; all diluted 1:1000). Reactivity (**Fig. 2**) was analyzed under a fluorescence microscope using Zeiss Axiovision software, by three investigators (MS, MP and JD) independently. Antibody titers were determined as the highest dilution of the patient's serum or CSF at which reactivity with HEK293 cells was still detectable.

Clinical vignettes

Patient #8

Four days after vaccination against yellow fever, a 10-month old previously healthy girl presented with acute recurrent focal motor seizures (brief episodes of head and eye deviation). A few days later, she became irritable, less interactive and developed choreic movements of the left arm and hypotonia, associated with motor regression (loss of sitting and raising the head). During the following three weeks she developed orofacial and limb dyskinesias, dystonic posturing of the trunk and head, loss of eye contact, decreased level of consciousness, and brainstem signs with bilateral internuclear ophthalmoplegia and dissociated abducting nystagmus (video1.mov). The focal seizures became refractory to antiepileptic medication (diazepam, phenytoin, phenobarbital, midazolam). EEG showed epileptiform discharges in the right fronto-temporal regions and intermittent diffuse slowing, mainly in the occipital regions. CSF cell count and protein concentration were normal (oligoclonal bands were not performed). Infectious work-up was negative and brain MRI was unremarkable. Seizures evolved to convulsive status epilepticus, requiring pharmacological coma (thiopental) and admission to the ICU; valproate and carbamazepine were introduced afterwards. Autonomic instability was also noted, including tachycardia, hypertension, and hyperhidrosis. The diagnosis of autoimmune encephalitis was suspected, and the patient's serum and CSF were found positive for GABA_AR antibodies. Additional studies for NMDAR, AMPAR, DPPX, GABA_BR, LGI1, and CASPR2 antibodies were negative.

Four weeks after symptom onset, she was started on IVIg (0,4 g/Kg/day for 5 days) and, since no improvement was noted after 3 weeks, she received intravenous methylprednisolone (30 mg/Kg/day for 5 days). These treatments were followed by progressive improvement, weaning from mechanical ventilation and discharge from the ICU (where she spent 39 days). Two months after

symptom onset, the seizures had ceased, the movement disorders had substantially subsided, and the patient showed improved motor and language skills. At 4 months after immunotherapy, the patient was almost completely recovered (video1.mov), although at last follow-up visit (8 months after symptom onset, at 18 months of age) she had mild motor and language delay.

Patient #15

A 5 week-old-old previously healthy baby girl presented with fever (38.5°C) and new onset multiple focal seizures (head turning and upper limb rhythmic clonic movements), at times accompanied with impairment of the level of consciousness. The seizures did not respond to initial antiepileptic medication (midazolam and levetiracetam) and evolved to convulsive status epilepticus for which she required admission to the ICU and pharmacological induced coma. EEG showed asymmetric background slowing, electroclinical seizures with multiple epileptic foci and bilateral frontal epileptiform discharges. CSF analysis showed 55 WBC/mm³, with a predominance of lymphocytes and monocytes, leading to empiric treatment with ampicillin, cefotaxime, and acyclovir. Repeat CSF analysis 24 hours later demonstrated 45 red blood cells/mm³, 37 WBC/mm³ (73% lymphocytes, 27% neutrophils), protein concentration (0.76 g/L), and normal glucose. HHV6 DNA was detected by PCR in blood (144 copies/mL) and CSF (100 copies/mL) and acyclovir was replaced by intravenous foscarnet. The remaining extensive infectious work-up was negative, including PCR for HSV1 and HSV2 in CSF, the antibiotics were stopped and the seizures were controlled on 5 antiepileptic drugs (valproate, levetiracetam, midazolam, phenobarbital and topiramate). Brain MRI showed extensive bilateral, asymmetric, cortical-subcortical abnormalities, mostly involving the frontal, temporal, and cerebellar regions, with hemosiderin deposits and diffusion restriction. Subsequently, the patient showed slow progressive improvement, which allowed weaning from mechanical ventilation, tapering of midazolam and valproate, and discharge from the ICU 1 week later. After 21 days of antiviral treatment, repeat CSF studies showed a traumatic tap with 800 red blood cells/mm³ and 95 WBC/mm³ along with negative PCR for HSV1, HSV2 and HHV6. Repeat brain MRI showed unchanged brain abnormalities with moderate

diffused brain atrophy. One month after symptom onset, the patient was seizure free on levetiracetam and topiramate, had mild neurological impairment (episodic irritability and mild hypotonia), and was back home.

One week later (5 weeks after disease onset, at 2.5 months of age), she became hypoactive and developed orofacial and limb dyskinesias, repetitive yawning, and decreased level of consciousness leading to hospital admission. EEG findings were similar to those of the previous study, including bilateral asymmetric diffuse slowing, predominantly in the fronto-temporal regions, with superimposed epileptiform discharges, without correlation with the abnormal movements. Brain MRI showed extensive residual, post-viral, areas of encephalomalacia with no new abnormalities. Repeat infectious work-up was negative, including CSF PCR for HSV1, HSV2 and HSV6. Routine CSF studies showed traumatic tap with 3200 red blood cells/mm³, 40 WBC/mm³, proteins (0.85 g/L). Autoimmune encephalitis was suspected, and the patient was started on IVIg (400mg/kg during 5 days), followed 1 week later by intravenous methylprednisolone (30mg/kg/day for 3 days), with oral tapering. Patient's serum and CSF demonstrated GABA_AR and NMDAR antibodies; no other antibodies were identified. At last follow-up, 6 months after disease onset, she did not have abnormal movements and the seizures were controlled with 3 antiepileptics, but she remained with substantial psychomotor retardation.

Legend to Videoclip (patient # 8): Dystonic posturing with hyperextension of the head and trunk and generalized dyskinesias involving orofacial and cervical regions as well as the upper and lower extremities, predominantly on the left side. The patient had bilateral exotropia and internuclear ophthalmoplegia. In the intensive care unit, her eyes were open but she did not establish eye contact or interact with the environment (no verbal output or motor exploration). Two months after IVIg and methylprednisolone, she was substantially improved, with mild oral dyskinesias, normal visual interaction, and improved motor and verbal performance. At 4 months after immunotherapy, she was almost completely recovered; the dyskinesias had resolved and she had good verbal and motor skills, although she was slightly delayed for her age.

Table e-1: Clinical features in patients with anti-GABA_AR encephalitis according to the presence or absence of a tumor

	Tumor	No tumor	p value
Number of patients (25)*	10	15	
Demographics			
- Median age (range), years	56.5 (16-88)	16 (2.5 mo-74)	< 0.01
- Gender (female)	7/10 (70%)	6/15 (36%)	0.22
Clinical manifestations			
- Prodrome	4/10	5/14	1
- Generalized seizures	4/10	13/15	0.02
- Focal seizures	7/10	13/15	0.35
- Status epilepticus/seizures (any type)	3/7	7/15	1
- Decreased level of consciousness	5/10	5/15	0.44
- Behavioral changes	3/10	9/15	0.22
- Cognitive decline	7/10	8/13	1
- Movement disorders	1/10	7/15	0.08
- Dysautonomia	2/10	2/14	1
Clinical severity			
- mRS \geq 4 at the peak of disease	5/8	9/13	1
- Admission to ICU	3/10	8/15	0.41
Complementary studies			
- MRI multifocal abnormalities	9/10	10/15	0.34
- EEG epileptiform discharges	4/7	11/13	0.28
- EEG focal/diffuse slowing	6/7	6/13	0.15
- CSF abnormal (cell count, proteins or OCB)	4/10	10/14	0.21
- Additional antineuronal antibodies	2/10	4/15	1
Immunotherapy			
- 1 st line only (steroids, PE, IVIg)	6/8	6/14	
- 1 st and 2 nd line (AZA, CTX, CyA, RTX)	2/8	6/14	0.08
- No immunotherapy	0/8	2/14	
Outcome			
- Partial improvement	6/8	8/13	
- Complete recovery	2/8	3/13	0.14
- Death	0/8	2/13	

*25/26 patients were investigated for a tumor; 1 patient was not investigated.

Current study (4 thymoma, 1 SCLC, 1 multiple myeloma, 1 rectal cancer); previous study⁸ (1

Hodgkin's lymphoma, 1 ovarian cancer). AZA=azathioprine; CTX=cyclophosphamide; CyA=cyclosporine; PE=plasma exchange; IVIg=intravenous immunoglobulins; OCB=oligoclonal bands; RTX=rituximab

Table e-2: Distribution of antibody reactivity with the GABA_AR subunits in 26 patients with anti-GABA_AR encephalitis

<p>Patients with antibodies reacting against one subunit (n=4):</p> <ul style="list-style-type: none"> - $\alpha 1$: 2 - $\beta 3$: 2 - $\gamma 2$: 0 	<p>Patients with antibodies reacting against the indicated subunits, in any combination (n=26):</p> <ul style="list-style-type: none"> - $\alpha 1$: 21/26 (81%) - $\beta 3$: 23/26 (88%) - $\gamma 2$: 8/26 (31%)
<p>Patients with antibodies reacting against two subunits (n=18) :</p> <ul style="list-style-type: none"> - $\alpha 1$ and $\beta 3$: 14 - $\beta 3$ and $\gamma 2$: 3 - $\alpha 1$ and $\gamma 2$: 1 	
<p>Patients with antibodies reacting against all three subunits (n=4):</p> <ul style="list-style-type: none"> - $\alpha 1$, $\beta 3$ and $\gamma 2$: 4 	

5.3. Paper III

Human neurexin-3 α antibodies associate with encephalitis and alter synapse development

Núria Gresa-Arribas, Jesús Planagumà, **Mar Petit-Pedrol**, Izumi Kawachi, Shinichi Katada, Carol A. Glaser, Mateus M. Simabukuro, Thaís Armangué, Eugenia Martínez-Hernandez, Francesc Graus, and Josep Dalmau

Neurology. 2016;86(24):2235-42.

Impact Factor JCR 2016 (percentile): 8.32 (D1)

Human neurexin-3 α antibodies associate with encephalitis and alter synapse development



Nuria Gresa-Arribas, PhD
Jesús Planagumà, PhD
Mar Petit-Pedrol, MS
Izumi Kawachi, MD,
PhD
Shinichi Katada, MD,
PhD
Carol A. Glaser, DVM,
MD
Mateus M. Simabukuro,
MD
Thaís Armangué, MD,
PhD
Eugenia Martínez-
Hernández, MD, PhD
Francesc Graus, MD,
PhD
Josep Dalmau, MD, PhD

Correspondence to
Dr. Dalmau:
jdalmau@clinic.ub.es

ABSTRACT

Objective: To report a novel autoimmune encephalitis in which the antibodies target neurexin-3 α , a cell adhesion molecule involved in the development and function of synapses.

Methods: Five patients with encephalitis and antibodies with a similar pattern of brain reactivity were selected. Antigen precipitation and determination of antibody effects on cultured rat embryonic neurons were performed with reported techniques.

Results: Immunoprecipitation and cell-based assays identified neurexin-3 α as the autoantigen of patients' antibodies. All 5 patients (median age 44 years, range 23–50; 4 female) presented with prodromal fever, headache, or gastrointestinal symptoms, followed by confusion, seizures, and decreased level of consciousness. Two developed mild orofacial dyskinesias, 3 needed respiratory support, and 4 had findings suggesting propensity to autoimmunity. CSF was abnormal in all patients (4 pleocytosis, 1 elevated immunoglobulin G [IgG] index), and brain MRI was abnormal in 1 (increased fluid-attenuated inversion recovery/T2 in temporal lobes). All received steroids, 1 IV immunoglobulin, and 1 cyclophosphamide; 3 partially recovered, 1 died of sepsis while recovering, and 1 had a rapid progression to death. At autopsy, edema but no inflammatory cells were identified. Cultures of neurons exposed during days in vitro (div) 7–17 to patients' IgG showed a decrease of neurexin-3 α clusters as well as the total number of synapses. No reduction of synapses occurred in mature neurons (div 18) exposed for 48 hours to patients' IgG. Neuronal survival, dendritic morphology, and spine density were unaffected.

Conclusion: Neurexin-3 α autoantibodies associate with a severe but potentially treatable encephalitis in which the antibodies cause a decrease of neurexin-3 α and alter synapse development. *Neurology*® 2016;86:2235–2242

GLOSSARY

ANA = antinuclear antibodies; **ANOVA** = analysis of variance; **div** = days in vitro; **IDIBAPS** = Institute of Biomedical Research August Pi i Sunyer; **IgG** = immunoglobulin G; **IVIg** = IV immunoglobulin; **LRRTM2** = leucine-rich repeat transmembrane neuronal 2; **NMDAR** = NMDA receptor.

Encephalitis is a severe inflammatory disorder of the brain with many possible causes and a complex differential diagnosis. Studies from different countries and a recent meta-analysis showed that in about 40% of patients with encephalitis the cause is never identified.^{1,2} Without reliable biomarkers, a response to empiric immunotherapy is frequently used to support that the disorder is immune-mediated, but a lack of response does not rule out an immune-mediated pathogenesis. For example, approximately 40% of patients with anti-NMDA receptor (NMDAR) encephalitis fail first-line immunotherapy (steroids, plasma exchange, or IV immunoglobulin [IVIg]) and require second-line therapies (rituximab or cyclophosphamide).^{3,4} However, second-line therapies are rarely used in encephalitis of unclear cause unless evidence of autoimmunity is provided. In this setting, the demonstration of autoantibodies to neuronal cell

Editorial, page 2222

Supplemental data
at Neurology.org

From the Neuroimmunology Program, Biomedical Research Institute August Pi i Sunyer (IDIBAPS) (N.G.-A., J.P., M.P.-P., T.A., E.M.-H., F.G., J.D.), and Service of Neurology, Hospital Clínic (F.G.), University of Barcelona, Spain; Department of Neurology (I.K., S.K.), Brain Research Institute, Niigata University, Japan; Division of Pediatric Infectious Diseases (C.A.G.), Kaiser Permanente, Oakland Medical Center and University of California, San Francisco; Neurology Division (M.M.S.), Hospital das Clínicas, São Paulo University (HC/FMUSP), Brazil; Pediatric Neuroimmunology Unit (T.A.), Sant Joan de Déu Children's Hospital; Department of Neurology (J.D.), University of Pennsylvania, Philadelphia; and Catalan Institution for Research and Advanced Studies (ICREA) (J.D.), Barcelona, Spain. N.G.-A. is currently affiliated with the Department of Neuroscience, Karolinska Institute, Stockholm, Sweden.

Go to Neurology.org for full disclosures. Funding information and disclosures deemed relevant by the authors, if any, are provided at the end of the article.

surface proteins is important for 3 reasons. First, they define the disorder as autoimmune regardless of a response to immunotherapy; second, they support the use of second-line immunotherapies or maintenance of intensive care if needed⁵; and finally, there is evidence that most of the antibodies are pathogenic.⁶ Some antibodies alter the surface dynamics of the cognate receptors causing their internalization (e.g., NMDAR^{7,8} or AMPA receptor⁹), while others block receptor function without altering its surface density (e.g., GABA_A receptor¹⁰). We report the clinical and immunologic features of a novel form of autoimmune encephalitis in which the antibodies target neurexin-3 α , a presynaptic cell adhesion molecule with critical roles in synapse development and function.¹¹ In addition, we show that patients' antibodies alter the formation of synapses.

METHODS Patients. Five patients with encephalitis of unclear cause and antibodies against a previously unknown neuronal cell surface autoantigen are the focus of this study. The 5 cases were identified over the last 10 years in the Laboratory of Neuroimmunology at the Institute of Biomedical Research August Pi i Sunyer (IDIBAPS), Hospital Clínic, University of Barcelona, and the Department of Neurology, University of Pennsylvania. The selection of the 5 cases was based on the distinctive pattern of serum and CSF reactivity with neuropil of rat brain, leading to the investigations reported here. Clinical data were provided by the treating physicians. Control samples (total 200) included serum or CSF of 179 patients with different types of neurologic disorders (well-characterized autoimmune encephalitis, suspected autoimmune encephalitis, neurodegenerative diseases, and multiple sclerosis) and 21 healthy blood donors (supplemental data on the *Neurology*[®] Web site at Neurology.org).

Standard protocol approvals, registrations, and patient consents. The study was approved by the institutional review boards of IDIBAPS and University of Pennsylvania and written consent was obtained.

Determination of antibodies, characterization of the target antigen, and development of a cell-based assay. The techniques involved in these studies are similar to those reported for other neuronal cell surface antibodies and antigens^{7,12,13} and are described in the supplemental data.

Analysis of the effects of the antibodies on cultures of neurons and confocal microscopy. To determine the effects of patients' antibodies at the cellular and synaptic levels, patient or control purified immunoglobulin G (IgG) (final concentration 80 μ g/mL media) were added to cultures of dissociated rat hippocampal neurons at 7, 10, and 14 days in vitro (div).¹⁴ On div 17, cultures were washed with phosphate-buffered saline, fixed with 4% paraformaldehyde, permeabilized with 0.3% Triton X-100, and blocked for 60 minutes with 1% bovine serum albumin. Cells were then incubated overnight at 4°C using single or double immunolabeling with the following antibodies:

anti-leucine-rich repeat transmembrane neuronal 2 (LRRTM2, sheep polyclonal diluted 1:100, AF5589; R&D Systems, Minneapolis, MN), anti-bassoon (mouse monoclonal, 1:400, SAP7F407; Enzo, Farmingdale, NY), or anti-homer1b (rabbit polyclonal, 1:100, PA5-21487; Pierce, Rockford, IL). To determine the levels of cell surface neurexin-3 α , human IgG with neurexin-3 α antibodies (diluted 1:50) was used as a reagent on the live neuronal cultures before permeabilization and fixation (as previously reported for studies with NMDAR antibodies^{7,15}). After the incubation with primary antibodies, slides were washed and incubated for 1 hour at room temperature with the corresponding secondary antibodies (all diluted 1:1,000; Molecular Probes, Eugene, OR), Alexa Fluor 594 donkey anti-sheep IgG (A-11016), Alexa Fluor 488 goat anti-mouse IgG (A-11001), Alexa Fluor 594 goat anti-rabbit IgG (A-11037), or Alexa Fluor 488 goat anti-human IgG (A11013). Slides were then mounted with ProLongGold with 4', 6-diamidino-2-phenylindole dihydrochloride (DAPI, P36935; Molecular Probes) and results scanned with a confocal microscope (Zeiss LSM710; Oberkochen, Germany) with EC-Plan NEOFLUAR CS 100 \times /1.3, 63 \times /1.4, or 20 \times /0.8 NA oil objectives.

To determine whether patients' antibodies caused alteration of neurexin-3 α levels and number of synapses in mature neurons, a similar set of experiments and markers as above were used in cultures of neurons (div 18) exposed for 48 hours to patient or control IgG.

Statistical analysis. The quantitation of neuronal cell death and number of dendritic spines was analyzed using one-way analysis of variance (ANOVA) and the quantitation of the number of dendrites and complexity with 2-way ANOVA (data shown in supplemental data). Confocal cluster densities of neurexin-3 α , LRRTM2, bassoon, or homer1b were analyzed using one-way ANOVA and post hoc testing with Tukey adjustment for multiple comparisons. A *p* value of <0.05 was considered significant. The α error was set at 0.05. All tests were done using GraphPad (La Jolla, CA) Prism (version 6).

RESULTS All 5 patients (median age 44 years, range 23–50 years; 4 female) presented with prodromal symptoms (fever, headache, nausea, or diarrhea) that rapidly progressed (1–7 days, median 3) to confusion, decreased level of consciousness, and seizures (table 1). One patient developed myoclonic jerks and 2 mild orofacial dyskinesias. Three patients required intensive care with respiratory support. Four of the patients had history or laboratory findings suggestive of systemic autoimmunity, such as increased antinuclear antibodies (ANA). One had been diagnosed with lupus 7 years earlier (fatigue, Raynaud phenomenon, proteinuria, decreased complement, double-stranded DNA antibodies, without neurologic symptoms), for which she had been treated with chronic oral steroids. The CSF was abnormal in all patients, showing moderate pleocytosis in 4 and mild increase of IgG index in 1 of 2 cases examined. Brain MRI was normal in 4 of 5 patients, and 1 patient had increased fluid-attenuated inversion recovery/T2 signal in the medial temporal lobes. All 5 patients received steroids, 1 also received IVIg, and 1 cyclophosphamide. Two patients died (patient 2 of

Table 1 Main clinical features of 5 patients with neurexin-3 α antibodies

Patient/ sex/age, y	Prodromal symptoms	Main neurologic symptoms	Other findings	CSF	MRI	Immunotherapy	Outcome
1/F/23	Headache	Confusion, somnolence, memory deficit, confabulation, acute episode of suspected central hypoventilation	Transient thrombocytopenia, leukopenia	1st: normal; 2nd: 20 WBC; normal proteins and glucose	Normal	Steroids	Follow-up at 36 mo: partial recovery; memory deficit, anxiety, respiratory problems (requiring BiPAP at night)
2/M/23	Fever, headache, vomiting, diarrhea	Confusion, extreme agitation, generalized seizures, autonomic instability, myoclonic jerks, coma, ventilatory support	Thrombocytopenia, leukopenia, ANA 1:80	31 WBC; normal proteins, glucose, and IgG index	Normal	Steroids	Unresponsive since hospital admission; died on day 17; autopsy: brain edema, herniation
3/F/50	Fever, headache	Abnormal behavior, seizures, decreased level of consciousness, mild orofacial dyskinesias, central hypoventilation	History of lupus: fatigue, Raynaud, ANA 108.2 index ($n < 20$); anti-dsDNA 16 IU/mL (< 12); anti-RNP 68.7 index (< 22); anti-SS-A 95.9 index (< 30); anti-SS-B 41.1 index (< 25)	Increased IgG index; normal cells, protein, glucose	Abnormal FLAIR/T2, DWI, in medial temporal lobes	Steroids, cyclophosphamide	Follow-up at 24 mo: partial recovery; cognitive deficit, refractory epilepsy
4/F/44	Fever, headache	Confusion, agitation, generalized seizures, incoherent speech, mild orofacial dyskinesias	ANA $> 1:1,280$ ($< 1:40$); negative anti-dsDNA and ANCA; normal C3, C4	10 WBC; normal proteins and glucose	Normal	Steroids, IVIg	Died on day 67 (sepsis); autopsy: mild subarachnoid hemorrhage; lungs with findings suggestive of cytomegalovirus infection
5/F/44	Nausea, diarrhea	Confusion, memory deficit, generalized seizures	Chronic arthralgias, ANA 99.3 index, anti-SS-A 123.9 index, anti-SS-B 147.7 index, thyroglobulin antibodies	24 WBC; proteins 64	Normal	Steroids	Follow-up at 2 mo: substantial recovery, mild cognitive deficit (still improving)

Abbreviations: ANA = antinuclear antibody; ANCA = antineutrophil cytoplasmic antibody; anti-RNP = anti-ribonucleoprotein antibody; BiPAP = bilevel positive airway pressure; dsDNA = double-stranded DNA; DWI = diffusion-weighted image; FLAIR = fluid-attenuated inversion recovery; SS-A/SS-B = Sjögren syndrome related antigen A or B; WBC = white blood cell count.

encephalitis, patient 4 of systemic complications while recovering from the encephalitis) and the other 3 patients had partial recovery after follow-ups of 2, 24, and 26 months. Despite extensive CSF investigations (and neuropathologic studies in 2 patients), no evidence of CNS infection was identified in any of the patients.

The autopsy of patient 2 showed substantial brain edema without evidence of inflammatory infiltrates and no remarkable systemic findings (blood and CSF studies for 16 different viruses studied at the California Encephalitis Project were all negative). The autopsy of patient 4 showed cytopathic changes in the lung compatible with cytomegalovirus infection. In the brain, there was focal and mild subarachnoid hemorrhage, sparse petechiae in the middle cerebellar peduncles, and moderate meningeal hemorrhage; no remarkable microscopic findings or evidence of CNS cytomegalovirus infection were identified.

All 5 patients had antibodies in serum and CSF that reacted with the neuropil of rat brain, producing a similar type of reactivity that was not present in control samples (figure 1, A and C). The pattern of immunostaining in the hippocampus (best seen in figure e-1A) was identical in the 5 patients and different from other neuronal cell surface antibodies reported to date. Studies with live hippocampal neuronal

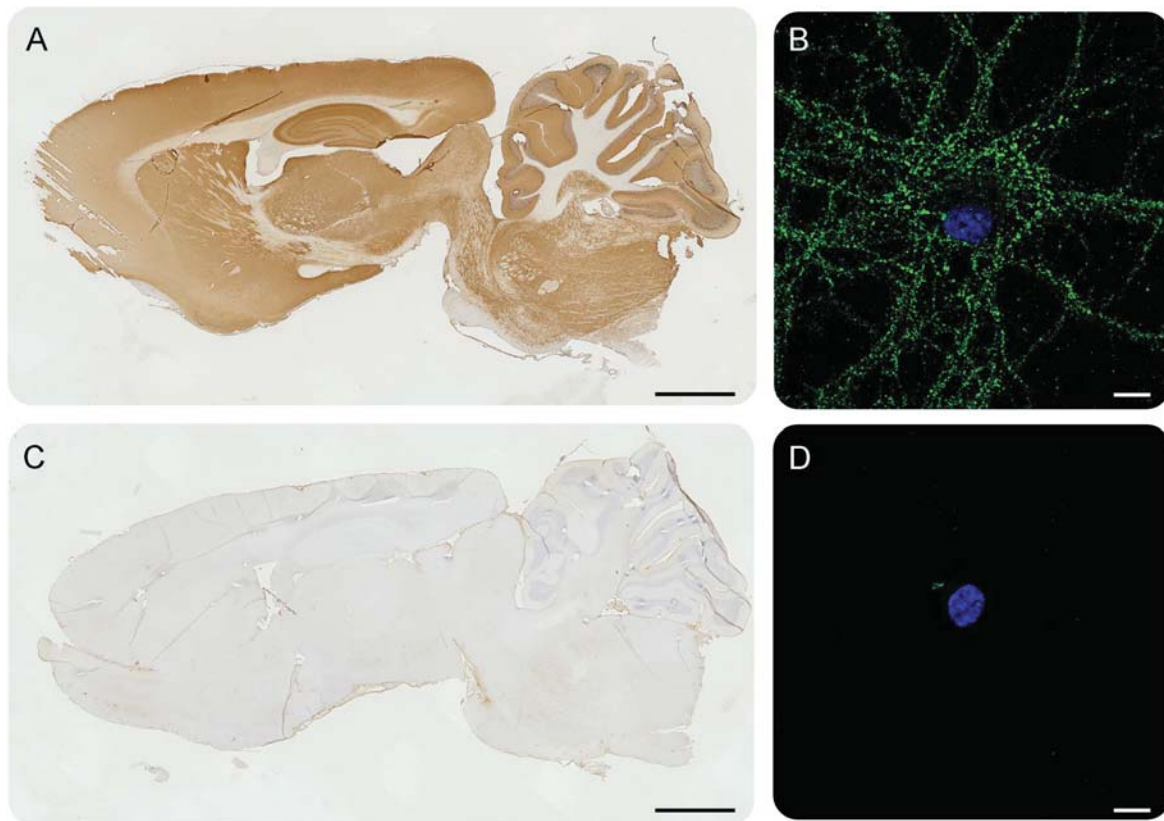
cultures showed that the epitopes were on the neuronal cell surface (figure 1B).

To further confirm that the patients' antibodies recognized the same antigen, we performed immunocompetition assays between the sera of 2 of the patients. This showed that preincubation of brain tissue with serum from one patient abrogated the reactivity of biotinylated IgG of the other patient, confirming that the antibodies of both patients recognized the same epitopes (figure e-1).

In order to identify the target antigen, 2 independent neuronal immunoprecipitations were carried out with sera from 2 different patients. Mass spectrometry of the precipitates showed several sequences of neurexin-3 α in both cases (table e-1).

To further assess that neurexin-3 α was the target antigen of patients' antibodies, patients' serum and CSF were tested in a cell-based assay with HEK293 cells expressing human neurexin-3 α or its ligand LRRTM2. Samples from the 5 patients but none of the 200 controls showed specific reactivity with neurexin-3 α (a representative case is shown in figure 2, A–F). Moreover, the pattern of brain reactivity of patients' antibodies was abrogated when a representative CSF sample was absorbed with HEK cells expressing neurexin-3 α (figure e-2). None of the 5 patients had antibodies against LRRTM2 (figure 2, G–L). To determine if LRRTM2 influenced the

Figure 1 Patients' antibodies react with brain tissue and neuronal cultures



Representative immunoreactivity of patient CSF (A, B) and control CSF (C, D) with sagittal sections of rat brain and cultures of dissociated rat hippocampal neurons. Patients' CSF antibodies (A) show a diffuse immunolabeling of neuropil that is not detected with control CSF (C). Patients' CSF also reacts with the cell surface of live rat hippocampal neurons (B), whereas the control CSF is negative (D). Scale bar for A and C = 2 mm, scale bar for B and D = 20 μ m.

antibody recognition of neurexin-3 α , patients' sera and CSF were incubated with HEK293 cells coexpressing neurexin-3 α and LRRTM2. Cotransfection of both proteins did not modify the intensity of staining of the positive samples (data not shown).

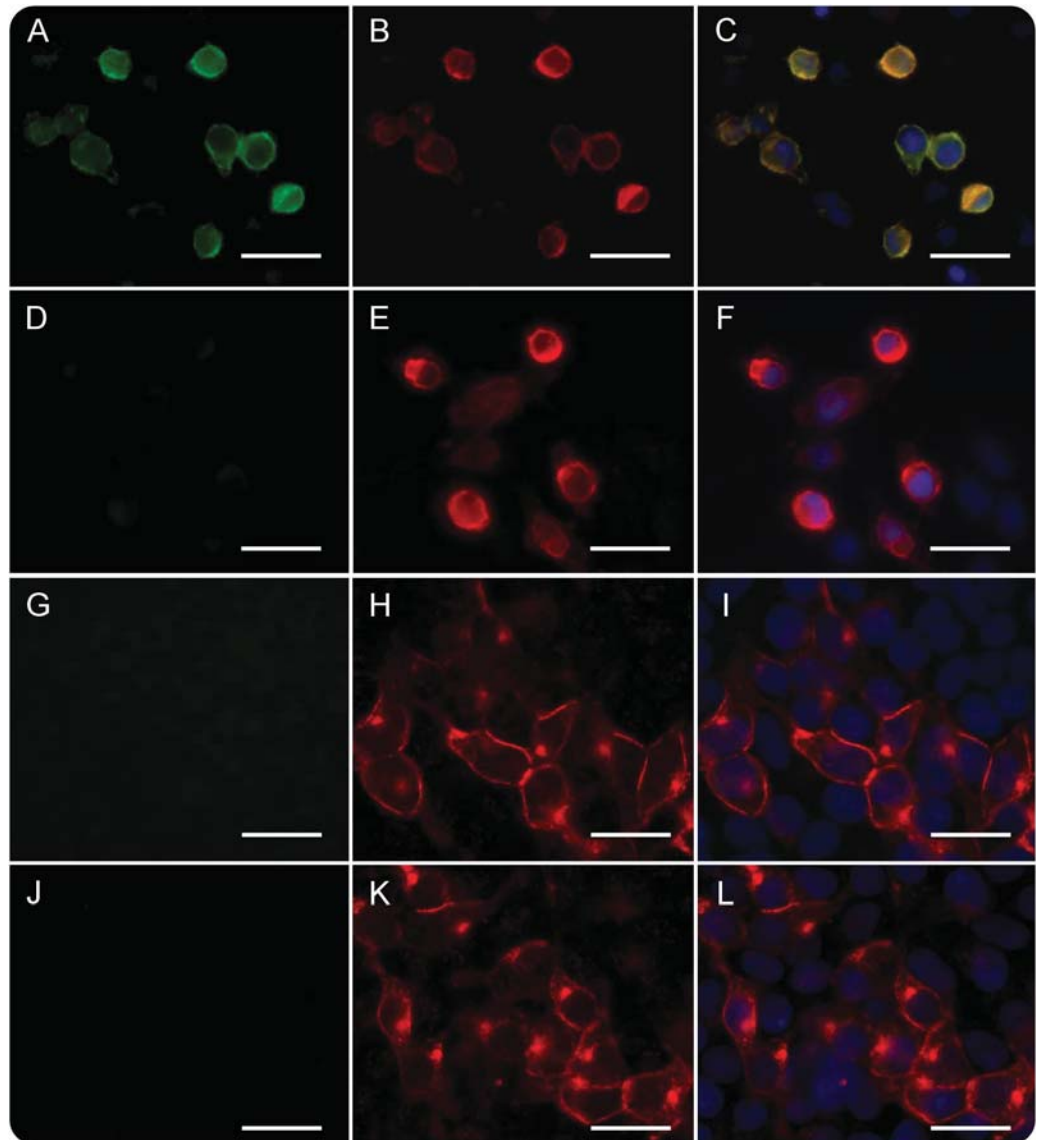
Having demonstrated that patients' antibodies target neurexin-3 α and considering the critical role of this protein in synapse development,¹¹ we next determined the effects of the antibodies on the levels of neurexin-3 α and formation of synapses, as well as on cell survival, number and complexity of dendrites, and spine density. For these studies, patient's IgG was added at regular intervals to dissociated cell cultures of rat embryonic neurons, div 7 to 14, a period during which there is robust development of neuronal processes and establishment of functional synaptic networks (the effects were examined on day 17).¹⁴ Compared to neurons treated with control IgG, those treated with patient IgG had a decrease of cell surface clusters of neurexin-3 α , as well as of clusters of neurexin-3 α colocalizing with LRRTM2; however, the density of clusters of LRRTM2 was not altered (figure 3). Additionally, neurons treated with patient IgG, but not control IgG, showed a decrease in the total number of synapses, defined by the colocalization

of a presynaptic marker (bassoon) with a postsynaptic marker (homer1b), as well as a decrease in the total clusters of bassoon and homer1b (figure 4). No effects were noted on neuronal survival (data not shown), number and complexity of dendrites, or spine density (figure e-3). Similar studies using mature neurons (div 18) exposed for 48 hours to patients' IgG showed a significant decrease of neurexin-3 α without affecting LRRTM2 or the number of synapses (figure e-4). Overall, these findings indicate that patients' antibodies cause a specific reduction of neurexin-3 α , which in turn decreases the total number of synapses in neurons undergoing development.

DISCUSSION We report a novel type of autoimmune encephalitis characterized by antibodies against extracellular epitopes of neurexin-3 α . The disorder is important for 3 reasons: first, symptoms are severe (with a rapid course to death in one patient) but potentially treatable; second, the initial clinical picture in some patients may suggest anti-NMDAR encephalitis; and third, the antibodies cause a decrease of neurexin-3 α and formation of synapses.

The combination of young age, rapid decline of the level of consciousness, seizures, orofacial

Figure 2 Patients' antibodies react with neurexin-3 α but not leucine-rich repeat transmembrane neuronal 2 (LRRTM2)



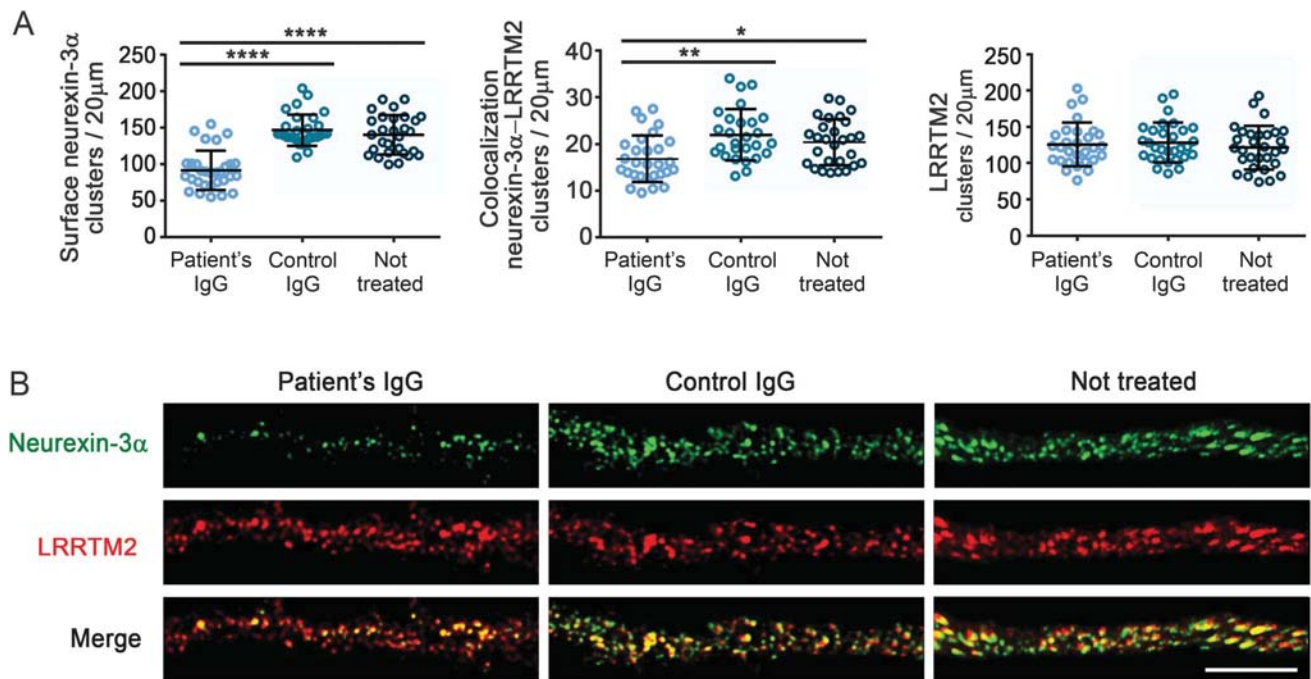
(A) The serum of a representative patient reacts with HEK293 cells expressing neurexin-3 α ; in contrast, no reactivity is observed with the serum of a healthy control (D). (B, E) Correspond to the same cells immunolabeled with a commercial neurexin-3 α antibody; (C, F) the merged reactivities. In (G-L), a similar experiment is shown with HEK293 cells expressing LRRTM2; no reactivity is observed with the patient's (G) or control (J) serum. Scale bar = 10 μ m.

dyskinesias, or central hypoventilation resembles the clinical picture of anti-NMDAR encephalitis.³ This diagnosis was clinically considered in patients 1, 3, and 4, but NMDAR antibody testing with cell-based assay was negative and the pattern of brain immunostaining, although robust and similar in all patients, was clearly different from that associated with NMDAR antibodies. None of the patients developed prolonged psychiatric symptoms or prominent abnormal movements other than mild orofacial dyskinesias or had teratoma, which are frequent features in adults with anti-NMDAR encephalitis. In line with other types of autoimmune encephalitis,^{13,16} 4 of the 5 patients had ANA or other non-neuronal

autoantibodies suggesting propensity to autoimmunity. Despite this, only 1 patient received second-line immunotherapy. This is probably due to the rapid course of the disease in patient 2, who died before aggressive immunotherapy could be tried, the limited knowledge on autoimmune encephalitis at the time patients 2 and 4 were studied (2006 and 2008, respectively), and the rapid response to steroids of patient 5.

The absence of brain inflammatory infiltrates in the autopsy of patients 2 and 4, despite both having CSF pleocytosis at symptom onset, is puzzling. In 4 patients, the antibody IgG isotype was investigated; 3 were only IgG1, and 1 IgG1 along with a minor

Figure 3 Patient antibodies cause a reduction in neurexin-3 α



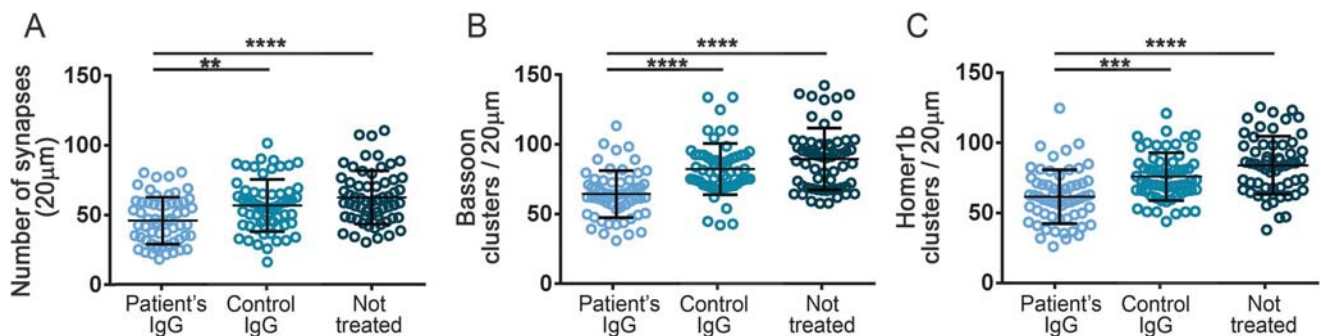
Hippocampal neurons treated during 10 days with patient immunoglobulin G (IgG), control IgG, or not treated were examined on days in vitro (div) 17 for the density of cell surface neurexin-3 α , the colocalization of neurexin-3 α with its ligand leucine-rich repeat transmembrane neuronal 2 (LRRTM2), and the density of LRRTM2. (A) Compared with control IgG or not treated neurons, patient IgG caused a significant reduction in the clusters of cell surface neurexin-3 α (left) as well as the colocalization of neurexin-3 α with its ligand LRRTM2 (middle), but had no effects on LRRTM (right). (B) Representative pictures of each condition. Note the significant reduction of the clusters of neurexin-3 α as well as the colocalization of neurexin-3 α with LRRTM2 (merge) in neurons treated with patient IgG. Scale bar = 5 μ m. All graphs represent mean \pm SD of 3 independent experiments (for each experiment, 10 dendrites per condition); * p < 0.05, ** p < 0.01, **** p < 0.0001.

component of IgG4 (data not shown), suggesting the potential for complement activation (not investigated) and recruitment of inflammatory infiltrates. We postulate the autopsy findings could be related to the fulminant disease of patient 2, whose death was likely caused by refractory seizures and brain edema, raising the possibility that mild inflammatory infiltrates could have been missed. Patient 4 died of sepsis and systemic complications after neurologic

improvement; the autopsy showed mild subarachnoid hemorrhage. In this case, it is possible that the brain inflammation had resolved by the time of the patient's death (day 67). Nevertheless, the absence of brain inflammation is in contrast to what is found in other autoimmune encephalitis cases and needs further study.^{17,18}

Neurexins are a family of synaptic cell adhesion molecules involved in synapse formation and maturation.

Figure 4 Patient antibodies interfere with the formation of synapses



Cultures of hippocampal neurons were treated for 10 days with patient immunoglobulin G (IgG) or control IgG or not treated, and the effect on the number of synapses (defined as clusters of the presynaptic marker bassoon colocalizing with the postsynaptic marker homer1b) was determined. The study shows that patient IgG antibodies, but not control IgG, caused a significant reduction of the number of synapses (A) as well as bassoon (B) and homer1b (C). All graphs represent mean \pm SD of 5 independent experiments (for each experiment, 10 dendrites per condition); ** p < 0.01, *** p < 0.001, **** p < 0.0001.

They are encoded by 3 genes—*NRX1*, *NRX2*, and *NRX3*—each of them providing 2 alternative splice products, a long α and a short β form.¹¹ Each neurexin can bind to a small number of postsynaptic ligands, including neuroligins, cerebellins, and LRRTMs^{11,19}; neurexin-3 α binds specifically to LRRTM2.^{20,21} The serum and CSF of our 5 patients contained antibodies against neurexin-3 α but not LRRTM2.

Neurexins act as a link between presynaptic and postsynaptic compartments, with the intracellular domain interacting with the presynaptic machinery for neurotransmitter release, and the extracellular domain binding to postsynaptic cell adhesion molecules.¹¹ Abrogating the expression of all 3 α neurexins in mice resulted in postnatal death and a dramatic reduction of Ca²⁺-triggered neurotransmitter release.²² Specific ablation of neurexin-3 showed different presynaptic and postsynaptic functions in distinct brain regions. For example, in the hippocampus, extracellular sequences of presynaptic neurexin-3 mediate transsynaptic regulation of postsynaptic AMPA receptors, whereas in the olfactory bulb, intracellular sequences of neurexin-3 are selectively required for GABA release.²³ Mutations in the neurexin genes have been associated with schizophrenia^{24–26} and autism.^{24,27–29}

Using rat embryonic neurons in the stage of maturation and development of functional synaptic networks (e.g., div 7–17), we found that patients' antibodies caused a specific reduction of the levels of neurexin-3 α as well as a decrease of the total number of synapses (defined by the colocalization of the presynaptic marker bassoon³⁰ with the postsynaptic marker homer1b³¹). A similar study using mature neurons (div 18) exposed for 48 hours to patients' antibodies showed a decrease of the levels of neurexin-3 α , without affecting the total number of synapses. Thus, the antibody-mediated decrease of neurexin-3 α affects synapse development. These findings are in line with studies showing that disruption of endogenous neurexin–neuroligin interaction by adding a recombinant neurexin reduces the number of presynaptic terminals and the number of inhibitory and excitatory synapses.^{32,33}

Our study has the limitation of a small number of patients. This often occurs in the initial description of a novel autoimmune encephalitis and prevents an estimation of disease frequency. For example, the first 2 reports on the clinical and immunologic findings of anti-NMDAR encephalitis had 4 and 12 patients^{12,34}; however, after the disorder was known and a diagnostic test developed, identification of cases increased and it is now considered one of the most frequent autoimmune encephalitis.³⁵ In some patients with neurexin-3 α antibodies, the clinical presentation

suggests an infectious etiology and the course of the disease can be fulminant (e.g., patient 2). It is likely that patients with these presentations are not considered for neuronal antibody testing, thus missing the diagnosis.

Future studies should aim to fully characterize the syndrome reported here and the mechanisms by which the antibodies decrease the levels of neurexin-3 α , which in turn alter the formation of synapses, and may affect presynaptic (neurotransmitter release) and postsynaptic functions (e.g., AMPA receptor regulation).²³ It is unclear whether the antibodies affect the maintenance of synapses in mature neurons; we did not see an effect after 48 hours of exposure but longer treatments may be necessary. The clinical features, immunologic findings, and diagnostic test provided in the current study are the first steps toward these goals.

AUTHOR CONTRIBUTIONS

Design/conceptualization of the study: N.G.-A. and J.D.; analysis/interpretation of the data: all authors; statistical analysis and figure development: N.G.-A., J.P., M.P.-P., J.D.; drafting/revising the manuscript: all authors.

ACKNOWLEDGMENT

The authors thank Dr. Thomas C. Südhof (Stanford University) for providing the plasmid with the human sequence of neurexin-3 α .

STUDY FUNDING

Supported in part by NIH RO1NS077851 (J.D.); Fondo de Investigaciones Sanitarias, FEDER, Spain (FIS PI12/00611, FG; FIS 14/00203, J.D.); Instituto de Salud Carlos III, Madrid, Spain (CM14/00081, TA; CD 14/00155, E.M.-H.); Asociación Española de Pediatría research grant from Dodot-Procter & Gamble (T.A.); and Fundació CELLEX (J.D.).

DISCLOSURE

N. Gresa-Arribas, J. Planagumà, M. Petit-Pedrol, I. Kawachi, S. Katada, C. Glaser, M. Simabukuro, T. Armangue, E. Martínez-Hernández, and F. Graus report no disclosures relevant to the manuscript. J. Dalmau has a research grant from Euroimmun and receives royalties from patents for the use of Ma2 and NMDAR as autoantibody tests. Go to Neurology.org for full disclosures.

Received November 25, 2015. Accepted in final form February 29, 2016.

REFERENCES

1. Vora NM, Holman RC, Mehal JM, Steiner CA, Blanton J, Sejvar J. Burden of encephalitis-associated hospitalizations in the United States, 1998–2010. *Neurology* 2014;82:443–451.
2. Glaser CA, Honarmand S, Anderson LJ, et al. Beyond viruses: clinical profiles and etiologies associated with encephalitis. *Clin Infect Dis* 2006;43:1565–1577.
3. Titulaer MJ, McCracken L, Gabilondo I, et al. Treatment and prognostic factors for long-term outcome in patients with anti-NMDA receptor encephalitis: an observational cohort study. *Lancet Neurol* 2013;12:157–165.
4. Nosadini M, Mohammad SS, Ramanathan S, Brilot F, Dale RC. Immune therapy in autoimmune encephalitis: a systematic review. *Expert Rev Neurother* 2015;15:1391–1419.

5. Dalmau J, Tuzun E, Wu HY, et al. Paraneoplastic anti-N-methyl-D-aspartate receptor encephalitis associated with ovarian teratoma. *Ann Neurol* 2007;61:25–36.
6. Leyboldt F, Armangue T, Dalmau J. Autoimmune encephalopathies. *Ann NY Acad Sci* 2015;1338:94–114.
7. Hughes EG, Peng X, Gleichman AJ, et al. Cellular and synaptic mechanisms of anti-NMDA receptor encephalitis. *J Neurosci* 2010;30:5866–5875.
8. Mikasova L, De Rossi P, Bouchet D, et al. Disrupted surface cross-talk between NMDA and Ephrin-B2 receptors in anti-NMDA encephalitis. *Brain* 2012;135:1606–1621.
9. Peng X, Hughes EG, Moscato EH, Parsons TD, Dalmau J, Balice-Gordon RJ. Cellular plasticity induced by anti-alpha-amino-3-hydroxy-5-methyl-4-isoxazolepropionic acid (AMPA) receptor encephalitis antibodies. *Ann Neurol* 2015;77:381–398.
10. Jain A, Lancaster E, Dalmau J, Balice-Gordon RJ. Autoantibodies in the CSF of anti-GABA receptor encephalitis patients block activation of GABA receptors in vitro (abstract M116, 140th annual meeting of the American Neurological Association). *Ann Neurol* 2015;78(suppl 19):S77.
11. Sudhof TC. Neuroligins and neuroligins link synaptic function to cognitive disease. *Nature* 2008;455:903–911.
12. Dalmau J, Gleichman AJ, Hughes EG, et al. Anti-NMDA-receptor encephalitis: case series and analysis of the effects of antibodies. *Lancet Neurol* 2008;7:1091–1098.
13. Lai M, Hughes EG, Peng X, et al. AMPA receptor antibodies in limbic encephalitis alter synaptic receptor location. *Ann Neurol* 2009;65:424–434.
14. Buchhalter JR, Dichter MA. Electrophysiological comparison of pyramidal and stellate nonpyramidal neurons in dissociated cell culture of rat hippocampus. *Brain Res Bull* 1991;26:333–338.
15. Planaguma J, Leyboldt F, Mannara F, et al. Human N-methyl D-aspartate receptor antibodies alter memory and behaviour in mice. *Brain* 2015;138:94–109.
16. Petit-Pedrol M, Armangue T, Peng X, et al. Encephalitis with refractory seizures, status epilepticus, and antibodies to the GABAA receptor: a case series, characterisation of the antigen, and analysis of the effects of antibodies. *Lancet Neurol* 2014;13:276–286.
17. Bien CG, Vincent A, Barnett MH, et al. Immunopathology of autoantibody-associated encephalitides: clues for pathogenesis. *Brain* 2012;135:1622–1638.
18. Martinez-Hernandez E, Horvath J, Shiloh-Malawsky Y, Sangha N, Martinez-Lage M, Dalmau J. Analysis of complement and plasma cells in the brain of patients with anti-NMDAR encephalitis. *Neurology* 2011;77:589–593.
19. Krueger DD, Tuffy LP, Papadopoulos T, Brose N. The role of neuroligins and neuroligins in the formation, maturation, and function of vertebrate synapses. *Curr Opin Neurobiol* 2012;22:412–422.
20. Siddiqui TJ, Pancaroglu R, Kang Y, Rooyackers A, Craig AM. LRRTMs and neuroligins bind neuroligins with a differential code to cooperate in glutamate synapse development. *J Neurosci* 2010;30:7495–7506.
21. Aoto J, Martinelli DC, Malenka RC, Tabuchi K, Sudhof TC. Presynaptic neuroligin-3 alternative splicing trans-synaptically controls postsynaptic AMPA receptor trafficking. *Cell* 2013;154:75–88.
22. Missler M, Zhang W, Rohlmann A, et al. Alpha-neuroligins couple Ca²⁺ channels to synaptic vesicle exocytosis. *Nature* 2003;423:939–948.
23. Aoto J, Foldy C, Ilcus SM, Tabuchi K, Sudhof TC. Distinct circuit-dependent functions of presynaptic neuroligin-3 at GABAergic and glutamatergic synapses. *Nat Neurosci* 2015;18:997–1007.
24. Gauthier J, Siddiqui TJ, Huashan P, et al. Truncating mutations in NRXN2 and NRXN1 in autism spectrum disorders and schizophrenia. *Hum Genet* 2011;130:563–573.
25. Rujescu D, Ingason A, Cichon S, et al. Disruption of the neuroligin 1 gene is associated with schizophrenia. *Hum Mol Genet* 2009;18:988–996.
26. Ikeda M, Aleksic B, Kinoshita Y, et al. Genome-wide association study of schizophrenia in a Japanese population. *Biol Psychiatry* 2011;69:472–478.
27. Feng J, Schroer R, Yan J, et al. High frequency of neuroligin 1beta signal peptide structural variants in patients with autism. *Neurosci Lett* 2006;409:10–13.
28. Liu Y, Hu Z, Xun G, et al. Mutation analysis of the NRXN1 gene in a Chinese autism cohort. *J Psychiatr Res* 2012;46:630–634.
29. Vaags AK, Lionel AC, Sato D, et al. Rare deletions at the neuroligin 3 locus in autism spectrum disorder. *Am J Hum Genet* 2012;90:133–141.
30. Tom DS, Sanmarti-Vila L, Langnaese K, et al. Bassoon, a novel zinc-finger CAG/glutamine-repeat protein selectively localized at the active zone of presynaptic nerve terminals. *J Cell Biol* 1998;142:499–509.
31. Hayashi MK, Tang C, Verpelli C, et al. The postsynaptic density proteins Homer and Shank form a polymeric network structure. *Cell* 2009;137:159–171.
32. Scheiffele P, Fan J, Choih J, Fetter R, Serafini T. Neuroligin expressed in nonneuronal cells triggers presynaptic development in contacting axons. *Cell* 2000;101:657–669.
33. Levinson JN, Chery N, Huang K, et al. Neuroligins mediate excitatory and inhibitory synapse formation: involvement of PSD-95 and neuroligin-1beta in neuroligin-induced synaptic specificity. *J Biol Chem* 2005;280:17312–17319.
34. Vitaliani R, Mason W, Ances B, Zwerdling T, Jiang Z, Dalmau J. Paraneoplastic encephalitis, psychiatric symptoms, and hypoventilation in ovarian teratoma. *Ann Neurol* 2005;58:594–604.
35. Granerod J, Ambrose HE, Davies NW, et al. Causes of encephalitis and differences in their clinical presentations in England: a multicentre, population-based prospective study. *Lancet Infect Dis* 2010;10:835–844.

Supplemental information

- Control samples (200 subjects)
- Immunohistochemistry of rat brain
- Immunocytochemistry on neuronal cultures
- Immunocompetition assay
- Immunoprecipitation
- Immunocytochemistry on HEK293 cells
- Immunoabsorption with HEK cells expressing neurexin-3 α
- Quantitation of neuronal death
- Quantitation of the number of dendrites, dendritic complexity, and spine density

Control samples (200 subjects)

Control samples included 21 sera from healthy blood donors, 14 sera from patients with neurodegenerative disorders, 20 sera from patients with multiple sclerosis, 38 sera (and 32 paired CSF) from patients with well-characterized autoimmune encephalitis (18 NMDAR, 8 LGI1, 3 AMPAR, 3 Caspr2, 3 GABAaR, 3 GABAbR), and 107 CSF (with 95 paired sera) from patients with encephalitis suspected to be autoimmune (reactivity against unknown neuropil antigens).

Immunohistochemistry with rat brain

Adult female Wistar rats were sacrificed without perfusion, and the brains removed and fixed by immersion in 4% paraformaldehyde for 1 hour at 4°C, cryoprotected in 40% sucrose for 24 hours, embedded in freezing compound media, and snap frozen in isopentane chilled with liquid nitrogen. Seven-micrometer-thick tissue sections were then sequentially incubated with 0.3% H₂O₂ for 15 minutes, 5% goat serum for 1 hour, and patient or control serum (1:200) or CSF (1:2) at 4°C overnight. After using a biotinylated secondary antibody against human IgG (diluted 1:2000; BA-3000, Vector laboratories) for 1 hour at room temperature (RT), the reactivity was developed with the avidin-biotin-peroxidase method. Results were photographed with an AxioCam MRc colour camera adapted to a confocal microscope (Zeiss LSM710) and analysed with Zen software (Zen 2012 blue edition 1.1.1.0, Zeiss).

Immunocytochemistry with neuronal cultures

Dissociated cell cultures of rat hippocampal neurons were prepared as reported.¹ Live neurons grown on coverslips were incubated for 1 hour at 37°C with patient or control serum (final dilution 1:200) or CSF (1:5). After removing the media and washing with

phosphate-buffered saline (PBS), neurons were fixed with 4% paraformaldehyde, permeabilized with 0.3% Triton X-100, and immunolabeled with Alexa Fluor 488 goat anti-human IgG (1:1000, A11013, Molecular Probes) for 1 hour at RT. Images were captured with an epifluorescence microscope using Zeiss Axiovision software (Zeiss, Thornwood, NY, USA).

Immunocompetition assay

To determine whether patients' antibodies were directed against similar epitopes of neurexin-3 α , immunocompetition studies were performed. IgG was isolated from a patient whose serum contained high levels of IgG antibodies against neurexin-3 α using protein A and G sepharose beads (20423, Pierce), and subsequently eluted and labelled with biotin (Vector, SP1200), as reported.² Then, sections of rat brain were pre-incubated with other patients' or control sera (diluted 1:5) overnight at 4°C, washed in PBS, incubated with the indicated human biotinylated IgG containing neurexin-3 α antibodies (diluted 1:20) for 1 hour at RT, and the reactivity was developed with the avidin-biotin-peroxidase method. Two sera were considered to compete for the same neurexin-3 α epitopes when pre-incubation of the tissue with one serum abrogated the reactivity of the other patient's IgG. Pictures were taken under a confocal microscope as described above.

Immunoprecipitation

Live neurons obtained as above, were grown in 100 mm dishes (density 1×10^6 neurons/dish), and incubated at 37°C with filtered patient serum (diluted 1:200) for 1 hour. Neurons were then washed with PBS, lysed with buffer (NaCl 150mM, EDTA 1mM, tris(hydroxymethyl)aminomethane [Tris]-HCl 100mM, deoxycholate acid 0.5%, 1% Triton X-100 [Sigma Labs], pH 7.5) containing protease inhibitors (P8340; Sigma Labs), and centrifuged at 16.1×10^3g for 20 minutes at 4°C. The supernatant was retained and incubated with protein A/G agarose beads (20423; Pierce) overnight at 4°C, centrifuged, and the pellet containing the beads with patient's antibodies bound to the target cell surface antigen was then washed with PBS, resuspended in Laemmli buffer, boiled for 5 minutes, separated in a 4 to 15% sodium dodecyl sulfate polyacrylamide gel electrophoresis, and the proteins visualized with EZBlue gel staining (G1041; Sigma Labs). Visible protein bands precipitated by patient's serum were excised from the gel and analyzed using mass

spectrometry at the Proteomics Core Facility of the Genomics Institute at the Abramson Cancer Center (University of Pennsylvania).

Immunocytochemistry on HEK293 cells

HEK293 cells were transfected with plasmids containing human neurexin-3 α (courtesy of Dr. Südhof) or LRRTM2 (sc-114672, Origene). Cells were grown for 24 hours after transfection before assessment. Transfected cells were fixed in 4% paraformaldehyde, permeabilized with 0.3% Triton X-100, blocked in 1% BSA for 60 minutes, and then incubated overnight at 4°C with patients' serum (1:40) or CSF (1:5) and depending on the antigen of interest one of the following antibodies, anti-neurexin-3 α (rabbit polyclonal diluted 1:2000, ABN96 Millipore) or anti-LRRTM2 (rabbit polyclonal diluted 1:500, ab106627 Abcam), followed by incubation with the corresponding fluorescent secondary antibodies, Alexa Fluor 488 goat anti-human IgG and Alexa Fluor 594 goat anti-rabbit IgG, (all used at 1:1000, A11013 and A11012 respectively, Molecular Probes) for 1h at RT. Results were imaged under Apotome 2 fluorescence microscope (Zeiss), using the Zen black software (Zeiss).

Immunoabsorption with HEK cells expressing neurexin-3 α

To determine if patients' serum or CSF samples contained additional antibodies that resulted in the indicated brain immunostaining, CSF (diluted 1:80) from a representative patient was pre-absorbed during 6 hours with HEK293 cells expressing neurexin-3 α or non-transfected cells. Every hour the culture media (2 ml) with patient's antibodies was moved to a new 3.5 cm plate containing HEK293 cells expressing or not expressing neurexin-3 α (6 sequential incubations at RT in 6 hours; all using fixed and permeabilized HEK293 cells). The reactivity of the pre-absorbed and post-absorbed CSF was then assessed using rat brain immunohistochemistry as above.

Quantitation of neuronal death

Hippocampal cultures were treated with patient's or control IgG as indicated above. At *div* 17 cells were washed with PBS, fixed with 4% paraformaldehyde, permeabilized with

0.3% Triton X-100, and blocked for 60 minutes with 1% BSA. Cells were then incubated overnight at 4°C with MAP2 antibody (mouse monoclonal, diluted 1:2000, M1406, Sigma-Aldrich), washed and incubated for 1 hour at RT with Alexa Fluor 594 goat anti-mouse (A-11005, Molecular probes), washed, and mounted with ProlonGold with DAPI (P36935, Molecular Probes). The number of neurons in 10 fields (20x objective) in 4 independent experiments (total 40 fields) were photographed and counted using the public domain Fiji ImageJ software (<http://fiji.sc/Fiji>).

Quantitation of the number of dendrites, dendritic complexity, and spine density

17 *div* hippocampal neurons treated with patient's IgG or control IgG were fixed and permeabilized as above and incubated with MAP2 antibodies (to identify dendrites; mouse monoclonal, diluted 1:2000, M1406, Sigma-Aldrich) and β -actin antibodies (to identify spines; mouse monoclonal, diluted 1:2000, A1978, Sigma-Aldrich), followed by the secondary antibody Alexa Fluor 594 goat anti-mouse (A-1100, Molecular Probes). Five fields from 3 independent experiments (total 15 fields) per condition were photographed with a 63x objective and 0.6 zoom and standardized z-stacks including 25 optical images were acquired using sequential scanning, 1024×1024 lateral resolution, and Nyquist optimized z sampling frequency. Images were deconvolved and analyzed using a filament tracer algorithm (Imaris suite 7.6.4, Bitplane). Dendrite length was expressed in μm , the number of dendrites was classified according to dendrite order, and dendrites from each category were expressed as percentage of total. To quantify the number of spines, only secondary and tertiary dendrites longer than 20 μm were analyzed. Density of spines was expressed as number of spines/20 μm .

Supplemental References

1. Buchhalter JR, Dichter MA. Electrophysiological comparison of pyramidal and stellate nonpyramidal neurons in dissociated cell culture of rat hippocampus. *Brain Res Bull* 1991;26:333-338.
2. Furneaux HM, Rosenblum MK, Dalmau J, Wong E, Woodruff P, Graus F, Posner JB. Selective expression of Purkinje-cell antigens in tumor tissue from patients with paraneoplastic cerebellar degeneration. *New England Journal of Medicine* 1990;322:1844-1851.

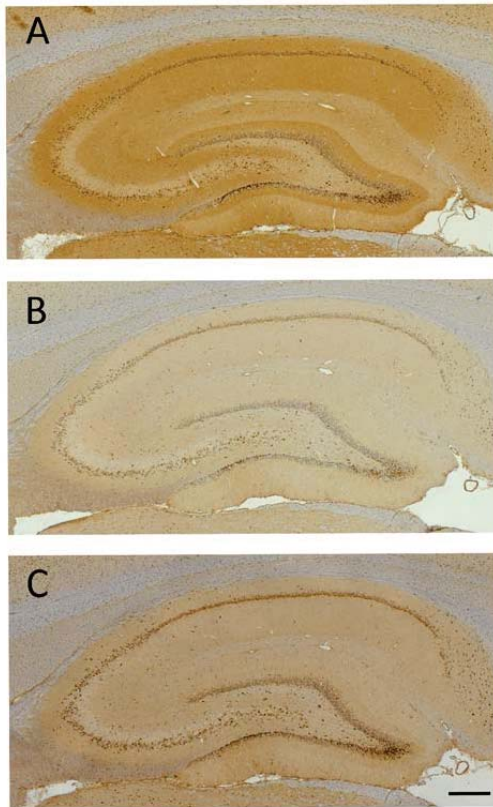
Table e-1: Sequences of neuronal protein immunoprecipitatesSerum 1:

Peptide sequence	Neurexin 3α peptide identification probability	Sequest X Corr	Sequest delta Cn
EASILSYDGSMYMK	95%	4,70	0,11
FICDCTGTGYWGR	95%	4,21	0,49
AYGLLVATTSR	95%	4,20	0,54
LEFHNIETGIMTEK	95%	3,88	0,33
MGSISFDFR	95%	3,53	0,46
TPVNDGKYHVVR	95%	3,53	0,43
SGGLILYTPANDRPSTR	95%	3,33	0,37
NGDIDYCELK	95%	3,23	0,36
LPDLINDALHR	95%	3,16	0,36
LMVNLDCIR	95%	3,16	0,36
QLAEMQNAAGVK	95%	3,14	0,36
GPETLYAGQK	95%	3,09	0,39
NGLLHTGK	95%	2,99	0,25
VVTQVINGAK	95%	2,91	0,33
IYGEVVK	95%	2,65	0,36
VIMPMVMHTEAEDVSFR	95%	2,46	0,40
EENVATFR	95%	2,14	0,30

Serum 2:

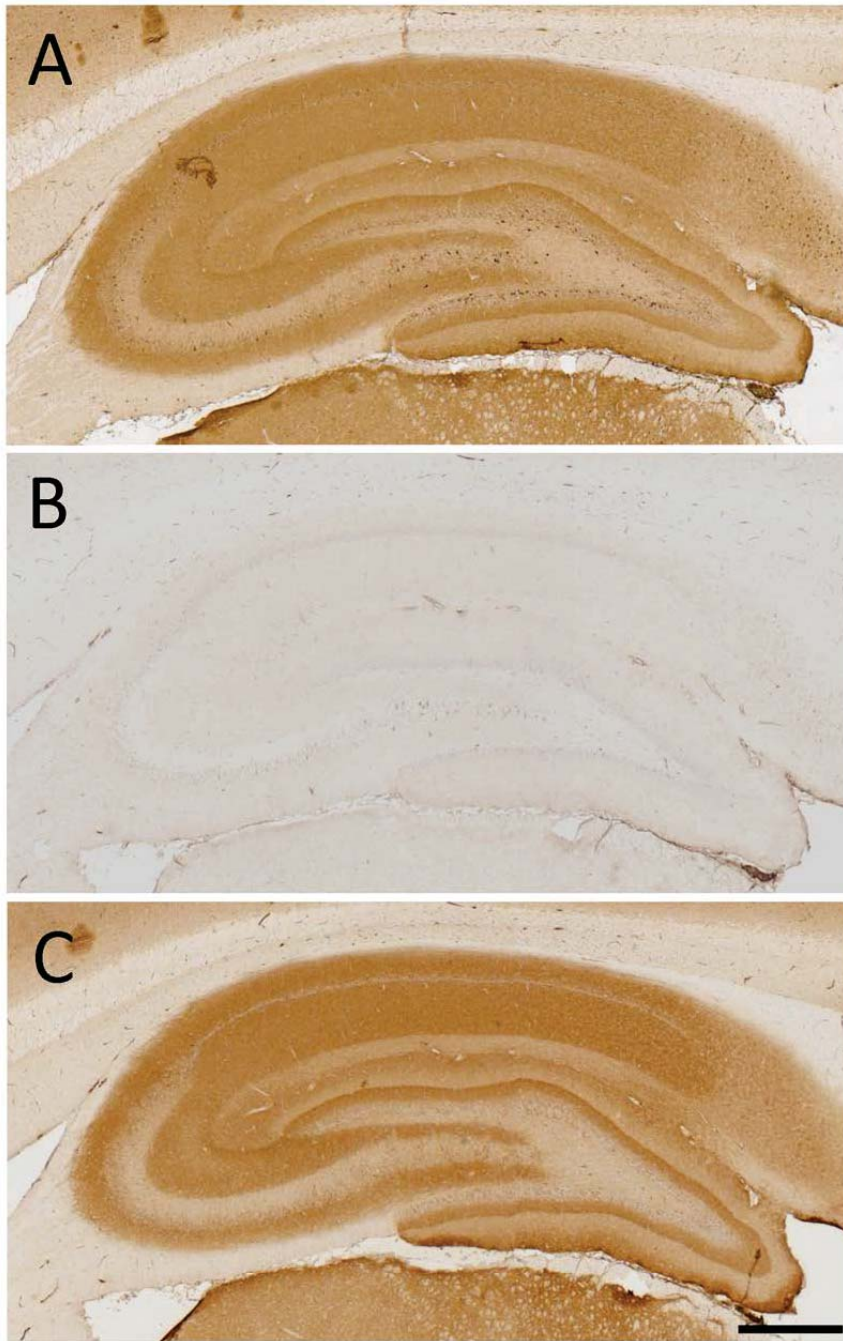
Peptide sequence	Neurexin 3α peptide identification probability	Sequest X Corr	Sequest delta Cn
AYGLLVATTSR	95%	4,42	0,53
TPVNDGKYHVVR	95%	3,48	0,47
VVTQVINGAK	95%	3,15	0,37
QLAEMQNAAGVK	95%	2,42	0,36
NGLIHTGK	95%	3,03	0,48
MGSISFDFR	95%	3,13	0,49
LMVNLDCIR	95%	2,93	0,27
GPETLYAGQK	95%	2,91	0,37

Figure e-1: Patients' antibodies compete for the same antigen



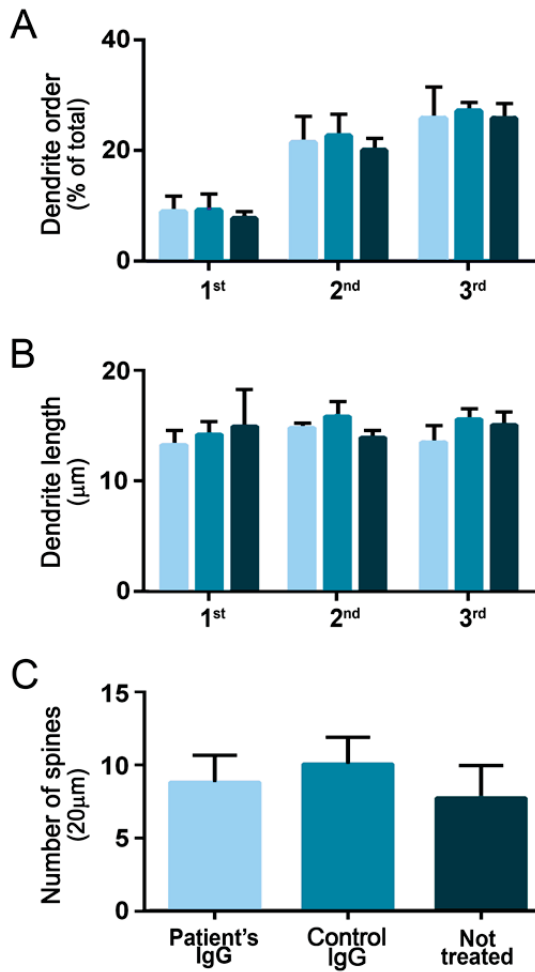
Reactivity of patient's biotinylated IgG with rat hippocampus pre-incubated with serum from a healthy subject (A), serum from the same patient whose IgG has been biotinylated (B), and serum from another patient with neurexin-3 α antibodies (C). Note the decrease of reactivity in panels B and C, indicating that the two patients have antibodies that compete for the same neurexin-3 α epitopes. Scale bar = 200 μ m

Figure e-2: Specific absorption of patients' antibodies with HEK293 cells expressing neurexin-3 α abrogates the reactivity with brain



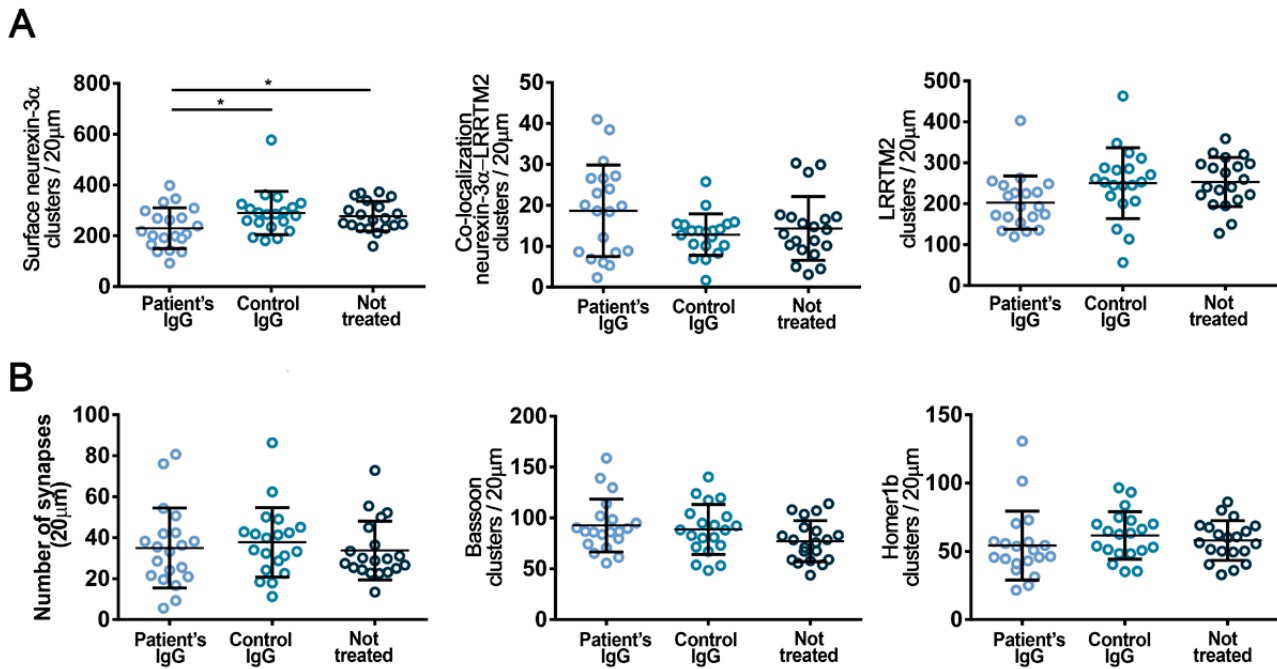
The reactivity of patients' antibodies with rat hippocampus (A) is abrogated after immunoadsorption with HEK293 expressing neurexin-3 α (B) but not after immunoadsorption with non-transfected HEK293 cells (C). Scale bar = 500 μ m

Figure e-3: Patients' IgG antibodies do not affect the number and complexity of dendrites, or the density of dendritic spines.



(A) Number of dendrites classified by dendrite order (1st, 2nd, 3rd) plotted as percentage of the total number of dendrites. (B) Dendrite length (μm) classified by dendrite order. (C) Number of spines for $20\mu\text{m}$ of dendrite (only 2nd and 3rd order dendrites plotted). For all panels the light blue column represents neurons treated with patient's IgG, the middle blue column neurons treated with control IgG, and the dark blue column neurons not treated (not treated). All graphs represent mean \pm SD of 3 independent experiments.

Figure e-4: Patients' IgG antibodies cause a reduction of neurexin-3 α in mature neurons but do not affect the number of synapses.



(A) Mature neurons (*div* 18) treated with patients' IgG for 48 hours, but not control IgG or untreated neurons, showed a significant reduction of the density of clusters of cell-surface neurexin-3 α (left), without change in the co-localization of neurexin-3 α with its ligand LRRTM2 (middle) or the density of LRRTM (right). All graphs represent mean \pm SD (20 dendrites per condition); * p <0.05.

(B) Mature neurons similarly treated as above show no significant reduction of the number of synapses (defined by the co-localization of the presynaptic marker bassoon with the postsynaptic marker homer1b; left), or the levels of bassoon (middle) or the levels of homer1b (right). All graphs represent mean \pm SD (20 dendrites per condition).

5.4. Paper IV

Human N-methyl D-aspartate receptor antibodies alter memory and behaviour in mice

Jesús Planagumà*, Frank Leypoldt*, Francesco Mannara*, Javier Gutiérrez-Cuesta, Elena Martín-García, Esther Aguilar, Maarten J. Titulaer, **Mar Petit-Pedrol**, Ankit Jain, Rita Balice-Gordon, Melike Lakadamyali, Francesc Graus, Rafael Maldonado and Josep Dalmau

* These authors contributed equally

Brain. 2015;138(Pt 1):94-109.

Impact Factor JCR 2015 (percentile): 10.103 (D1)

Human *N*-methyl *D*-aspartate receptor antibodies alter memory and behaviour in mice

Jesús Planagumà,^{1,2,*} Frank Leypoldt,^{1,3,*} Francesco Mannara,^{1,4,*} Javier Gutiérrez-Cuesta,⁴ Elena Martín-García,⁴ Esther Aguilar,¹ Maarten J. Titulaer,⁵ Mar Petit-Pedrol,¹ Ankit Jain,⁶ Rita Balice-Gordon,⁶ Melike Lakadamyali,² Francesc Graus,^{1,7} Rafael Maldonado⁴ and Josep Dalmau^{1,8,9}

Anti-*N*-methyl *D*-aspartate receptor (NMDAR) encephalitis is a severe neuropsychiatric disorder that associates with prominent memory and behavioural deficits. Patients' antibodies react with the N-terminal domain of the GluN1 (previously known as NR1) subunit of NMDAR causing in cultured neurons a selective and reversible internalization of cell-surface receptors. These effects and the frequent response to immunotherapy have suggested an antibody-mediated pathogenesis, but to date there is no animal model showing that patients' antibodies cause memory and behavioural deficits. To develop such a model, C57BL6/J mice underwent placement of ventricular catheters connected to osmotic pumps that delivered a continuous infusion of patients' or control cerebrospinal fluid (flow rate 0.25 µl/h, 14 days). During and after the infusion period standardized tests were applied, including tasks to assess memory (novel object recognition in open field and V-maze paradigms), anhedonic behaviours (sucrose preference test), depressive-like behaviours (tail suspension, forced swimming tests), anxiety (black and white, elevated plus maze tests), aggressiveness (resident-intruder test), and locomotor activity (horizontal and vertical). Animals sacrificed at Days 5, 13, 18, 26 and 46 were examined for brain-bound antibodies and the antibody effects on total and synaptic NMDAR clusters and protein concentration using confocal microscopy and immunoblot analysis. These experiments showed that animals infused with patients' cerebrospinal fluid, but not control cerebrospinal fluid, developed progressive memory deficits, and anhedonic and depressive-like behaviours, without affecting other behavioural or locomotor tasks. Memory deficits gradually worsened until Day 18 (4 days after the infusion stopped) and all symptoms resolved over the next week. Accompanying brain tissue studies showed progressive increase of brain-bound human antibodies, predominantly in the hippocampus (maximal on Days 13–18), that after acid extraction and characterization with GluN1-expressing human embryonic kidney cells were confirmed to be against the NMDAR. Confocal microscopy and immunoblot analysis of the hippocampus showed progressive decrease of the density of total and synaptic NMDAR clusters and total NMDAR protein concentration (maximal on Day 18), without affecting the post-synaptic density protein 95 (PSD95) and α -amino-3-hydroxy-5-methyl-4-isoxazolepropionic acid (AMPA) receptors. These effects occurred in parallel with memory and other behavioural deficits and gradually improved after Day 18, with reversibility of symptoms accompanied by a decrease of brain-bound antibodies and restoration of NMDAR levels. Overall, these findings establish a link between memory and behavioural deficits and antibody-mediated reduction of NMDAR, provide the biological basis by which removal of antibodies and antibody-producing cells improve neurological function, and offer a model for testing experimental therapies in this and similar disorders.

1 Institut d'Investigacions Biomèdiques August Pi i Sunyer (IDIBAPS), Hospital Clínic, Universitat de Barcelona, Barcelona, Spain

2 ICFO-Institut de Ciències Fotòniques, Barcelona, Spain

3 Institute of Clinical Chemistry, Neuroimmunology Unit, University Medical Centre Schleswig-Holstein Campus Lübeck, Germany

4 Laboratori de Neurofarmacologia, Facultat de Ciències de la Salut i de la Vida, Universitat Pompeu Fabra, Barcelona, Spain

5 Department of Neurology, Erasmus Medical Centre, Rotterdam, The Netherlands

6 Department of Neuroscience, University of Pennsylvania, PA, USA

7 Servei de Neurologia, Hospital Clínic, Universitat de Barcelona, Barcelona, Spain

8 Department of Neurology, University of Pennsylvania, Philadelphia, PA, USA

9 Institució Catalana de Recerca i Estudis Avançats (ICREA), Barcelona, Spain

*These authors contributed equally to this work.

Correspondence to: Josep Dalmau, MD, PhD,
IDIBAPS-Hospital Clínic,
Universitat de Barcelona, Department of Neurology,
c/Villarroel 170, 08036, Barcelona, Spain
E-mail: jdalmau@clinic.ub.es

Keywords: animal model; anti-NMDAR encephalitis; antibodies; pathogenesis; mechanism

Abbreviations: AMPAR = α -amino-3-hydroxy-5-methyl-4-isoxazolepropionic acid receptor; NMDAR = *N*-methyl D-aspartate receptor; PSD95 = post-synaptic density protein 95

Introduction

Memory, learning, and behaviour depend on the proper function of the excitatory glutamate *N*-methyl D-aspartate receptor (NMDAR) and α -amino-3-hydroxy-5-methyl-4-isoxazolepropionic acid receptor (AMPA) and underlying mechanisms of synaptic plasticity (Lau and Zukin, 2007; Shepherd and Huganir, 2007). The critical role of NMDAR in these functions has been shown in animal models in which the NMDAR are altered genetically (Mohn *et al.*, 1999; Belforte *et al.*, 2010) or pharmacologically (Jentsch and Roth, 1999; Mouri *et al.*, 2007). In humans this evidence comes from more indirect observations such as studies investigating the effects of phen-cyclidine or ketamine (non-competitive antagonists of NMDAR that cause psychosis) (Weiner *et al.*, 2000; Gunduz-Bruce, 2009), and brain tissue studies of patients with schizophrenia or Alzheimer's disease in which several molecular pathways that modulate glutamate receptor trafficking or function are affected (Snyder *et al.*, 2005; Hahn *et al.*, 2006). In 2007 we identified a novel disorder (anti-NMDAR encephalitis) that occurs with highly specific antibodies against extracellular epitopes located at the amino terminal domain of the GluN1 subunit of NMDAR (Dalmau *et al.*, 2007; Gleichman *et al.*, 2012). The resulting syndrome resembles the spectrum of symptoms that occurs in genetic or pharmacologic models of NMDAR hypofunction, including memory loss and neuropsychiatric alterations ranging from psychosis to coma (Dalmau *et al.*, 2008; Irani *et al.*, 2010; Viacoz *et al.*, 2014). Regardless of the type of presentation, most patients develop severe problems forming new memories and amnesia of the disease. Symptoms are usually accompanied by systemic and intrathecal synthesis of antibodies, the latter likely produced by plasma cells contained in brain inflammatory infiltrates (Dalmau *et al.*, 2008; Martinez-Hernandez *et al.*, 2011). These long-lived plasma cells and persistent antibody synthesis may explain the lengthy symptoms of most patients (average hospitalization \sim 3 months) (Dalmau *et al.*, 2008). Yet, despite the severity and duration of the disease, 80% of the patients have substantial recovery after immunotherapy (accompanied by removal of an underlying tumour, usually an ovarian

teratoma, when appropriate), or sometimes spontaneously (Iizuka *et al.*, 2008; Titulaer *et al.*, 2013).

Investigations on the potential pathogenic role of patients' antibodies using cultured neurons showed that the antibodies caused crosslinking and selective internalization of NMDARs that correlated with the antibody titres, and these effects were reversible after removing the antibodies (Hughes *et al.*, 2010; Mikasova *et al.*, 2012). In contrast, patients' antibodies did not alter the localization or expression of other synaptic proteins, number of synapses, dendritic spines, dendritic complexity, or cell survival (Hughes *et al.*, 2010). In parallel experiments, the density of NMDAR was also significantly reduced in the hippocampus of rats infused with patients' antibodies, a finding comparable to that observed in the hippocampus of autopsied patients (Hughes *et al.*, 2010). Overall, these studies suggested an antibody-mediated pathogenesis, but the demonstration that patients' antibodies caused symptoms remained pending. Modelling symptoms and showing that these correlate with antibody-mediated reduction of NMDAR would prove the pathogenicity of patients' antibodies, support the use of treatments directed toward decreasing the levels of antibodies or antibody-producing cells, and help to investigate experimental therapies in this and similar disorders. We report here such a model using continuous 14-day cerebroventricular infusion of patients' CSF in mice. The aims were to determine (i) if patients' antibodies altered memory and behaviour; (ii) whether mice symptoms correlated with brain antibody-binding and reduction of NMDAR; and (iii) whether the clinical and molecular alterations recovered after stopping the antibody infusion.

Materials and methods

Animals

Male C57BL/6J mice (Charles River), 8–10 weeks old (25–30 g) were housed in cages of five until 1 week before surgery when they were housed individually. The room was maintained at a controlled temperature ($21 \pm 1^\circ\text{C}$) and humidity ($55 \pm 10\%$)

with illumination at 12-h cycles; food and water were available *ad libitum*. All experiments were performed during the light phase, and animals were habituated to the experimental room for 1 week before starting the tests. All procedures were conducted in accordance with standard ethical guidelines (European Communities Directive 86/609/EU) and approved by the local ethical committees: Comitè Ètic d'Experimentació Animal, Institut Municipal d'Assistència Sanitària (Universitat Pompeu Fabra), and Institutional Animal Care and Use Committee (University of Pennsylvania).

Patients' CSF samples

CSF from 25 patients with high titre NMDAR antibodies (all >1:320) were pooled and used for cerebroventricular infusion. CSF from 25 subjects without NMDAR antibodies (11 with normal pressure hydrocephalus and 14 with non-inflammatory CNS disorders) were similarly pooled and used as controls. Before loading the osmotic pumps (discussed below), the pooled CSF samples from patients and controls were dialyzed (Slide-A-Lyzer 7K, Thermo) against sterile phosphate-buffered saline (PBS) overnight at 4°C, and the concentration of total IgG normalized to the CSF physiologic concentration of 2 mg/dl. All mice received the same pooled CSF either from patients or controls. Studies were approved by the institutional review board of Hospital Clínic and Institut d'Investigacions Biomèdiques August Pi i Sunyer (IDIBAPS), Universitat de Barcelona.

Surgery, placement of ventricular catheters and osmotic pumps

Cerebroventricular infusion of CSF was performed using osmotic pumps (model 1002, Alzet) with the following characteristics: volume 100 µl, flow rate 0.25 µl/h, and duration 14 days. Twenty-four hours before surgery, two osmotic pumps per animal were each loaded with 100 µl of patient or control CSF. The pumps were then connected to a 0.28 mm IM (internal diameter) polyethylene tube (C314CT, PlasticsOne) and left overnight in sterile PBS at 37°C. The next day, mice were deeply anaesthetized by intraperitoneal injection of a mixture of ketamine (100 mg/kg) and xylazine (10 mg/kg) along with subcutaneous administration of the analgesic meloxicam (1 mg/kg). Mice were then placed in a stereotaxic frame, and a bilateral catheter (PlasticsOne, model 3280PD-2.0/SP) was inserted into the ventricles (0.02 mm anterior and 1.00 mm lateral from bregma, depth 0.22 mm) and secured with dental cement. Each arm of the catheter was connected to one osmotic pump, which was subcutaneously implanted on the back of the mice. Appropriate ventricular placement of the catheters was assessed in randomly selected mice injecting methylene blue through the catheters (Fig. 1A–C).

Cognitive tasks

All behavioural tasks were performed by researchers blinded to experimental conditions using standardized tests reported by us (Maldonado *et al.*, 1970; Filliol *et al.*, 2000; Berrendero *et al.*, 2005; Bura *et al.*, 2007, 2010, 2013; Aso *et al.*, 2008; Puighermanal *et al.*, 2009; Burokas *et al.*, 2012; Llorente-Berzal *et al.*, 2013) and others (Porsolt *et al.*, 1977; Crawley

and Goodwin, 1980; Handley and Mithani, 1984; Steru *et al.*, 1985; Konig *et al.*, 1996; Caille *et al.*, 1999; Strelakova *et al.*, 2006; Tagliatela *et al.*, 2009; Ennaceur, 2010) and following the schedule summarized in Fig. 1D. The tasks were aimed to assess memory (novel object recognition in open field and V-maze), anhedonic behaviours (sucrose preference test), depressive-like behaviours (tail suspension, and forced swimming tests), anxiety (black and white and elevated plus maze tests), aggressiveness (resident-intruder test) and locomotor activity (horizontal and vertical activity assessment). A brief description of each task is provided in the [Supplementary material](#).

Brain tissue processing

To determine the effects of patients' antibodies on mouse brain, animals were sacrificed at the indicated time points (Fig. 1D, Days 5, 13, 18, 26 and 46) with CO₂. Brains were harvested, sagittally split, and transferred to ice-cold PBS. Half of the brain was fixed by immersion in 4% paraformaldehyde (PFA) for 1 h at 4°C, cryoprotected with 40% sucrose for 48 h at 4°C, embedded with freezing media, and snap-frozen with isopentane chilled with liquid nitrogen. The other half-brain was used for dissection of hippocampus and cerebellum for IgG and protein extraction (see below).

Immunohistochemistry and quantitative peroxidase staining

For determination of antibodies bound to brain tissue using immunoperoxidase staining, 7-µm thick tissue sections were sequentially incubated with 0.25% H₂O₂ for 10 min at 4°C, 5% goat serum for 15 min at room temperature, biotinylated goat anti-human IgG (1:2000, Vector labs) overnight at 4°C, and the reactivity developed using avidin-biotin-peroxidase and diaminobenzidine. Sections were mildly counterstained with haematoxylin, and results photographed under a Leica DMD108 microscope. Images were prepared creating a mask for diaminobenzidine colour, converting the mask to greyscale intensities, and inverting the pixels using Adobe Photoshop CS6 package. Hippocampal, frontal cortex, striatum and cerebellar regions were manually outlined; intensity and area were quantified in two serial sections using the public domain Fiji ImageJ software (<http://fiji.sc/Fiji>). Values were divided by area and normalized to the group with the highest mean (defined as 100%, patients' CSF treated animals sacrificed at Day 18).

Immunofluorescence and confocal microscopy with brain tissue

For determination of antibodies bound to brain tissue using immunofluorescence, 5-µm-thick tissue sections were blocked with 5% goat serum and 1% bovine serum albumin for 60 min at room temperature, and incubated overnight at 4°C with Alexa Fluor® 488 goat anti-human IgG (A11013, diluted 1:1000, Molecular Probes/ Life Technologies). Slides were then mounted with ProLong® Gold (P36930, Molecular Probes) and results scanned under a LSM710 Zeiss confocal microscope. Sections from all animals were analysed in parallel. Quantification of fluorescent intensity in areas of CA1, CA3 and dentate gyrus was done using Fiji ImageJ software.

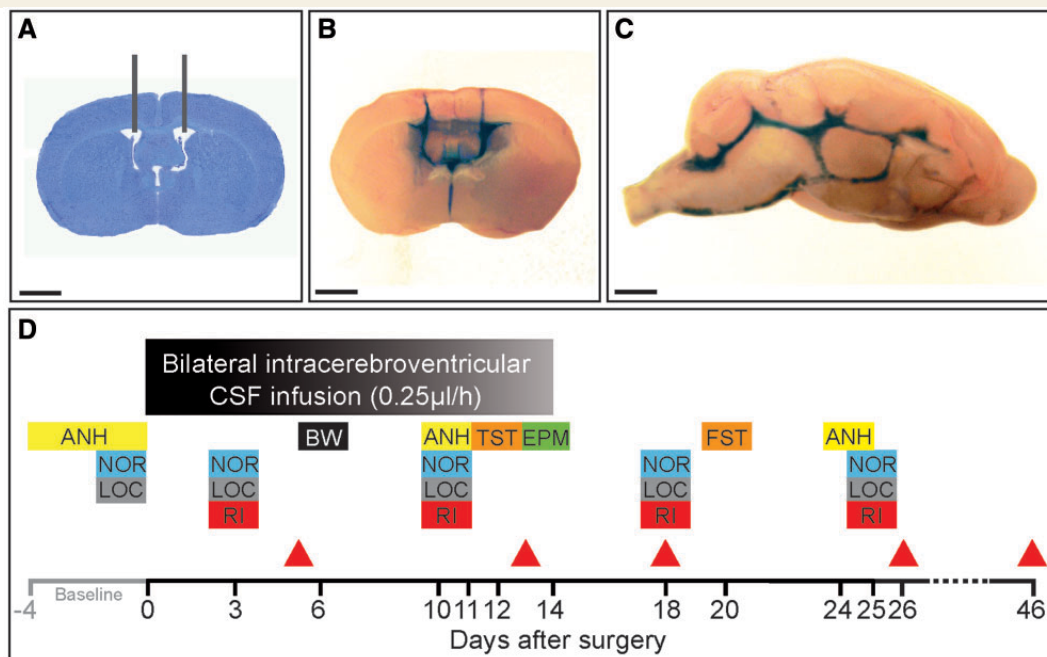


Figure 1 Experimental design and placement of ventricular catheters. (A) Representative coronal mouse brain section with catheter placement. Scale bar = 2 mm. (B and C) Coronal and sagittal mouse brain sections demonstrating cerebroventricular diffusion of methylene blue after ventricular infusion. Scale bars = 2 mm. (D) Schedule of cognitive testing and animal sacrifice. At Day 0, catheters and osmotic pumps were placed and bilateral ventricular infusion of patients' or control CSF started. Infusion lasted for 14 days. Memory [novel object recognition (NOR)], anhedonia [sucrose preference test (ANH)], depressive-like behaviour [tail suspension test (TST) and forced swimming test (FST)], anxiety [black and white test (BW) and elevated plus maze test (EPM)], aggressiveness [resident intruder test (RI)] and locomotor activity (LOC) were assessed blinded to treatment at the indicated days. The novel object recognition was assessed in open field and V-maze paradigms in two different cohorts of mice. Animals were habituated for 1 to 4 days before surgery (baseline) to novel object recognition, anhedonia, and locomotor activity. Red arrowheads indicate the days of sacrifice for studies of effects of antibodies in brain.

Background was subtracted and intensity divided by area. Mean intensity of IgG immunostaining in animals treated with patients' CSF and sacrificed at Day 18 was defined as 100%.

To determine the effects of patients' antibodies on total and synaptic NMDAR clusters and PSD95, non-permeabilized 5-µm thick sections were blocked with 5% goat serum and 1% bovine serum albumin as above, incubated with human CSF antibodies for 2 h at room temperature, washed with PBS, permeabilized with TritonTM X-100 0.3% for 10 min at room temperature, and incubated with rabbit polyclonal antibody against PSD95 (diluted 1:250, Clone 18258 Abcam) overnight at 4°C. Next day, the slides were washed and incubated with the corresponding secondary antibodies, Alexa Fluor[®] 594 goat anti-human IgG and Alexa Fluor[®] 488 goat anti-rabbit IgG (A-11014, A-11008, both diluted 1:1000, Molecular Probes) for 1 h at room temperature. Slides were mounted as above and results scanned with a confocal microscope (Zeiss LSM710) with EC-Plan NEOFLUAR CS ×100/1.3 NA oil objective. Standardized z-stacks including 50 optical images were acquired from five different, equally spaced areas of CA1, CA3 and dentate gyrus of hippocampus using sequential scanning, 1024 × 1024 lateral resolution, and Nyquist optimized z-sampling frequency. Images were deconvolved with 20 iterations using theoretical point spread functions and maximum likelihood estimation

algorithms of Huygens Essential software (Scientific Volume Imaging). For cluster density analysis a spot detection algorithm from Imaris suite 7.6.4 (Bitplane) was used based on automatic segmentation of the images to spots (Banovic et al., 2010). Density of clusters was expressed as spots/µm³. Three-dimensional colocalization of clusters (e.g. NMDAR and PSD95) was done using a spot co-localization algorithm implemented in Imaris suite 7.6.4. Synaptic localization was defined as co-localization of NMDAR or AMPAR with post-synaptic PSD95. Synaptic cluster density was expressed as colocalized spots/µm³. For each animal, five identical image stacks in each hippocampal area (CA1, CA2 and dentate gyrus) were acquired and the mean densities calculated for total and synaptic NMDAR and AMPAR. Densities were normalized to the mean density of control CSF treated animals (100%). For the AMPAR the antibody used was guinea pig GluA1 antibody (1:100, clone AGP-009, Alomone), and as secondary antibody Alexa Fluor[®] 594 goat anti-guinea pig IgG (A11076, 1:1000, Molecular Probes).

The presence of apoptosis, cellular infiltrates, and complement was assessed in the hippocampal region (CA3) in mice sacrificed on Day 18 and corresponding controls. Apoptosis was determined by standard terminal deoxynucleotidyl transferase mediated biotinylated UTP nick end labelling (TUNEL) using the TACS 2TdT-Fluor *in situ* apoptosis detection kit (Trevigen), and immunolabelling of cleaved caspase 3 (1:200,

#9661 Cell Signalling, Technologies) using a goat anti-rabbit Alexa Fluor[®] 488 as secondary antibody (1:1000 Molecular Probes). The presence of complement was assessed using rabbit anti-mouse C5b-9 (1:500, Abcam) and Alexa Fluor[®] 488 goat anti-rabbit IgG (1:500, #A11008, Molecular Probes). Immunolabelling for T and B lymphocytes was done using rabbit anti-mouse CD3 (1:1000, #ab16669 Abcam) followed by secondary antibody goat anti-rabbit Alexa Fluor[®] 488 (1:1000, Molecular Probes), and rat anti-CD45R (1/10000, #ab64100) followed by goat anti-rat Alexa Fluor[®] 594 (1/1000, #A-11007 Molecular Probes). Results were scanned with a confocal microscope Zeiss LSM710.

Extraction of human IgG bound to mice brain

Under a dissection microscope (Zeiss stereomicroscope, Stemi 2000), the hippocampus and cerebellum were isolated, weighed, snap-frozen, and stored at -80°C . Tissue (10 mg) was homogenized in 0.5 ml ice-cold PBS with protease inhibitors (Sigma-Aldrich) and centrifuged at 16 000g for 5 min. All steps were performed at 4°C . Washing was repeated four times to remove unbound IgG. The last wash was done in 100 μl and the supernatant saved as pre-extraction fraction. To extract the specifically bound antibodies, the pellet was solubilized for 5 min in acid (86 μl 0.1 M Na-citrate buffer pH 2.7), centrifuged at 16 000g for 5 min, and the supernatant neutralized with 14 μl 1.5 M Tris pH 8.8, and used to determine the presence of NMDAR (GluN1) antibodies (see below).

Immunofluorescence with HEK293 cells expressing GluN1

The presence of GluN1 antibodies in IgG extracts from brain was determined using a HEK293 cell-based assay expressing GluN1, as reported (Dalmau *et al.*, 2008). After fixation with 4% paraformaldehyde and permeabilization with 0.3% Triton[™] X-100, cells were blocked with 1% bovine serum albumin for 90 min, and incubated with undiluted acid-extracted IgG or pre-extraction fraction from brain of infused mice, at 4°C overnight. The next day, cells were washed and incubated with a mouse monoclonal antibody against a non-competing GluN1 epitope located at amino acid 660-811 (1:20 000; clone MAB363, Millipore) for 1 h at room temperature, followed by the corresponding Alexa Fluor[®] secondary antibodies (A11013, A11032, both diluted 1:1000, Molecular Probes) for 1 h at room temperature. The titre of positive samples was calculated by serial dilutions until the reactivity was no longer visible. Results were photographed under a fluorescence microscope using Zeiss Axiovision software.

Immunoblot analyses

Total protein from hippocampus and cerebellum was obtained by dissecting these regions from 20- μm thick paraformaldehyde-fixed sagittal mouse brain sections on glass slides at 4°C under a Zeiss stereomicroscope (Stemi 2000). Two consecutive sections of isolated hippocampus or cerebellum were then transferred to an Eppendorf tube in PBS supplemented with protease inhibitors. Loading buffer (RotiLoad) was added, the solubilized tissue boiled for 5 min, and the proteins

separated in a 10% SDS gel electrophoresis with semi-dry blotting on PVDF membranes. Membranes were blocked in 5% non-fat skimmed milk and incubated overnight at 4°C with the following polyclonal rabbit antibodies: GluN1 (1:1000, Sigma-Aldrich), GluR2/3 (1:1000, Abcam), and PSD95 (1:1000, Synaptic Systems), or a monoclonal mouse anti- β -actin (1:20 000, Sigma-Aldrich). Membranes were incubated with secondary antibodies for 1 h at room temperature (anti-rabbit IgG HRP 1:1000, anti-mouse IgG HRP 1:10 000) and analysed by enhanced chemiluminescence (all Amersham GE Healthcare) on a LAS4000 (GE Healthcare). All studies were done in duplicate. Analysed films were in the linear range of exposure, digitally scanned, and signals quantified using Fiji ImageJ software. The signal intensity of each antigen was normalized to that of actin in the same lane. The mean intensity of signal in control CSF treated animals was defined as 100% and all other intensities expressed in per cent relative to this value.

Statistics

Behavioural tests were analysed using repeated measures two-way ANOVA for tests with multiple time points (novel object recognition, sucrose preference test, resident-intruder test, locomotor activity), independent sample *t*-tests for tests with single time points (forced swimming test, black and white test, elevated plus maze test) or by Mann Whitney-U for skewed distributions (tail suspension test). Non-normally distributed parameters were log-transformed (black and white test, elevated plus maze test). Significance of NMDAR antibody titre in acid-extracted IgG fractions was calculated using the Kruskal-Wallis test and Dunn's *post hoc* test compared to titres at Day 46. Human IgG intensity, confocal cluster density and immunoblot data (GluN1, PSD95) from different time points or regions were analysed using two-way ANOVA with Sidak-Holm *post hoc* testing to calculate multiplicity-adjusted *P*-values. Confocal cluster density in the different hippocampal subregions (CA1, CA3, dentate gyrus) were not significantly different and were analysed pooled. All experiments were assessed visually for outliers (e.g. one animal with very different results from the other animals at the same time point), but none were identified, so measurements were pooled per time point and treatment (patient or control CSF). For confocal AMPAR cluster density measured at single time points, independent sample *t*-tests were used. A *P*-value of <0.05 was considered significant in *post hoc* testing after correction for multiple testing (Sidak-Holm). In the two-way ANOVA the cut-off for interaction between two factors was set at 0.10; if the *P*-value for interaction was <0.10 , the effects of treatment were considered for the separate time points (*post hoc* analysis). All tests were done using GraphPad Prism (Version 6).

Results

One-hundred and eleven mice were included in the studies, 56 for cognitive and behavioural tests, and 55 for assessment of antibody binding to brain and the effects on total and synaptic NMDAR (Fig. 1).

Cerebroventricular infusion of patients' CSF alters memory and behaviour in mice

The most robust effect during the 14-day infusion of patients' CSF was on the novel object recognition test in both the open field and V-maze paradigms (Fig. 2A and B). Compared with animals infused with control CSF, those infused with patients' CSF showed a progressive decrease of the object recognition index, indicative of a memory deficit (Bura *et al.*, 2007; Puighermanal *et al.*, 2009; Tagliatela *et al.*, 2009). The memory deficit became significant on Day 10 and was maximal on Day 18 (4 days after the infusion of CSF had stopped). On Day 25, the object recognition index had normalized and was similar to that of animals treated with control CSF (Fig. 2A and B). For all time-points, the total time spent exploring both objects (internal control) was similar in animals infused with control or patients' CSF (Supplementary Table 1).

The preference to drink sweetened water (sucrose preference test) was used as a measure of anhedonic behaviour. Mice infused with patients' CSF and tested during the infusion period (Day 10) had less preference for sucrose compared with mice infused with control CSF (Fig. 2C). In contrast, the same mice tested 10 days after the infusion of CSF had stopped (Day 24) showed a preference for sucrose similar to that of the control mice. The total consumption of water with and without sucrose was similar in both groups (internal control, Supplementary Table 1). In addition, two tests of depressive-like behaviour were performed. The tail suspension test, performed on Day 12, showed that animals infused with patients' CSF had longer periods of immobility compared with those infused with control CSF (Fig. 2D). In contrast, 6 days after the infusion of CSF had stopped (Day 20), no differences were noted with the forced swimming test (examining immobility in inescapable situations; Fig. 2E and Supplementary Table 1). Overall, these findings suggest that the infusion of NMDAR antibodies was associated with anhedonic and depressive-like behaviours.

In contrast to the prominent memory deficit, along with anhedonia and depressive behaviour, no significant differences were noted in tests of anxiety (black and white test, elevated plus maze test), aggression (resident-intruder test) and locomotor activity (Fig. 3A–D).

Patients' antibodies bind to NMDAR in mouse brain

Animals infused with patients' CSF, but not control CSF, had progressively increasing human IgG immunostaining (representing IgG bound to brain) that correlated with the duration of the infusion. The distribution of IgG immunostaining predominated in regions with high density of NMDAR, mainly the hippocampus (Fig. 4A), resembling that obtained with brain sections directly incubated with

patients' CSF or a monoclonal antibody against GluN1 (Dalmau *et al.*, 2008). Upon quantification of immunostaining, the maximal antibody binding was identified in mice sacrificed on Day 18, which had received 14 days of CSF infusion, compared with mice sacrificed on Days 5 or 13 (Fig. 4B and C). In animals sacrificed on Days 26 and 46 the presence of IgG immunostaining progressively decreased. In frontal cortex the dynamics of IgG binding were similar to those of the hippocampus (Supplementary Fig. 1), but the amount of IgG was substantially less; in other brain regions such as the cerebellum and striatum, the IgG immunostaining was sparse and not significantly different between animals infused with patients' CSF or control CSF (data not shown).

Studies with immunofluorescence and confocal microscopy showed that in animals infused with patients' CSF the presence of hippocampal IgG was visible as a punctate immunolabelling on the surface of neurons and neuronal processes in contrast to mice infused with control CSF where minor amounts of IgG reactivity without preference for neuronal structures were noted (Fig. 4D–G). In addition, the amount of human IgG bound to all selected regions of hippocampus was significantly higher than in the control group (Fig. 4H).

To determine if the IgG immunostaining represented brain-bound NMDAR antibodies, IgG was extracted from several brain regions and examined for reactivity with HEK cells expressing GluN1. These studies showed that the IgG extracted from hippocampus of mice infused with patients' CSF reacted specifically with GluN1 (Fig. 5A). The NMDAR antibody concentration in the extracts correlated with the duration of infusion of CSF; it increased until Day 13, reached the maximal concentration on Days 13–18, and decreased afterwards (Fig. 5A and C). NMDAR antibodies were also detected in IgG extracts from other brain regions (frontal cortex, cerebellum) but at lower concentration to that obtained from hippocampus (Fig. 5D). Demonstration that the extracted antibodies were specifically bound to the NMDAR was provided by the lack of GluN1 reactivity in the pre-extraction fractions (Fig. 5B and E). Parallel studies with tissue from animals infused with control CSF did not show NMDAR antibodies (Supplementary Fig. 2).

Effects of patients' antibodies on NMDAR

To determine the effects of patients' antibodies on NMDAR, we focused on the hippocampus, which was the region with maximal concentration of NMDAR-bound antibodies. Compared with animals infused with control CSF, those infused with patients' CSF had on Days 13 and 18 a significant decrease of the density of total and synaptic hippocampal NMDAR clusters followed by a gradual recovery after Day 18 (pooled analysis of CA1, CA3 and dentate gyrus; Fig. 6A–D). No significant

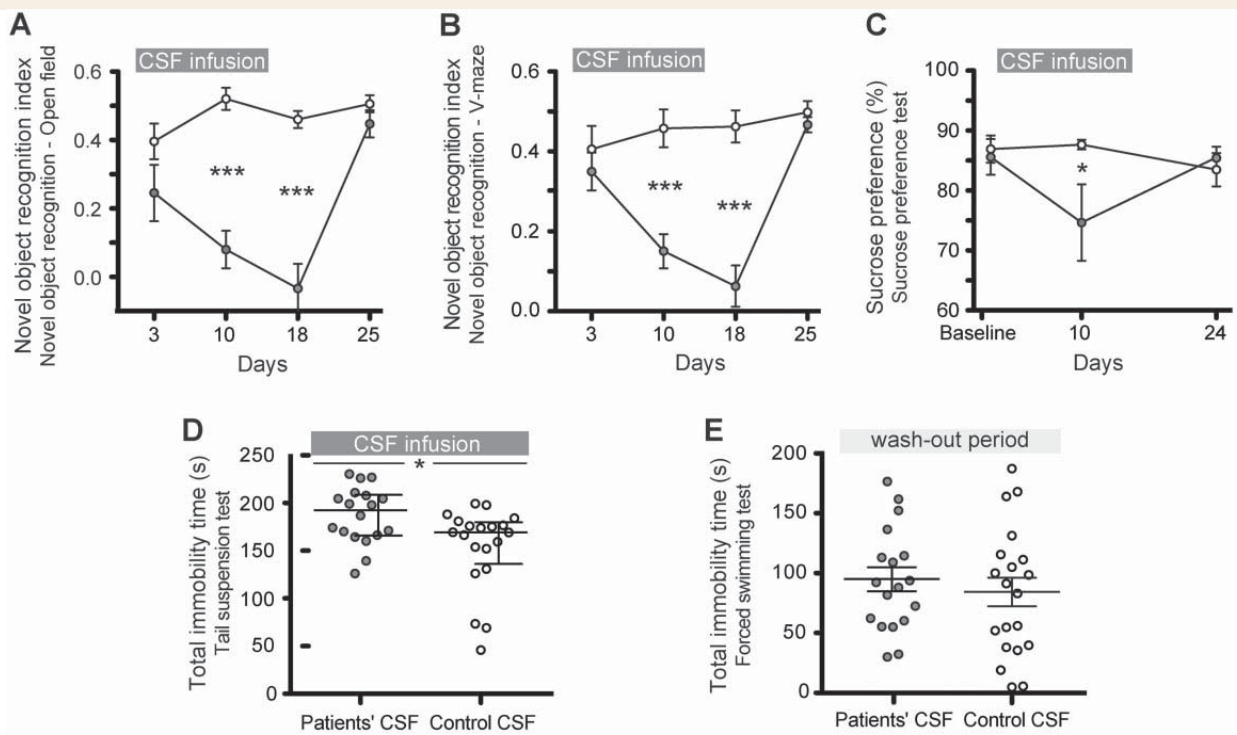


Figure 2 Infusion of CSF from patients with NMDAR antibodies causes deficits in memory, anhedonia and depressive-like behaviour. (A and B) Novel object recognition index in open field (A) or V-maze paradigms (B) in animals treated with patients' CSF (grey circles) or control CSF (white circles). A high index indicates better object recognition memory. (C) Preference for sucrose-containing water in animals infused with patients' CSF (grey) or control CSF (white). Lower percentages indicate anhedonia. (D and E) Total time of immobility in tail-suspension test during the infusion period (D, Day 12) and in forced swimming test after the infusion period (E, Day 20). Data are presented as mean \pm SEM (median \pm IQR in D). Number of animals: patients' CSF $n = 18$ (open field novel object recognition $n = 8$), control CSF $n = 20$ (open field novel object recognition $n = 10$). Significance of treatment effect was assessed by two-way ANOVA (A–C) with an α -error of 0.05 and *post hoc* testing with Sidak-Holm adjustment (asterisks), unpaired *t*-test (E) or Mann-Whitney U test (D). * $P < 0.05$, *** $P < 0.001$. See Supplementary Table 1 for detailed statistics.

differences in between hippocampal subregions (CA1, CA3, dentate gyrus) were observed (not shown). In contrast, patients' antibodies did not alter the density of PSD95 or AMPAR clusters (Fig. 6E and F).

Immunoblot analysis of total protein extracted from hippocampus showed that on Days 13 and 18, mice infused with patients' CSF had a significant decrease of total NMDAR protein concentration compared with mice infused with control CSF (Fig. 7A and B). The magnitude of this effect was greater in animals with higher concentration of IgG bound to hippocampus (Fig. 7C). Parallel studies examining the effect on the protein concentrations of PSD95 (Fig. 7A and E) and AMPAR (Fig. 7D) demonstrated no significant differences between mice infused with patients' CSF or control CSF.

In cerebellum, no significant effects on the cluster density or total protein concentration of NMDAR, PSD95 and AMPAR were noted in animals infused with patients' CSF compared to those infused with control CSF (data not shown).

Immunohistochemical studies for neuronal apoptosis, infiltrates of T or B cells, and deposits of complement in

hippocampus of animals infused with patients' or control CSF, examined on Day 18, showed no abnormalities (Fig. 8).

Discussion

We report that passive transfer of NMDAR antibodies by continuous ventricular infusion of CSF from patients with anti-NMDAR encephalitis causes memory and behavioural deficits in mice, and that the effects are likely mediated by the binding of antibodies to NMDAR resulting in a specific decrease of the density of these receptors. Data from earlier reports showing that despite the severity and duration of symptoms, most patients with anti-NMDAR encephalitis respond to immunotherapy (Gresa-Arribas *et al.*, 2014), and findings at the cellular level demonstrating that patients' antibodies cause a titre-dependent decrease of synaptic NMDAR receptors fulfilled most of the Witebsky's criteria for an antibody-mediated disease (Rose and Bona, 1993), but the transfer of symptoms to animals was pending. In the current study, four sets of experiments satisfy

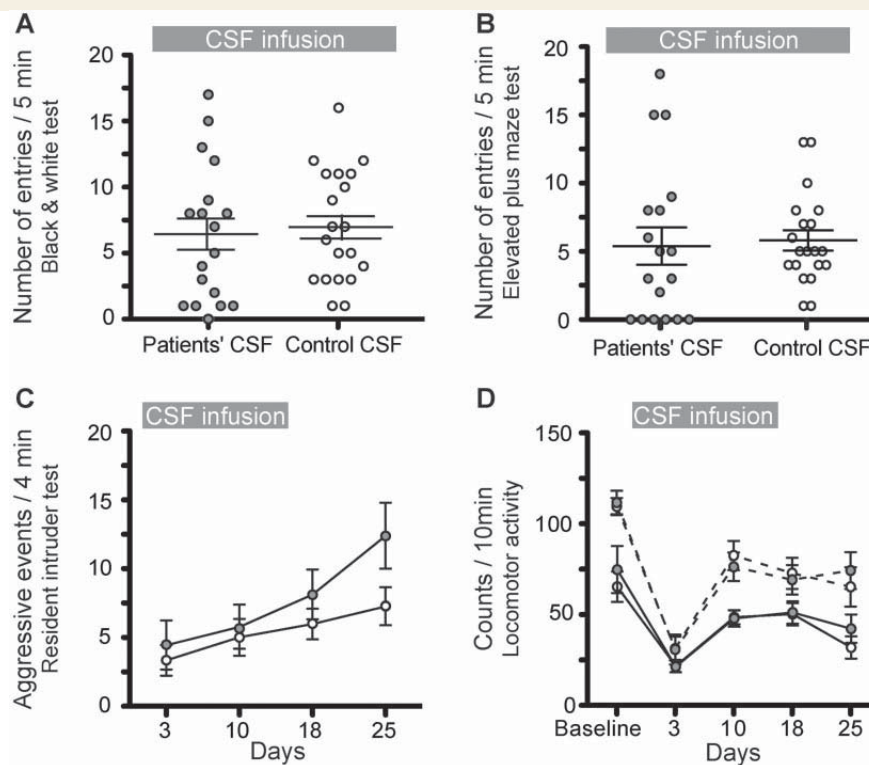


Figure 3 Infusion of CSF from patients with NMDAR antibodies does not alter the tests of anxiety, aggression and locomotor activity. (A and B) Number of entries into bright/open compartments during a 5 min period in a standard black and white (A, Day 6) or elevated plus maze test (B, Day 14) in animals treated with patients' CSF (filled circles) or control CSF (open circles). (C) Number of aggressive events over a 4-min period in a resident intruder paradigm in both treatment groups. (D) Horizontal (solid lines) and vertical (dashed lines) movement count over a 10 min period in both treatment groups. Data are presented as mean \pm SEM. Number of animals: patients' CSF $n = 18$, control CSF $n = 20$. Statistical assessment as indicated in Fig. 2 and Supplementary Table 1.

this postulate: (i) the development of symptoms in animals infused with patients' CSF, but not control CSF; (ii) the demonstration that the infused antibodies reacted predominantly with brain regions with high density of NMDAR (e.g. hippocampus) and specifically recognized these receptors; (iii) the identification of a selective decrease of the density of total and synaptic NMDAR clusters and total NMDAR protein concentration without affecting PSD95, and that these effects correlated with the concentration of brain-bound antibodies; and (iv) the correlation noted between the intensity of the abovementioned findings and time-course of patients' antibody infusion, as well as between the reversibility of symptoms and restoration of NMDAR levels after stopping the infusion of CSF antibodies.

Approximately 75% of patients with anti-NMDAR encephalitis present with mood and psychiatric alterations ranging from manic or depressive behaviour to psychosis, often followed by stereotyped movements, seizures, or decreased level of consciousness (Kayser *et al.*, 2013; Titulaer *et al.*, 2013). Regardless of the presentation, most patients develop severe problems forming new memories and have amnesia of the disease. Close examination during the phase of recovery shows, in some patients,

impairment in the visual recognition of objects or faces (e.g. physicians, nurses) (Frechette *et al.*, 2011). Owing to the wide range of symptoms of the disease and lack of previous studies examining the distribution of brain tissue NMDAR-antibody binding when these antibodies are infused intraventricularly, we used standardized memory and behavioural tests. The most notable effects were observed in the tests of memory (novel object recognition) using different groups of animals in two different paradigms (open field and V-maze). While the first depends predominantly on normal hippocampal function, the second is dependent of perirhinal-hippocampal structures (Winters *et al.*, 2004). Compared with animals infused with control CSF, those infused with patients' CSF developed progressive memory deficits, which were maximal on Days 13–18 when the highest concentration of brain-bound NMDAR antibodies and lowest density of NMDAR occurred. Other paradigms affected were related to depressive-like behaviours (tail suspension test) and anhedonic behaviours (sucrose preference test). We did not find significant abnormalities in the tests of aggression and anxiety, which are often present in the human disease, or in locomotor activity (an expected finding given that paralysis rarely occurs in patients).

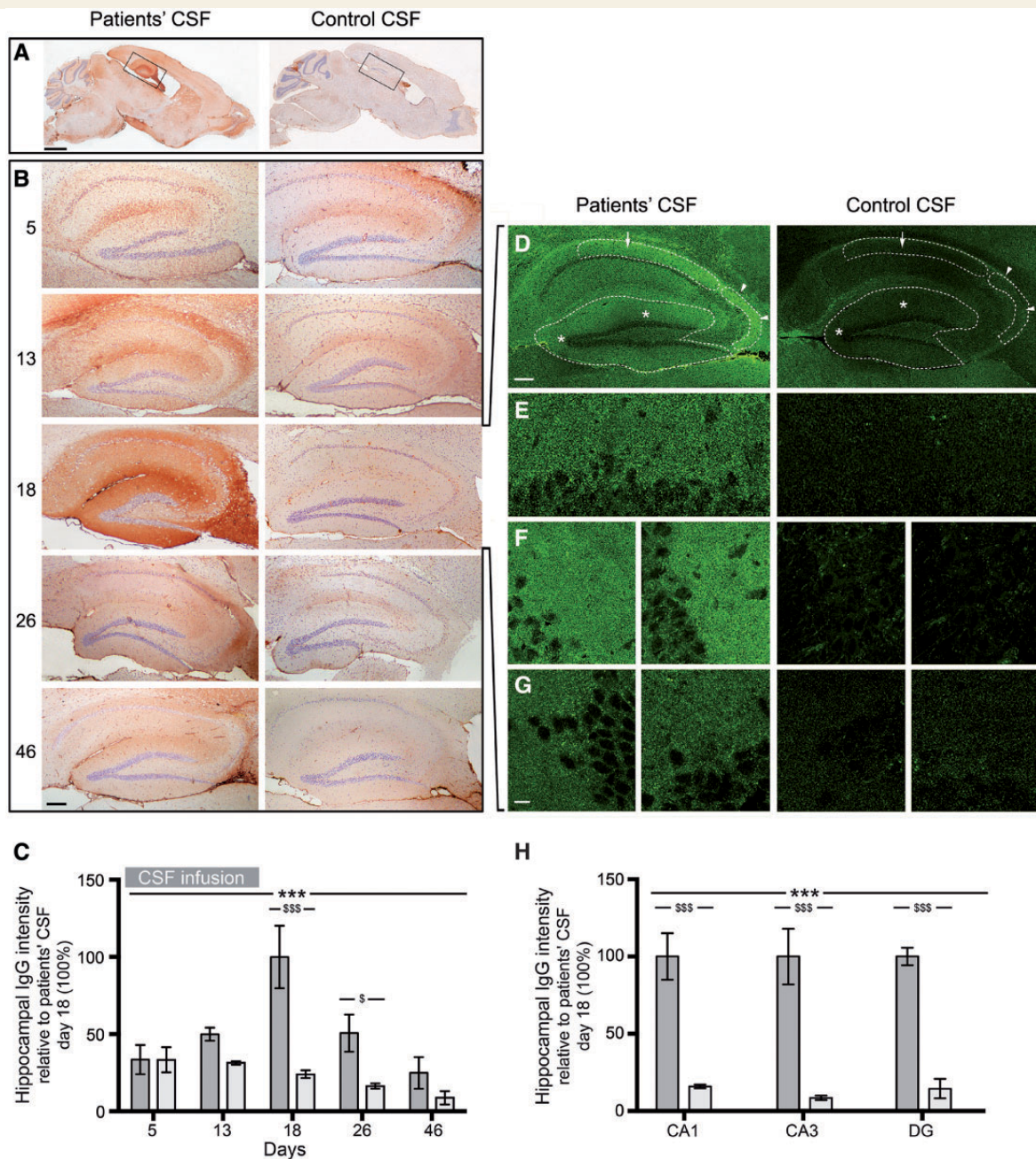


Figure 4 Animals infused with patient's CSF have a progressive increase of human IgG bound to hippocampus. (A and B) Immunostaining of human IgG in sagittal brain sections (A) and hippocampus (B) of representative animals infused with patients' CSF (left) and control CSF (right), sacrificed at the indicated experimental days. In animals infused with patients' CSF there is a gradual increase of IgG immunostaining until Day 18, followed by decrease of immunostaining. Scale bars: A = 2 mm; B = 200 μ m. (C) Quantification of intensity of human IgG immunolabelling in hippocampus of mice infused with patients' CSF (dark grey columns) and control CSF (light grey columns) sacrificed at the indicated time points. (D–H) Confocal microscopy analysis of IgG bound to the hippocampus on Day 18. (D) Sagittal section of the hippocampus with areas examined at higher magnification in E (arrow in CA1), F (arrow heads in CA3) and G (asterisks in dentate gyrus). Note the fine punctate IgG immunolabelling surrounding neuronal bodies in mice infused with patients' CSF; this immunolabelling is similar to that reported in brain sections directly incubated with patients' antibodies, as in Dalmau *et al.* (2008). Scale bars: D = 200 μ m; E–G = 10 μ m. (H) Quantification of the intensity of human IgG immunofluorescence in the indicated areas in animals infused with patients' CSF (dark grey columns) or control CSF (light grey columns). For all quantifications, mean intensity of IgG immunostaining in the group with the highest value (animals treated with patients' CSF and sacrificed at Day 18) was defined as 100%. All data are presented as mean \pm SEM. For each time point five animals infused with patients' CSF and five with control CSF were examined. Significance of treatment effect was assessed by two-way ANOVA with an α -error of 0.05 (*) and *post hoc* testing with Sidak-Holm adjustment (\$). ***: \$\$\$ p < 0.001; \$ p < 0.05. See Supplementary Table 2 for detailed statistics.

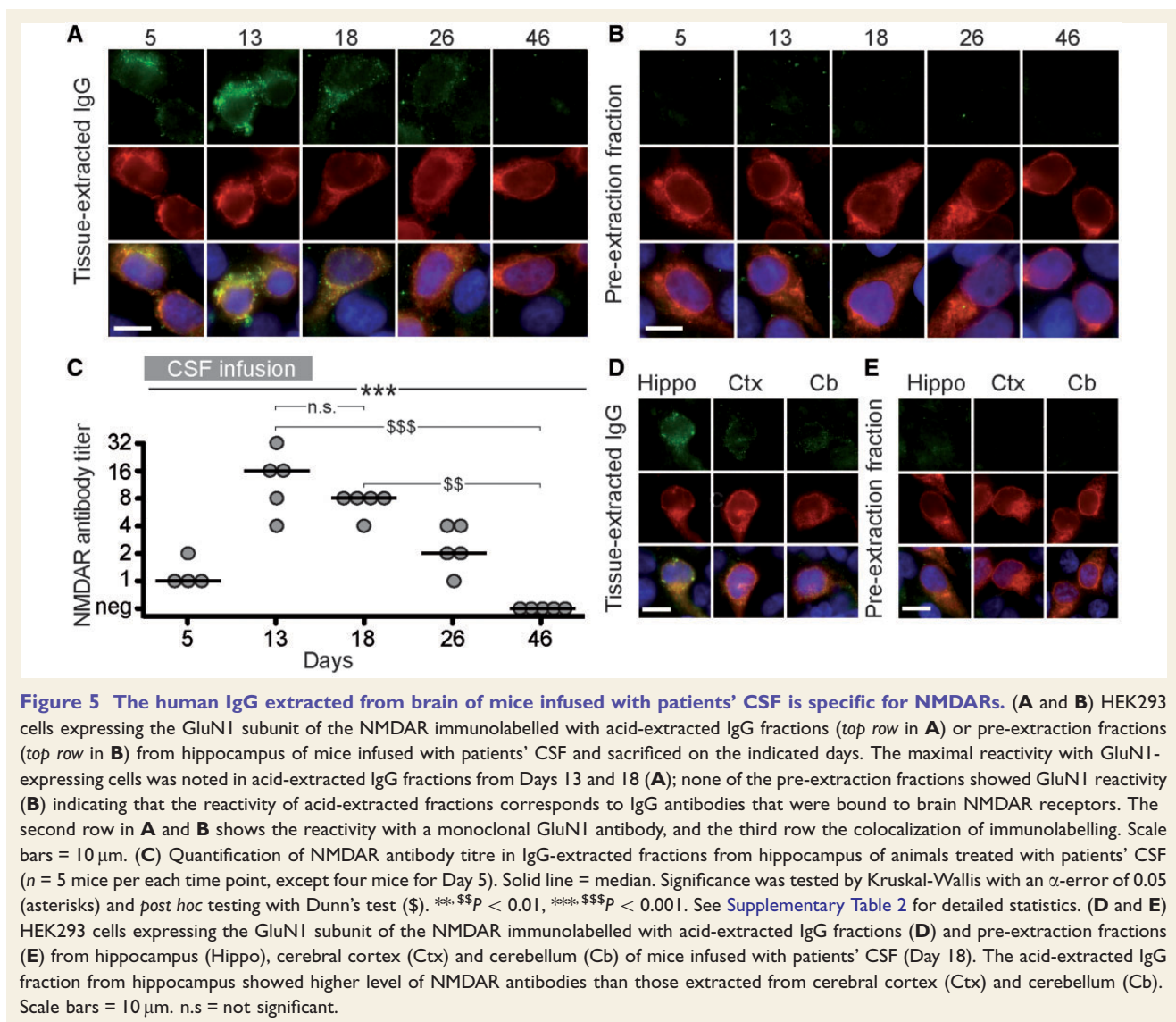


Figure 5 The human IgG extracted from brain of mice infused with patients' CSF is specific for NMDARs. (A and B) HEK293 cells expressing the GluN1 subunit of the NMDAR immunolabelled with acid-extracted IgG fractions (top row in A) or pre-extraction fractions (top row in B) from hippocampus of mice infused with patients' CSF and sacrificed on the indicated days. The maximal reactivity with GluN1-expressing cells was noted in acid-extracted IgG fractions from Days 13 and 18 (A); none of the pre-extraction fractions showed GluN1 reactivity (B) indicating that the reactivity of acid-extracted fractions corresponds to IgG antibodies that were bound to brain NMDAR receptors. The second row in A and B shows the reactivity with a monoclonal GluN1 antibody, and the third row the colocalization of immunolabelling. Scale bars = 10 μ m. (C) Quantification of NMDAR antibody titre in IgG-extracted fractions from hippocampus of animals treated with patients' CSF ($n = 5$ mice per each time point, except four mice for Day 5). Solid line = median. Significance was tested by Kruskal-Wallis with an α -error of 0.05 (asterisks) and *post hoc* testing with Dunn's test (\$). ***, \$\$\$ $p < 0.01$, ****, \$\$\$ $p < 0.001$. See Supplementary Table 2 for detailed statistics. (D and E) HEK293 cells expressing the GluN1 subunit of the NMDAR immunolabelled with acid-extracted IgG fractions (D) and pre-extraction fractions (E) from hippocampus (Hippo), cerebral cortex (Ctx) and cerebellum (Cb) of mice infused with patients' CSF (Day 18). The acid-extracted IgG fraction from hippocampus showed higher level of NMDAR antibodies than those extracted from cerebral cortex (Ctx) and cerebellum (Cb). Scale bars = 10 μ m. n.s. = not significant.

The high levels of brain-bound NMDAR antibodies between Days 13–18 suggests that after stopping the infusion of patients' CSF on Day 14, the NMDAR antibodies continued being distributed from mice cerebroventricular system to parenchyma. This distribution occurred slowly; for example, 5 days after starting the infusion of patients' CSF the amount of NMDAR antibodies that had reached the hippocampus was very limited compared to that seen on Days 13–18 (shown in Fig. 4B). Moreover, previous studies using cultured neurons treated with patients' CSF showed that once the antibodies bound to the NMDARs, the reduction of receptors was microscopically visible in 2 h but it took 12 h to result in the lowest receptor density. Subsequently, there was a steady state of low NMDAR density for as long as the neurons were exposed to patients' antibodies (Moscato *et al.*, 2014). Together, these findings explain the progressive worsening of symptoms along with continued antibody binding and decrease of NMDAR for

at least 4 days after the ventricular infusion stops and the subsequent recovery starts.

Although the hippocampus was the region with the highest concentration of brain-bound NMDAR antibodies, these antibodies were also extracted from cerebral cortex or cerebellum though at much lower levels. The higher concentration of antibodies and predominant decrease of NMDAR in the hippocampus are consistent with the predominant binding of human antibodies to this brain region when sections of rodent brain are directly incubated with patients' antibodies (Dalmau *et al.*, 2007; Moscato *et al.*, 2014). Additionally, because of the close spatial relationship to the ventricles, the intraventricular infusion of human CSF antibodies might have contributed to the preferential binding to the hippocampus.

The correlation between the concentration of brain-bound antibodies and selective reduction of NMDAR cluster density and protein concentration was similar to

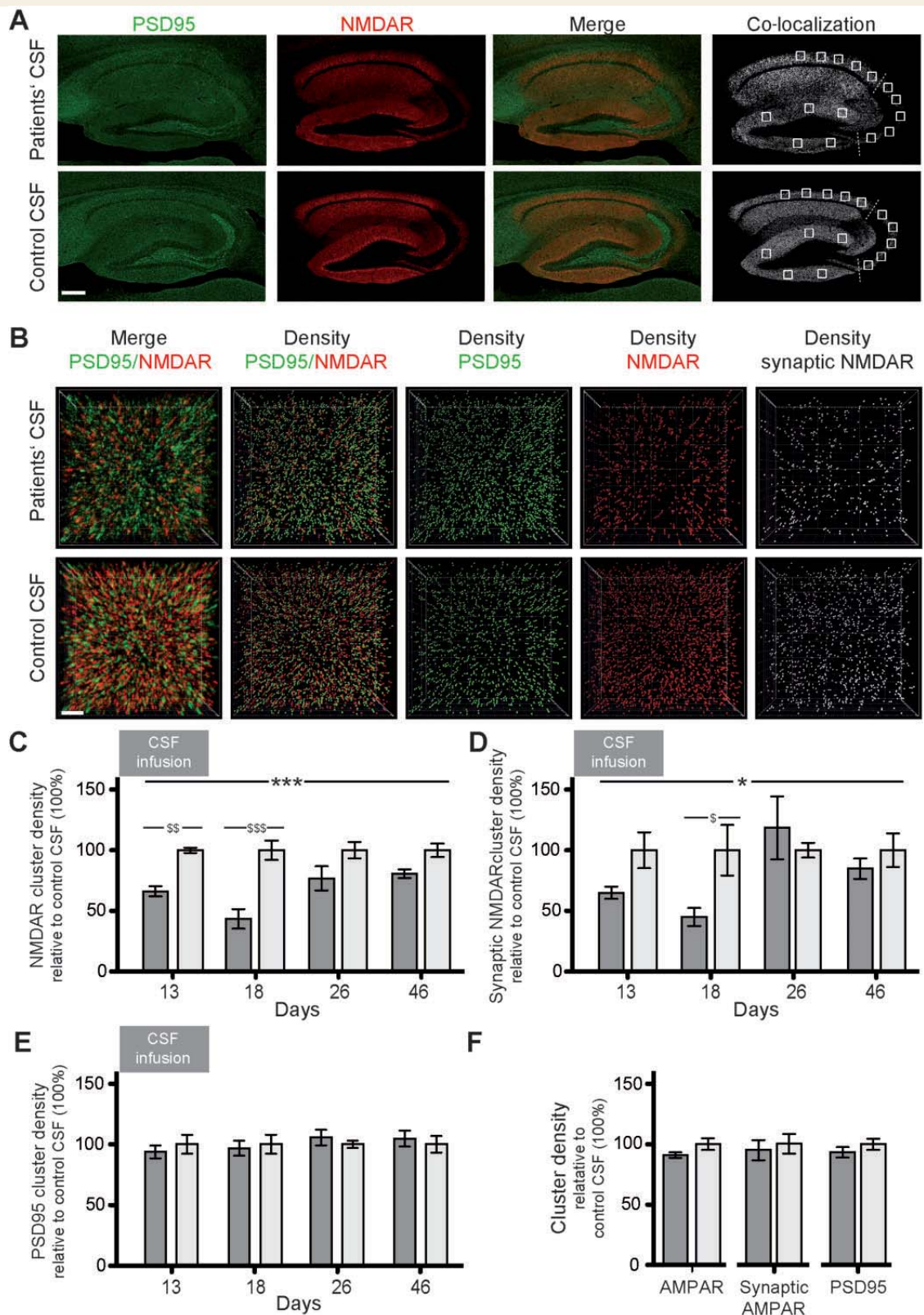


Figure 6 Patients' NMDAR antibodies selectively reduce the density of total and synaptic NMDAR clusters in hippocampus of mice. (A) Hippocampus of mice infused for 14 days (Day 18) with patients' CSF (upper row) or control CSF (lower row) immunolabelled for PSD95 and NMDAR. Images were merged (merge) and post-processed to demonstrate co-localizing clusters (co-localization). Squares in 'co-localization' indicate the analysed areas in CA1, CA3 and dentate gyrus. Scale bar = 200 μ m. (B) Three-dimensional projection and analysis of the density of

(continued)

that reported using *in vitro* studies with cultured rat hippocampal neurons (Hughes *et al.*, 2010; Moscato *et al.*, 2014). Moreover, autopsies of patients with anti-NMDAR encephalitis showed that the hippocampal regions with highest concentration of brain-bound antibodies were also the areas with lower expression of NMDAR (Dalmau *et al.*, 2007). In the current model, patients' antibodies did not alter AMPAR cluster density or protein concentration; these findings are in line with those reported with cultured neurons where the clusters of AMPAR and AMPAR-mediated currents were not directly affected (Hughes *et al.*, 2010). These experiments, however, did

not explore whether paradigms that normally induce long-term potentiation, and therefore increase the number of synaptic AMPAR, were altered by patients' antibodies. Mikasova *et al.* (2012) showed that neurons exposed to patients' NMDAR antibodies failed to show an increase in cell surface AMPAR after induction of chemical long-term potentiation. Another study examining the acute metabolic effects of patients' antibodies after injection into rat brain showed impairment of NMDA and AMPA-mediated synaptic function (Manto *et al.*, 2010). In the present model, we did not perform electrophysiological studies on acute slices of brain (a goal of future

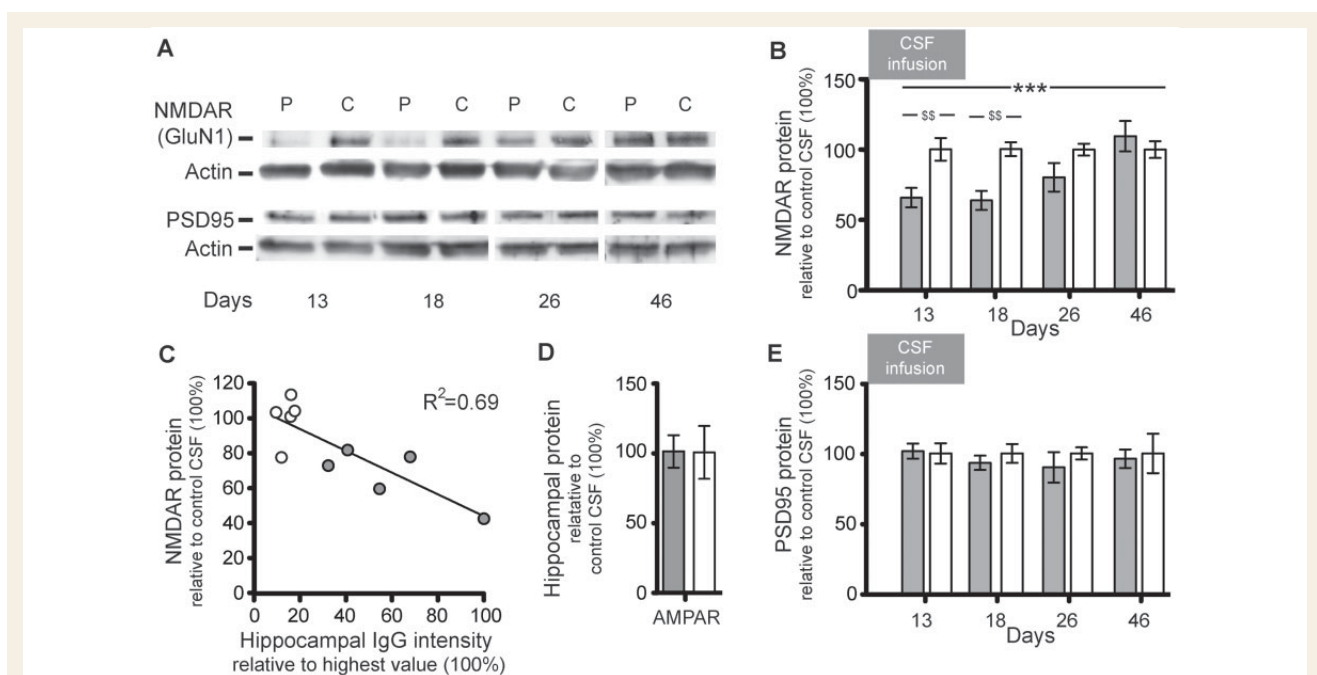


Figure 7 Patients' NMDAR antibodies selectively reduce the protein concentration of NMDAR in hippocampus of mice. (A) Representative immunoblots of proteins extracted from hippocampus of animals infused with patients' CSF (P) or control CSF (C) sacrificed at the indicated time points and probed for expression of GluN1 (NMDAR), PSD95 and β -actin (loading control). Note that there is less visible GluN1 expression on Days 13 and 18. (B, D and E) Quantification of total NMDAR (B), AMPAR (D) or PSD95 (E) protein in animals treated with patients' CSF (filled columns) or control CSF (open columns) sacrificed at the indicated time points (AMPA Day 18 only, D). Results were normalized to β -actin (loading control). Mean band density of animals treated with control CSF was defined as 100%. Data are presented as mean \pm SEM. For each time point six animals infused with patients' CSF and six with control CSF were examined (for Days 26 and 46, only five animals treated with patient's CSF were available). Significance of treatment effect was assessed by two-way ANOVA with an α -error of 0.05 (asterisks) and *post hoc* testing with Sidak-Holm adjustment (\$). $^{**}P < 0.01$; $^{***}P < 0.001$. See [Supplementary Table 2](#) for detailed statistics. (C) Correlation between concentration of human IgG bound to hippocampus (x-axis, highest hippocampal IgG intensity was defined as 100%) and hippocampal NMDAR protein concentration in mice sacrificed on Day 18 ($R^2 = 0.69$, $P = 0.003$). Filled circles: mice infused with patients' CSF ($n = 5$), open circles: mice infused with control CSF ($n = 5$).

Figure 6 Continued

total clusters of PSD95 and NMDAR, and synaptic clusters of NMDAR (defined as NMDAR clusters colocalizing with PSD95) in a representative CA3 region (square in **A** 'co-localization'). Merged images (merge, PSD95 green, NMDAR red) were post-processed and used to calculate the density of clusters (density = spots/ μm^3). Scale bar = $2\mu\text{m}$. (C-F) Quantification of the density of total (C) and synaptic (D) NMDAR clusters, PSD95 clusters (E), and total/synaptic AMPAR and PSD95 clusters (Day 18 only, F) in a pooled analysis of hippocampal subregions (CA1, CA3, dentate gyrus) in animals treated with patients' CSF (dark grey) or control CSF (light grey) on the indicated days. Mean density of clusters in control CSF treated animals was defined as 100%. Data are presented as mean \pm SEM. For each time point five animals infused with patients' CSF and five with control CSF were examined. Significance of treatment effect was assessed by two-way ANOVA with an α -error of 0.05 (asterisks) and *post hoc* testing with Sidak-Holm adjustment (\$) (C-E) or unpaired *t*-test (F). $^{*}P < 0.05$; $^{**}P < 0.01$; $^{***}P < 0.001$. See [Supplementary Table 2](#) for detailed statistics.

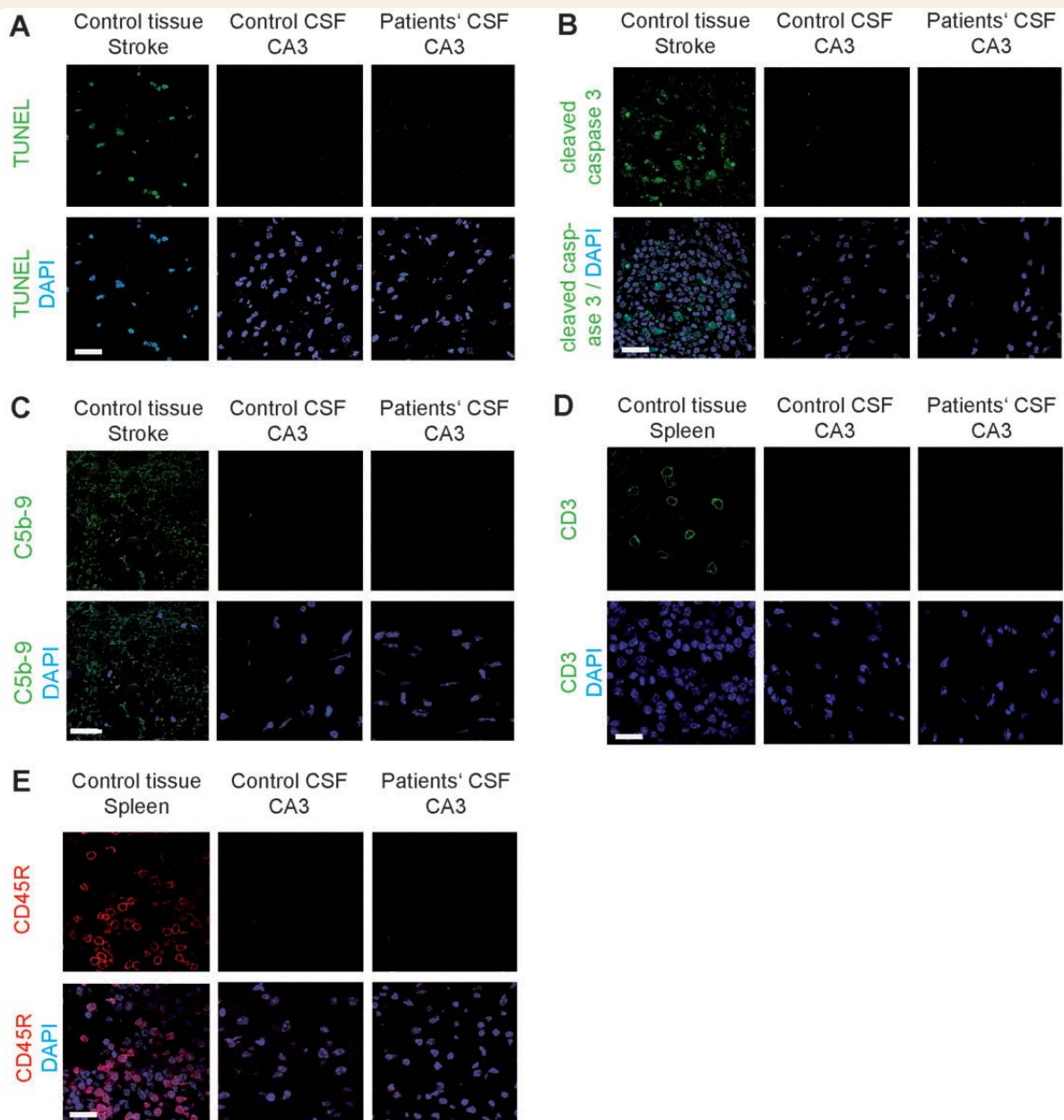


Figure 8 Absence of neuronal apoptosis, deposits of complement, and lymphocytic infiltrates in the hippocampus of mice infused with patients' CSF. (A and B) TUNEL and cleaved caspase 3 immunolabelling of a representative area of CA3 (area with maximal IgG binding and lower NMDAR concentration) of an animal infused with patients' CSF, showing lack of apoptotic cells. A section of the same region in an animal with transient middle cerebral artery occlusion (stroke model) shows apoptotic cells in the penumbra (*left*). (C) Same CA3 region as in (A) immunostained for C5b-9 showing lack of deposit of complement. A section of the same region in the indicated stroke model shows presence of complement in the penumbra (*left*). (D and E) Same CA3 region as in (A) immunostained for T (CD3) and B (CD45R) lymphocytes showing absence of inflammatory infiltrates. A section of spleen was used as control tissue showing the presence of CD3 (green) and CD45R (red) cells. Scale bar = 10 μ m. Total number of animals examined: patients' CSF $n = 5$; control CSF $n = 5$. Scale bars = 20 μ m.

studies); however, there is reported evidence that patients' NMDAR antibodies suppress induction of long-term potentiation when directly applied to mouse hippocampal slices (Zhang *et al.*, 2012). Work with cultured neurons indicates that the decrease of synaptic NMDAR currents is likely a result of the antibody-mediated low receptor

levels, as no direct antibody blockade was detected (Moscato *et al.*, 2014).

Our study has limitations related to the type of disease and symptoms to model. For example, different from other models of antibody-mediated CNS disorders where the antibodies result in characteristic symptoms (e.g.

amphiphysin antibodies and visible muscle spasms (Sommer *et al.*, 2005) or focal deficits with visible tissue changes (e.g. AQP4 antibodies and neuromyelitis optica) (Hinson *et al.*, 2012; Bradl and Lassmann, 2014), anti-NMDAR encephalitis results in a broader spectrum of symptoms where memory and behavioural deficits occur early, and the structural alterations are not visible unless the NMDAR clusters or protein concentration are measured. It is not surprising that in the current model the full spectrum of symptoms, such as seizures, dyskinesias or coma, did not occur. Studies with NMDAR antagonists have shown that the progression of symptoms (from behavioural and memory deficits to unresponsiveness with catatonic features and coma) correlated with the intensity of the decrease of receptor function (Javitt and Zukin, 1991). Therefore, it is likely that prolonged infusion or higher concentration of patients' antibodies would cause additional symptoms. This is supported by the current model, in which the time course of symptom development, brain-bound antibody concentration, and decrease of synaptic NMDAR correlated well with each other. Future experiments using prolonged infusion or higher concentration of patients' antibodies may also result in symptoms beyond hippocampal-parahippocampal regions. Compared with the hippocampus, other brain regions normally have lower density of NMDAR, and appeared to be less accessible to the ventricularly infused antibodies. Direct injection of antibodies into those brain regions can be considered, but we previously tried bilateral hippocampal infusion using the same osmotic pump approach, resulting in more limited antibody diffusion and no symptoms (data not published). Moreover, the phenotype of the current model is likely influenced by the strain of mice. In this study we used C57BL6/J mice because we were interested in the effects on memory and behaviour, but this strain is one of the most resistant to develop seizures (Ferraro *et al.*, 2002).

The antibody-induced depletion of synaptic NMDAR along with the similarities between the human disease and the phenotypes induced by NMDAR antagonists (phencyclidine, ketamine or MK801) have suggested points of convergence with one of the most influential theories of schizophrenia, the NMDA-hypofunction model (Olney and Farber, 1995; Kehrer *et al.*, 2008). The presence of positive (hallucinations, delusions, hyperactivity) and negative (decreased motivation, flat affect, deficit of memory and learning) symptoms is, however, not identical among the drug-induced phenotypes and also varies among animal species (Javitt and Zukin, 1991). It has been suggested that NMDAR-bearing parvalbumin-positive GABAergic interneurons are disproportionately more sensitive to NMDAR antagonists than other neurons (Li *et al.*, 2002). Interestingly, a genetic model of partial ablation of the GluN1 subunit of NMDAR in corticolimbic GABAergic interneurons resulted in symptoms partially resembling our GluN1 immunological model of receptor depletion, including memory deficits and anhedonic behaviours (Belforte *et al.*, 2010). Differences related to the underlying

mechanisms (pharmacologic blockade, genetic or immunologic NMDAR depletion) and regions where the NMDAR function is depleted (general, corticolimbic, or hippocampal-parahippocampal) likely influence the clinical phenotypes.

Overall, the current findings provide robust evidence that antibodies from patients with anti-NMDAR encephalitis alter memory and behaviour through reduction of cell-surface and synaptic NMDAR, and therefore support the use of treatments directed at decreasing the levels of antibodies or antibody-producing cells. This approach can now be adapted to (i) model other aspects of the disease by changing the duration and dosing of antibody infusion, or strain of mice; (ii) investigate other disorders of memory and behaviour that occur in association with antibodies against other cell surface or synaptic proteins, such as AMPAR or GABA(B)R (Lai *et al.*, 2009; Lancaster *et al.*, 2010); and (iii) determine whether compounds such as Ephrin-B2 ligand that has been shown to prevent the destabilizing NMDAR crosslinking effects of patients' antibodies improve or alter the course of the disease (Mikasova *et al.*, 2012).

Acknowledgements

We thank Anna Planas and Vanessa Brait for providing stroke brain tissue and Jordi Andilla for technical support.

Funding

This work was supported by the National Institutes of Health RO1NS077851 (J.D.), RO1MH094741 (R.B.-G. and J.D.), Fundació La Marató de TV3 #101530 (J.D.), Fondo de Investigaciones Sanitarias/Instituto Carlos III (FIS PI11/01780 J.D.), ErasmusMC fellowship (M.T.), and Forschungsförderungsfonds Hamburg-Eppendorf FL).

Conflict of interest

Dr Dalmau holds a patent for the use of NMDA receptor as an autoantibody test. Dr Dalmau has received a research grant from Euroimmun Inc.

Supplementary material

Supplementary material is available at *Brain* online.

References

- Aso E, Ozaita A, Valdizan EM, Ledent C, Pazos A, Maldonado R, *et al.* BDNF impairment in the hippocampus is related to enhanced despair behavior in CB1 knockout mice. *J Neurochem* 2008; 105: 565–72.

- Banovic D, Khorramshahi O, Oswald D, Wichmann C, Riedt T, Fouquet W, et al. Drosophila neuroligin 1 promotes growth and postsynaptic differentiation at glutamatergic neuromuscular junctions. *Neuron* 2010; 66: 724–38.
- Belforte JE, Zsiros V, Sklar ER, Jiang Z, Yu G, Li Y, et al. Postnatal NMDA receptor ablation in corticolimbic interneurons confers schizophrenia-like phenotypes. *Nat Neurosci* 2010; 13: 76–83.
- Berrrendero F, Mendizabal V, Robledo P, et al. Nicotine-induced antinociception, rewarding effects, and physical dependence are decreased in mice lacking the preproenkephalin gene. *J Neurosci* 2005; 25: 1103–12.
- Bradl M, Lassmann H. Experimental models of neuromyelitis optica. *Brain Pathol* 2014; 24: 74–82.
- Bura AS, Guegan T, Zamanillo D, Vela JM, Maldonado R. Operant self-administration of a sigma ligand improves nociceptive and emotional manifestations of neuropathic pain. *Eur J Pain* 2013; 17: 832–43.
- Bura SA, Burokas A, Martin-Garcia E, Maldonado R. Effects of chronic nicotine on food intake and anxiety-like behaviour in CB(1) knockout mice. *Eur Neuropsychopharmacol* 2010; 20: 369–78.
- Bura SA, Castane A, Ledent C, Valverde O, Maldonado R. Genetic and pharmacological approaches to evaluate the interaction between the cannabinoid and cholinergic systems in cognitive processes. *Br J Pharmacol* 2007; 150: 758–65.
- Burokas A, Gutierrez-Cuesta J, Martin-Garcia E, Maldonado R. Operant model of frustrated expected reward in mice. *Addict Biol* 2012; 17: 770–82.
- Caille S, Espejo EF, Reneric JP, Cador M, Koob GF, Stinus L. Total neurochemical lesion of noradrenergic neurons of the locus ceruleus does not alter either naloxone-precipitated or spontaneous opiate withdrawal nor does it influence ability of clonidine to reverse opiate withdrawal. *J Pharmacol Exp Ther* 1999; 290: 881–92.
- Crawley J, Goodwin FK. Preliminary report of a simple animal behavior model for the anxiolytic effects of benzodiazepines. *Pharmacol Biochem Behav* 1980; 13: 167–70.
- Dalmau J, Gleichman AJ, Hughes EG, Rossi JE, Peng X, Lai M, et al. Anti-NMDA-receptor encephalitis: case series and analysis of the effects of antibodies. *Lancet Neurol* 2008; 7: 1091–8.
- Dalmau J, Tuzun E, Wu HY, Masjuan J, Rossi JE, Voloschin A, et al. Paraneoplastic anti-N-methyl-D-aspartate receptor encephalitis associated with ovarian teratoma. *Ann Neurol* 2007; 61: 25–36.
- Ennaceur A. One-trial object recognition in rats and mice: methodological and theoretical issues. *Behav Brain Res* 2010; 215: 244–54.
- Ferraro TN, Golden GT, Smith GG, DeMuth D, Buono RJ, Berrettini WH. Mouse strain variation in maximal electroshock seizure threshold. *Brain Res* 2002; 936: 82–6.
- Filliol D, Ghozland S, Chluba J, et al. Mice deficient for delta- and mu-opioid receptors exhibit opposing alterations of emotional responses. *Nat Genet* 2000; 25: 195–200.
- Frechette ES, Zhou L, Galetta SL, Chen L, Dalmau J. Prolonged follow-up and CSF antibody titers in a patient with anti-NMDA receptor encephalitis. *Neurology* 2011; 76: S64–6.
- Gleichman AJ, Spruce LA, Dalmau J, Seeholzer SH, Lynch DR. Anti-NMDA receptor encephalitis antibody binding is dependent on amino acid identity of a small region within the GluN1 amino terminal domain. *J Neurosci* 2012; 32: 11082–94.
- Gresa-Arribas N, Titulaer MJ, Torrents A, Aguilar E, McCracken L, Leypoldt F, et al. Antibody titres at diagnosis and during follow-up of anti-NMDA receptor encephalitis: a retrospective study. *Lancet Neurol* 2014; 13: 167–77.
- Gunduz-Bruce H. The acute effects of NMDA antagonism: from the rodent to the human brain. *Brain Res Rev* 2009; 60: 279–86.
- Hahn CG, Wang HY, Cho DS, Talbot K, Gur RE, Berrettini WH, et al. Altered neuregulin 1-erbB4 signaling contributes to NMDA receptor hypofunction in schizophrenia. *Nat Med* 2006; 12: 824–8.
- Handley SL, Mithani S. Effects of alpha-adrenoceptor agonists and antagonists in a maze-exploration model of 'fear'-motivated behaviour. *Naunyn Schmiedebergs Arch Pharmacol* 1984; 327: 1–5.
- Hinson SR, Romero MF, Popescu BF, Lucchinetti CF, Fryer JP, Wolburg H, et al. Molecular outcomes of neuromyelitis optica (NMO)-IgG binding to aquaporin-4 in astrocytes. *Proc Natl Acad Sci USA* 2012; 109: 1245–50.
- Hughes EG, Peng X, Gleichman AJ, Lai M, Zhou L, Tsou R, et al. Cellular and synaptic mechanisms of anti-NMDA receptor encephalitis. *J Neurosci* 2010; 30: 5866–75.
- Iizuka T, Sakai F, Ide T, Monzen T, Yoshii S, Iigaya M, et al. Anti-NMDA receptor encephalitis in Japan: long-term outcome without tumor removal. *Neurology* 2008; 70: 504–11.
- Irani SR, Bera K, Waters P, et al. N-methyl-D-aspartate antibody encephalitis: temporal progression of clinical and paraclinical observations in a predominantly non-paraneoplastic disorder of both sexes. *Brain* 2010; 133: 1655–67.
- Javitt DC, Zukin SR. Recent advances in the phencyclidine model of schizophrenia. *Am J Psychiatry* 1991; 148: 1301–8.
- Jentsch JD, Roth RH. The neuropsychopharmacology of phencyclidine: from NMDA receptor hypofunction to the dopamine hypothesis of schizophrenia. *Neuropsychopharmacology* 1999; 20: 201–25.
- Kayser MS, Titulaer MJ, Gresa-Arribas N, Dalmau J. Frequency and characteristics of isolated psychiatric episodes in anti-N-methyl-d-aspartate receptor encephalitis. *JAMA Neurol* 2013; 70: 1133–9.
- Kehrer C, Maziashvili N, Dugladze T, Gloveli T. Altered excitatory-inhibitory balance in the NMDA-hypofunction model of schizophrenia. *Front Mol Neurosci* 2008; 1: 6.
- Konig M, Zimmer AM, Steiner H, Holmes PV, Crawley JN, Brownstein MJ, et al. Pain responses, anxiety and aggression in mice deficient in pre-proenkephalin. *Nature* 1996; 383: 535–8.
- Lai M, Hughes EG, Peng X, Zhou L, Gleichman AJ, Shu H, et al. AMPA receptor antibodies in limbic encephalitis alter synaptic receptor location. *Ann Neurol* 2009; 65: 424–34.
- Lancaster E, Lai M, Peng X, Hughes E, Constantinescu R, Raizer J, et al. Antibodies to the GABA(B) receptor in limbic encephalitis with seizures: case series and characterisation of the antigen. *Lancet Neurol* 2010; 9: 67–76.
- Lau CG, Zukin RS. NMDA receptor trafficking in synaptic plasticity and neuropsychiatric disorders. *Nat Rev Neurosci* 2007; 8: 413–26.
- Li Q, Clark S, Lewis DV, Wilson WA. NMDA receptor antagonists disinhibit rat posterior cingulate and retrosplenial cortices: a potential mechanism of neurotoxicity. *J Neurosci* 2002; 22: 3070–80.
- Llorente-Berzal A, Puighermanal E, Burokas A, Ozaita A, Maldonado R, Marco EM, et al. Sex-dependent psychoneuroendocrine effects of THC and MDMA in an animal model of adolescent drug consumption. *PLoS One* 2013; 8: e78386.
- Maldonado JE, Kyle RA, Ludwig J. Meningeal myeloma. *Arch Intern Med* 1970; 126: 660–3.
- Manto M, Dalmau J, Didelot A, Rogemond V, Honnorat J. *In vivo* effects of antibodies from patients with anti-NMDA receptor encephalitis: further evidence of synaptic glutamatergic dysfunction. *Orphanet J Rare Dis* 2010; 5: 31.
- Martinez-Hernandez E, Horvath J, Shiloh-Malawsky Y, Sangha N, Martinez-Lage M, Dalmau J. Analysis of complement and plasma cells in the brain of patients with anti-NMDAR encephalitis. *Neurology* 2011; 77: 589–93.
- Mikasova L, De RP, Bouchet D, Georges F, Rogemond V, Didelot A, et al. Disrupted surface cross-talk between NMDA and Ephrin-B2 receptors in anti-NMDA encephalitis. *Brain* 2012; 135: 1606–21.
- Mohn AR, Gainetdinov RR, Caron MG, Koller BH. Mice with reduced NMDA receptor expression display behaviors related to schizophrenia. *Cell* 1999; 98: 427–36.
- Moscato EH, Peng X, Jain A, Parsons TD, Dalmau J, Balice-Gordon RJ. Acute mechanisms underlying antibody effects in anti-

- N-methyl-D-aspartate receptor encephalitis. *Ann Neurol* 2014; 76: 108–90.
- Mouri A, Noda Y, Noda A, Nakamura T, Tokura T, Yura Y, et al. Involvement of a dysfunctional dopamine-D1/N-methyl-d-aspartate-NR1 and Ca²⁺/calmodulin-dependent protein kinase II pathway in the impairment of latent learning in a model of schizophrenia induced by phencyclidine. *Mol Pharmacol* 2007; 71: 1598–609.
- Olney JW, Farber NB. Glutamate receptor dysfunction and schizophrenia. *Arch Gen Psychiatry* 1995; 52: 998–1007.
- Porsolt RD, Bertin A, Jalfre M. Behavioral despair in mice: a primary screening test for antidepressants. *Arch Int Pharmacodyn Ther* 1977; 229: 327–36.
- Puighermanal E, Marsicano G, Busquets-Garcia A, Lutz B, Maldonado R, Ozaita A. Cannabinoid modulation of hippocampal long-term memory is mediated by mTOR signaling. *Nat Neurosci* 2009; 12: 1152–8.
- Rose NR, Bona C. Defining criteria for autoimmune diseases (Witebsky's postulates revisited). *Immunol Today* 1993; 14: 426–30.
- Shepherd JD, Huganir RL. The cell biology of synaptic plasticity: AMPA receptor trafficking. *Annu Rev Cell Dev Biol* 2007; 23: 613–43.
- Snyder EM, Nong Y, Almeida CG, Paul S, Moran T, Choi EY, et al. Regulation of NMDA receptor trafficking by amyloid-beta. *Nat Neurosci* 2005; 8: 1051–8.
- Sommer C, Weishaupt A, Brinkhoff J, Biko L, Wessig C, Gold R, et al. Paraneoplastic stiff-person syndrome: passive transfer to rats by means of IgG antibodies to amphiphysin. *Lancet* 2005; 365: 1406–11.
- Steru L, Chermat R, Thierry B, Simon P. The tail suspension test: a new method for screening antidepressants in mice. *Psychopharmacology (Berl)* 1985; 85: 367–70.
- Strekalova T, Gorenkova N, Schunk E, Dolgov O, Bartsch D. Selective effects of citalopram in a mouse model of stress-induced anhedonia with a control for chronic stress. *Behav Pharmacol* 2006; 17: 271–87.
- Tagliatela G, Hogan D, Zhang WR, Dineley KT. Intermediate- and long-term recognition memory deficits in Tg2576 mice are reversed with acute calcineurin inhibition. *Behav Brain Res* 2009; 200: 95–9.
- Titulaer MJ, McCracken L, Gabilondo I, Armangué T, Glaser C, Iizuka T, et al. Treatment and prognostic factors for long-term outcome in patients with anti-NMDA receptor encephalitis: an observational cohort study. *Lancet Neurol* 2013; 12: 157–65.
- Viaccoz A, Desestret V, Ducray F, Picard G, Cavillon G, Rogemond V, et al. Clinical specificities of adult male patients with NMDA receptor antibodies encephalitis. *Neurology* 2014; 82: 556–63.
- Weiner AL, Vieira L, McKay CA, Bayer MJ. Ketamine abusers presenting to the emergency department: a case series. *J Emerg Med* 2000; 18: 447–51.
- Winters BD, Forwood SE, Cowell RA, Saksida LM, Bussey TJ. Double dissociation between the effects of peri-postrhinal cortex and hippocampal lesions on tests of object recognition and spatial memory: heterogeneity of function within the temporal lobe. *J Neurosci* 2004; 24: 5901–8.
- Zhang Q, Tanaka K, Sun P, Nakata M, Yamamoto R, Sakimura K, et al. Suppression of synaptic plasticity by cerebrospinal fluid from anti-NMDA receptor encephalitis patients. *Neurobiol Dis* 2012; 45: 610–15.

Supplemental material

Behavioral animal tests and references

Supplemental Tables 1 and 2

Supplemental Figures 1 and 2

Behavioral animal tests

Novel object recognition (NOR) test: This test was performed in two paradigms, open field (45x45x40 cm, Panlab, Spain) and in V-maze (40 cm per side, Panlab, Spain) using two different groups of animals, as reported by us and others [Bura *et al.* 2007; Tagliabattola *et al.* 2009; Puighermanal *et al.* 2009]. On day 1 (same day of osmotic pump implantation, before surgery) mice were habituated for 30 minutes in the open field arena, or 9 minutes in the V-maze. On days 3, 10, 18 and 25, mice were put back into the open field arena or into the V-maze for 9 minutes; two identical objects were presented, and the time the mice spent exploring each object was recorded. After a retention phase of 3 hours, the mice were placed for another 9 minutes into the open field arena or into the V-maze; in each paradigm one of the familiar objects was replaced with a novel object and the total time spent exploring each object (novel and familiar) was registered. During the test phase of the open field paradigm, the objects were positioned in the opposite corners of those used in the training phase and the novel object was presented in 50% of trials on the right and in 50% of trials on the left side. Object exploration was defined as the orientation of the nose to the object at a distance of less than 2 cm. A discrimination index was calculated as the difference of the time spent exploring the novel and the time spent exploring the familiar object divided by the total time exploring both objects. A

higher discrimination index is considered to reflect greater memory retention for the familiar object [Puighermanal, Marsicano, Busquets-Garcia, Lutz, Maldonado, and Ozaita2009;Ennaceur 2010].

Sucrose preference test: This test was performed on days 10 and 24 after surgery, as previously reported [Bura *et al.* 2013;Strekalova *et al.* 2006]. During the 4 days preceding surgery, two bottles of water, one with 2% sucrose and the other without, were placed in the cage. Every day the position of the bottles was exchanged, and the consumption from each bottle measured. On the day of the test, the two bottles were placed again in the cage and the consumption from each recorded after a 24h interval. The preference for sucrose was calculated as the relative amount of water with sucrose versus total liquid (water with and without sucrose) consumed by the mice.

Tail suspension test (TST): This test was performed on day 12 after surgery, as previously reported [Steru *et al.* 1985;Aso *et al.* 2008]. Mice were suspended 50 cm above a solid surface by the use of adhesive tape applied to the tail (3/4 of the distance from the base of mouse tail). During a six minutes interval, the total time of immobility was recorded. Long periods of immobility are characteristic of a depressive-like state; an alternative test is the forced swimming test, which was also applied at a different time point (see below).

Forced swimming test (FST): This test was performed on day 20 after surgery, as previously reported [Filliol *et al.* 2000;Porsolt *et al.* 1977]. The mouse was placed in a plastic cylinder containing warm water (27-28 °C), deep enough to prevent touching the bottom of the cylinder and forcing the mouse to swim. The trial lasted 6 minutes and the total time of immobility after

minute 2:00 was recorded. Time of immobility was defined as the time that the animal stopped swimming and only used minimal movements to keep the head above the water.

Black and white test: This test was performed on day 6 after surgery, as reported [Bura *et al.* 2010;Crawley and Goodwin 1980]. It measures the conflict between the natural tendency of rodents to explore new environments and the tendency to avoid brightly illuminated areas. The box consisted of two compartments (20 cm wide × 20 cm long × 30 cm high) connected by a 6 cm wide by 6 cm high tunnel. One compartment was painted black and maintained at 10 lux, while the other compartment was painted white, brightly illuminated (500 lux), and subdivided into three sections (distal, medial and proximal), based on the distance from the tunnel. The floor of both compartments was subdivided into squares (5x5 cm) to measure the locomotor activity. At the start of the session, mice were placed in the black compartment, head facing a corner. The latency of first entry into the white compartment and section reached in each entry, together with time spent, squares crossed, and number of entries into both compartments were recorded and used to evaluate anxiety.

Elevated plus maze test: This test was performed on day 14 after surgery, as reported [Handley and Mithani 1984;Llorente-Berzal *et al.* 2013]. The test is based on the same principle as the black and white test, and measures the conflict between the natural tendency of mice to avoid an illuminated and elevated surface, and the natural tendency to explore new environments. It consisted of a plastic black cross with arms 40 cm long and 6 cm wide placed 50 cm above the floor. Two opposite arms were surrounded by walls (15 cm high, closed arms, 10 lux), while the two other arms were devoid of such walls (open arms, 200 lux). The four arms were connected

by a central platform. At the start of the session, the mouse was placed at the end of a closed arm facing the wall. During the 5-minute trial, the number of entries and the time spent in each arm were recorded. Anxiety was assessed as both the time spent avoiding the open arms and the number of entries into them.

Resident-intruder test: This test, performed on days 3, 10, 18 and 25 after surgery, evaluates aggressive behavior in rodents, as reported [Konig *et al.* 1996;Burokas *et al.* 2012]. Resident mice were housed individually for at least 10 days before the test. Intruder animals of similar age and weight were housed five per cage. Each session consisted of putting together resident and intruder mice for a period of 4 minutes, measuring the latency of the first aggressive event and frequency of events.

Locomotor activity: This test was performed on days 3, 10, 18 and 25 after surgery. Animals were assessed in locomotor activity boxes (9×20×11 cm; Imetronic, Passac, France), equipped with 2 rows of photocell detectors, and placed in a low-luminosity environment (20–25 lux), as previously described [Caille *et al.* 1999;Berrendero *et al.* 2005]. The mouse locomotor activity was recorded for 10 minutes as horizontal activity and vertical activity.

Legends to supplemental figures

Supplemental Figure 1: Quantification of human IgG present in mice cerebral cortex

Quantification of the intensity of immunolabeling of human IgG present in frontal cortex of mice infused with patients' CSF (grey columns) or control CSF (white columns) sacrificed at the indicated time points. The change over time of the amount of patients' IgG detected in frontal cortex is similar to that demonstrated in hippocampus (see Figure 4 C: progressive increase until day 18 followed by a wash out period). Note that despite the similarity in the dynamics of patient's IgG detection, in all time points the amount of patients' IgG in frontal cortex was substantially less than that found in hippocampus (5% versus 100%)

Mean intensity of immunostaining of patients' IgG detected in hippocampus in the group with the highest value (animals infused with patients' CSF examined at day 18) was defined as 100%.

All data are presented as mean \pm s.e.m. For each time point 5 animals infused with patients' CSF and 5 with control CSF were examined. Significance of treatment effect was assessed by two-way ANOVA with an α -error of 0.05 (*) and post-hoc testing with Sidak-Holm adjustment (\$). ***, \$\$\$ $P < 0.001$; \$, $P < 0.05$.

Supplemental Figure 2: Absence of brain-bound NMDAR-specific IgG in mice infused with CSF from NMDAR antibody negative patients (control)

HEK293 cells expressing the GluN1 subunit of the NMDAR immunolabeled with acid-extracted IgG fractions (top row) from hippocampus of mice infused with control CSF and sacrificed on the indicated days. No reactivity is observed. The second row shows the reactivity with a monoclonal GluN1 antibody, and the third row the co-localization of immunolabeling. Scale bars=10 μ m.

References

- Aso E, Ozaita A, Valdizan EM *et al.* BDNF impairment in the hippocampus is related to enhanced despair behavior in CB1 knockout mice. *J Neurochem* 2008; 105: 565-572.
- Berrendero F, Mendizabal V, Robledo P *et al.* Nicotine-induced antinociception, rewarding effects, and physical dependence are decreased in mice lacking the preproenkephalin gene. *J Neurosci* 2005; 25: 1103-1112.
- Bura AS, Guegan T, Zamanillo D, Vela JM, Maldonado R. Operant self-administration of a sigma ligand improves nociceptive and emotional manifestations of neuropathic pain. *Eur J Pain* 2013; 17: 832-843.
- Bura SA, Burokas A, Martin-Garcia E, Maldonado R. Effects of chronic nicotine on food intake and anxiety-like behaviour in CB(1) knockout mice. *Eur Neuropsychopharmacol* 2010; 20: 369-378.
- Bura SA, Castane A, Ledent C, Valverde O, Maldonado R. Genetic and pharmacological approaches to evaluate the interaction between the cannabinoid and cholinergic systems in cognitive processes. *Br J Pharmacol* 2007; 150: 758-765.
- Burokas A, Gutierrez-Cuesta J, Martin-Garcia E, Maldonado R. Operant model of frustrated expected reward in mice. *Addict Biol* 2012; 17: 770-782.
- Caille S, Espejo EF, Reneric JP, Cador M, Koob GF, Stinus L. Total neurochemical lesion of noradrenergic neurons of the locus ceruleus does not alter either naloxone-precipitated or spontaneous opiate withdrawal nor does it influence ability of clonidine to reverse opiate withdrawal. *J Pharmacol Exp Ther* 1999; 290: 881-892.
- Crawley J, Goodwin FK. Preliminary report of a simple animal behavior model for the anxiolytic effects of benzodiazepines. *Pharmacol Biochem Behav* 1980; 13: 167-170.
- Ennaceur A. One-trial object recognition in rats and mice: methodological and theoretical issues. *Behav Brain Res* 2010; 215: 244-254.
- Filliol D, Ghozland S, Chluba J *et al.* Mice deficient for delta- and mu-opioid receptors exhibit opposing alterations of emotional responses. *Nat Genet* 2000; 25: 195-200.
- Handley SL, Mithani S. Effects of alpha-adrenoceptor agonists and antagonists in a maze-exploration model of 'fear'-motivated behaviour. *Naunyn Schmiedebergs Arch Pharmacol* 1984; 327: 1-5.
- Konig M, Zimmer AM, Steiner H *et al.* Pain responses, anxiety and aggression in mice deficient in pre-proenkephalin. *Nature* 1996; 383: 535-538.
- Llorente-Berzal A, Puighermanal E, Burokas A *et al.* Sex-dependent psychoneuroendocrine effects of THC and MDMA in an animal model of adolescent drug consumption. *PLoS ONE* 2013; 8: e78386.

Porsolt RD, Bertin A, Jalfre M. Behavioral despair in mice: a primary screening test for antidepressants. *Arch Int Pharmacodyn Ther* 1977; 229: 327-336.

Puighermanal E, Marsicano G, Busquets-Garcia A, Lutz B, Maldonado R, Ozaita A. Cannabinoid modulation of hippocampal long-term memory is mediated by mTOR signaling. *Nat Neurosci* 2009; 12: 1152-1158.

Steru L, Chermat R, Thierry B, Simon P. The tail suspension test: a new method for screening antidepressants in mice. *Psychopharmacology (Berl)* 1985; 85: 367-370.

Strekalova T, Gorenkova N, Schunk E, Dolgov O, Bartsch D. Selective effects of citalopram in a mouse model of stress-induced anhedonia with a control for chronic stress. *Behav Pharmacol* 2006; 17: 271-287.

Tagliatela G, Hogan D, Zhang WR, Dineley KT. Intermediate- and long-term recognition memory deficits in Tg2576 mice are reversed with acute calcineurin inhibition. *Behav Brain Res* 2009; 200: 95-99.

Supplemental Table 1: Statistical analysis of cognitive and memory tests

2way ANOVA analysis					Post-hoc analysis						
Test	Variable	Source of variation	Uncorrected P-value	F-value	Day	Mean patients' CSF	Mean control CSF	Difference	Multiplicity-adjusted P-value ^{&}		
Memory	Novel object recognition - open field	Novel object recognition index	Time	<0.001	9.96	3	0.25	0.40	-0.15	0.066	
			Treatment	<0.001	67.5	10	0.08	0.52	-0.44	<0.001	
			Interaction	<0.001	9.45	18	-0.03	0.46	-0.49	<0.001	
						25	0.45	0.51	-0.06	0.40	
		Total time of exploration (Internal control)	Time	0.003	5.48						
			Treatment	0.37	0.86						
			Interaction	0.18	1.76						
		Novel object recognition - V-maze	Novel object recognition index	Time	<0.001	12.6	3	0.35	0.41	-0.056	0.066
			Treatment	<0.001	24.2	10	0.15	0.46	-0.31	<0.001	
			Interaction	<0.001	11.3	18	0.06	0.26	-0.40	<0.001	
					25	0.47	0.50	-0.031	0.40		
	Total time of exploration (Internal control)	Time	<0.001	14.8							
		Treatment	0.39	0.76							
		Interaction	0.37	1.07							
Anhedonia	Sucrose preference test	Percentage of sucrose preference	Time	0.30	1.22	-4 to 0	85.60	86.92	-1.33	0.89	
			Treatment	0.10	2.87	10	74.64	87.66	-13.02	0.016	
			Interaction	0.068	2.82	24	85.40	83.47	1.93	0.89	
		Total fluid consumption (Internal control)	Time	<0.001	10.1						
		Treatment	0.50	0.46							
		Interaction	0.87	0.14							
Locomotion	Locomotor activity test	Horizontal Activity	Time	<0.001	14.6						
			Treatment	0.40	0.73						
			Interaction	0.85	0.34						
		Vertical Activity	Time	<0.001	39.0						
		Treatment	0.98	0.001							
		Interaction	0.80	0.41							
Aggressiveness	Resident-intruder test	Frequency	Time	<0.001	7.08						
			Treatment	0.16	2.04						
			Interaction	0.36	1.07						
		Latency of aggressive events	Time	0.46	0.85						
		Treatment	0.29	1.14							
		Interaction	0.98	0.068							
Unpaired t-test / Mann Whitney-U test											
Test, Day		Variable	mean patients' CSF (95% CI)		mean control CSF (95% CI)		Uncorrected P-value				
Depression	Tail suspension test day 12	Time of immobility	169.2 (136.2-179.8)*		192.4 (165.8-208.7)*		0,017*				
	Forced swimming test day 20	Time of immobility	93.8 (72.5-115)		83.1 (58.0-108)		0.50				
Anxiety	Black and white test day 6	Latency	67.8 (21.1-114)		29.2 (8.41-50.1)		0.25				
		% Time in white box	12.4 (6.58-18.3)		14.9 (9.99-19.7)		0.19				
		Entries in white box	6.39 (3.77-9.01)		7.00 (5.00-9.00)		0.70				
	Elevated plus maze test day 14	Entries in distal section	2.94 (1.46-4.43)		3.35 (2.20-4.50)		0.46				
		% Time in open arms	6.27 (2.18-10.4)		6.75 (4.12-9.38)		0.15				
	Entries in open arms	5.39 (2.51-8.26)		5.80 (4.24-7.36)		0.79					

In the 2-way ANOVA analysis a p-value of 0.05 is considered significant for the treatment effect. An interaction p-value < 0.10 is considered a sign of different treatment effects at different time points, warranting post-hoc analysis. Significant results for treatment effect or interaction of treatment and time are shown in bold. * Median, IQR and result of significance testing using Mann Whitney-U test indicated because of non-normality. & Multiplicity-adjusted P-value using Sidak-Holm post-hoc procedure.

Supplemental Table 2: Statistical analysis of human IgG and receptor studies

2way ANOVA analysis					Post-hoc analysis				
Test	Variable	Source of variation	P-value	F-value	Day	Mean patients' CSF	Mean control CSF	Difference	Multiplicity-adjusted P-value ^{&}
Immuno-histo-chemistry (Figure 4)	Human IgG intensity in hippocampus – Percent of patients' CSF treated animals (100%)	Time	0.0005	6.23	3	33.6	33.3	0.28	0.98
		Treatment	<0.0001	24.7	10	49.9	31.4	18.5	0.42
		Interaction	0.003	4.89	18	100.0	24.0	76.0	<0.0001
					25	50.7	16.4	34.4	0.048
					46	25.0	8.84	16.1	0.42
Immuno-fluores-cence (Figure 4)	Human IgG intensity in hippocampus - Percent of patients' CSF treated animals (100%)	Region	0.93	0.077	CA1	100.0	16.0	84.1	<0.0001
		Treatment	<0.0001	109.2	CA3	100.0	8.38	91.6	<0.0001
		Interaction	0.93	0.077	DG	100.0	14.4	85.6	<0.0001
Confocal cluster density (Figure 6)	NMDAR - Percent of control CSF treated animals (100%)	Time	0.032	3.30	13	66.2	100.0	33.8	0.004
		Treatment	<0.0001	51.8	18	43.4	100.0	56.6	<0.0001
		Interaction	0.032	3.30	26	76.8	100.0	23.2	0.054
					46	80.8	100.0	19.2	0.18
					13	65.0	100.0	35.0	0.33
Confocal cluster density (Figure 6)	Synaptic NMDAR - Percent of control CSF treated animals (100%)	Time	0.086	2.40	18	44.9	100.0	55.1	0.044
		Treatment	0.039	2.40	26	118.5	100.0	-18.5	0.82
		Interaction	0.086	4.60	46	84.8	100.0	15.3	0.92
Total protein - Immuno-blot (Figure 7)	PSD95 - Percent of control CSF treated animals (100%)	Time	0.73	1.13					
		Treatment	0.97	0.028					
		Interaction	0.73	1.13					
Total protein - Immuno-blot (Figure 7)	NMDAR GluN1 - Percent of control CSF treated animals (100%)	Time	0.022	3.63	13	65.6	100.0	34.4	0.0082
		Treatment	0.0008	13.2	18	63.7	100.0	36.3	0.0067
		Interaction	0.022	3.63	26	80.3	100.0	19.7	0.19
					46	110.0	100.0	-9.54	0.40
Total protein - Immuno-blot (Figure 7)	PSD95 - Percent of control CSF treated animals (100%)	Time	0.91	0.18					
		Treatment	0.43	0.64					
		Interaction	0.91	0.18					

Kruskal-Wallis analysis				Post-hoc analysis				
Test	Variable	P-value	Test statistic	Pairwise Day	Mean rank 1	Mean rank 2	Difference	P [@]
IgG extraction hippo-campus (Figure 5)	NMDAR antibody titer	0.0004	20.6	46 vs. 5	3	8.38	-5.38	1.0
				46 vs. 13	3	20.5	-17.5	0.0004
				46 vs. 18	3	18.1	-15.1	0.0031
				46 vs. 26	3	11.7	-8.7	0.24
				13 vs. 18	18.1	20.5	-2.4	1.0

Unpaired t-test				
Test	Variable	mean patients' CSF (95% CI)	mean control CSF (95% CI)	Uncorrected P-value
Confocal cluster density (Figure 6)	AMPA - Percent of control CSF treated animals (100%)	90.9 (84.6-97.2)	100.0 (86.6-113.5)	0.14
	Synaptic AMPAR - Percent of control CSF treated animals (100%)	94.8 (71.6-118.0)	100.0 (77.8-122.2)	0.66
	PSD95 - Percent of control CSF treated animals (100%)	93.4 (82.4-104.4)	100.0 (86.9-113.1)	0.33
Immuno-blot (Figure 7)	AMPA - Percent of control CSF treated animals (100%) - day 18	106.5 (76.4-136.5)	100.0 (58.5-151.5)	0.75

In the 2-way ANOVA analysis a p-value of 0.05 is considered significant for the treatment effect. An interaction p-value < 0.10 is considered a sign of different treatment effects at different time points, warranting post-hoc analysis. Significant results for treatment effect or interaction of treatment and time are shown in bold. [&]Multiplicity-adjusted P-value using Sidak-Holm post-hoc procedure. [@]Multiplicity-adjusted P-value by Dunn's post-hoc procedure.

5.5. Paper V

Ephrin-B2 prevents N-methyl-D-aspartate receptor antibody effects on memory and neuroplasticity

Jesús Planagumà*, Holger Haselmann*, Francesco Mannara*, **Mar Petit-Pedrol**, Benedikt Grünewald, Esther Aguilar, Louis Röpke, Elena Martín-García, Marteen J. Titulaer, Pablo Jercog, Francesc Graus, Rafael Maldonado, Christian Geis, Josep Dalmau

*These authors contributed equally

Ann Neurol. 2016; 80(3):388-400

Impact Factor JCR 2016 (percentile): 9.89 (D1)

Ephrin-B2 Prevents N-Methyl-D-Aspartate Receptor Antibody Effects on Memory and Neuroplasticity

Jesús Planagumà, PhD,¹ Holger Haselmann, BS,^{2,3} Francesco Mannara, PhD,¹
 Mar Petit-Pedrol, BS,¹ Benedikt Grünewald, PhD,^{2,3} Esther Aguilar, BS,¹
 Luise Röpke, MD,² Elena Martín-García, PhD,⁴ Maarten J. Titulaer, MD, PhD,⁵
 Pablo Jercog, PhD,¹ Francesc Graus, MD, PhD,^{1,6} Rafael Maldonado, PhD,⁴
 Christian Geis, MD,^{2,3} and Josep Dalmau, MD, PhD^{1,7,8,9}

Objective: To demonstrate that ephrin-B2 (the ligand of EphB2 receptor) antagonizes the pathogenic effects of patients' N-methyl-D-aspartate receptor (NMDAR) antibodies on memory and synaptic plasticity.

Methods: One hundred twenty-two C57BL/6J mice infused with cerebrospinal fluid (CSF) from patients with anti-NMDAR encephalitis or controls, with or without ephrin-B2, were investigated. CSF was infused through ventricular catheters connected to subcutaneous osmotic pumps over 14 days. Memory, behavioral tasks, locomotor activity, presence of human antibodies specifically bound to hippocampal NMDAR, and antibody effects on the density of cell-surface and synaptic NMDAR and EphB2 were examined at different time points using reported techniques. Short- and long-term synaptic plasticity were determined in acute brain sections; the Schaffer collateral pathway was stimulated and the field excitatory postsynaptic potentials were recorded in the CA1 region of the hippocampus.

Results: Mice infused with patients' CSF, but not control CSF, developed progressive memory deficit and depressive-like behavior along with deposits of NMDAR antibodies in the hippocampus. These findings were associated with a decrease of the density of cell-surface and synaptic NMDAR and EphB2, and marked impairment of long-term synaptic plasticity without altering short-term plasticity. Administration of ephrin-B2 prevented the pathogenic effects of the antibodies in all the investigated paradigms assessing memory, depressive-like behavior, density of cell-surface and synaptic NMDAR and EphB2, and long-term synaptic plasticity.

Interpretation: Administration of ephrin-B2 prevents the pathogenic effects of anti-NMDAR encephalitis antibodies on memory and behavior, levels of cell-surface NMDAR, and synaptic plasticity. These findings reveal a strategy beyond immunotherapy to antagonize patients' antibody effects.

ANN NEUROL 2016;00:000–000

Anti-N-methyl-D-aspartate receptor (NMDAR) encephalitis is an inflammatory disorder of the brain that results in prominent neurological and psychiatric symptoms

in association with immunoglobulin G (IgG) antibodies against the GluN1 subunit of the receptor.¹ In recent years, several studies have provided evidence that the antibodies

View this article online at wileyonlinelibrary.com. DOI: 10.1002/ana.24721

Received Feb 27, 2016, and in revised form Jun 14, 2016. Accepted for publication Jun 27, 2016.

Address correspondence to Dr Josep Dalmau, IDIBAPS-Hospital Clínic, Universitat de Barcelona, Department of Neurology, c/ Villarroel 170, 08036 Barcelona, Spain. E-mail: jdalmau@clinic.ub.es

From the ¹Institut d'Investigacions Biomèdiques August Pi i Sunyer (IDIBAPS), Hospital Clínic, Universitat de Barcelona, Barcelona, Spain; ²Hans-Berger Department of Neurology, Jena University Hospital, Jena, Germany; ³Center for Sepsis Control and Care (CSCC), Jena University Hospital, Jena, Germany; ⁴Laboratori de Neurofarmacologia, Facultat de Ciències de la Salut i de la Vida, Universitat Pompeu Fabra, Barcelona, Spain; ⁵Erasmus Medical Center, Rotterdam, The Netherlands; ⁶Servei de Neurologia, Hospital Clínic, Universitat de Barcelona, Barcelona, Spain; ⁷Department of Neurology, University of Pennsylvania, Philadelphia, PA; ⁸Centro de Investigación Biomédica en Red Enfermedades Raras (CIBERER); and ⁹Institució Catalana de Recerca i Estudis Avançats (ICREA), Barcelona, Spain

Additional supporting information can be found in the online version of this article

alter synaptic function and likely result in the clinical syndrome.²⁻⁴ Approximately 80% of the patients improve with immunotherapy or sometimes spontaneously indicating that, despite the severity and protracted course of the disease, the altered NMDAR signaling is largely reversible.^{1,5-7} To date, the antibody effects have been mainly studied in cultured neurons exposed to patients' cerebrospinal fluid (CSF), demonstrating internalization of NMDAR and a decrease in their surface density and NMDAR-mediated currents.^{2,4} At the synapse, the antibodies disrupt the interaction between NMDAR and ephrin type B2 receptor (EphB2), displacing the NMDAR to extrasynaptic sites before they are internalized.³ This process of NMDAR internalization is antibody-titer dependent, reversible upon removing the antibodies, and highly specific for NMDAR, without per se affecting the density of α -amino-3-hydroxy-5-methyl-4-isoxazolepropionic acid receptor (AMPA).² Furthermore, antibody-treated neurons failed to increase the levels of AMPAR after chemical induction of long-term potentiation (LTP), suggesting that the mechanisms of plasticity were altered.³ Disruption of long-term plasticity was also suggested by a study in which the antibodies were applied for 5 minutes onto slices of normal mouse hippocampus.⁸ However, none of these studies determined whether long-term synaptic plasticity was altered in the brain of mice with symptoms related to NMDAR antibodies or whether the mechanisms of short-term plasticity were affected at the presynaptic level.

A definite link between development of memory and behavioral alterations and antibody-mediated decrease of NMDAR was recently established in a mouse model of cerebroventricular infusion of patients' CSF antibodies.⁹ The study showed a correlation between the intensity of the symptoms and the time course of antibody administration as well as between the reversibility of the symptoms and the restoration of levels of NMDAR after discontinuing the antibody infusion. In the current study, we first reproduced these findings using CSF from another group of patients and then applied the model to investigate whether the antibodies alter synaptic plasticity using electrophysiological paradigms of short- and long-term plasticity at the Schaffer collateral pathway. Additionally, given that previous work showed that ephrin-B2 antagonized the antibody-mediated changes in cell-surface dynamics of NMDAR,³ we have investigated in vivo whether this ligand prevents development of symptoms and antagonizes the mechanisms of disease in sets of experiments examining memory and behavioral responses, levels of cell-surface and synaptic NMDAR and EphB2, and synaptic plasticity in hippocampal networks. The results show a marked antibody-mediated impairment of the mechanisms of long-term synaptic plasticity, revealing a strategy to prevent the pathogenic effect of the antibodies that may lead to novel therapies.

Materials and Methods

Animals, Preparation of CSF, and Cerebroventricular Infusion of Antibodies

One hundred twenty-two male C57BL/6J mice (Charles River Laboratories, Wilmington, MA), 8 to 10 weeks old (25–30 g), were used for the studies. Some animals were used for more than one study (51 for memory and behavior, 60 for immunohistochemistry, and 29 for electrophysiological studies). Animal care, anesthesia, insertion of bilateral ventricular catheters (model 3280PD-2.0/SP; coordinates: 0.2mm anterior and 1.00mm lateral from bregma, depth 2.2mm; PlasticsOne Inc., Roanoke, VA), and connection of each catheter to a subcutaneous osmotic pump for continuous infusion of CSF (volume 100 μ l, flow rate 0.25 μ l/h for 14 days; Alzet, Cupertino, CA) have been reported.⁹ The CSF infused was pooled from samples of 34 patients with high-titer IgG GluN1 antibodies (all > 1:320) and 12 patients with normal pressure hydrocephalus without NMDAR antibodies (control samples). The patients used as controls had a history of rapidly progressive (median, 4 months; range, 2–9) memory deficits, cognitive decline, gait unsteadiness, or sphincter dysfunction; none of them had CSF inflammatory changes or autoantibodies.

To avoid the presence of other antibodies or small molecules that may have biological activity, patients' CSF samples were selected and prepared using the following studies: (1) confirmation that patients' CSF only had NMDAR antibodies by immunoadsorption of a representative sample of pooled CSF with HEK293 cells expressing the GluN1 subunit of the NMDARs showing abrogation of reactivity with mouse brain and NMDAR (tested in a cell-based assay [CBA]); (2) demonstration of the absence of antibodies against EphB2 receptor (confirmed by CBA, data not shown); and (3) CSF filtration (Amicon Ultracel 30K; Sigma-Aldrich, St. Louis, MO), dialysis against phosphate-buffered saline (PBS), and normalization to a physiological concentration of 2mg of IgG/dl, as reported.⁹

Four experimental groups were established: mice infused with patients' CSF without or with ephrin-B2 (50ng of ephrin-B2 added to the 100 μ l of CSF in each osmotic pump; two pumps per mouse; Sino Biological Inc, North Wales, PA), and mice infused with control CSF without or with ephrin-B2. The total dose of ephrin-B2 (100ng infused over 14 days) was based in a previous study using a single hippocampal injection (eg, 10ng/1 day).³ Animal procedures were conducted in accord with standard ethical guidelines (European Communities Directive 86/609/EU) and approved by the local ethical committees.

Cognitive Tasks and Locomotor Activity

These tasks were aimed to assess memory (novel object recognition [NOR]) discrimination index) and depressive-like behavior (tail suspension, and forced swimming tests) along with locomotor activity (local motor, horizontal and vertical activity). The selection and timing of these tasks were based on the findings of our previous study showing that patients' CSF antibodies, but not control CSF, caused memory deficits and depressive-like behaviors without

significant change of locomotor activity.⁹ All behavioral tasks were performed by researchers blinded to experimental conditions.

Immunohistochemistry, Confocal Microscopy, and Immunoprecipitation

All techniques related to immunolabeling of live cultures of dissociated rodent hippocampal neurons,² immunoabsorption of patients' samples with antigen-expressing HEK cells,¹⁰ brain tissue processing, quantitative brain tissue immunoperoxidase staining, extraction of human IgG bound to mice brain, and determination of NMDAR specificity of brain-extracted IgG have been previously reported on.⁹ To quantify the effects of patients' antibodies on total cell-surface and synaptic NMDAR clusters and PSD95, nonpermeabilized 5- μ m brain sections were blocked with 5% goat serum, incubated with human CSF antibodies (1:20; used here as primary NMDAR antibody) for 2 hours at room temperature (RT), washed with PBS, permeabilized with Triton X-100 0.3% for 10 minutes at RT, and serially incubated with rabbit polyclonal anti-PSD95 (1:250, ab18258; Abcam, Cambridge, MA) overnight at 4°C and the corresponding secondary antibodies, Alexa Fluor 594 or 488 goat antihuman Fab-specific IgG (109-585-097 or 109-545-097; Jackson ImmunoResearch Laboratories, Inc., West Grove, PA) and Alexa Fluor 488 goat antirabbit IgG (A-11008; Thermo Fisher Scientific, Waltham, MA), all diluted 1:1,000, for 1 hour at RT. Clusters of EphB2 were identified using non-permeabilized tissue and a goat anti-EphB2 as primary antibody (1:100, AF467; R&D Systems, Minneapolis, MN) overnight at 4°C, followed by a secondary antibody, Alexa Fluor 594 donkey antigoat IgG (A-11058, 1:1000; Thermo Fisher Scientific), for 1 hour at RT. Slides were mounted and results scanned with a confocal microscope (Zeiss LSM710; Carl Zeiss GmbH, Jena, Germany) as reported.⁹ Standardized z-stacks including 50 optical images were acquired from 18 hippocampal regions per animal, including CA1, CA2, CA3, and dentate gyrus, as reported.⁹ For cluster density analysis, a spot detection algorithm from Imaris suite 7.6.4 (Bitplane, Zurich, Switzerland) was used. Density of clusters in each hippocampal region was expressed as spots/ μ m³. Synaptic localization is defined as colocalization of NMDAR with postsynaptic PSD95, and synaptic cluster density is expressed as colocalized spots/ μ m³. For animals treated with patients' CSF with or without ephrin-B2 or control CSF with ephrin-B2, the mean densities of all 18 hippocampal regions were calculated for total and synaptic NMDAR and EphB2, and normalized to the mean density of the 18 hippocampal regions in animals treated with control CSF (= 100%).

To demonstrate the binding of ephrin-B2 to EphB2, nonpermeabilized brain sections were obtained from animals infused for 5 days with patients' CSF with or without ephrin-B2, processed as above and sequentially incubated with rabbit anti-ephrin-B2 antibodies (1:500, ab131536; Abcam) for 2 hours at 4°C, washed, goat anti-EphB2 antibody (1:200, AF467; R&D Systems) overnight at 4°C, washed, and the secondary antibodies, Alexa Fluor 594 donkey antigoat followed by goat-anti-rabbit 488 (A-11058 or A-11008;

Thermo Fisher Scientific), all diluted 1:1,000, for 1 hour at RT. For each animal, three identical image stacks representing CA1 were examined. Intensity of ephrin-B2 immunostaining was calculated with ImageJ software (National Institutes of Health [NIH], Bethesda, MD), and colocalization of clusters of ephrin-B2 and EphB2 was determined with Imaris suite 7.6.4 (Bitplane). Results were normalized to the mean values obtained in animals treated with patients' CSF + ephrin-B2 (100%).

To determine the phosphorylation of EphB2 by ephrin-B2, permeabilized brain tissue sections were blocked as above and sequentially incubated with rabbit anti-phospho-EphB2 (dilution 1:50, E22-65BR; SignalChem, Richmond, British Columbia, Canada) overnight at 4°C and a secondary antibody, Alexa 488 goat anti-rabbit (1:1,000, A-11008; Thermo Fisher Scientific), for 1 hour at RT. Slides were then mounted and scanned with confocal microscope as above.

To demonstrate the specificity of neuronal-bound IgG, we used an immunoprecipitation method similar to that previously reported.¹¹ In brief, cultures of live hippocampal neurons were incubated for 1 hour with aliquots of the samples (patients' or control CSF with or without ephrin-B2) used for mice cerebroventricular infusion, washed, lysed, and neuronal-bound IgG precipitated with protein A and G sepharose beads. Immunoprecipitates were then run in a gel and incubated with a rabbit antibody specific for the NR1 subunit of the NMDAR (#G8913; Sigma-Aldrich), diluted 1:1,000, for 1 hour at room temperature, followed by a biotinylated anti-rabbit antibody (diluted 1:1,000, BA-1000; Vector Laboratories, Burlingame, CA), and the reactivity developed with the avidin-biotin peroxidase technique.

Electrophysiological Studies

Seventeen to 23 days after activation of osmotic pumps, mice were deeply anesthetized with isoflurane and decapitated. Brains were removed, placed in ice-cold, high-sucrose extracellular artificial fluid 1 (artificial CSF [aCSF] 1; 40mM of NaCl, 25mM of NaHCO₃, 10mM of glucose, 150mM of sucrose, 4mM of KCl, 1.25mM of NaH₂PO₄, 0.5mM of CaCl₂, and 7mM of Mg₂Cl; purged with 95% O₂/5% CO₂ [pH 7.35]) and subdivided into the hemispheres. Thick (400- μ m) coronal slices of hippocampus were obtained with a vibratome (VT1200 S; Leica Microsystems, Wetzlar, Germany) and transferred into an incubation beaker with extracellular aCSF 2 appropriate for electrophysiological recordings (aCSF 2; 124mM of NaCl, 26mM of NaHCO₃, 10mM of glucose, 3.4mM of KCl, 1.2mM of NaH₂PO₄, 2mM of CaCl₂, and 2mM of MgSO₄; purged with 95% O₂/5% CO₂ [pH 7.35]). Slices were kept at 34°C for 60 minutes and subsequently at RT for at least 60 additional minutes. For field potential measurements, single slices were then transferred into a measurement chamber perfused with aCSF 2 at 1.3 to 2.5ml/min at 32°C to 33°C (control CSF: number of acute slices: n = 7, prepared from brain hemisections of 4 mice; control CSF + ephrin-B2: n = 7, from hemisections of 6 mice; patients' CSF: n = 7, from

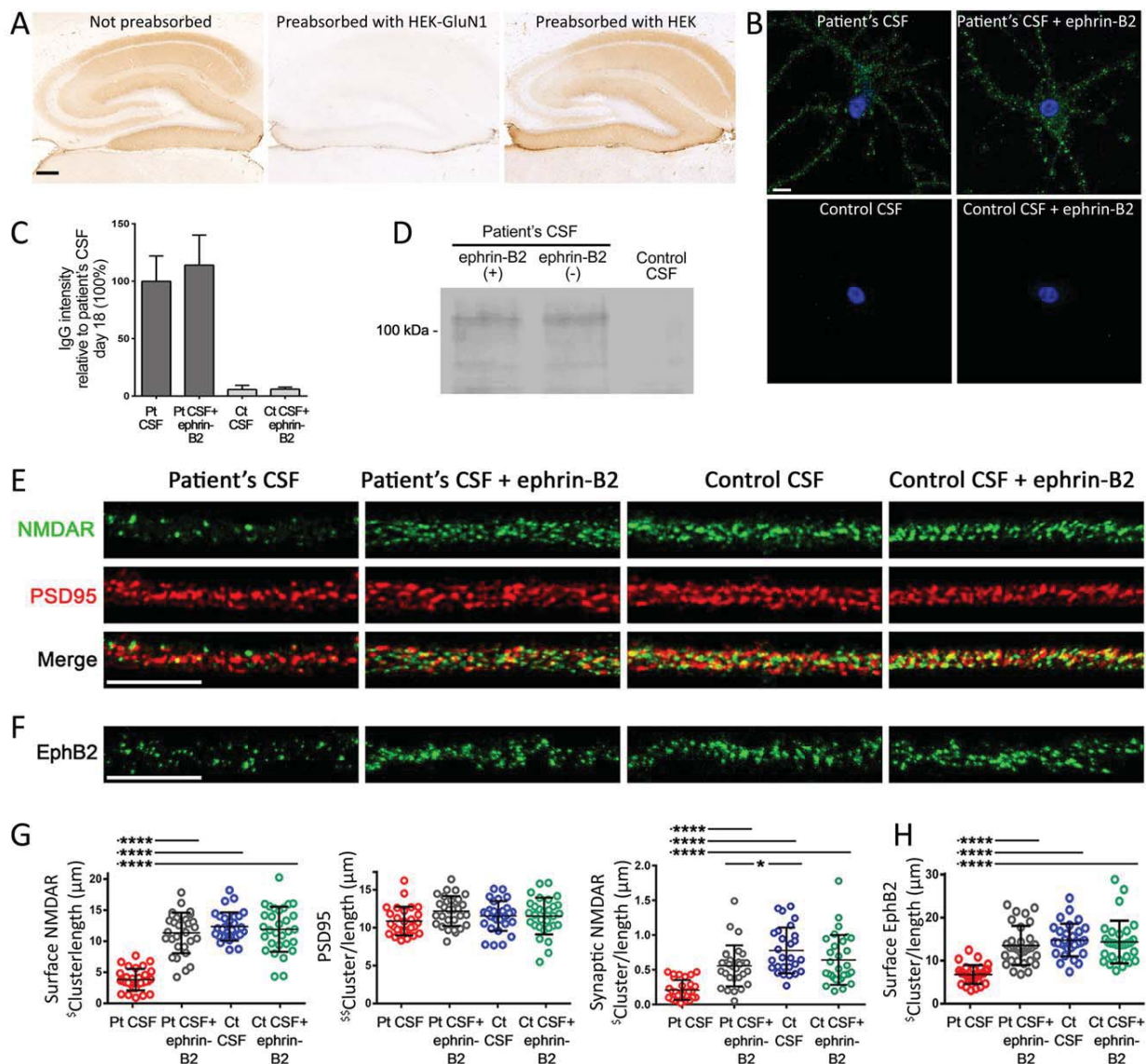


FIGURE 1: Soluble ephrin-B2 does not interfere with antibody binding and prevents antibody-induced reduction of surface NMDAR and EphB2 clusters in cultures of neurons. (A) Sections of mouse hippocampus incubated with pooled CSF from patients with anti-NMDAR encephalitis not preabsorbed (left), and pre-absorbed with HEK293 cells expressing (middle) and not expressing (right) the GluN1 subunit of the NMDARs. Preabsorption with GluN1 abrogates patients' CSF reactivity with brain; scale bar = 200 μm . (B) Cultured rat hippocampal neurons incubated for 1 hour with patients' or control CSF with or without ephrin-B2 show similar immunolabeling by patients' antibodies regardless of the presence of ephrin-B2; scale bar = 10 μm . (C) Quantification of intensity of CSF IgG reactivity (10 dendrites per condition); bars show the mean intensity + standard error of the mean in percentage relative to patients' CSF IgG reactivity. Significance assessed by one-way analysis of variance (ANOVA; $p < 0.0001$) with Bonferroni post-hoc correction; **** $p < 0.0001$. (D) Immunoprecipitation of the neuronal antigen bound to patients' IgG showed that the target was the NMDAR (band at $\sim 110\text{kDa}$); the same result was obtained in neurons incubated with patients' CSF with or without ephrin-B2. (E) Representative dendrite of hippocampal neurons immunostained for surface NMDAR (green) and PSD95 (red) after 24-hour treatment with patients' CSF antibodies (Pt CSF) or control CSF (Ct CSF) without or with ephrin-B2. Patients' antibodies reacted with surface NMDAR in nonpermeabilized neurons; synaptic NMDARs were defined by the colocalization of reactivity with PSD95 (yellow). (F) Immunostaining of surface EphB2 after 24-hour treatment with Pt CSF or Ct CSF without or with ephrin-B2. Scale bars = 10 μm . (G) Quantification of the density of surface and synaptic NMDAR: The presence of ephrin-B2 prevented the antibody-mediated reduction of surface and synaptic NMDAR clusters. PSD95 was not affected by ephrin-B2. (H) Quantification of the density of EphB2: The presence of ephrin-B2 prevented the antibody-mediated reduction of EphB2 (n = 10 cells per condition; three independent experiments). Cluster density analysis was performed with a spot detection algorithm from Imaris suite 7.6.4 (Bitplane). ($^{\circ}$) in Y axis represents the number of surface clusters (NMDAR or EphB2) or synaptic clusters (NMDAR) per dendrite (measured three-dimensionally [3D])/length of the dendrite; ($^{\circ}$) represents the number of intracellular clusters of PSD95 (measured in 3D)/length of dendrite. Significance of treatment effect was assessed by one-way ANOVA ($p < 0.0001$ for NMDAR, synaptic NMDAR, and EphB2) with Bonferroni post-hoc correction; **** $p < 0.0001$. CSF = cerebrospinal fluid; IgG = immunoglobulin G; NMDAR = N-methyl-D-aspartate receptor.

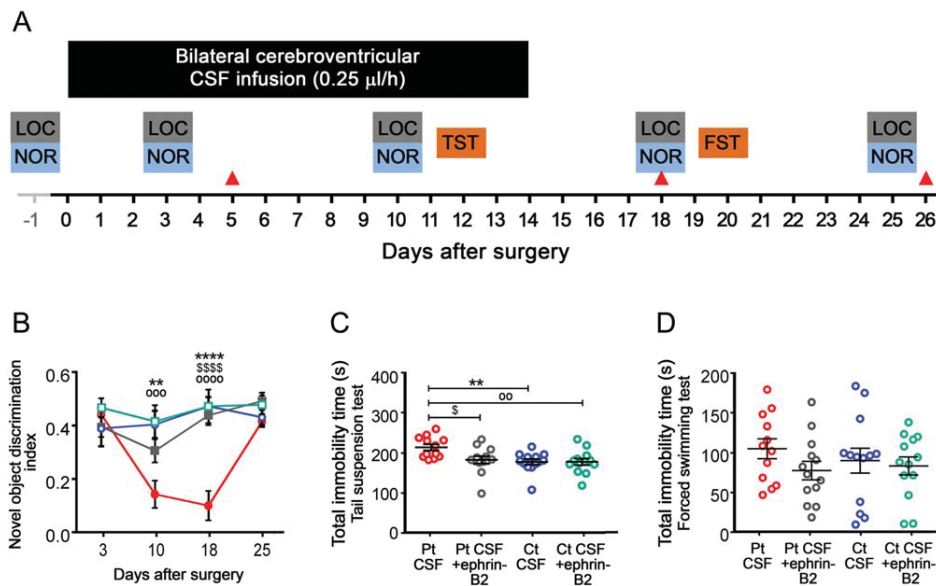


FIGURE 2: Intraventricular infusion of CSF from patients with NMDAR antibodies causes deficits in memory and depressive-like behavior that are prevented by ephrin-B2. (A) Schedule of cognitive testing and animal sacrifice. Memory (novel object recognition [NOR] discrimination index), depressive-like behavior (tail suspension test [TST] and forced swimming test [FST]), and locomotor activity (LOC) were assessed blinded to treatment at the indicated days. The NOR discrimination index was assessed in open field in four different cohorts of mice. Animals were habituated the day before surgery (baseline) to NOR and LOC. Red arrow heads indicate the days of sacrifice for studies of effects of antibodies in brain. (B) NOR index in open-field paradigm in animals treated with patients' CSF antibodies (Pt CSF; solid circles), Pt CSF + ephrin-B2 (open circles), control CSF (Ct CSF; solid squares), or Ct CSF + ephrin-B2 (open squares). A high index indicates better object recognition memory. (C) Total time of immobility in TST during the infusion period (day 12). (D) Total time of immobility in FST (day 20). Data are presented as mean \pm standard error of the mean (median \pm interquartile range IQR in C and D). Number of animals: patients' CSF, $n = 12$; patients' CSF + ephrin-B2, $n = 13$; control CSF, $n = 13$; and control CSF + ephrin-B2, $n = 13$. Significance of treatment effect was assessed by repeated-measures two-way analysis of variance (ANOVA; $p = 0.0001$; B) with post-hoc testing with Bonferroni adjustment (asterisks), or one-way ANOVA ($p = 0.0032$) and Bonferroni post-hoc correction (C). Patients' CSF versus control CSF: $**p < 0.01$; $****p < 0.0001$; patients' CSF versus patients' CSF + ephrin-B2: $^{\circ}p < 0.05$; $^{\circ\circ\circ\circ}p < 0.0001$; patients' CSF versus control CSF + ephrin-B2: $^{\circ\circ}p < 0.01$; $^{\circ\circ\circ}p < 0.001$; $^{\circ\circ\circ\circ}p < 0.0001$. CSF = cerebrospinal fluid; NMDAR = N-methyl-D-aspartate receptor.

hemisections of 4 mice; patients' CSF + ephrin-B2: $n = 5$, from hemisections of 5 mice). A custom made bipolar stimulation electrode was placed in the Schaffer collateral pathway. Recording electrodes were made with a puller (P-1000; Sutter Instrument Company, Novato, CA) from thick-walled borosilicate glass with a diameter of 2mm (Science Products, Hofheim, Germany). The recording electrode filled with aCSF 2 was placed in the dendritic branching of the CA1 region for local field potential measurement (field excitatory postsynaptic potential; fEPSP). A stimulus isolation unit (Isoflex; A.M.P.I., Jerusalem, Israel) was used to elicit stimulation currents between 70 and 260 μ A. Before baseline recordings for long-term potentiation (LTP) measurements, input-output curves were recorded for each slice at 0.03Hz (control CSF: $n = 8$ slices from $N = 5$ mice; control CSF + ephrin-B2: $n = 8$, $N = 6$; patients' CSF: $n = 9$, $N = 5$; patients' CSF + ephrin-B2: $n = 7$, $N = 5$). The stimulation current was then adjusted in each recording to evoke fEPSP at which the population spike could first be distinguished from the field potential and was then reduced by 10%.¹² The final intensities of stimulation ranged from 60% to 70% of maximum fEPSP slopes and were unchanged in between the experimental groups. After baseline recordings for

25 minutes with 0.03Hz, LTP was induced by theta-burst stimulation (TBS; 10 theta bursts of four pulses of 100Hz with an interstimulus interval of 200ms repeated 10 times with 0.03Hz).¹³ After LTP induction, fEPSPs were recorded for additional 65 minutes with 0.03Hz. Paired-pulse fEPSPs in the test pathway were measured directly before and 30 minutes after LTP induction with 0.03Hz and an interstimulus interval of 100ms. The fEPSP of the first paired-pulse stimulus was included in fEPSP analysis. All recordings were filtered at 2.9 and 10kHz using Bessel filters of the amplifier. Traces were analyzed by IGOR Pro software (WaveMetrics, Lake Oswego, OR).

Statistical Analysis

Behavioral tests with multiple time points (NOR, locomotor activity) were analyzed using repeated-measures two-way analysis of variance (ANOVA). The tail suspension test (behavioral paradigm with single time point) was analyzed with one-way ANOVA. All experiments were assessed for outliers, but none were identified, so measurements were pooled per time point and treatment (patient or control CSF). Human IgG intensity from different time points and electrophysiological data (LTP-induced changes in fEPSP slope and absolute fEPSP slope

values) were analyzed with two-way ANOVA. Intensity of reactivity of patients' antibodies with cultures of neurons, confocal cluster densities (GluN1, PSD95, and EphB2) at one time point, and assessment of fEPSP stimulation strength were analyzed using one-way ANOVA. Electrophysiological data from

the paired-pulse experiment were analyzed with repeated-measures two-way ANOVA. Post-hoc analyses for all experiments used Bonferroni correction for multiple testing. The EphB2 activation experiment was assessed by two-tailed *t* test. A *p* value of < 0.05 was considered significant. The α -error was

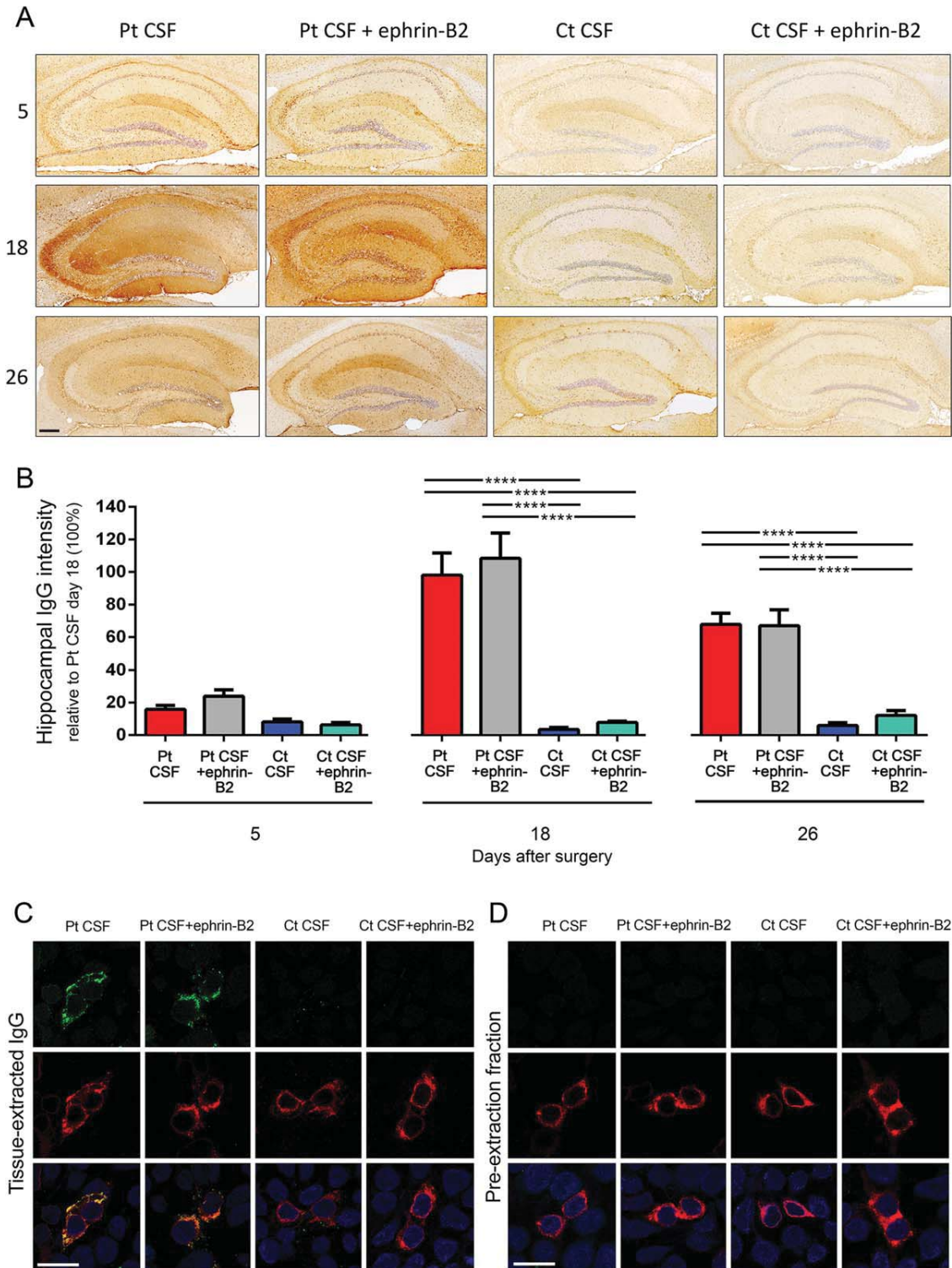


FIGURE 3.

set at 0.05. All tests were done using GraphPad Prism software (version 6; GraphPad Software Inc., La Jolla, CA).

Results

Patients' Antibodies Cause Memory and Behavioral Deficits That Are Prevented by Ephrin-B2

We first confirmed that (1) pooled patients' CSF only had GluN1 NMDAR antibodies (Fig 1A), (2) ephrin-B2 did not block binding of patients' antibodies (Fig 1B,C), and (3) binding of patients' antibodies to the neuronal surface was specific for NMDARs (eg, patients' antibodies precipitated this receptor; Fig 1D). We also confirmed in cultured neurons that patients' antibodies removed NMDARs from synapses causing their internalization² and that these effects were antagonized by ephrin-B2³ (Fig 1E–G). Next, we used patients' CSF samples for cerebroventricular infusions to mice. Animals infused for 14 days with patients' CSF antibodies, but not control CSF, showed a progressive impairment of memory (NOR discrimination index) that was maximal on day 18 and recovered on day 25 (Fig 2A,B). Compared with animals infused with control CSF, those infused with patients' CSF developed depressive-like behavior (longer time of immobility during the tail suspension test [TST] on day 10; Fig 2C) that recovered after the CSF infusion stopped (assessed by forced swimming test [FST] on day 20; Fig 2D). The reason for using two different tests to assess a similar task is that mice cannot be re-exposed to TST or FST test because of behavioral learning acquired during the first exposure. Although these tests are considered equivalent,^{14,15} future studies should confirm this in our model.

In contrast to the above-mentioned findings, mice that received patients' CSF along with ephrin-B2 showed a

mild, not significant, decrease of memory on day 10 and normal memory on day 18. In addition, mice that received ephrin-B2 did not develop depressive-like behavior (Fig 2B,C; Supplementary Table 1A,B). No significant difference in motor activity was noted among the different groups (Supplementary Table 2). Overall, these findings confirm those of our previous study and demonstrate, for the first time, that the alteration of memory and behavior caused by patients' NMDAR antibodies can be largely prevented by administration of ephrin-B2.

Ephrin-B2 Does Not Alter the Specific Binding of Patients' Antibodies to Mouse NMDAR

Mice infused with patients' CSF, but not control CSF, showed progressive accumulation of brain-bound human IgG, predominantly in the hippocampus (Fig 3A,B). Compared with mice not receiving ephrin-B2, those infused with this ligand showed increased density of ephrin-B2 bound to EphB2 and increased levels of EphB2 phosphorylated (data not shown). The dynamics and the degree of IgG binding to the brain were not altered by adding ephrin-B2 to patients' CSF (Fig 3A,B; Supplementary Table 3). NMDAR specificity of brain-bound human IgG (confirmed in immunoabsorption experiments before infusion in mice; Fig 1A) was further determined by acid extraction of the IgG bound to hippocampus and testing it with a CBA for NMDAR. IgG extracted from hippocampus of mice infused with patients' CSF with or without ephrin-B2, but not control CSF, was specific for NMDAR (Fig 3C). Confirmation that extracted IgG represented antibodies bound to the hippocampus and not unbound antibodies (eg, present in blood vessels) was provided by the absence of reactivity in the pre-extraction fraction (tissue wash fraction before applying acid; Fig 3D).

FIGURE 3: Animals infused with patients' CSF have a progressive increase of human anti-NMDAR IgG bound to hippocampus that is not altered by ephrin-B2. (A) Immunostaining of human IgG in sagittal hippocampal sections of mice infused with patients' CSF antibodies (Pt CSF), Pt CSF + ephrin-B2, control CSF (Ct CSF), and Ct CSF + ephrin-B2, sacrificed at the indicated experimental days. In animals infused with patients' CSF and patients' CSF + ephrin-B2, there is a gradual increase of IgG immunostaining until day 18, followed by a decrease of immunostaining. Scale bar: A = 200 μ m. **(B)** Quantification of intensity of human IgG immunostaining in hippocampus of mice infused with patients' CSF (red bars), patients' CSF + ephrin-B2 (gray bars), control CSF (blue bars), and control CSF + ephrin-B2 (cyan bars) sacrificed at the indicated time points. For all quantifications, mean intensity of IgG immunostaining in the group with the highest value (animals treated with patients' CSF and sacrificed at day 18) was defined as 100%. All data are presented as mean \pm standard error of the mean. For each time point, 5 animals of each experimental group were examined. Significance of treatment effect was assessed by two-way analysis of variance (ANOVA; time points, treatment, and interaction, all $p < 0.0001$), and post-hoc analyses were performed with Bonferroni correction; **** $p < 0.0001$. **(C and D)** Demonstration that the human IgG in mouse brain has NMDAR specificity: HEK293 cells expressing the GluN1 subunit of the NMDAR immunolabeled with acid-extracted IgG fractions (top row in C) or pre-extraction fractions (top row in D) from hippocampus of mice infused with patients' CSF antibodies (Pt CSF), Pt CSF + ephrin-B2, control CSF (Ct CSF), or Ct CSF + ephrin-B2 at day 18. The intense reactivity with GluN1-expressing cells was noted in acid-extracted IgG fractions from Pt CSF and Pt CSF + ephrin-B2 groups (C); none of the pre-extraction fractions from any animal group showed GluN1 reactivity (D). The second row in (C) and (D) shows the reactivity with a monoclonal GluN1 antibody, and the third row the colocalization of immunolabeling. Scale bars = 10 μ m. Pt CSF (n = 5), Pt CSF + ephrin-B2 (n = 5), Ct CSF (n = 5), and Ct CSF + ephrin-B2 (n = 5). CSF = cerebrospinal fluid; IgG = immunoglobulin G; NMDAR = N-methyl-D-aspartate receptor.

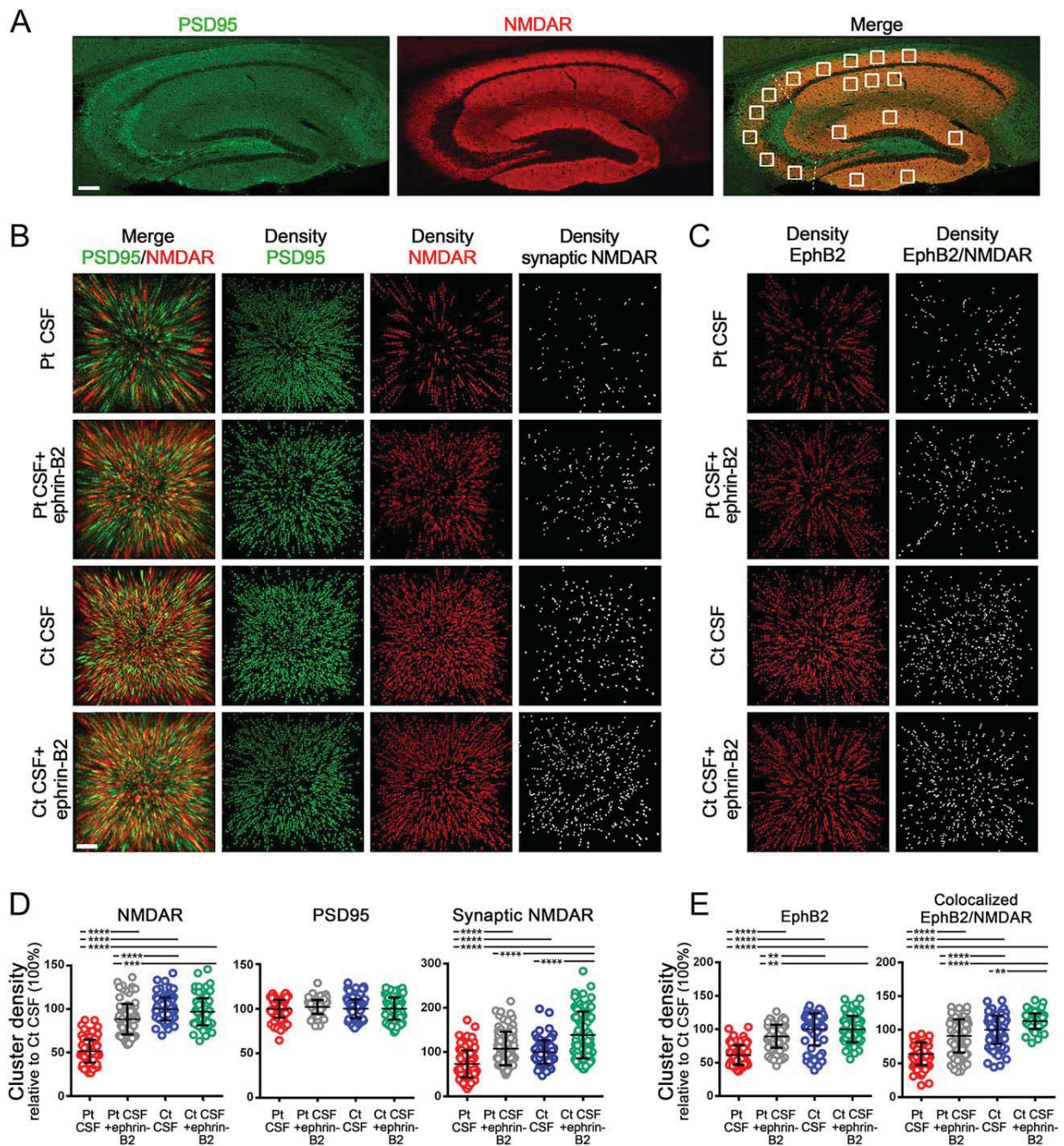


FIGURE 4: Soluble ephrin-B2 antagonizes the antibody-mediated reduction of NMDAR and EphB2 in mice hippocampus. (A) Hippocampus of mouse immunolabeled for PSD95 and NMDAR. Images were merged (merge) and postprocessed to demonstrate colocalizing clusters. Squares in "merge" indicate the analyzed areas in CA1, CA2, CA3, and dentate gyrus. Each square is a three-dimensional (3D) stack of 50 sections. Scale bar = 200 μm . (B) 3D projection and analysis of the density of total clusters of PSD95 and NMDAR, and synaptic clusters of NMDAR (defined as NMDAR clusters colocalizing with PSD95) in a CA3 region (square in A "merge") from a representative animal of each experimental group. Merged images (merge: PSD95 [green]/ NMDAR [red]) were postprocessed and used to calculate the density of clusters (density = spots/ μm^3). Scale bar = 2 μm . (C) Density of total clusters of EphB2 and EphB2 colocalizing with NMDAR. Scale bar = 2 μm . (D) Quantification of the density of total (left) and synaptic (right) NMDAR clusters, and (E) total EphB2 and EphB2 colocalizing with NMDAR at day 18 in a pooled analysis of hippocampal areas (CA1, CA2, CA3, and dentate gyrus) in animals treated with patients' CSF antibodies (Pt CSF; red), Pt CSF + ephrin-B2 (gray), control CSF (Ct CSF; blue), and control Ct CSF + ephrin-B2 (cyan). Mean density of clusters in control CSF treated animals was defined as 100%. Data are presented as scatterplot + mean \pm standard error of the mean. For each condition, 5 animals were examined (18 hippocampal areas per animal = 90 hippocampal areas per condition). Significance of treatment effect was assessed by one-way analysis of variance ($p < 0.0001$) and by post-hoc analysis with Bonferroni correction; ** $p < 0.01$; *** $p < 0.001$; **** $p < 0.0001$. CSF = cerebrospinal fluid; NMDAR = N-methyl-D-aspartate receptor.

These experiments show that ephrin-B2 did not alter the specific binding of patients' antibodies to mouse hippocampal NMDAR, although it prevented the memory and behavioral deficits caused by the antibodies.

The Antibody-Mediated Reduction of Synaptic NMDAR and EphB2 Is Antagonized by Ephrin-B2

To determine whether the protective effects of ephrin-B2 occurred *in vivo*, we infused this ligand along with patients' antibodies into the cerebroventricular system of our mouse model. We then compared the effects of patients' antibodies on the density of total and synaptic NMDAR in the hippocampus of mice infused with patients' or control CSF, with or without ephrin-B2. Eighteen hippocampal areas with 50 z -sections per area, representing a total of 900 sections per animal (5 animals per group), were investigated (Fig 4A). Animals infused with patients' CSF antibodies, but not control CSF, showed a significant decrease of the density of total and synaptic NMDAR clusters. These effects were largely prevented when ephrin-B2 was coinjected with patients' antibodies (Fig 4B,D).

Patients' antibodies also caused a decrease of the density of EphB2 that was prevented by coinjection of ephrin-B2 (Fig 4C,E) similar to the results observed with cultured neurons (Fig 1F,H). Furthermore, we observed an increase in the density of colocalized EphB2/NMDAR in animals receiving ephrin-B2 either with patients' or control CSF (Fig 4E). This increase of colocalized EphB2/NMDAR, but not the total number of cell-surface EphB2 in the control group, is in line with studies showing that activation of EphB2 facilitates interaction with NMDAR and increases formation of EphB2/NMDAR clusters.¹⁶ Our findings confirm that CSF antibodies from patients with anti-NMDAR encephalitis cause a decrease of cell-surface and synaptic NMDAR *in vitro* and *in mice*, and show that these molecular effects as well as the resulting memory and behavioral deficits are prevented by the activation of EphB2 with ephrin-B2 *in vivo*.

Ephrin-B2 Antagonizes Antibody-Mediated Impairment of Hippocampal Long-Term Synaptic Plasticity

Acute brain slices from mice infused with patients' or control CSF, without or with ephrin-B2, were used to record fEPSPs in the CA1 region of the hippocampus (Fig 5A). Animals infused with patients' CSF showed a substantial reduction of LTP compared with animals infused with control CSF, as shown by analysis of fEPSP slope change (Fig 5B,C). Quantitative analysis comparing median changes in slope values of minutes 40 to 90 of the recordings (15

minutes after TBS) demonstrated a reduced potentiation of fEPSP in mice receiving patients' CSF in comparison to those receiving control CSF (Fig 5D). Coadministration of patients' CSF antibodies with ephrin-B2 partially abrogated the NMDAR antibody-mediated impairment of potentiation (Fig 5C,D; $p < 0.0001$). Administration of ephrin-B2 together with control CSF had no effects on the potentiation of fEPSP.

In contrast to severe reduction of hippocampal LTP, short-term plasticity was not affected in animals infused with patients' CSF antibodies. We performed a paired-pulse protocol before and after TBS in the CA3-CA1 synapse. As expected, fEPSP recordings showed significant paired-pulse facilitation (Fig 5E) according to increased presynaptic release probability. This effect was preserved in mice receiving patients' CSF regardless of the presence of ephrin-B2. Moreover, the fEPSP slope values of the first of the paired stimuli before and after TBS did not change in mice infused with patients' CSF, but they significantly increased in mice infused with patients' CSF and ephrin-B2, consistent with the antibody-induced impairment of LTP shown in Figure 5C. Input-output curves of fEPSPs reflecting glutamatergic transmission in the CA1/Schaffer collateral pathway at increasing stimulus intensities revealed an exponential rise of fEPSP slope values to a maximum plateau phase that is finally reached by complete stimulation of the fiber tract. In animals that received patients' CSF, absolute fEPSP slope values were reduced at nearly all stimulation intensities and also in the plateau phase compared to those of control animals. Coinjection of ephrin-B2 led to improvement of antibody-induced reduction of fEPSP slope (Fig 5F; $p = 0.001$ compared to patients' CSF). fEPSPs in slices of mice infused with control CSF and ephrin-B2 showed no differences compared to animals infused with control CSF alone. Thus, we found severe impairment of postsynaptic, but not presynaptic, plasticity after TBS in animals that received patients' CSF.

Discussion

We have used a mouse model of chronic cerebroventricular infusion of patients' NMDAR antibodies to demonstrate the antibody pathogenicity at multiple levels from behavior to synaptic plasticity, and that all antibody-mediated effects can be at least partially prevented by administration of ephrin-B2, suggesting a novel molecular intervention with potential therapeutic implications.

Our results with CSF from a new group of patients with anti-NMDAR encephalitis accurately reproduced those of our previous study,⁹ as expected, knowing the limited GluN1 epitope repertoire in patients with this disorder.¹⁷ A novel finding was that patients' antibodies

caused a reduction of EphB2, a receptor that stabilizes the NMDAR at the synapsis.¹⁸

Previous work with cultured neurons showed that patients GluN1 antibodies interfered with NMDAR signaling by reducing NMDAR-mediated miniature excitatory postsynaptic currents (mEPSCs).^{2,17} GluN1 is the obligatory subunit for formation of functional NMDAR, and GluN1 knockout mice die within hours after birth.¹⁹ Hippocampal CA1 region-specific GluN1 knockouts show

impaired spatial and temporal learning with severe impairment of formation of LTP in the Schaffer collateral/CA1 synapse, demonstrating the role of NMDAR in establishing synaptic plasticity and memory formation.^{20,21} Our findings show that similar hippocampal network alterations occur when the NMDAR is targeted by GluN1 antibodies from patients with anti-NMDAR encephalitis. Indeed, LTP recordings in the CA3-CA1 synapses of acute brain slices of our mouse model showed severe impairment of

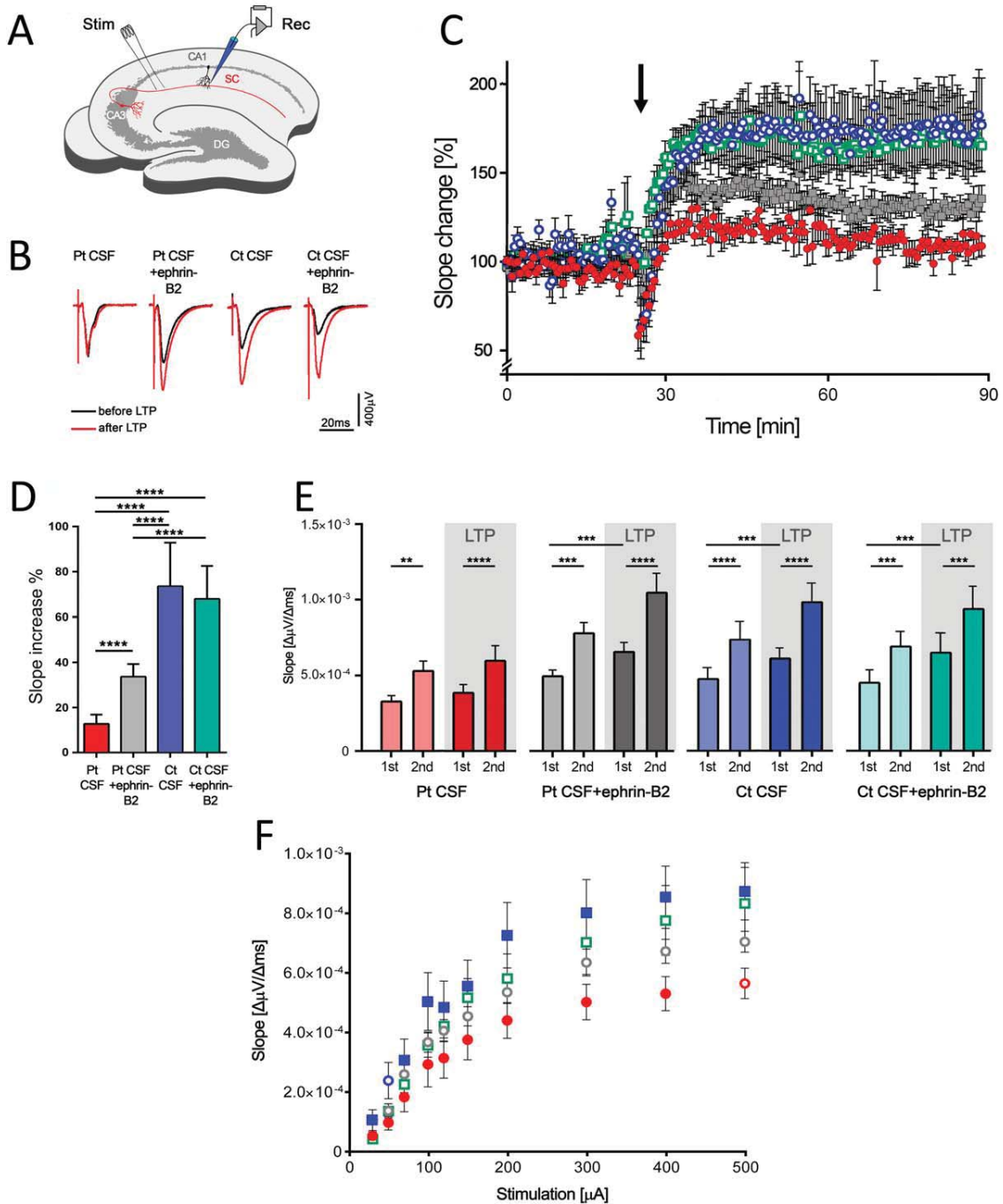


FIGURE 5.

hippocampal synaptic plasticity. This finding possibly accounts for the memory and behavioral deficits observed in our animal model. Long-term impairment of synaptic plasticity by altered NMDAR function may result in reduction of activity-induced incorporation of high-conductance AMPARs in synaptic receptor fields, which is one of the main postsynaptic mechanisms of LTP.²² In contrast to these postsynaptic alterations, paired-pulse facilitation was unaffected accounting for largely intact presynaptic release mechanisms.²³

A study using bilateral single injection of patients' CSF into the dentate gyrus of rats showed impairment of spatial memory along with a reduction of NMDAR-evoked excitatory postsynaptic potentials and long-term potentiation.²⁴ However, these alterations appeared to be irreversible and similar to those of a commercial GluN1 antibody, the binding of which requires cell permeabilization, suggesting that antibody-independent factors may have been involved.⁴ Another study that aimed to model seizures in mice by single cerebroventricular injection of patients' IgG showed no spontaneous epileptic activity, but a decrease of seizure threshold.²⁵ The NMDAR specificity of these effects (eg,

change of synaptic NMDAR cluster density or NMDAR synaptic currents) was not investigated.

Eph receptors are a family of receptor tyrosine kinases that modulate LTP probably through their interaction with NMDAR and stabilization and clustering of this receptor in the postsynaptic membrane.^{16,26–28} Ephrin signaling, such as ephrin-B2 binding to the EphB2, is important to establish LTP in CA3-CA1 synapses for which downstream kinase signaling upon EphB activation is not critical as intracellular truncated forms of EphB do not interfere with LTP.^{26,29} In our mouse model, we hypothesize that autoantibody-induced disruption of the direct extracellular interaction of NMDAR with EphB2¹⁶ results in reduction of synaptically located NMDAR, leading to memory and behavioral deficits and reduced LTP. Moreover, ligand-dependent direct interaction of EphB2 and NMDAR may also influence phosphorylation status or subunit composition of NMDAR and, in this way, modulate synaptic plasticity.¹⁸ In cultured neurons, the antibody-mediated disruption of the cross-talk of NMDAR and EphB2 leading to NMDAR synaptic displacement and internalization is efficiently

FIGURE 5: Patients' antibodies cause severe impairment of long-term synaptic plasticity in the hippocampus that is partially prevented by ephrin-B2. (A) The Schaffer collateral pathway (SC, red) was stimulated (Stim) and field potentials were recorded in the CA1 region of the hippocampus (Rec). Long-term potentiation (LTP) was induced by theta-burst stimulation (TBS); DG = dentate gyrus; CA = Cornu Ammonis. (B) Example traces of individual recordings showing average traces of baseline recording before LTP induction (black traces) and after LTP (red traces). Slope and peak amplitude of fEPSPs are increased after TBS in mice infused with control CSF (Ct CSF) and Ct CSF + ephrin-B2, whereas manifestation of LTP is strongly impaired in animals infused with patients' CSF antibodies (Pt CSF). In mice infused with Pt CSF + ephrin-B2, the increase of slope is improved. Note that initial peak amplitude of fEPSP may vary within individual recordings. (C) Time course of fEPSP recordings demonstrating robust changes in fEPSP slope in the Ct CSF ($n = 7$ recordings, blue open circles) and Ct CSF + ephrin-B2 group ($n = 7$, cyan open squares), which is stable throughout the recording period after TBS (arrow). In animals chronically infused with Pt CSF ($n = 7$, red solid circles), the induction of synaptic LTP is markedly impaired. Recordings from the Pt CSF + ephrin-B2 group ($n = 5$, gray solid squares) show partially resolved effects on synaptic plasticity after LTP induction. (D) Quantitative analysis of LTP-induced changes in fEPSPs in the plateau interval after TBS depicted as comparison to each individual baseline value (slope increase as median values \pm standard error of the mean in the consolidation phase during the last 50 minutes of each recording, starting 15 minutes after TBS). Chronic application of Pt CSF results in marked reduction of LTP ($13.3 \pm 4.1\%$ slope increase vs $73.6 \pm 19.3\%$ and $68.3 \pm 14.7\%$ in Ct CSF and Ct CSF + ephrin-B2, respectively). Coadministration of soluble ephrin-B2 improved fEPSP potentiation to levels of $33.7 \pm 5.5\%$. Significance of treatment effect was assessed by two-way analysis of variance (ANOVA; $p < 0.0001$ for treatment group) and by post-hoc analysis with Bonferroni correction; $***p < 0.001$. (E) Patients' antibodies do not alter short-term plasticity, as revealed by paired-pulse facilitation. Short-term plasticity in the Schaffer collateral-CA1 synaptic region shows paired pulse facilitation as measured by mean slope values of the first (1st) and second (2nd) stimulus in the group of mice infused with control CSF (Ct CSF, blue), Ct CSF + ephrin-B2 (cyan), patients' CSF antibodies (Pt CSF, red), or Pt CSF + ephrin-B2 (grey) before (pale color) and after (dark color) LTP induction. Analysis of 2nd versus 1st stimulation reveals a significant increase of fEPSPs in all groups and at both time points before LTP induction (Ct CSF: $p < 0.0001$; Ct CSF + ephrin-B2: $p = 0.0002$; Pt CSF: $p = 0.0012$; Pt CSF + ephrin-B2: $p = 0.0004$) and after LTP (Ct CSF: $p < 0.0001$; Ct CSF + ephrin-B2: $p = 0.0009$; Pt CSF: $p < 0.0001$; Pt CSF + ephrin-B2: $p < 0.0001$). Comparison of fEPSPs after the first stimulus before and after LTP induction shows a significant increase in the Pt CSF + ephrin-B2 ($p = 0.0007$) and both control CSF groups (Ct CSF: $p = 0.0003$; Ct CSF + ephrin-B2: $p = 0.0004$), but not in the Pt CSF group ($p = 0.21$). Analysis was performed using repeated-measures two-way ANOVA ($p < 0.0001$ for treatment groups) and post-hoc analysis with Bonferroni correction; $**p < 0.01$; $***p < 0.001$; $****p < 0.0001$. (F) Analysis of fEPSP absolute slope values depending on stimulus amplitude. Increasing stimulation leads to higher slope values reaching a plateau phase at stimulation strength $> 400 \mu\text{A}$ (maximum slope and peak amplitude of fEPSP). The fEPSP slope is significantly reduced in mice infused with patients' CSF antibodies (Pt CSF; red circles). In the Pt CSF + ephrin-B2 group (gray circles), the fEPSP slope is partially restored in comparison to mice infused with Pt CSF. Blue and cyan squares indicate animals infused with control CSF (Ct CSF) and Ct CSF + ephrin-B2, respectively. Two-way ANOVA showed $p < 0.0001$ for increasing stimulation and treatment; post-hoc analysis with Bonferroni correction showed difference between the groups of mice infused with Pt CSF compared with Ct CSF with or without ephrin-B2 ($p < 0.0001$); Pt CSF compared with Pt CSF + ephrin-B2 ($p = 0.001$); and Pt CSF + ephrin-B2 compared with Ct CSF ($p = 0.0007$). CSF = cerebrospinal fluid.

antagonized by stimulation of EphB2.³ Here, we provide evidence that in mice receiving patients' antibodies, treatment with ephrin-B2 is able to partially prevent the antibody-induced impairment of LTP and glutamatergic transmission in the hippocampus.

Direct quantification of ephrin-B2-induced restoration of NMDAR-mediated individual currents awaits further experimental evidence by evaluating synaptic currents using patch-clamp experiments at the single-cell level. These effects *ex vivo* are supported by the morphological findings demonstrating abrogation of the antibody-induced reduction of NMDAR and EphB2 in the ephrin-B2-treated mice. Thus, stabilization of NMDAR expression in the postsynaptic receptor fields mediated by stimulation of Eph2B receptors may account for the rescue of memory and behavioral deficits in this animal model.

Different from the current model in which the antibodies are infused by a pump that stops after 14 days, in the human disease the exposure of brain to central nervous system (CNS) antibodies decreases slowly over months.^{30,31} A relevant source of CNS antibodies are the plasma cells demonstrated in pathological studies^{32,33} and associated with intrathecal synthesis of antibodies.^{1,6} Current treatments (plasma exchange, intravenous immune globulin, or rituximab) have limited efficacy on removing antibodies and plasma cells from the CNS. Thus, prolonged exposure of the human brain to NMDAR antibodies may disturb synaptic networks, as suggested by our observed decrease of synaptic NMDAR and alteration of synaptic plasticity in our model. It is important to keep in mind that a period of 14 days in 2-month-old mice is equivalent to 60 weeks in humans.³⁴ Additionally, in the human disease, the presence of inflammatory cells, mediators of inflammation, and frequent clinical complications (eg, intensive care unit complications, autonomic instability) may modify the outcome of the disorder.³⁵

An important finding of this study is that all antibody-mediated deficits, from memory to synaptic plasticity, were substantially prevented by ephrin-B2, providing a potential treatment strategy with peptides or small-molecule agonists of EphB2. There is precedence for the clinical use of agonists of other types of Ephrin receptors, such as the EphA2 agonist, doxazosin, which is used for treatment of benign prostate hypertrophy, but in experimental models also inhibits tumor cell migration and metastases.³⁶ In antibody-mediated disorders of the neuromuscular junction, such as myasthenia gravis or Lambert-Eaton syndrome, the discovery of the physiopathological underpinnings led to the development of drugs that antagonize the effects of the corresponding antibodies (eg, anticholinesterases and 3,4-diaminopyridine).³⁷ One envisions

a similar result in anti-NMDAR and perhaps other autoimmune encephalitis, in which the combined use of immunotherapy and small molecules crossing the blood-brain barrier and antagonizing antibody effects could represent a future treatment approach. For anti-NMDAR encephalitis, such drugs may lead to a faster control of the severe symptoms of the disease, stabilizing the function of the NMDAR in the synapses.

Acknowledgments

This study was supported, in part, by Instituto Carlos III/FEDER (FIS 15/00377 [to F.G.], FIS 14/00203 and CIBERER [to J.D.], and RETICS-RTA and RD12/0028/0023 [to R.M.]), NIH RO1NS077851 (to J.D.), MINECO (SAF2014-59648-P; to R.M.), European Commission (HEALTH-F2-2013-602891; to R.M.), Fundació Cellex (to J.D.), the Netherlands Organisation for Scientific Research (NWO, Veni incentive; to M.T.), an Erasmus MC fellowship (to M.T.), and the German Research Council (DFG; GE 2519/3-1 and CRC-TR 166/1 B2 [to C.G.]).

We thank Dr Melike Lakadamyali (ICFO-Institut de Ciències Fotòniques, Barcelona) and Dr Myrna Rosenfeld (IDIBAPS, University of Barcelona) for their critical review of the manuscript and useful suggestions and Dr Thaís Armangué (IDIBAPS, University of Barcelona) for her comments on the statistical analysis.

Author Contributions

J.D. and C.G. were responsible for conception and design of the study. F.M., M.P.-P., E.M.-G., R.F., and J.D. were responsible for acquisition and analysis of animal behavior. J.P., M.J.T., P.J., F.G., and J.D. were responsible for acquisition and analysis of immunohistochemistry and confocal microscopy. H.H., B.G., L.R., and C.G. were responsible for acquisition and analysis of electrophysiological studies. J.P., H.H., C.G., and J.D. were responsible for drafting of the manuscript and figures. J.P., H.H., and F.M. contributed equally. C.G. and J.D. share seniority.

Potential Conflicts of interest

Dr Dalmau holds a patent for the use of NMDA receptor as an autoantibody test. Dr Dalmau has received a research grant from Euroimmun Inc.

References

1. Dalmau J, Gleichman AJ, Hughes EG, et al. Anti-NMDA-receptor encephalitis: case series and analysis of the effects of antibodies. *Lancet Neurol* 2008;7:1091-1098.

2. Hughes EG, Peng X, Gleichman AJ, et al. Cellular and synaptic mechanisms of anti-NMDA receptor encephalitis. *J Neurosci* 2010;30:5866–5875.
3. Mikasova L, De Rossi P, Bouchet D, et al. Disrupted surface cross-talk between NMDA and Ephrin-B2 receptors in anti-NMDA encephalitis. *Brain* 2012;135:1606–1621.
4. Moscato EH, Peng X, Jain A, et al. Acute mechanisms underlying antibody effects in anti-N-methyl-D-aspartate receptor encephalitis. *Ann Neurol* 2014;76:108–119.
5. Titulaer MJ, McCracken L, Gabilondo I, et al. Treatment and prognostic factors for long-term outcome in patients with anti-NMDA receptor encephalitis: an observational cohort study. *Lancet Neurol* 2013;12:157–165.
6. Irani SR, Bera K, Waters P, et al. N-methyl-D-aspartate antibody encephalitis: temporal progression of clinical and paraclinical observations in a predominantly non-paraneoplastic disorder of both sexes. *Brain* 2010;133:1655–1667.
7. Viacoz A, Desestret V, Ducray F, et al. Clinical specificities of adult male patients with NMDA receptor antibodies encephalitis. *Neurology* 2014;82:556–563.
8. Zhang Q, Tanaka K, Sun P, et al. Suppression of synaptic plasticity by cerebrospinal fluid from anti-NMDA receptor encephalitis patients. *Neurobiol Dis* 2012;45:610–615.
9. Planaguma J, Leypoldt F, Mannara F, et al. Human N-methyl D-aspartate receptor antibodies alter memory and behaviour in mice. *Brain* 2015;138:94–109.
10. Petit-Pedrol M, Armangue T, Peng X, et al. Encephalitis with refractory seizures, status epilepticus, and antibodies to the GABAA receptor: a case series, characterisation of the antigen, and analysis of the effects of antibodies. *Lancet Neurol* 2014;13:276–286.
11. Lai M, Hughes EG, Peng X, Dalmau J. AMPA receptor antibodies in limbic encephalitis alter synaptic receptor location. *Ann Neurol* 2009;65:424–434.
12. Grover LM, Kim E, Cooke JD, Holmes WR. LTP in hippocampal area CA1 is induced by burst stimulation over a broad frequency range centered around delta. *Learn Mem* 2009;16:69–81.
13. Raymond CR. LTP forms 1, 2 and 3: different mechanisms for the “long” in long-term potentiation. *Trends Neurosci* 2007;30:167–175.
14. Schmuckermair C, Gaburro S, Sah A, et al. Behavioral and neurobiological effects of deep brain stimulation in a mouse model of high anxiety- and depression-like behavior. *Neuropsychopharmacology* 2013;38:1234–1244.
15. Kordjazy N, Haj-Mirzaian A, Amiri S, et al. Involvement of N-methyl-d-aspartate receptors in the antidepressant-like effect of 5-hydroxytryptamine 3 antagonists in mouse forced swimming test and tail suspension test. *Pharmacol Biochem Behav* 2015;141:1–9.
16. Dalva MB, Takasu MA, Lin MZ, et al. EphB receptors interact with NMDA receptors and regulate excitatory synapse formation. *Cell* 2000;103:945–956.
17. Gleichman AJ, Spruce LA, Dalmau J, et al. Anti-NMDA receptor encephalitis antibody binding is dependent on amino acid identity of a small region within the GluN1 amino terminal domain. *J Neurosci* 2012;32:11082–11094.
18. Nolt MJ, Lin Y, Hruska M, et al. EphB controls NMDA receptor function and synaptic targeting in a subunit-specific manner. *J Neurosci* 2011;31:5353–5364.
19. Forrest D, Yuzaki M, Soares HD, et al. Targeted disruption of NMDA receptor 1 gene abolishes NMDA response and results in neonatal death. *Neuron* 1994;13:325–338.
20. Huerta PT, Sun LD, Wilson MA, Tonegawa S. Formation of temporal memory requires NMDA receptors within CA1 pyramidal neurons. *Neuron* 2000;25:473–480.
21. Tsien JZ, Huerta PT, Tonegawa S. The essential role of hippocampal CA1 NMDA receptor-dependent synaptic plasticity in spatial memory. *Cell* 1996;87:1327–1338.
22. Zamanillo D, Sprengel R, Hvalby O, et al. Importance of AMPA receptors for hippocampal synaptic plasticity but not for spatial learning. *Science* 1999;284:1805–1811.
23. Oertner TG, Sabatini BL, Nimchinsky EA, Svoboda K. Facilitation at single synapses probed with optical quantal analysis. *Nat Neurosci* 2002;5:657–664.
24. Wurdemann T, Kersten M, Tokay T, et al. Stereotactic injection of cerebrospinal fluid from anti-NMDA receptor encephalitis into rat dentate gyrus impairs NMDA receptor function. *Brain Res* 2015;1633:10–18.
25. Wright S, Hashemi K, Stasiak L, et al. Epileptogenic effects of NMDAR antibodies in a passive transfer mouse model. *Brain* 2015;138:3159–3167.
26. Henderson JT, Georgiou J, Jia Z, et al. The receptor tyrosine kinase EphB2 regulates NMDA-dependent synaptic function. *Neuron* 2001;32:1041–1056.
27. Kullander K, Klein R. Mechanisms and functions of Eph and ephrin signalling. *Nat Rev Mol Cell Biol* 2002;3:475–486.
28. Lisabeth EM, Falivelli G, Pasquale EB. Eph receptor signaling and ephrins. *Cold Spring Harb Perspect Biol* 2013;5 pii: a009159. doi: 10.1101/cshperspect.a009159.
29. Grunwald IC, Korte M, Wolfer D, et al. Kinase-independent requirement of EphB2 receptors in hippocampal synaptic plasticity. *Neuron* 2001;32:1027–1040.
30. Gresa-Arribas N, Titulaer MJ, Torrents A, et al. Antibody titres at diagnosis and during follow-up of anti-NMDA receptor encephalitis: a retrospective study. *Lancet Neurol* 2014;13:167–177.
31. Leypoldt F, Hofberger R, Titulaer MJ, et al. Investigations on CXCL13 in anti-N-methyl-D-aspartate receptor encephalitis: a potential biomarker of treatment response. *JAMA Neurol* 2015;72:180–186.
32. Martinez-Hernandez E, Horvath J, Shiloh-Malawsky Y, et al. Analysis of complement and plasma cells in the brain of patients with anti-NMDAR encephalitis. *Neurology* 2011;77:589–593.
33. Bien CG, Vincent A, Barnett MH, et al. Immunopathology of autoantibody-associated encephalitides: clues for pathogenesis. *Brain* 2012;135:1622–1638.
34. Flurkey K, Curren JM, Harrison DE. The mouse in aging research. In: Fox JGea, ed. *The Mouse in Biomedical Research*. Burlington, MA: American College Laboratory Animal Medicine (Elsevier); 2015:637–672.
35. Dalmau J, Lancaster E, Martinez-Hernandez E, Rosenfeld MR, Balice-Gordon R. Clinical experience and laboratory investigations in patients with anti-NMDAR encephalitis. *Lancet Neurol* 2011;10:63–74.
36. Petty A, Myshkin E, Qin H, et al. A small molecule agonist of EphA2 receptor tyrosine kinase inhibits tumor cell migration in vitro and prostate cancer metastasis in vivo. *PLoS One* 2012;7:e42120.
37. Newsom-Davis J. Therapy in myasthenia gravis and Lambert-Eaton myasthenic syndrome. *Semin Neurol* 2003;23:191–198.

Suppl. Table 2

Test	2-way ANOVA analysis			
	Source of variation	p-value	F-value	
Locomotor Activity	Motor Activity	Interaction	0.90	0.51
		Time	< 0.0001	26.92
		Treatment	0.94	0.13
	Horizontal Activity	Interaction	0.86	0.58
		Time	< 0.0001	23.95
		Treatment	0.47	0.85
Vertical Activity	Interaction	0.81	0.63	
	Time	< 0.0001	36.95	
	Treatment	0.82	0.30	
Weight	% Difference weight	Interaction	0.16	1.35
		Time	< 0.0001	9.08
		Treatment	0.26	1.36

Suppl. Tab. 3

2-way ANOVA analysis				Post-hoc analysis OR Index *					
Source of variation	P-value	F-value	Pt CSF vs Ct CSF						
			Day	Mean Pt CSF	Mean Ct CSF	difference	95% CI	P-value	
IgG deposits	Interaction	< 0.0001	11.02	5	11.31	4.61	6.70	-13.87 to 27.28	> 0.05
				18	69.94	2.50	67.44	48.04 to 86.84	< 0.0001
				26	48.33	4.25	44.09	24.69 to 63.49	< 0.0001
	Treatment	< 0.0001	60.55	Pt CSF vs Ct CSF + ephrin-B2					
				Day	Mean Pt CSF	Mean Ct CSF + ephrin-B2	difference	95% CI	P-value
				5	11.31	4.03	7.28	-12.12 to 26.29	> 0.05
	Time	< 0.0001	32.38	18	69.94	5.50	64.44	45.04 to 83.84	< 0.0001
				26	48.33	8.60	39.74	20.33 to 59.14	< 0.0001
				Pt CSF + ephrin-B2 vs Ct CSF					
Day	Mean Pt CSF + ephrin-B2	Mean Ct CSF	difference	95% CI	P-value				
5	17.02	4.61	12.41	-8.16 to 32.99	> 0.05				
18	77.40	2.50	74.91	55.51 to 94.31	< 0.0001				
26	47.75	4.25	43.50	24.10 to 62.90	< 0.0001				
Pt CSF + ephrin-B2 vs Ct + ephrin-B2									
Day	Mean Pt CSF + ephrin-B2	Mean Ct CSF + ephrin-B2	difference	95% CI	P-value				
5	17.02	4.03	12.99	-6.41 to 32.39	> 0.05				
18	77.40	5.50	71.90	52.50 to 91.30	< 0.0001				
26	47.75	8.60	39.15	19.75 to 58.55	< 0.0001				

* Post-hoc data for comparisons of Pt CSF vs Pt CSF + ephrin-B2 and Ct CSF vs Ct CSF + ephrin-B2 revealed no significant differences.

5.6. Paper VI (unpublished paper)

LGI1 antibodies alter Kv1.1 and AMPA receptors changing synaptic excitability, plasticity and memory

Mar Petit-Pedrol*, Josefine Sell*, Jesús Planagumà, Francesco Mannara, Marija Radosevic, Holger Haselmann, Mihai Ceanga, Lidia Sabater, Marianna Spatola, David Soto, Xavier Gasull, Josep Dalmau, and Christian Geis

*These authors contributed equally



LGI1 antibodies alter Kv1.1 and AMPA receptors changing synaptic excitability, plasticity and memory

Journal:	<i>Brain</i>
Manuscript ID	Draft
Manuscript Type:	Original Article
Date Submitted by the Author:	n/a
Complete List of Authors:	<p>Petit-Pedrol, Mar; Institut d'Investigacions Biomèdiques August Pi i Sunyer (IDIBAPS), Hospital Clínic, Universitat de Barcelona</p> <p>Sell, Josefine; Hans-Berger Department of Neurology; Center for Sepsis Control and Care (CSCC), Jena University Hospital</p> <p>Planagumà, Jesús; Institut d'Investigacions Biomèdiques August Pi i Sunyer (IDIBAPS), Hospital Clínic, Universitat de Barcelona</p> <p>Mannara, Francesco; Institut d'Investigacions Biomèdiques August Pi i Sunyer (IDIBAPS), Hospital Clínic, Universitat de Barcelona</p> <p>Radosevic, Marija; Institut d'Investigacions Biomèdiques August Pi i Sunyer (IDIBAPS), Hospital Clínic, Universitat de Barcelona</p> <p>Haselmann, Holger; Hans-Berger Department of Neurology; Center for Sepsis Control and Care (CSCC), Jena University Hospital</p> <p>Ceanga, Mihai; Hans-Berger Department of Neurology</p> <p>Sabater, Lidia; Institut d'Investigacions Biomèdiques August Pi i Sunyer (IDIBAPS), Hospital Clínic, Universitat de Barcelona</p> <p>Spatola, Marianna; Institut d'Investigacions Biomèdiques August Pi i Sunyer (IDIBAPS), Hospital Clínic, Universitat de Barcelona; University of Lausanne (UNIL)</p> <p>Soto, David; Institut d'Investigacions Biomèdiques August Pi i Sunyer (IDIBAPS), Hospital Clínic, Universitat de Barcelona; Laboratori de Neurofisiologia, Departament de Biomedicina, Facultat de Medicina i Ciències de la Salut, Institut de Neurociències, Universitat de Barcelona</p> <p>Gasull, Xavier; Institut d'Investigacions Biomèdiques August Pi i Sunyer (IDIBAPS), Hospital Clínic, Universitat de Barcelona; Laboratori de Neurofisiologia, Departament de Biomedicina, Facultat de Medicina i Ciències de la Salut, Institut de Neurociències, Universitat de Barcelona</p> <p>Dalmau, Josep; Institut d'Investigacions Biomèdiques August Pi i Sunyer (IDIBAPS), Hospital Clínic, Universitat de Barcelona; Department of Neurology, University of Pennsylvania; Centro de Investigación Biomédica en Red Enfermedades Raras (CIBERER); Institució Catalana de Recerca i Estudis Avançats (ICREA)</p> <p>Geis, Christian; Hans-Berger Department of Neurology; Center for Sepsis Control and Care (CSCC), Jena University Hospital</p>
Subject category:	Multiple sclerosis and neuroinflammation
To search keyword list, use whole or part words followed	Limbic encephalitis < MULTIPLE SCLEROSIS AND NEUROINFLAMMATION, Neuroimmunology < MULTIPLE SCLEROSIS AND NEUROINFLAMMATION,

by an *:	Synaptic transmission < SYSTEMS/DEVELOPMENT/PHYSIOLOGY, Plasticity < SYSTEMS/DEVELOPMENT/PHYSIOLOGY, Memory < DEMENTIA

SCHOLARONE™
Manuscripts

For Peer Review

LGI1 antibodies alter Kv1.1 and AMPA receptors changing synaptic excitability, plasticity and memory

Mar Petit-Pedrol^{1,*}, Josefina Sell^{2,*}, Jesús Planagumà¹, Francesco Mannara¹, Marija Radosevic¹, Holger Haselmann^{2,3}, Mihai Ceanga², Lidia Sabater¹, Marianna Spatola^{1,4}, David Soto^{1,5}, Xavier Gasull^{1,5}, Josep Dalmau^{1,6,7,8,\$}, and Christian Geis^{2,3,\$}

¹Institut d'Investigacions Biomèdiques August Pi i Sunyer (IDIBAPS), Hospital Clínic, Universitat de Barcelona, Barcelona, Spain; ²Hans-Berger Department of Neurology,

³Center for Sepsis Control and Care (CSCC), Jena University Hospital, Jena, Germany;

⁴University of Lausanne (UNIL), Lausanne, Switzerland; ⁵Laboratori de

Neurofisiologia, Departament de Biomedicina, Facultat de Medicina i Ciències de la Salut, Institut de Neurociències, Universitat de Barcelona, Barcelona, Spain;

⁶Department of Neurology, University of Pennsylvania, Philadelphia, USA; ⁷Centro de Investigación Biomédica en Red Enfermedades Raras (CIBERER); ⁸Institució Catalana de Recerca i Estudis Avançats (ICREA), Barcelona, Spain.

*** Contributed equally**

\$ Share seniority

Corresponding author: Josep Dalmau, MD, PhD, IDIBAPS-Hospital Clínic,

University of Barcelona, Casanova, 143; Floor 3^a, Barcelona 08036 (Spain); Phone: +34

932 271 738 Fax: +34 932 271 726. E-mail: Jdalmau@clinic.cat

Running title: Mechanisms of anti-LGI1 encephalitis

Abstract

Autoimmune encephalitis with antibodies against leucine-rich glioma-inactivated 1 (LGI1) protein is the most frequent form of immune-mediated limbic encephalitis usually presenting with severe impairment in memory formation preceded by faciobrachial dystonic seizures that often respond to immunotherapy. LGI1 is a neuronal secreted synaptic linker protein that connects presynaptic voltage-gated potassium channels Kv1.1 with postsynaptic α -amino-3-hydroxy-5-methyl-4-isoxazolepropionic acid (AMPA) receptors through the interaction with the transmembrane disintegrin and metalloprotease domain family members ADAM23 and 22, respectively. Despite evidence suggesting the disorder is immune-mediated the pathophysiology of how human LGI1 antibodies cause disease symptoms is largely unknown. Here we used highly specific patient-derived immunoglobulin G to determine the main epitope regions, the potential antibody interference of the interaction between LGI1 and ADAM23 and 22, and the effects on behavior, presynaptic Kv1.1 and postsynaptic AMPA receptors, synaptic transmission, and plasticity. Purified immunoglobulin G samples of 25 patients and 20 controls, and experiments with 118 mice including behavioral test, brain tissue analysis with confocal microscopy, and electrophysiology were used in the study. All patients' samples prevented binding of LGI1 to ADAM23, but only 60% to ADAM22. Using deletion constructs of LGI1 we found obligate binding of patients' antibodies to the leucine rich repeat domain and less frequent binding to the epitempin domain. Passive cerebroventricular transfer of patients' immunoglobulin G antibodies to mice led to prolonged but reversible deficits in memory function. Confocal analysis of hippocampal brain slices showed reduced total and synaptic levels of Kv1.1 following the time course of animal memory deficit, with complete recovery 33 days after the end of the infusion. Reduction of AMPA

receptors was present in a time-displaced manner following the loss of Kv1.1. In acute slice preparations of hippocampus, patch-clamp analysis from dentate gyrus granule cells revealed neuronal hyperexcitability with increased glutamatergic transmission and higher presynaptic release probability most likely induced by the reduced expression of Kv1.1. Analysis of synaptic plasticity by recording field potentials in the CA1 region of the hippocampus revealed severely affected long-term potentiation consistent with the memory deficits observed in mice. Different from genetic models of LGI1 deficiency, we did not observe aberrant dendritic sprouting or defective synaptic pruning as major pathology underlying disease symptoms. Overall, these findings reveal several LGI1 antibody-mediated pathogenic mechanisms that interfere with LGI1-associated pathways, altering presynaptic and postsynaptic signaling, and resulting in synaptic hyperexcitability, decreased plasticity, and memory deficits.

Keywords

Limbic encephalitis, LGI1, AMPA receptors, Kv1.1, synaptic hyperexcitability

Introduction

Autoimmune encephalitides refer to a group of inflammatory brain diseases that manifest with prominent neuropsychiatric symptoms and are associated with antibodies against neuronal cell surface proteins, ion channels or receptors (Dalmau *et al.*, 2017). One of the most frequent types of autoimmune encephalitis predominantly affects the limbic system (limbic encephalitis) and can result from autoantibodies against different antigens, such as leucine-rich glioma-inactivated 1 (LGI1) protein, the α -amino-3-hydroxy-5-methyl-4-isoxazolepropionic acid receptor (AMPA), the γ -aminobutyric acid (GABA) type B receptor, or contactin-associated protein-like 2 (Caspr2), each of

them manifesting with a core syndrome that includes severe difficulty in forming new memories (anterograde or short-term memory deficit), changes of mood and behavior, and variable presence of seizures (Dalmau and Graus, 2018). The most frequent is autoimmune limbic encephalitis with antibodies against LGI1 (Irani *et al.*, 2010; Lai *et al.*, 2010). Patients with this disorder often present with faciobrachial dystonic seizures or hyponatremia that precede or develop together with the aforementioned core syndrome of limbic dysfunction (Irani *et al.*, 2013). Less frequently, patients with LGI1 antibodies present with rapidly progressive dementia which, as the other clinical manifestations, is responsive to immunotherapy (Arino *et al.*, 2016; Gadoth *et al.*, 2017).

Anti-LGI1 associated limbic encephalitis (or anti-LGI1 encephalitis) has an estimated incidence of 0.83 per 1 million persons (van Sonderen *et al.*, 2016), strongly associates with DRB1*07:01-DQB1*02:02 and HLA-DRB4 (Kim *et al.*, 2017; van Sonderen *et al.*, 2017b), and rarely presents as a paraneoplastic manifestation of an underlying thymoma (van Sonderen *et al.*, 2017a). Different from the other autoantigens of limbic encephalitis, which are synaptic receptors or cell membrane proteins, LGI1 is a secreted neuronal protein that has several binding partners, possibly organizing a trans-synaptic complex that includes the pre-synaptic ADAM23 and Kv1.1 potassium channels, and the postsynaptic ADAM22 and AMPAR (Sirerol-Piquer *et al.*, 2006; Fukata *et al.*, 2010). Mutations of LGI1 are linked to a disorder named “autosomal dominant lateral temporal lobe epilepsy” (ADTLE), an inherited form of epilepsy characterized by partial seizures with acoustic or visual hallucinations (Poza *et al.*, 1999; Morante-Redolat *et al.*, 2002; Staub *et al.*, 2002). Several transgenic mouse models expressing a truncated LGI1 mutant that causes the inherited human disease, as well as LGI1 knock-out mice, showed an increase of excitatory synaptic transmission as

compared with wild-type mice (Zhou *et al.*, 2009; Boillot *et al.*, 2016; Seagar *et al.*, 2017). These findings and evidence from experiments in oocytes after overexpression of Kv1.1, Kvbeta1, LGI1, and mutated LGI (Schulte *et al.*, 2006) suggested that LGI1 decreases presynaptic release probability by upregulating presynaptic Kv1 channel activity *in vivo*. On the other hand, LGI1 knock-out mice also had decreased levels of post-synaptic AMPAR in the hippocampal dentate gyrus (Ohkawa *et al.*, 2013).

A previous study examining the synaptic effects of patients' LGI1 antibodies showed that they disrupted the interaction of LGI1 with ADAM22 and reversibly reduced the postsynaptic clusters of AMPAR *in vitro* in rat hippocampal neurons (Ohkawa *et al.*, 2013). The antibodies also altered the interaction of LGI1 with a soluble construct of ADAM23 (Ohkawa *et al.*, 2013) but the effects on Kv1.1 potassium channels and plasticity, the effects in an animal model, and whether patients' antibodies can impair memory were not reported. Considering the interaction of LGI1 with ADAM23, we reasoned that patients' antibodies would have a downstream effect on the Kv1.1 potassium channels. Moreover, since anti-LGI1 encephalitis usually results in a treatable hippocampal syndrome with difficulty in forming new memories (Arino *et al.*, 2016; van Sonderen *et al.*, 2016), we postulated that patients' antibodies would alter memory in a mouse model of cerebroventricular transfer of the antibodies. Our findings reveal a complex pathogenic mechanism of LGI1 antibodies involving both the Kv1.1 potassium channels and AMPAR, which lead to alterations of plasticity and to prolonged but reversible memory deficits.

Material and Methods

Patients' serum samples

Serum samples of 25 patients with anti-LGI1 encephalitis were included in the assays (Supplementary Table 1). In all cases the presence of LGI1 antibodies was confirmed with rat brain tissue immunohistochemistry and a cell-based assay with human embryonic kidney (HEK)293 cells expressing LGI1 (Lai *et al.*, 2010). Serum samples from 20 antibody-negative healthy blood donors were used as controls. In a subset of experiments (field potential recordings) we additionally used CSF from patients and controls. Studies were approved by the institutional review board of Hospital Clínic and Institut d'Investigacions Biomèdiques August Pi i Sunyer (IDIBAPS), University of Barcelona and Jena University Hospital.

Serum IgG purification

Sera from 8 high-titer LGI1 antibody positive patients with prominent limbic encephalitis were pooled and the IgG (LGI1 IgG) isolated using agarose beads columns (#20423, Pierce), as reported (Gresa-Arribas *et al.*, 2016). IgG similarly isolated from serum of antibody-negative healthy blood donors was used as control (control IgG). After IgG isolation, samples were dialyzed, normalized to a concentration of 4 μ g/ μ l using Amicon Ultracentrifugal filters 30K (#UFC903024, Sigma-Aldrich), filtered, and kept at -80 C° until use. The LGI1 specificity of the sample preparation was determined by immunoabsorption with HEK293 cells expressing LGI1, which showed abrogation of reactivity with brain, LGI1-expressing HEK293 cells, and cultured neurons (Supplementary Fig. 1), and by immunohistochemistry with brain of LGI1 null mice which showed lack of immunostaining (Supplementary Fig. 2).

Production of soluble LGI1

HEK293 cells were transfected with a human LGI1 plasmid (Origene, human sequence sc-116925) as reported (Lai *et al.*, 2010). Six hours after transfection, culture medium was replaced with OptiMem medium (#51985-026, Gibco) and cells were

incubated for 15 hours at 37°C, 95% O₂, 5% CO₂. The medium was then collected and concentrated (total protein, 3 mg/ml) using Amicon Ultracentrifugal filters 30K (#UFC903024, Millipore). The LGI1 enriched medium was then filtered through 0.22µm polyvinylidenedifluoride (PVDF) membrane filters (#sc-358812, Santa Cruz), and the presence of LGI1 in the media was determined by immunoblot using a commercial LGI1 antibody (1:200, #ab30868, Abcam), as described in Supplementary material. The same steps were carried out for the media of non-transfected HEK293 cells (used as control).

LGI1 deletion mutants

To identify the main epitope regions of LGI1, human full length LGI1 DNA, (SC116925; NM_005097, Origene) cloned in pCMV6-AC-GFP plasmid was used as template to generate deletion mutants. The cloning procedures were performed by GenScript (USA, Inc, Piscataway, NJ, USA). Clone #1 corresponded to the indicated human full length LGI1 DNA; clone #2 contained the signal peptide (1-34 nucleotides) and the leucine rich repeat (LRR) domain (35-223 nucleotides); clone #3 contained the signal peptide and the epitempin (EPTP) domains (224-557 nucleotides), and clone #4 had the signal peptide (SP) and the immunoglobulin domain 3 of IgLON5 (218-307 nucleotides of IgLON5) (Sabater *et al.*, 2016) and served as control. In order to anchor the constructs to the cell membrane, all four clones had the glycosylphosphatidylinositol (GPI) sequence and the green fluorescence protein (GFP) sequence of human IgLON5 (RG225495; NM_001101372, Origene) added to the C-terminus. The presence of patients' serum antibodies against each of these clones was determined with a conventional HEK293 cell-based assay, using serum dilutions 1:20 for 1 hour at room temperature, and a secondary goat anti-human IgG Alexa Fluor 594 (1:1000, A11014, Invitrogen) for 1 hour.

LGI1 binding assay

HEK293 cells were transfected with ADAM22 or ADAM23 (rat sequences containing an HA tag) as reported (Lai *et al.*, 2010), and their expression was confirmed with a mouse polyclonal antibody against HA 6E2 (1:200, #2367, Cell Signaling). To show that soluble LGI1 was able to bind to ADAM22 or ADAM23, HEK293 cells expressing ADAM22 or ADAM23 were exposed to the indicated LGI1 enriched medium (1:3) in Dulbecco's Modified Eagle's medium (DMEM) for 2 hours at 37°C, washed with DMEM, and sequentially incubated for 45 minutes at 37°C with patients' LGI1 IgG or control IgG (1:50) and goat anti-human IgG Alexa Fluor 488 (1:1000, #A11013, Invitrogen). A similar experiment was performed using goat polyclonal antibody against LGI1 (diluted 1:100, #sc9583, Santa Cruz) instead of human LGI1 IgG; in this setting the secondary antibody was donkey anti-goat Alexa Fluor 488 (1:1000, #A11055, Invitrogen).

Parallel studies in which the indicated medium with soluble LGI1 had been pre-incubated with excess patients' or control IgG (total IgG concentration 0.5 mg/ml) for 2 hours at 37°C, were used to determine whether patient's antibodies interfered with the binding of soluble LGI1 to cells expressing ADAM22 or ADAM23.

Mice, placement of osmotic pumps, and behavioral tasks

Male C57BL6/J mice (Charles River), 8-10 weeks old (25-30 g) were used in the studies. Animal experiments were performed in accordance to the ARRIVE guidelines for reporting animal research (Kilkenny, Browne, Cuthill, Emerson, & Altman, 2010) and the procedures were approved by the local ethics committee at the Universities of Barcelona and Jena. Detailed information on the animal studies including surgery, placement of ventricular catheters and osmotic pumps, and behavioral tests is provided as supplemental information and has been previously reported (Planaguma *et al.*, 2015).

The distribution of behavioral tests in relation to the infusion of LGII IgG control IgG is shown in Supplementary Fig. 3. Overall, a total of 118 mice were used for these studies: 83 for behavioral and brain tissue studies (quantification of Kv1.1 and AMPAR clusters; antibody extraction; immunoprecipitation) and 35 for electrophysiological studies.

Immunofluorescence and confocal microscopy with brain tissue

Representative groups of mice were deeply anesthetized with isoflurane, perfused with PBS, and sacrificed at different time points (days 1, 5, 13, 18, 26, 47). The brains were removed and sagittally split into the two hemispheres. One hemisphere was fixed with 4% PFA for 1 hour, cryopreserved in 40% sucrose for 48 hours, embedded in optimal cutting temperature compound (#4583, Tissue-Tek), and snap frozen in isopentane chilled with liquid nitrogen.

To determine the levels of presynaptic Kv1.1 potassium channels, 5 μm thick cryostat sections were sequentially incubated with a polyclonal rabbit antibody against Kv1.1 (1:100, #ab32433, Abcam) for 2 hours at RT, washed in PBS containing 0,3% Triton, and incubated with a mouse monoclonal antibody against the presynaptic marker Bassoon (1:250, #SAP7F407, Enzo), overnight at 4°C. Secondary antibodies included goat anti-rabbit Alexa Fluor 488 and goat anti-mouse Alexa Fluor 594 (both 1:1000, #A11008 and A11005, Invitrogen).

To determine whether the post-synaptic levels of AMPAR were affected, brain sections were incubated with a polyclonal guinea pig antibody against GluA1 (1:200, #AGP009, Alomone) for 2 hours at RT, washed in PBS containing 0,3% Triton, and incubated with a rabbit polyclonal antibody against the post-synaptic marker PSD95 (1:250, #18258, Abcam) overnight at 4°C. Secondary antibodies included goat anti-guinea pig Alexa Fluor 488, and goat anti-rabbit Alexa Fluor 594 (1:1000, #A11073 and

A11012, Invitrogen). The AMPAR that co-localized with PSD95 were defined as synaptic.

Cell-surface and synaptic clusters of the indicated proteins were visualized and quantified by confocal imaging (LSM710, Carl-Zeiss, Germany) using Imaris suite 7.6.4 (Bitplane AG, Zürich, Switzerland), as reported (Planaguma *et al.*, 2015).

Acid-extraction of human antibodies from hippocampal tissue

The contralateral hippocampus was dissected under a magnifying glass (Zeiss stereomicroscope, Stemi 2000), washed with cold PBS, homogenized in PBS containing a cocktail of protease inhibitors (1:50, #P8340, Sigma-Aldrich), and centrifuged at 16000 rpm for 5 minutes. The supernatant was separated and kept as pre-extraction fraction; the pellet was resuspended in 0.1M Na-citrate buffer pH 2.7 for 15 minutes on ice, centrifuged (16000 rpm, 5 minutes), and the supernatant containing the acid-extracted human IgG was separated and neutralized with 1.5 M Tris buffer pH8.8 (extraction fraction). The presence of human LGI1 antibodies in the pre-extraction and extraction fractions was assessed with the indicated HEK293-LGI1 cell-based assay (Lai *et al.*, 2010).

LGI1 immunoprecipitation from brain tissue

Representative mice brain from animals infused for 14 days with LGI1 IgG or control IgG were used for this experiment. Brains were removed, washed with PBS, and homogenized with cold lysis buffer (NaCl 150 mM, EDTA 1 mM, Tris-HCl 100mM, Deoxycholic acid 0.5%, Triton X-100 1%) and a cocktail of protease inhibitors (1:50, #P8340, Sigma). After centrifugation (16000 rpm for 20 minutes), the supernatant was retained and the IgG contained in the supernatant was isolated with protein A/G agarose beads (#20424, Thermo Fisher). The precipitated beads containing IgG were then run in a 4-12% BisTris electrophoresis gel (#NP03222 NuPage, Invitrogene), transferred into a

nitrocellulose membrane (#1704158, Biorad), probed with a commercial antibody against LGI1 (1:200, #ab30868, Abcam), and the reactivity developed with a peroxidase-linked secondary antibody (Anti-rabbit 1:1000, #NA934V, GE HealthCare) using the chemiluminescence method and read with an ImageQuant LAS 4000 Control Software (GE Healthcare).

Electrophysiological Recordings

Preparation of acute hippocampal brain slices was done 14-16 days after pump implantation. Mice were deeply anesthetized, decapitated, and the brain was removed in ice-cold protective cutting artificial cerebrospinal fluid (aCSF1 for patch-clamp recordings (in mM); 95 N-Methyl-D-glutamine, 30 NaHCO₃, 20 HEPES, 25 glucose, 2.5 KCl, 1.25 NaH₂PO₄, 2 thiourea, 5 sodium ascorbate, 3 sodium pyruvate, 10 MgSO₄, 0.5 CaCl₂, 12 N-acetylcysteine, adjusted to pH 7.3 and an osmolarity of 300 to 310 mOsmol, purged with 95% O₂/5% CO₂)(Grunewald *et al.*, 2017) or in high-sucrose extracellular artificial fluid (aCSF2 for field potential recordings (in mM); 206 sucrose, 1.3 KCl, 1 CaCl₂, 10 MgSO₄, 26 NaHCO₃, 11 glucose, 1.25 NaH₂PO₄; purged with 95% CO₂/5% O₂, pH 7.4). The brain was then subdivided into the hemispheres and coronal hippocampal slices (300 μm for patch-clamp recordings and 380 μm for field potential recordings) were prepared on a vibratome (Leica, Wetzlar, Germany; Leica VT1200 S).

Whole-cell patch-clamp recordings of dentate gyrus granule cells

Slices were then incubated in aCSF1 at 34°C for 12 minutes and transferred into another incubation beaker with protective storage aCSF3 (in mM: 125 NaCl, 25 NaHCO₃, 25 glucose, 2.5 KCl, 1.25 NaH₂PO₄, 1 MgCl₂, 2 CaCl₂, 2 thiourea, 5 sodium ascorbate, 3 sodium pyruvate, 12 N-acetylcysteine, adjusted to pH 7.3 and an

osmolarity of 300 to 310 mOsmol, purged with 95% O₂/5% CO₂) at RT for at least 1 hour until recording.

Electrophysiological measurements were performed with a HEKA EPC-10 double patch-clamp amplifier with a sampling rate of 20 kHz. All recordings were filtered at 2.9 and 10 kHz using Bessel filters of the amplifier. For whole-cell patch-clamp recordings single slices were transferred into a recording chamber and continuously submerged with recording aCSF4 (in mM: 125 NaCl, 25 NaHCO₃, 25 Glucose, 2.5 KCl, 1.25 NaH₂PO₄, 1 MgCl₂, 2 CaCl₂, purged with 95% O₂/5% CO₂) at RT (Haselmann *et al.*, 2015). Measurements were done on dentate gyrus granule cells of the hippocampus at holding potentials of -70 mV. Patch pipettes were pulled from thick-walled borosilicate glass and filled with intracellular solution (in mM: 120 K-gluconate, 20 KCl, 10 HEPES, 0.1 EGTA, 4 Mg-ATP, 0.2 Na₂-GTP, 2 MgCl₂, 10 Na-Phosphocreatine, adjusted to pH 7.3 with CsOH and an osmolarity of 280 mOsmol) and had a final resistance of 2.5 – 5 MΩ. Series resistance was compensated (70-80%) and monitored during the recordings. For evaluation of evoked excitatory postsynaptic currents (eEPSCs) the medial perforant path (MPP) was stimulated by a theta glass bipolar electrode filled with aCSF4 and connected to a stimulus isolation unit (Isoflex, A.M.P.I, Jerusalem, Israel). Supramaximal stimulation was determined when increasing stimulation did not result in an increase of eEPSC and ranged from 200 – 400 μA. For isolation of AMPAR-mediated glutamatergic transmission, 50 μM 2-amino-5-phosphonovalerate (AP-5, #0106, Tocris) and 20 μM bicuculline (#0109, Tocris) in aCSF4 perfusion were used to block NMDA receptor and GABA_A receptor, respectively. Paired-pulse facilitation of eEPSC was measured with interstimulus intervals of 50 ms after supramaximal stimulation. Whole cell recordings were analyzed by NeuroMatic plugin of Igor Pro Software 6 or 7 (Wavemetrics, Portland, OR, USA).

Cells with series resistance $>30\text{M}\Omega$ or series resistance changes of $>20\%$ during measurement were discarded. Liquid junction potential of 10 mV was corrected offline for all whole-cell patch clamp recordings.

Field potential recordings and analysis of long-term potentiation (LTP)

380 μm thick coronal hippocampal slices were transferred into an incubation beaker with aCSF5 (in mM: 119 NaCl, 2.5 KCl, 2.5 CaCl₂, 1.25 NaH₂PO₄, 1.5 MgSO₄, 25 NaHCO₃, 11 glucose, purged with 95 % CO₂/5 % O₂ pH 7.4). Slices were kept at 32°C for 60 minutes and subsequently at RT for at least 60 additional minutes. Slices were then transferred into a measurement chamber perfused with aCSF5 at 32°C. A bipolar stimulation electrode (Platinum-Iridium stereotrode, Science Products) was placed in the Schaffer collateral pathway (Planaguma *et al.*, 2016). Recording electrodes were made from borosilicate glass (BF150-86-10, Sutter Instruments). The recording electrode filled with aCSF5 was placed in the dendritic branching of the CA1 region for local field potential measurement (field excitatory postsynaptic potential, fEPSP). Signals were amplified and stored using AxoClamp 2B amplifier (Molecular Devices). A stimulus isolation unit A385 (World Precision Instruments) was used to elicit stimulation currents. Before baseline recordings, input-output curves were determined for each slice with stimulation currents ranging from 25 to 700 μA at 0.03 Hz. The stimulation current was adjusted for each recording to evoke fEPSP which was at half of its maximal evoked amplitude. After baseline recordings for 30 minutes with 0.03 Hz, LTP was induced by theta-burst stimulation (TBS; 10 theta bursts of 4 pulses of 100 Hz with an interstimulus interval of 200ms, repeated 7 times with 0.03 Hz). After LTP induction, fEPSPs were recorded for additional 60 minutes with 0.03 Hz. Recordings with unstable baseline measurements (variations higher than 20% in baseline fEPSPs) were discarded.

The recordings were done and analyzed using Axon pCLAMP Software (Molecular Devices, version 10.6). Slopes of all recordings were measured within 1-1.5ms of the linear part of the rising fEPSP before it reaches the peak and starting after the fiber volley. For determination of TBS induced LTP, mean slope values of fEPSPs after TBS until end of the recording were compared between the experimental groups.

Golgi–Cox staining, Sholl analysis, and synaptic spine quantification

Morphological dendrite and spine analysis were performed in granule cells of the dentate gyrus and pyramidal neurons of the CA1 region from the contralateral brain hemisphere of mice used in neurophysiological recordings. Directly after removal, Golgi silver impregnation was conducted with the FD Rapid GolgiStain™ Kit (FD NeuroTechnologies, Inc., Columbia, USA) according to manufacturer's instructions. Dendritic complexity was assessed with the Sholl ring method, including analysis of total dendritic length, number of branch ends, and number of dendrites per branch order. Density of dendritic spines was analyzed in tertiary branches of CA1 pyramidal neurons. Spines were subclassified (thin, mushroom, stubby, filopodia or branched) according to previous reports (McKinney, 2010). Detailed information on Golgi-Cox staining Sholl and dendritic spine analysis is provided as supplemental information.

Statistical analysis

Confocal cluster densities of GluA1, Kv1.1, PSD95, or Bassoon, and behavioral tests with multiple time points (NOR, LOC, RI, ANH) were analyzed using two-way analysis of variance (ANOVA). All behavioral paradigms with single time points (BW, EPM) were analyzed with independent sample *t*-tests; *Post-hoc* analyses for all experiments used Bonferroni correction for multiple testing.

Electrophysiological measurements of In-Out curves were analyzed with two-way ANOVA followed by Holm-Sidak *post-hoc* test. Group comparisons of independent

recordings were made using two-tailed *t*-tests. The alpha-level used to determine significance was $P < 0.05$. All tests were done using GraphPad Prism (Version 7) or SigmaPlot (Version 13.0).

Results

Patients' LGI1 IgG preferentially prevents the binding of LGI1 to ADAM23 as compared to ADAM22

To determine whether patients' LGI1 IgG recognized soluble LGI1 and prevented its binding to ADAM22 or ADAM23, HEK293 cells expressing each of these proteins were incubated with LGI1-enriched or control media. The presence of LGI1 in the media was first confirmed with immunoblot (Fig. 1A, lane 1), and the binding of soluble LGI1 to ADAM22 or ADAM23 was demonstrated in HEK293 cells expressing each of these proteins incubated with soluble LGI1 followed by patients' LGI1 IgG (Fig. 1B) or a commercial LGI1 antibody (data not shown). Pre-incubation of soluble LGI1 with excess patients' LGI1 IgG, but not control IgG, abrogated the binding of LGI1 to ADAM23 (25 of 25 cases [100%]) more consistently than to ADAM22 (15/25 [60%]) (Fig. 1B, and Supplementary Fig. 4).

The target epitopes of LGI1 IgG are more frequently located in the LRR than in the EPTP domains

All patients' samples strongly reacted with clones 1 and 2 which contained the LRR domain; 12/25 samples mildly reacted with clone 3 which contained the EPTP domain, and none with clone 4 which contained the signal peptide (SP) domain of LGI1 sequence followed by the immunoglobulin domain 3 of IgLON5 (Fig. 2). None of 20 control sera showed reactivity with any of the four clones (data not shown). These

findings indicate that patients' IgG is directed against epitopes located in the LRR and flanking regions, and less frequently in the EPTP domains.

Passive transfer of patients' LGI1 IgG causes memory deficits in mice

Compared with animals infused with control IgG, those infused with patients' LGI1 IgG showed a progressive decrease of the object recognition index, indicative of a memory deficit (Bura *et al* 2007; Tagliabata *et al.* 2009; Puighermanal *et al.* 2009). The memory deficit became significant on day 3 and persisted until day 25 (11 days after the infusion of IgG had stopped). At the last time point (day 47), the object recognition index had normalized and was similar to that of animals treated with control IgG (Fig. 3). For all time-points, the total time spent exploring both objects (internal control) was similar in animals infused with control or patients' LGI1 IgG (data not shown).

No significant differences were noted in tests of anxiety (black and white test, elevated plus maze test), aggression (resident-intruder test) and locomotor activity (Supplementary Fig. 5).

Passive transfer of patients' LGI1 IgG causes a decrease of Kv1.1 potassium channels and AMPAR

The presence of patients' IgG bound to LGI1 in mice brain tissue was demonstrated with two techniques: immunoprecipitation of LGI1 using protein A/G agarose beads (Supplementary Fig. 6A), and acid-extraction of human antibodies from hippocampus that reacted with LGI1 expressed in HEK293 cells (Supplementary Fig. 6B). To determine whether patients' LGI1 IgG had effects on Kv1.1 and AMPAR clusters we focused on the hippocampus (Fig. 4A). This region was selected because anti-LGI1 encephalitis predominantly affects the hippocampus which has close proximity to the lateral ventricles where the IgG fractions were infused. Compared with animals infused

with control IgG those infused with patients' LGI1 IgG had on days 13, 18, and 26 a significant decrease of the density of cell surface and synaptic Kv1.1 clusters (Fig. 4B-D) followed by a gradual recovery after day 26 (pooled analysis of the subregions in CA1, CA3, and dentate gyrus [DG] indicated in Fig. 4A). In contrast, patients' LGI1 IgG did not affect the density of the presynaptic marker Bassoon (Fig. 4E).

In parallel we investigated whether the levels of cell surface and synaptic AMPAR (GluA1) clusters were affected in the same hippocampal subregions used for the Kv1.1 studies. The findings showed that mice infused with patients' LGI1 IgG had on day 18 a significant decrease of cell surface and synaptic AMPAR compared with mice infused with control IgG (Fig. 5A-C). The total cell surface AMPAR appeared to decrease and recover faster than the synaptic AMPAR. No significant differences were noted in the levels of PSD95 clusters comparing mice infused with patients' or control IgG (Fig. 5D).

Patients' LGI1 IgG increases excitatory synaptic transmission

To investigate the pathophysiological role of patients' LGI1 IgG in synaptic transmission, we examined the glutamatergic transmission by whole-cell patch-clamp recordings in acute brain slices of mice after the indicated 14-day cerebroventricular infusion of patients' LGI1 IgG or control IgG. LGI1 is predominantly expressed in the hippocampal formation where it colocalizes with Kv1.1 in the middle molecular layer of the dentate gyrus (Schulte et al., 2006). We therefore recorded electrically evoked (e)EPSCs in the DG granule cells (GC) of the hippocampus. We did not observe any differences in membrane properties, e.g. series resistance, resting membrane potential, or cell capacitance in both groups (not shown). Incremental stimulation of axons in the MPP from the entorhinal cortex led to increased peak amplitudes of eEPSCs in slices of mice infused with patients' LGI1 IgG as compared to control IgG, whereas eEPSC

kinetics remained unchanged (Fig. 6A-D). This increase of excitatory synaptic transmission could either result from altered AMPAR formation on the postsynaptic density or from an increased presynaptic release of glutamate. To determine whether short-term plasticity was altered in patients' LGI1 IgG treated mice, we performed paired-pulse recordings in the MPP-GC pathway. Mice infused with patients' LGI1 IgG showed reduced paired-pulse facilitation as compared to control IgG infused mice (Fig. 6E, F). Together, these data suggest that mice with chronic infusion of LGI1-IgG have alterations in presynaptic function characterized by increased neurotransmitter release.

Patients' LGI1 IgG alters synaptic plasticity

Next, we examined synaptic plasticity in the hippocampus by recording field potentials (fEPSPs) in the CA1 pathway after stimulation of the Schaffer collateral in hippocampal slices of mice infused with patients' LGI1 IgG and control IgG. The findings showed impaired LTP in slices of mice infused with patients' LGI1 IgG as shown by reduced fEPSP slope values throughout the recording period up to 60 minutes after theta-burst stimulation (Fig. 7A-C).

Dendritic pruning is unaffected by patient's LGI1 IgG

In a previous report using a transgenic mouse model with a truncated form of LGI1, abnormal dendritic pruning and increased spine density was associated with increased excitatory synaptic transmission (Zhou *et al.*, 2009). Here, we investigated dendritic pruning and spine morphology in mice infused with patients' LGI1 IgG and control IgG. Sholl analysis with concentric shells and neuroLucida reconstructions of dentate gyrus granule cells showed unchanged dendritic arborization and dendrite length after infusion of patients' LGI1 IgG (Fig. 8A-E). Analysis of synaptic spines in CA1 apical dendrites revealed identical spine density and unchanged spine morphology in both

experimental groups (Fig. 8F-H). Thus, changes in excitatory transmission and synaptic plasticity were not mediated by defective synaptic maturation.

Discussion

We show that patients' LGI1 antibodies alter the levels of Kv1.1 potassium channels and AMPAR causing a severe impairment of memory, plasticity, and neuronal transmission in a passive transfer mouse model of patient-derived antibodies. Previous clinical reports demonstrated that despite the severity of anterograde memory deficits most patients improved with immunotherapy (Arino *et al.*, 2016; van Sonderen *et al.*, 2016; Gadoth *et al.*, 2017), and experimental studies provided evidence that patients' antibodies caused a decrease of AMPAR in cultured neurons (Ohkawa *et al.*, 2013). Together, these findings suggested the pathogenicity of LGI1 autoantibodies but the effects on an animal model were pending to investigate. Here we used a model of cerebroventricular transfer of patients' antibodies to mice because the proximity of the lateral ventricles to the hippocampus facilitates exploring the alterations on memory and plasticity. It is likely that defective plasticity in the hippocampus of mice treated with patients' LGI1 IgG may underlie the observed memory deficit and that similar mechanisms apply to the short-term memory deficit of the patients.

LGI1 is a neuronal secreted protein containing an N-terminal LRR-domain and a C-terminal EPTP domain (Fukata *et al.*, 2006; Sirerol-Piquer *et al.*, 2006). Previous studies have shown that LGI1 interacts with the transmembrane metalloproteases ADAM23 and ADAM22 (Fukata *et al.*, 2006) that serve as receptors associated with presynaptic and axonal complexes containing Kv1.1 channels and postsynaptic AMPAR, respectively. Using IgG fractions of 25 patients with anti-LGI1 encephalitis we found that all patients' IgG strongly reacted with the LRR domain of LGI1 and only

12 of 25 samples showed reactivity with the EPTP domain, thus suggesting that the LGI1 LRR domain contains dominant epitopes of LGI1 antibodies. Since the EPTP domain is essential for binding of LGI1 to ADAM22 (Fukata *et al.*, 2006), we hypothesize that pathogenic antibodies more frequently affect the interaction of LGI1 with presynaptic ADAM23. Nevertheless, we and others have observed that 60% of the patients harbor antibodies that also inhibit the interaction of LGI1 with ADAM22 (Ohkawa *et al.*, 2013).

Mice with mutated or deficient LGI1 show a severe epileptic phenotype with premature death (Zhou *et al.*, 2009; Chabrol *et al.*, 2010; Fukata *et al.*, 2010; Yu *et al.*, 2010). In these models, two potential underlying mechanisms have been reported including, loss of synaptic AMPAR leading to reduction of AMPAR-mediated glutamatergic transmission (Fukata *et al.*, 2010; Lovero *et al.*, 2015), and defective function of axonal and presynaptic Kv1.1 resulting in enhanced excitatory transmission (Yu *et al.*, 2010; Boillot *et al.*, 2016; Seagar *et al.*, 2017). Here, after continuous intraventricular infusion of patients' LGI1 IgG, we found significant reduction of AMPAR and Kv1.1 clusters in the hippocampus, corroborating previous observations in LGI1 knockout mouse models (Fukata *et al.*, 2010; Lovero *et al.*, 2015; Seagar *et al.*, 2017). Moreover, in acute sections of hippocampus of mice infused with LGI1 IgG, but not in those infused with control IgG, we found distinct functional evidence for hyperexcitability and enlarged glutamatergic transmission in the MPP-GC pathway compatible with increased presynaptic release.

These findings are in agreement with a previous report showing increased firing frequency and enlarged evoked glutamatergic transmission in CA3 neurons after preincubation of brain slices with IgG from patients with limbic encephalitis and antibodies against proteins of the voltage-gated K⁺ channel complex (Lalic *et al.*, 2011)

which presumably were directed against LGI1 (Irani *et al.*, 2010; Lai *et al.*, 2010). It is known that presynaptic Kv1.1 potassium channel inactivation enhances release probability by increased and prolonged depolarization, Ca²⁺ influx, and subsequent potentiation of excitatory transmission (Geiger and Jonas, 2000). Indeed, recent studies in slice cultures or acute slices of LGI1 knockout mice showed evidence for enhanced neuronal excitability, increased release of presynaptic glutamate, and enlarged excitatory synaptic drive (Boillot *et al.*, 2016; Seagar *et al.*, 2017). In an oocyte expression system LGI1 has been shown to prevent the N-type inactivation of Kv1.1 channels. Mutated LGI1 reversed this effect, thus leading to rapid inactivation possibly contributing to an increase of action potential broadening and glutamate release (Schulte *et al.*, 2006). Together, in the passive-transfer model of LGI1 IgG we identified several underlying pathophysiological mechanisms that are in good agreement with previous observations in LGI1 deficient model systems. Our findings point toward interference with LGI1 associated pathways that affect LGI1 signaling via post- and presynaptic mechanisms.

In our model of ventricular transfer of antibodies we did not observe seizures, but electrographic recordings were not performed. The mouse strain of our model was selected to determine the LGI1 antibody effects on memory and behavior, but there are mouse strains more appropriate to investigate potential increased seizure susceptibility (Ferraro *et al.*, 2002). At the synaptic level the findings in the LGI1 deficient models as well as in our immune-mediated model make difficult to explain how reduced AMPAR function associates with epileptic seizures in patients with ADTLE or anti-LGI1 encephalitis. Homeostatic downregulation of postsynaptic AMPAR in response to an ongoing presynaptic hyperexcitability has been proposed but it remains speculative and is not yet supported by experimental evidence (Seagar *et al.*, 2017). This hypothesis

however, is in line with the observation that patients' LGI1 IgG caused a reduction of Kv1.1 expression (from day 5 after onset of antibody infusion) that preceded the reduction of AMPAR clusters (from day 13) in the hippocampus of infused mice.

In ADAM23 deficient mice (Owuor *et al.*, 2009) as well as in a transgenic model with truncated LGI1 (Zhou *et al.*, 2009), abnormal maturation of hippocampal synapses was observed. These changes consisted of decreased dendritic arborization in ADAM23 deficient mice but defective synaptic pruning and increased spine density in LGI mutant mice. Different from these observations in germline knockout strains, application of LGI1 antibodies in adult mice did not induce changes in spine density or dendritic arborization. Furthermore, we did not detect any differences in neuronal membrane properties such as cell capacitance or input resistance. This is likely explained by the acute disturbance of LGI1 function by specific autoantibodies in the mature brain in contrast to chronic changes and adaptations in neuronal network following genetic mutation. Corroborating these findings, a recent report revealed unchanged synaptic density and dendritic arborization in very young LGI1 knockout mice before onset of epileptic activity (Boillot *et al.*, 2016).

Overall, intraventricular application of patients' LGI1 IgG caused severe impairment of memory and plasticity along with neuronal hyperexcitability and alterations of the levels of Kv1.1 and AMPAR similar to those reported in models of genetic alteration of LGI1, providing evidence of antibody pathogenicity. Since LGI1 is a neuronal secreted linker protein, the antibody-mediated disturbance of this synaptic complex signaling pathway leads to fundamentally different pathophysiological mechanisms as compared with those associated with other antibody-mediated diseases, such as anti-NMDAR or anti-AMPA encephalitis, where the antibodies alter the cell surface dynamics of the targets and cause their internalization (Mikasova *et al.*, 2012;

Peng *et al.*, 2015). Interestingly, among the few antibody-mediated encephalitides that more frequently manifest as limbic encephalitis (Dalmau and Graus, 2018), two of them associate with antibodies that cause an important reduction of AMPAR, either by direct binding of the antibodies to the receptor (anti-AMPAR encephalitis) or by binding to synaptic partners, as shown here for LGI1. A task for the future is to clarify how antibody-binding to the protein-protein interaction domains of LGI1 (LRR, EPTP) affects LGI1 conformation and reactivity to its binding partners, and whether different approaches of antibody transfer (parenchymal, cortical) in different strains of mice lead to epileptic activity and seizures.

Acknowledgements

We thank Claudia Sommer (Jena), Esther Aguilar (Barcelona), and Mercè Alba (Barcelona) for providing expert technical assistance in animal experiments.

Funding

This work was supported by the Deutsche Forschungsgemeinschaft (CRC-TR 166 [TP B2 to C.G. GE2519_3-1 to C.G.], by the IZKF and CSCC Jena to C.G.), Instituto Carlos III/FEDER (FIS PI15/00377, FG; FIS PI14/00203, JD, FIS PI14/00141, XG; FIS PI17/00296, XG; RETIC RD16/0008/0014, XG), Fondation de l'Université de Lausanne et Centre Hospitalier Universitaire Vaudois (UNIL/CHUV), Lausanne, Switzerland (MS), NIH (RO1NS077851, JD), Ministerio de Economía, Industria y Competitividad, Spain (BFU2017-83317-P, DS), AGAUR (SGR93, JD; SGR737, XG), CERCA Programme / Generalitat de Catalunya,), (PERIS) (SLT002/16/00346, JP), and Fundació CELLEX (JD). The authors declare no conflict of interest.

Legends to figures

Figure 1: Patient's LGI1 IgG blocks the binding of soluble LGI1 to ADAM22 and ADAM23

The media of HEK293 cells transfected with LGI1 contains secreted LGI1 (A, lane 1) whereas the media of non-transfected cells does not contain LGI1 (A, lane 2). HEK293 cells expressing ADAM22 or ADAM23 bind soluble LGI1 present in the media of HEK293 cells expressing LGI1 (B, first row) but not present in control media (B, second row). When the media with soluble LGI1 is pre-incubated with a representative patient's LGI1 IgG the binding of LGI1 to ADAM22 or ADAM23 is abrogated (B, third row); in contrast, no blocking of the binding is observed when the media is pre-incubated with control IgG (B, fourth row). Scale bar = 20 μm .

Figure 2: Reactivity of a patient's serum with deletion constructs of LGI1

Serum from a representative patient with anti-LGI1 encephalitis shows predominant reactivity with the full-length sequence of LGI1 (clone 1), and the construct that contains the LRR domain (clone 2); milder reactivity is shown with the construct that contains the EPTP domain (clone 3). The construct generated by clone 4 contains the signal peptide (SP) but does not include any LGI1 sequence. Scale bar = 20 μm .

Figure 3: Cerebroventricular infusion of patients' LGI1 IgG causes decrease of memory

Novel object recognition index in mice treated with patients' IgG (red, n = 16) or control IgG (grey, n = 14). A high index indicates better memory. Data is presented as mean \pm SEM. * P <0.05; ** P <0.01.

Figure 4: Patients' LGI1 IgG causes a decrease of total cell surface and synaptic Kv1.1 clusters in the hippocampus

Sagittal section of hippocampus of a representative mouse infused with patients' LGI1 IgG demonstrating the immunostaining of Kv1.1, Bassoon, and the merging reactivities (A). Squares in "Analysis" indicate the analyzed subregions in CA1, CA3, and DG for each animal. Scale bar = 200 μ m. 3D projection and analysis of the density of total cell surface clusters of Kv1.1 and Bassoon, and synaptic clusters of Kv1.1 (defined as Kv1.1 clusters that co-localized with Bassoon) in one of the indicated CA3 subregions (A "Analysis"). Merged images (B, left upper and lower squares; Kv1.1 green, and Bassoon red) were post-processed and used to calculate the density of the indicated clusters (density = spots/ μ m³). Scale bar = 2 μ m. Quantification of the density of total cell surface (C) and synaptic (D) Kv1.1 clusters, and Bassoon clusters (E) in a pooled analysis of hippocampal subregions (CA1, CA3, DG) in animals treated with patients' LGI1 IgG (red) or control IgG (black) on the indicated days. Mean density of clusters in control IgG treated animals was defined as 100%. Data are presented as mean \pm SEM. For each time point five animals infused with patients' LGI1 IgG and five with control IgG were examined. Significance of treatment effect was assessed by two-way ANOVA with an alpha-error of 0.05 (asterisks) and *post-hoc* testing with Sidak-Holm adjustment. ** P < 0.01; *** P <0.001; **** P <0.0001.

Figure 5: Patients' LG1 IgG causes a decrease of total cell surface and synaptic AMPAR clusters in the hippocampus

3D projection and analysis of the density of total cell surface clusters of GluA1 AMPAR and PSD95, and synaptic clusters of AMPAR (defined as AMPAR clusters that co-localized with PSD95) in one of the CA3 subregions indicated in Fig. 4A, "Analysis". Merged images (A, left upper and lower squares; GluA1 green, and PSD95 red) were post-processed and used to calculate the density of the indicated clusters (density = spots/ μm^3). Scale bar = 2 μm . Quantification of the density of total cell surface (B) and synaptic (C) GluA1 AMPAR clusters, and PSD95 clusters (D) in a pooled analysis of hippocampal subregions (CA1, CA3, DG) in animals treated with patients' LG1 IgG (red) or control IgG (black) on the indicated days. Mean density of clusters in control IgG treated animals was defined as 100%. Data are presented as mean \pm SEM. For each time point five animals infused with patients' IgG and five with control IgG were examined. Significance of treatment effect was assessed by two-way ANOVA with an alpha-error of 0.05 (asterisks) and *post-hoc* testing with Sidak-Holm adjustment. * $P < 0.05$; ** $P < 0.01$; *** $P < 0.001$; **** $P < 0.0001$.

Figure 6: Patients' LG1 IgG increases excitatory synaptic transmission

Evoked excitatory postsynaptic currents (eEPSCs) in dentate gyrus granule cells upon incremental stimulation of medial perforant path (MPP) afferent fibers are increased in acute brain slices of mice that received patient's LG1 IgG (A and B). Example traces of an individual recording are shown in (A). In/out characteristics of granule cell neurons of control IgG and patients' LG1 IgG treated mice (B; $n_{\text{control IgG}} = 13$; $n_{\text{LG1 IgG}} = 15$; data are presented as mean \pm SEM; two-way ANOVA and Holm-Sidak *post-hoc* test. *** $P < 0.001$). Peak amplitude of eEPSCs (example traces in C) is increased after

infusion of antibodies against LGI1, whereas rise and decay time is unchanged ($n_{\text{control IgG}} = 13$; $n_{\text{LGI1 IgG}} = 15$; data are presented as mean \pm SEM; unpaired *t*-test. $**P < 0.01$) (C and D). Paired pulse facilitation with an interstimulus interval of 50 ms is reduced in granule cell neurons from mice after infusion of patients' LGI1 IgG indicating increased release probability. Example traces in E; dashed lines indicate peak amplitude of the first pulse ($n_{\text{control IgG}} = 11$; $n_{\text{LGI1 IgG}} = 13$; data are presented as mean \pm SEM; unpaired *t*-test. $*P < 0.05$) (E and F).

Figure 7: Patients' LGI1 IgG alters synaptic plasticity

Example traces of individual field excitatory postsynaptic potential (fEPSP) recordings in the CA1 region before and after theta burst stimulation (TBS) of Schaffer collateral afferents show reduced fEPSP potentiation in brain slices of mice that received patient's LGI1 IgG (A). Time course and quantitative analysis of long-term potentiation (LTP) after TBS (arrow), demonstrates persistent reduction of fEPSP slope values in slices of mice after infusion of patient's LGI1 IgG indicating disturbed synaptic plasticity. Quantification of fEPSP slope change is decreased in LGI1 IgG infused mice (B and C, $n_{\text{control IgG}} = 10$; $n_{\text{LGI1 IgG}} = 13$; data are presented as mean \pm SEM; unpaired *t*-test. $*P < 0.05$).

Figure 8: Dendritic pruning is unaffected by patients' LGI1 IgG

Dendritic arborization of a dentate gyrus granule cell; example neuron is shown after Golgi silver impregnation (left) and in NeuroLucida reconstruction for Sholl analysis (right) (A, scale bar = 50 μm). Sholl analysis revealed unchanged dendritic arborization in control IgG and patients' LGI1 IgG infused mice as shown by the length of hippocampal granule cell dendrites (B and C) and by number and intersection of

dendritic branches (D and E). Synaptic spines of tertiary dendrites of CA1 pyramidal neurons (F, scale bar = 10 μ m). Quantification of spine density (G) and of spine morphology (H) is unchanged in control IgG and patients' LGI1 IgG infused mice (all data are presented as mean \pm SEM).

For Peer Review

References

- Arino H, Armangue T, Petit-Pedrol M, Sabater L, Martinez-Hernandez E, Hara M, *et al.* Anti-LGI1-associated cognitive impairment: Presentation and long-term outcome. *Neurology* 2016; 87(8): 759-65.
- Boillot M, Lee CY, Allene C, Leguern E, Baulac S, Rouach N. LGI1 acts presynaptically to regulate excitatory synaptic transmission during early postnatal development. *Sci Rep* 2016; 6: 21769.
- Chabrol E, Navarro V, Provenzano G, Cohen I, Dinocourt C, Rivaud-Pechoux S, *et al.* Electroclinical characterization of epileptic seizures in leucine-rich, glioma-inactivated 1-deficient mice. *Brain* 2010; 133(9): 2749-62.
- Dalmau J, Geis C, Graus F. Autoantibodies to Synaptic Receptors and Neuronal Cell Surface Proteins in Autoimmune Diseases of the Central Nervous System. *Physiol Rev* 2017; 97(2): 839-87.
- Dalmau J, Graus F. Antibody-Mediated Encephalitis. *N Engl J Med* 2018; 378(9): 840-51.
- Ferraro TN, Golden GT, Smith GG, DeMuth D, Buono RJ, Berrettini WH. Mouse strain variation in maximal electroshock seizure threshold. *Brain Res* 2002; 936(1-2): 82-6.
- Fukata Y, Adesnik H, Iwanaga T, Brecht DS, Nicoll RA, Fukata M. Epilepsy-related ligand/receptor complex LGI1 and ADAM22 regulate synaptic transmission. *Science* 2006; 313(5794): 1792-5.
- Fukata Y, Lovero KL, Iwanaga T, Watanabe A, Yokoi N, Tabuchi K, *et al.* Disruption of LGI1-linked synaptic complex causes abnormal synaptic transmission and epilepsy. *Proc Natl Acad Sci USA* 2010; 107(8): 3799-804.

- Gadoth A, Pittock SJ, Dubey D, McKeon A, Britton JW, Schmeling JE, *et al.* Expanded phenotypes and outcomes among 256 LGI1/CASPR2-IgG-positive patients. *Ann Neurol* 2017; 82(1): 79-92.
- Geiger JR, Jonas P. Dynamic control of presynaptic Ca(2+) inflow by fast-inactivating K(+) channels in hippocampal mossy fiber boutons. *Neuron* 2000; 28(3): 927-39.
- Gresa-Arribas N, Planaguma J, Petit-Pedrol M, Kawachi I, Katada S, Glaser CA, *et al.* Human neurexin-3alpha antibodies associate with encephalitis and alter synapse development. *Neurology* 2016; 86(24): 2235-42.
- Grunewald B, Lange MD, Werner C, O'Leary A, Weishaupt A, Popp S, *et al.* Defective synaptic transmission causes disease signs in a mouse model of juvenile neuronal ceroid lipofuscinosis. *Elife* 2017; 6.
- Haselmann H, Ropke L, Werner C, Kunze A, Geis C. Interactions of Human Autoantibodies with Hippocampal GABAergic Synaptic Transmission - Analyzing Antibody-Induced Effects ex vivo. *Front Neurol* 2015; 6: 136.
- Irani SR, Alexander S, Waters P, Kleopa KA, Pettingill P, Zuliani L, *et al.* Antibodies to Kv1 potassium channel-complex proteins leucine-rich, glioma inactivated 1 protein and contactin-associated protein-2 in limbic encephalitis, Morvan's syndrome and acquired neuromyotonia. *Brain* 2010; 133(9): 2734-48.
- Irani SR, Stagg CJ, Schott JM, Rosenthal CR, Schneider SA, Pettingill P, *et al.* Faciobrachial dystonic seizures: the influence of immunotherapy on seizure control and prevention of cognitive impairment in a broadening phenotype. *Brain* 2013; 136(Pt 10): 3151-62.
- Kim TJ, Lee ST, Moon J, Sunwoo JS, Byun JI, Lim JA, *et al.* Anti-LGI1 encephalitis is associated with unique HLA subtypes. *Ann Neurol* 2017; 81(2): 183-92.

- Lai M, Huijbers MG, Lancaster E, Graus F, Bataller L, Balice-Gordon R, *et al.*
Investigation of LGI1 as the antigen in limbic encephalitis previously attributed to potassium channels: a case series. *Lancet Neurol* 2010; 9(8): 776-85.
- Lalic T, Pettingill P, Vincent A, Capogna M. Human limbic encephalitis serum enhances hippocampal mossy fiber-CA3 pyramidal cell synaptic transmission. *Epilepsia* 2011; 52(1): 121-31.
- Lovero KL, Fukata Y, Granger AJ, Fukata M, Nicoll RA. The LGI1-ADAM22 protein complex directs synapse maturation through regulation of PSD-95 function. *Proc Natl Acad Sci U S A* 2015; 112(30): E4129-37.
- McKinney RA. Excitatory amino acid involvement in dendritic spine formation, maintenance and remodelling. *J Physiol* 2010; 588(Pt 1): 107-16.
- Mikasova L, P. DR, Bouchet D, Georges F, Rogemond V, Didelot A, *et al.* Disrupted surface cross-talk between NMDA and Ephrin-B2 receptors in anti-NMDA encephalitis. *Brain* 2012; 135(Pt 5): 1606-21.
- Morante-Redolat JM, Gorostidi-Pagola A, Piquer-Sirerol S, Saenz A, Poza JJ, Galan J, *et al.* Mutations in the LGI1/Epitempin gene on 10q24 cause autosomal dominant lateral temporal epilepsy. *Hum Mol Genet* 2002; 11(9): 1119-28.
- Ohkawa T, Fukata Y, Yamasaki M, Miyazaki T, Yokoi N, Takashima H, *et al.*
Autoantibodies to epilepsy-related LGI1 in limbic encephalitis neutralize LGI1-ADAM22 interaction and reduce synaptic AMPA receptors. *J Neurosci* 2013; 33(46): 18161-74.
- Owuor K, Harel NY, Englot DJ, Hisama F, Blumenfeld H, Strittmatter SM. LGI1-associated epilepsy through altered ADAM23-dependent neuronal morphology. *Mol Cell Neurosci* 2009; 42(4): 448-57.

- Peng X, Hughes EG, Moscato EH, Parsons TD, Dalmau J, Balice-Gordon RJ. Cellular plasticity induced by anti-alpha-amino-3-hydroxy-5-methyl-4-isoxazolepropionic acid (AMPA) receptor encephalitis antibodies. *Ann Neurol* 2015; 77(3): 381-98.
- Planaguma J, Haselmann H, Mannara F, Petit-Pedrol M, Grunewald B, Aguilar E, *et al.* Ephrin-B2 prevents N-methyl-D-aspartate receptor antibody effects on memory and neuroplasticity. *Ann Neurol* 2016; 80(3): 388-400.
- Planaguma J, Leyboldt F, Mannara F, Gutierrez-Cuesta J, Martin-Garcia E, Aguilar E, *et al.* Human N-methyl D-aspartate receptor antibodies alter memory and behaviour in mice. *Brain* 2015; 138(Pt 1): 94-109.
- Poza JJ, Saenz A, Martinez-Gil A, Cheron N, Cobo AM, Urtasun M, *et al.* Autosomal dominant lateral temporal epilepsy: clinical and genetic study of a large Basque pedigree linked to chromosome 10q. *Ann Neurol* 1999; 45(2): 182-8.
- Sabater L, Planaguma J, Dalmau J, Graus F. Cellular investigations with human antibodies associated with the anti-IgLON5 syndrome. *J Neuroinflammation* 2016; 13(1): 226.
- Schulte U, Thumfart JO, Klocker N, Sailer CA, Bildl W, Biniossek M, *et al.* The epilepsy-linked Lgi1 protein assembles into presynaptic Kv1 channels and inhibits inactivation by Kvbeta1. *Neuron* 2006; 49(5): 697-706.
- Seagar M, Russier M, Caillard O, Maulet Y, Fronzaroli-Molinieres L, De San Feliciano M, *et al.* LGI1 tunes intrinsic excitability by regulating the density of axonal Kv1 channels. *Proc Natl Acad Sci U S A* 2017; 114(29): 7719-24.
- Sirerol-Piquer MS, Ayerdi-Izquierdo A, Morante-Redolat JM, Herranz-Perez V, Favell K, Barker PA, *et al.* The epilepsy gene LGI1 encodes a secreted glycoprotein that binds to the cell surface. *Hum Mol Genet* 2006; 15(23): 3436-45.

Staub E, Perez-Tur J, Siebert R, Nobile C, Moschonas NK, Deloukas P, *et al.* The novel EPTP repeat defines a superfamily of proteins implicated in epileptic disorders. *Trends Biochem Sci* 2002; 27(9): 441-4.

van Sonderen A, Petit-Pedrol M, Dalmau J, Titulaer MJ. The value of LGI1, Caspr2 and voltage-gated potassium channel antibodies in encephalitis. *Nat Rev Neurol* 2017a; 13(5): 290-301.

van Sonderen A, Roelen DL, Stoop JA, Verdijk RM, Haasnoot GW, Thijs RD, *et al.* Anti-LGI1 encephalitis is strongly associated with HLA-DR7 and HLA-DRB4. *Ann Neurol* 2017b; 81(2): 193-8.

van Sonderen A, Thijs RD, Coenders EC, Jiskoot LC, Sanchez E, de Bruijn MA, *et al.* Anti-LGI1 encephalitis: Clinical syndrome and long-term follow-up. *Neurology* 2016; 87(14): 1449-56.

Yu YE, Wen L, Silva J, Li Z, Head K, Sossey-Alaoui K, *et al.* Lgi1 null mutant mice exhibit myoclonic seizures and CA1 neuronal hyperexcitability. *Hum Mol Genet* 2010; 19(9): 1702-11.

Zhou YD, Lee S, Jin Z, Wright M, Smith SE, Anderson MP. Arrested maturation of excitatory synapses in autosomal dominant lateral temporal lobe epilepsy. *Nat Med* 2009; 15(10): 1208-14.

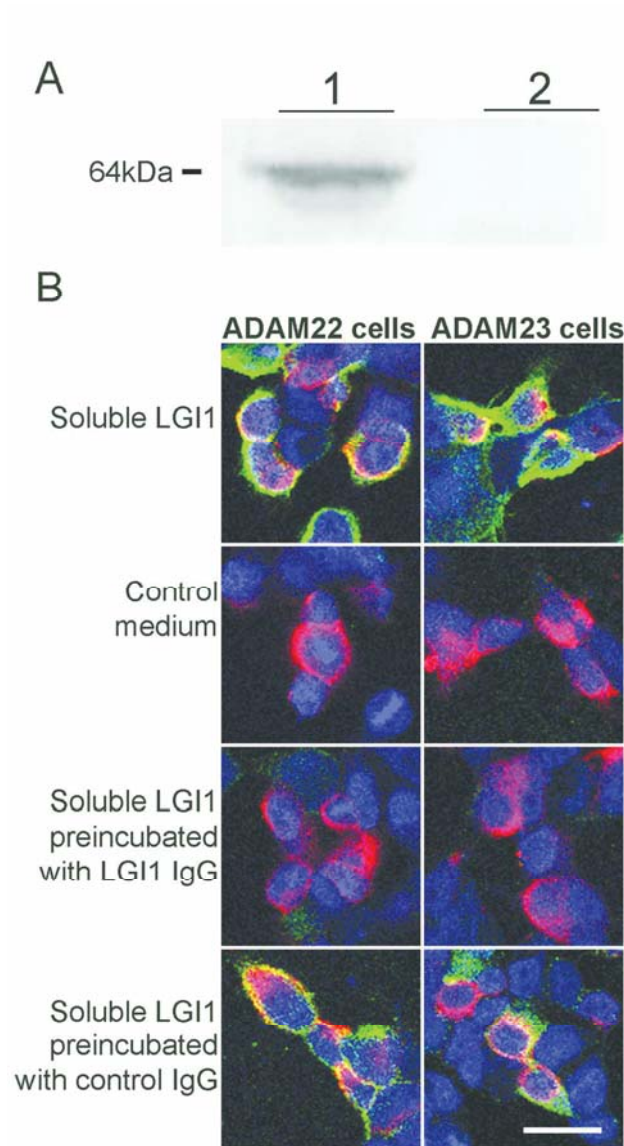


Figure 1: Patient's LGI1 IgG blocks the binding of soluble LGI1 to ADAM22 and ADAM23 The media of HEK293 cells transfected with LGI1 contains secreted LGI1 (A, lane 1) whereas the media of non-transfected cells does not contain LGI1 (A, lane 2). HEK293 cells expressing ADAM22 or ADAM23 bind soluble LGI1 present in the media of HEK293 cells expressing LGI1 (B, first row) but not present in control media (B, second row). When the media with soluble LGI1 is pre-incubated with a representative patient's LGI1 IgG the binding of LGI1 to ADAM22 or ADAM23 is abrogated (B, third row); in contrast, no blocking of the binding is observed when the media is pre-incubated with control IgG (B, fourth row). Scale bar = 20 μ m.

90x169mm (300 x 300 DPI)

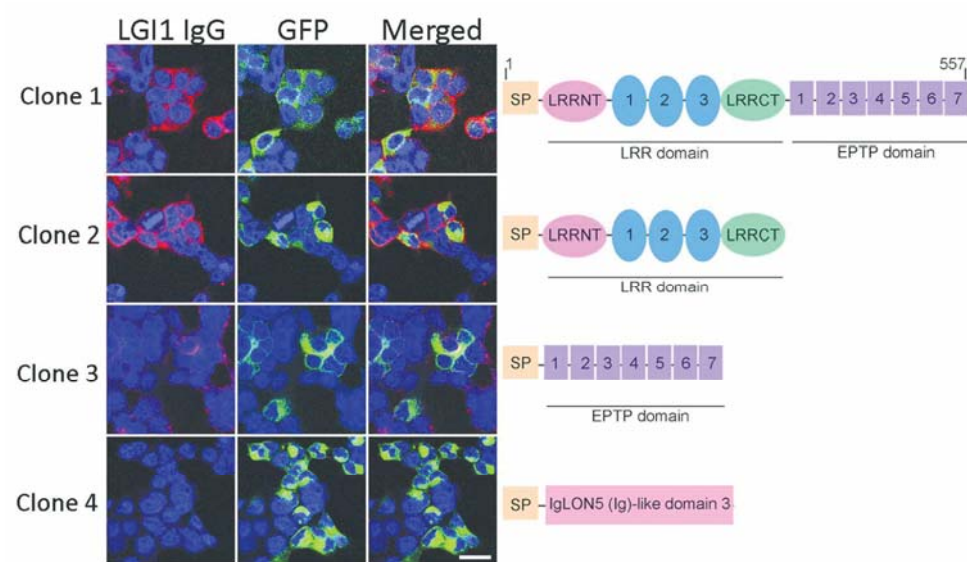


Figure 2: Reactivity of a patient's serum with deletion constructs of LGI1 Serum from a representative patient with anti-LGI1 encephalitis shows predominant reactivity with the full-length sequence of LGI1 (clone 1), and the construct that contains the LRR domain (clone 2); milder reactivity is shown with the construct that contains the EPTP domain (clone 3). The construct generated by clone 4 contains the signal peptide (SP) but does not include any LGI1 sequence. Scale bar = 20 μ m.

127x74mm (300 x 300 DPI)

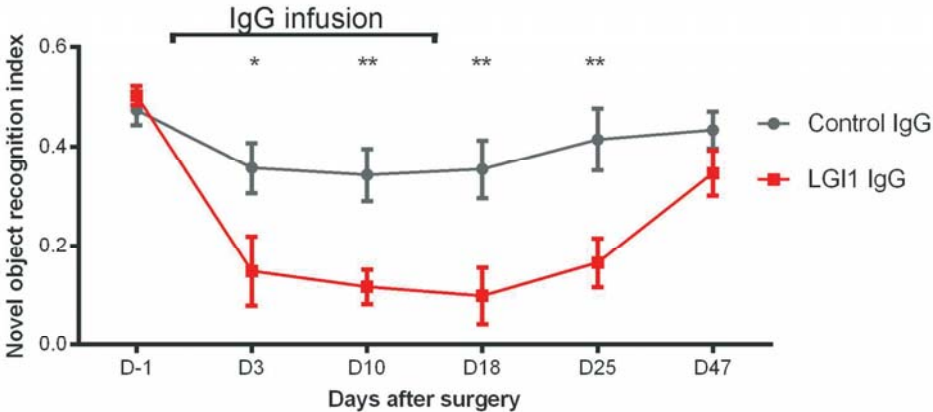


Figure 3: Cerebroventricular infusion of patients' LGI1 IgG causes decrease of memory Novel object recognition index in mice treated with patients' IgG (red, n = 16) or control IgG (grey, n = 14). A high index indicates better memory. Data is presented as mean ± SEM. * $P < 0.05$; ** $P < 0.01$.

165x74mm (300 x 300 DPI)

Peer Review

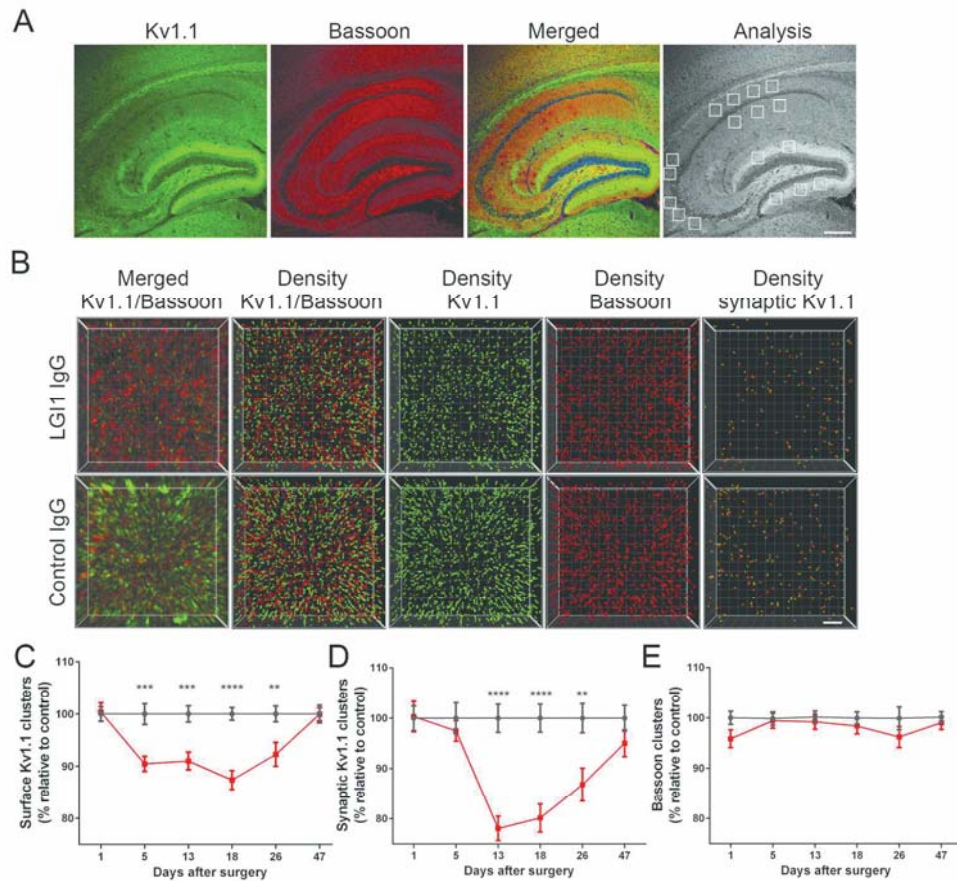


Figure 4: Patients' LGI1 IgG causes a decrease of total cell surface and synaptic Kv1.1 clusters in the hippocampus Sagittal section of hippocampus of a representative mouse infused with patients' LGI1 IgG demonstrating the immunostaining of Kv1.1, Bassoon, and the merging reactivities (A). Squares in "Analysis" indicate the analyzed subregions in CA1, CA3, and DG for each animal. Scale bar = 200 μm . 3D projection and analysis of the density of total cell surface clusters of Kv1.1 and Bassoon, and synaptic clusters of Kv1.1 (defined as Kv1.1 clusters that co-localized with Bassoon) in one of the indicated CA3 subregions (A "Analysis"). Merged images (B, left upper and lower squares; Kv1.1 green, and Bassoon red) were post-processed and used to calculate the density of the indicated clusters (density = spots/ μm^3). Scale bar = 2 μm . Quantification of the density of total cell surface (C) and synaptic (D) Kv1.1 clusters, and Bassoon clusters (E) in a pooled analysis of hippocampal subregions (CA1, CA3, DG) in animals treated with patients' LGI1 IgG (red) or control IgG (black) on the indicated days. Mean density of clusters in control IgG treated animals was defined as 100%. Data are presented as mean \pm SEM. For each time point five animals infused with patients' LGI1 IgG and five with control IgG were examined. Significance of treatment effect was assessed by two-way ANOVA with an alpha-error of 0.05 (asterisks) and post-hoc testing with Sidak-Holm adjustment. ** $P < 0.01$; *** $P < 0.001$; **** $P < 0.0001$.

199x183mm (300 x 300 DPI)

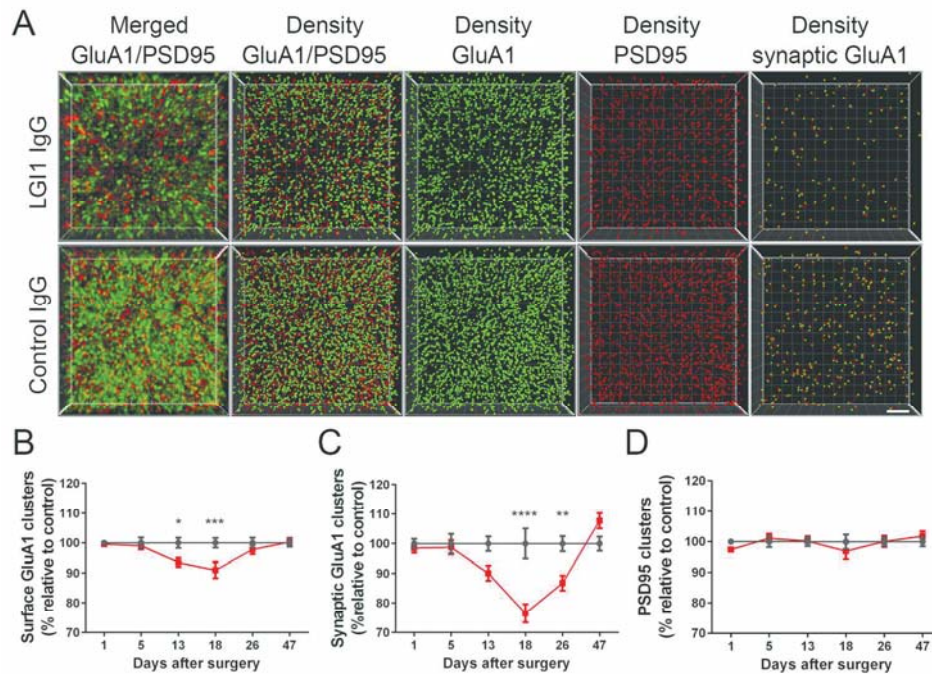


Figure 5: Patients' LG1 IgG causes a decrease of total cell surface and synaptic AMPAR clusters in the hippocampus 3D projection and analysis of the density of total cell surface clusters of GluA1 AMPAR and PSD95, and synaptic clusters of AMPAR (defined as AMPAR clusters that co-localized with PSD95) in one of the CA3 subregions indicated in Fig. 4A, "Analysis". Merged images (A, left upper and lower squares; GluA1 green, and PSD95 red) were post-processed and used to calculate the density of the indicated clusters (density = spots/ μm^3). Scale bar = 2 μm . Quantification of the density of total cell surface (B) and synaptic (C) GluA1 AMPAR clusters, and PSD95 clusters (D) in a pooled analysis of hippocampal subregions (CA1, CA3, DG) in animals treated with patients' LGI1 IgG (red) or control IgG (black) on the indicated days. Mean density of clusters in control IgG treated animals was defined as 100%. Data are presented as mean \pm SEM. For each time point five animals infused with patients' IgG and five with control IgG were examined. Significance of treatment effect was assessed by two-way ANOVA with an alpha-error of 0.05 (asterisks) and post-hoc testing with Sidak-Holm adjustment. * $P < 0.05$; ** $P < 0.01$; *** $P < 0.001$; **** $P < 0.0001$.

199x147mm (300 x 300 DPI)

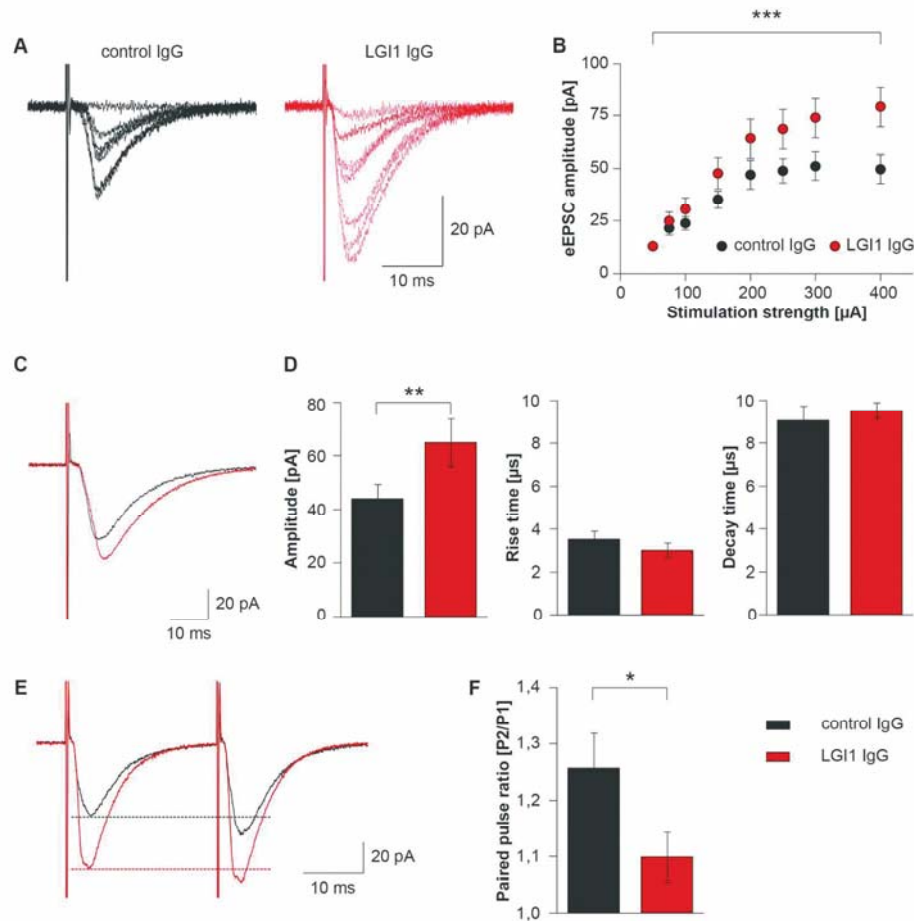


Figure 6: Patients' LGI1 IgG increases excitatory synaptic transmission Evoked excitatory postsynaptic currents (eEPSCs) in dentate gyrus granule cells upon incremental stimulation of medial perforant path (MPP) afferent fibers are increased in acute brain slices of mice that received patient's LGI1 IgG (A and B). Example traces of an individual recording are shown in (A). In/out characteristics of granule cell neurons of control IgG and patients' LGI1 IgG treated mice (B; $n_{\text{control IgG}} = 13$; $n_{\text{LGI1 IgG}} = 15$; data are presented as mean \pm SEM; two-way ANOVA and Holm-Sidak post-hoc test. *** $P < 0.001$). Peak amplitude of eEPSCs (example traces in C) is increased after infusion of antibodies against LGI1, whereas rise and decay time is unchanged ($n_{\text{control IgG}} = 13$; $n_{\text{LGI1 IgG}} = 15$; data are presented as mean \pm SEM; unpaired t-test. ** $P < 0.01$) (C and D). Paired pulse facilitation with an interstimulus interval of 50 ms is reduced in granule cell neurons from mice after infusion of patients' LGI1 IgG indicating increased release probability. Example traces in E; dashed lines indicate peak amplitude of the first pulse ($n_{\text{control IgG}} = 11$; $n_{\text{LGI1 IgG}} = 13$; data are presented as mean \pm SEM; unpaired t-test. * $P < 0.05$) (E and F).

204x195mm (300 x 300 DPI)

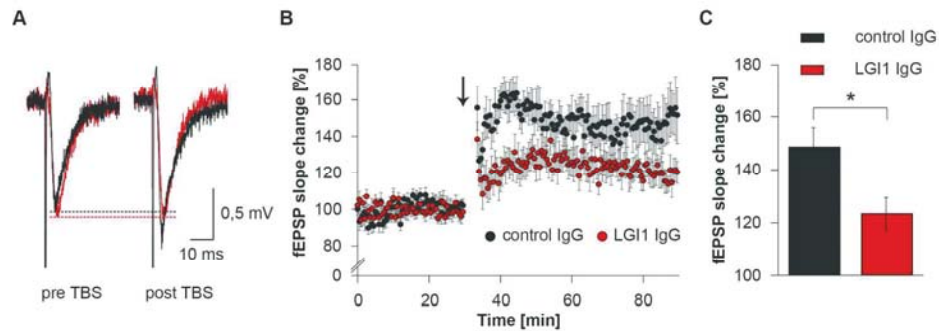


Figure 7: Patients' LGI1 IgG alters synaptic plasticity Example traces of individual field excitatory postsynaptic potential (fEPSP) recordings in the CA1 region before and after theta burst stimulation (TBS) of Schaffer collateral afferents show reduced fEPSP potentiation in brain slices of mice that received patient's LGI1 IgG (A). Time course and quantitative analysis of long-term potentiation (LTP) after TBS (arrow), demonstrates persistent reduction of fEPSP slope values in slices of mice after infusion of patient's LGI1 IgG indicating disturbed synaptic plasticity. Quantification of fEPSP slope change is decreased in LGI1 IgG infused mice (B and C, $n_{\text{control IgG}} = 10$; $n_{\text{LGI1 IgG}} = 13$; data are presented as mean \pm SEM; unpaired t-test. $*P < 0.05$).

206x73mm (300 x 300 DPI)

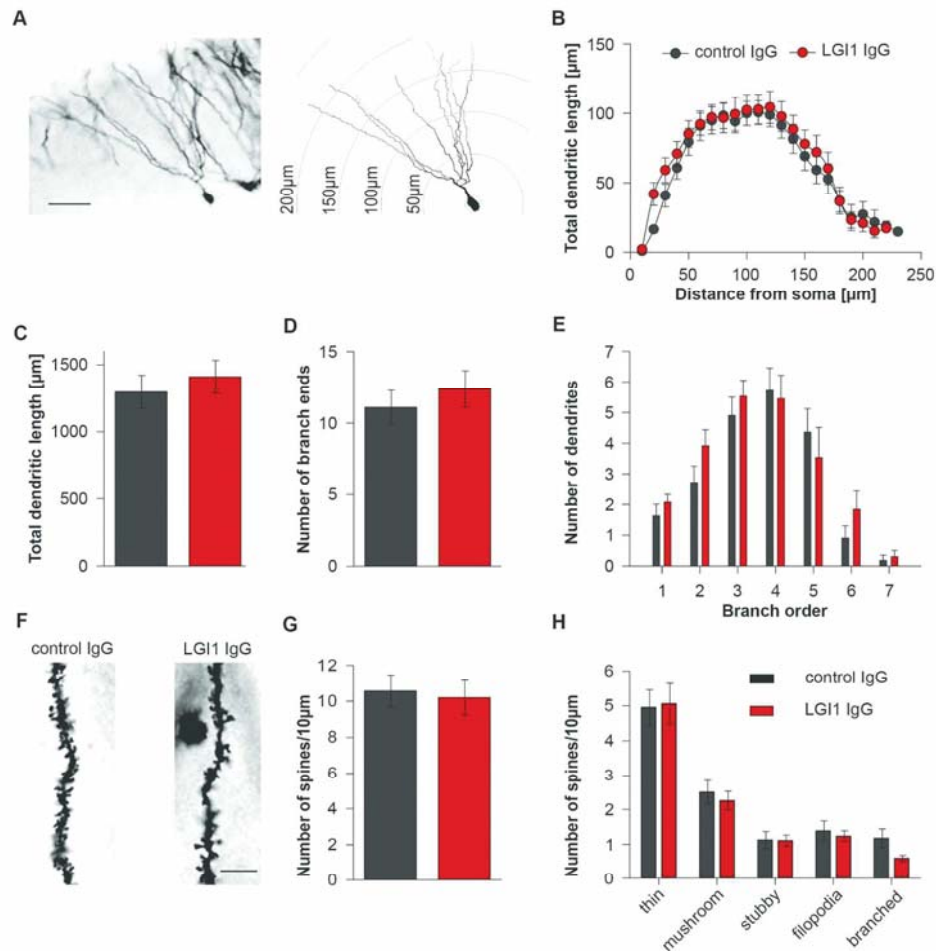


Figure 8: Dendritic pruning is unaffected by patients' LGI1 IgG Dendritic arborization of a dentate gyrus granule cell; example neuron is shown after Golgi silver impregnation (left) and in NeuroLucida reconstruction for Sholl analysis (right) (A, scale bar = 50 μm). Sholl analysis revealed unchanged dendritic arborization in control IgG and patients' LGI1 IgG infused mice as shown by the length of hippocampal granule cell dendrites (B and C) and by number and intersection of dendritic branches (D and E). Synaptic spines of tertiary dendrites of CA1 pyramidal neurons (F, scale bar = 10 μm). Quantification of spine density (G) and of spine morphology (H) is unchanged in control IgG and patients' LGI1 IgG infused mice (all data are presented as mean ± SEM).

203x203mm (300 x 300 DPI)

Supplementary material

- Immunoblot of soluble LGI1
- Mice, surgery, placement of ventricular catheters and osmotic pumps
- Behavioral tasks
- Golgi-Cox staining
- Sholl analysis
- Supplementary Table 1
- Supplementary Figure 1: Immunoabsorption of patients' purified IgG with LGI1-expressing HEK293 cells
- Supplementary Figure 2: LGI1 IgG isolated from patients' serum does not react with brain of LGI1 null mice
- Supplementary Figure 3: Distribution of behavioral tests, period of infusion, and brain tissue studies
- Supplementary Figure 4: Patients' LGI1 IgG blocks the binding of LGI1 to ADAM23 more frequently than to ADAM22
- Supplementary Figure 5: Tests of anxiety, aggression, and locomotor activity
- Supplementary Figure 6: Presence of patients' antibodies bound to LGI1 in brain of infused mice

Immunoblot of soluble LGI1

Media from the indicated LGI1-expressing HEK293 cells, and media from non-transfected cells, were normalized in protein concentration, and 100 µg of protein diluted 1:2 with Rotiload (#K929.1, Roth) boiled for 5 minutes, and separated in a 10% polyacrylamide gel electrophoresis. After transferring the proteins to a PVDF membrane, they were probed with a monoclonal rabbit antibody against LGI1 (1:200, #ab30868, Abcam) for 2 hours at 4°C, and the reactivity developed using the avidin-biotin immunoperoxidase method.

Mice, surgery, placement of ventricular catheters and osmotic pumps

Male C57BL6/J mice (Charles River), 8-10 weeks old (25-30 grams) were housed in cages of five until one week before surgery when they were housed individually. The room was maintained at a controlled temperature (21±1°C) and humidity (55±10%) with

illumination at 12-hour cycles; food and water were available *ad libitum*. All experiments were performed during the light phase, and animals were habituated to the experimental room for 1 week before starting the tests.

Cerebroventricular infusion of patients' LGI1 IgG or control IgG was performed using osmotic pumps (model 1002, Alzet, Cupertino, CA) with the following characteristics: volume 100 μ l, flow rate 0.25 μ l/hour, and duration 14 days, as reported (Planaguma *et al.*, 2015). In brief, 24 hours before surgery, two osmotic pumps per animal were each loaded with 100 μ l of purified patients' LGI1 IgG or control IgG (1 μ g/ μ l). Mice were then placed in a stereotaxic frame, and a bilateral cannula (model 3280PD-2.0/SP, PlasticsOne) was inserted into the ventricles (coordinates: 0.2 mm posterior and \pm 1.00 mm lateral from bregma, depth 2.2 mm), as reported (Planaguma *et al.*, 2015). Each arm of the cannula was connected to one osmotic pump, which was subcutaneously implanted on the back of the mice (two pumps per animal). Appropriate ventricular placement of the catheters was assessed in randomly selected mice injecting methylene blue through the catheters, as reported (Planaguma *et al.*, 2015).

Behavioral tasks

Multiple behavioral tasks were applied at different time points related to the day of pump implantation and initiation of the ventricular infusion of patients' LGI1 IgG or control IgG. They included the novel object recognition (NOR) index and spontaneous locomotor activity (LOC), which were tested 1 day before surgery and on days 3, 10, 18, 25 and 47 after surgery, black and white test (BW, day 7), elevated plus maze (EPM, day 17), and resident-intruder test (RI, days 11 and 26). The distribution of behavioral tests in relation to the infusion period is shown in Supplementary Fig. 3.

Detailed information on these tests has been previously reported (Planaguma *et al.*, 2015).

Golgi-Cox staining

Golgi silver impregnation was conducted with the FD Rapid GolgiStain™ Kit (#PK401, FD NeuroTechnologies, Inc., Columbia, USA) according to manufacturer's instructions. Briefly, the tissue was rinsed in aCSF1 to remove blood residues, and was then transferred into equal amounts of solution A+B of the FD Rapid GolgiStain™ Kit. After renewal of solutions on the second day the tissue was subsequently left in the dark for two weeks at room temperature. Thereafter, brain hemispheres were transferred into solution C of the FD Rapid GolgiStain™ Kit, which was changed after one day, and were left in solution at 4°C for 5 days. Hemispheres were then stored at -80°C until further use. Thereafter, hemispheres were cut into 150µm thick coronal slices in the area of the hippocampus using a Leica CM3050S cryostat and mounted on object slides. For the last step of staining procedure, slices were washed in purified water (2 x 4 minutes), incubated in a mix of 1/4 solution D, 1/4 solution E and 1/2 purified water for 10 minutes, washed again, and then dehydrated in an ascending alcohol series (50%, 75%, 95% for 4 minutes each, and 2 x 100 % for 8 minutes). Finally, slices were immersed in xylene (2 x 5 minutes), and then quickly coverslipped with Entellan® (Merck KGaG, Darmstadt, Germany) and dehumidified overnight.

Sholl analysis

To evaluate dendritic morphology, a Zeiss Axioskop 2 mot plus (Zeiss, Oberkochen, Germany) and a computer-based system (NeuroLucida; MicroBrightField) was used to generate three-dimensional neuron tracings that were subsequently analyzed using the

NeuroExplorer Software (MicroBrightField). Golgi-impregnated cells were selected for reconstruction if they fulfilled the following criteria: (1) the neuron was located in the dentate gyrus with soma in outer granule layer of the superior or inferior blade, (2) the neuron was distinguishable from neighboring cells to allow for identification of dendrites, (3) the dendrites were not truncated or broken, and (4) the cell exhibited dark and well filled impregnation throughout whole dendrites including spines. Selected cells were traced manually using the NeuroLucida system at 40x magnification. For each reconstructed neuron an estimate of dendritic complexity was obtained using the Sholl ring method (Zhou *et al.*, 2009). Additionally, the total dendritic length, the number of branch ends and the number of dendrites per branch order were calculated.

For analysis of dendritic spines, positively stained neurons in the CA region were randomly selected and used for analysis as described previously (Orlowski and Bjarkam, 2012). Neuronal apical dendrites were followed up to tertiary branches without visible disruptions and without further split up using a Zeiss Axioskop 2 mot plus with a 100x oil immersion objective (PLAN-Neofluar). For correct analysis of dendrite length, tertiary branches were chosen to be in an even z-layer. Number and type of spines (thin, mushroom, stubby, filopodia or branched) were counted manually by the same blinded investigator according to previous reports (McKinney, 2010). Total spine density was calculated as number of spines per 10 μm of dendritic length. Morphological subclassification was outlined in proportion of all spines regardless of spine properties.

Supplementary Table 1: Patients clinical and immunological features

Patient	Age	Gender	Main clinical syndrome	Facio-brachial dystonic seizures	Other seizure types	MRI T2/FLAIR increased signal	Clones reactivity	Blocking with ADAM23	Blocking with ADAM22
1	62	F	Limbic encephalitis	No	Generalized	No	LRR	Yes	No
2	54	F	Limbic encephalitis	Yes	No	Unilateral mesiotemporal	LRR	Yes	Yes
3	73	M	Limbic encephalitis	Yes	No	No	LRR	Yes	Yes
4	65	M	Limbic encephalitis	No	Generalized	Unilateral mesiotemporal	LRR, EPTP	Yes	Yes
5	65	M	Limbic encephalitis	No	Focal	Bilateral mesiotemporal	LRR	Yes	No
6	63	F	Limbic encephalitis	No	Focal and generalized	Bilateral mesiotemporal	LRR, EPTP	Yes	No
7	52	F	Limbic encephalitis	No	Generalized	Bilateral mesiotemporal	LRR	Yes	No
8	59	M	Limbic encephalitis	Yes	Focal and generalized	Basal ganglia, frontal, insula	LRR	Yes	Yes
9	71	F	Limbic encephalitis	Yes	Focal and generalized	No	LRR	Yes	Yes
10	57	M	Limbic encephalitis	No	Focal and generalized	Bilateral mesiotemporal	LRR, EPTP	Yes	No
11	63	M	Limbic encephalitis	Yes	Focal and generalized	Bilateral mesiotemporal	LRR, EPTP	Yes	Yes
12	72	M	Limbic encephalitis	Yes	No	Unilateral mesiotemporal sclerosis	LRR, EPTP	Yes	No
13	80	M	Limbic encephalitis	No	Focal	No	LRR	Yes	No
14	71	F	Limbic encephalitis	No	Generalized	Bilateral mesiotemporal	LRR, EPTP	Yes	Yes
15	61	M	Limbic encephalitis	No	Focal and generalized	Bilateral mesiotemporal	LRR, EPTP	Yes	Yes

						and basal ganglia			
16	74	M	Limbic encephalitis	Yes	Focal	Bilateral mesiotemporal	LRR, EPTP	Yes	Yes
17	59	M	Limbic encephalitis	Unknown	Focal and generalized	No	LRR	Yes	No
18	56	M	Limbic encephalitis	No	Focal	Unilateral mesiotemporal	LRR	Yes	No
19	54	F	Limbic encephalitis	Unknown	NA	Bilateral mesiotemporal	LRR, EPTP	Yes	Yes
20	58	M	Limbic encephalitis	No	No	Bilateral mesiotemporal	LRR, EPTP	Yes	Yes
21	65	M	Limbic encephalitis	Yes	Focal and generalized	Unilateral insula	LRR	Yes	Yes
22	41	M	Limbic encephalitis	Yes	Focal	No	LRR	Yes	Yes
23	56	M	Limbic encephalitis	Unknown	Focal	Unilateral mesiotemporal	LRR	Yes	No
24	53	F	Limbic encephalitis	Yes	Focal	No	LRR, EPTP	Yes	Yes
25	58	F	Limbic encephalitis	Yes	Focal	Bilateral mesiotemporal	LRR, EPTP	Yes	Yes

Supplementary figures

Supplementary Figure 1: Immunoabsorption of patients' purified IgG with LGI1-expressing HEK293 cells

Reactivity of patients' LGI1 IgG with rat brain (A), HEK293 cells that express LGI1 (B) and live cultures of neuron (C). Pre-absorption of patients' LGI1 IgG with HEK293 cells expressing LGI1 abolished the reactivity in all three conditions (D, E, F). In contrast, pre-absorption with HEK293 cells without LGI1 did not alter the reactivity in the three indicated conditions (G, H, I). Scale bar in G = 2 mm; Scale bar in H = 20 μ m; Scale bar in I = 50 μ m.

Supplementary Figure 2: LGI1 IgG isolated from patients' serum does not react with brain of LGI1 null mice

Purified LGI1 IgG from patients intensively reacts with hippocampus of wild type mice but it does not react with hippocampus of LGI1 null mice (tissue obtained as reported, (Lai *et al.*, 2010)). Purified IgG from healthy participants (control) does not show reactivity with any of the brains. Scale bar = 200 μ m.

Supplementary Figure 3: Distribution of behavioral tests, period of infusion, and brain tissue studies

At day 0, catheters and osmotic pumps were placed and bilateral ventricular infusion of patients' LGI1 IgG or control IgG started. Infusion lasted for 14 days. Memory (novel object recognition [NOR]), locomotor activity (LOC), anxiety (black and white test [BW] and elevated plus maze test [EPM]), and aggressiveness (resident intruder test [RI]) were assessed blinded to treatment at the indicated days. Animals were habituated

for 1 to 4 days before surgery (baseline) to NOR and LOC. Red arrowheads indicate the days of sacrifice for studies of effects of antibodies in brain.

Supplementary Figure 4: Patients' LGI1 IgG blocks the binding of LGI1 to ADAM23 more frequently than to ADAM22

Sera from four additional representative patients show that all block the binding of LGI1 to ADAM23, but two of them (serum 3 and 4) do not block the binding of LGI1 to ADAM22. Scale bar = 20 μ m.

Supplementary Figure 5: Tests of anxiety, aggression, and locomotor activity

Tests of anxiety (black and white test, A, and elevated plus maze, B), aggression (resident intruder, C), and locomotor activity (D) did not show significant differences between mice infused with patients' LGI1 IgG and control (CT) IgG. B entries = black entries; W entries = white entries; CA entries = closed arm entries; OA = open arm entries. D = day of the experiment related to first day of IgG infusion; Hab = habituation.

Supplementary Figure 6: Presence of patients' antibodies bound to LGI1 in brain of infused mice

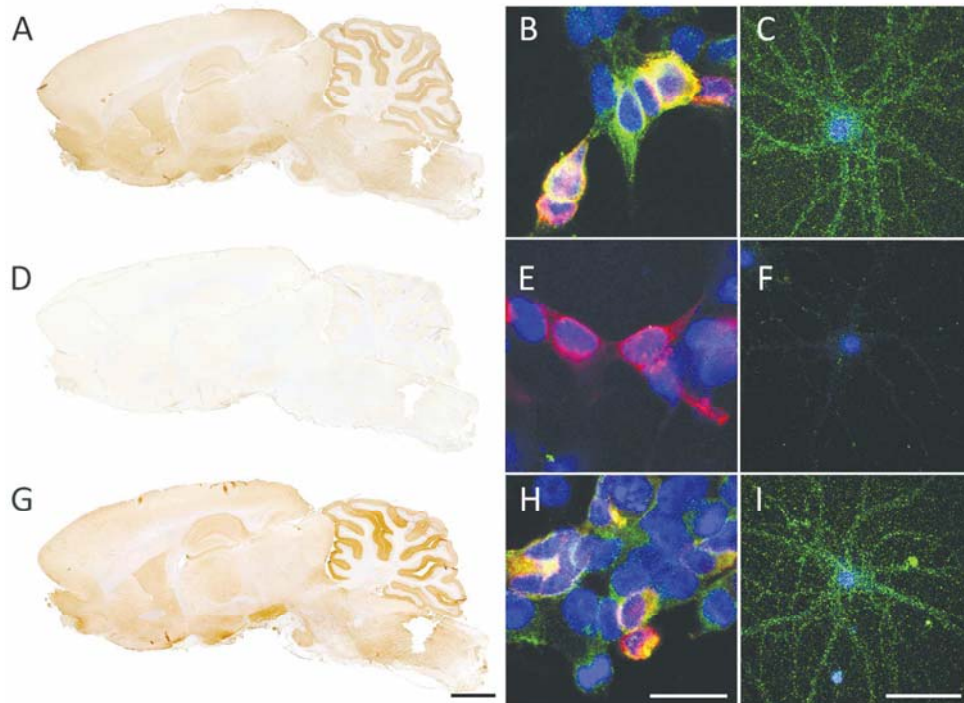
In mice infused with patients' LGI1 IgG (A, lanes 1 and 2), but not in mice infused with control IgG (A, lanes 3 and 4), the extraction and precipitation of IgG from brain show that it is bound to LGI1 (64 kDa protein band in lanes 1 and 2).

In another experiment, acid-extracted IgG from hippocampus of mice infused with patients' IgG shows the presence of LGI1 antibodies, which are demonstrated in a cell-

based assay with HEK293 cells expressing LGI1 (first row in B). In contrast no LGI1 antibodies are detected in the tissue-wash before the acid extraction (second row) suggesting the acid-extracted IgG contained antibodies specifically bound to LGI1 in tissue. Similar experiments with samples obtained from mice infused with control IgG show absence of LGI1 antibodies (third and fourth rows). For all rows the expression of LGI1 in HEK293 cells was confirmed with a monoclonal rabbit antibody against LGI1 (1:1000, #ab30868, Abcam) showing the merged reactivities of the human and monoclonal antibodies. Scale bar = 20 μm .

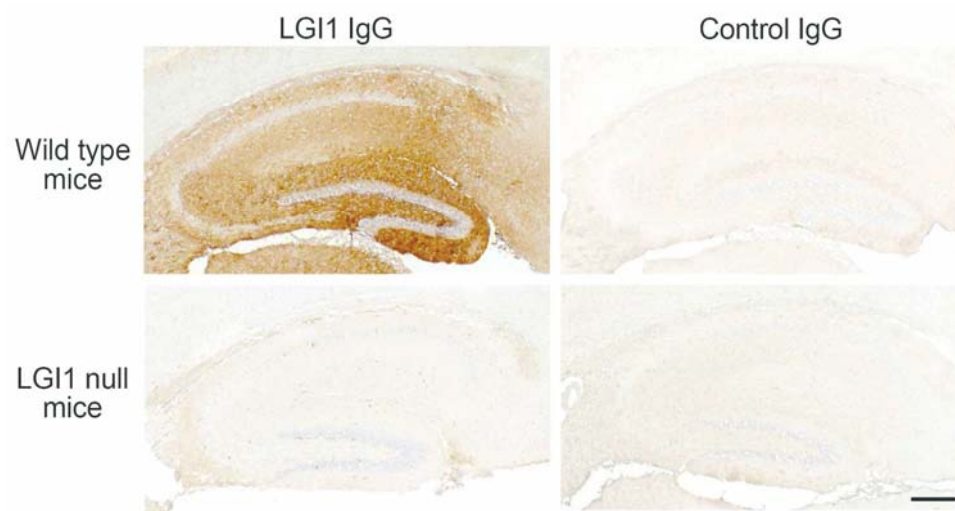
Supplementary References

- Lai M, Huijbers MG, Lancaster E, Graus F, Bataller L, Balice-Gordon R, *et al*. Investigation of LGI1 as the antigen in limbic encephalitis previously attributed to potassium channels: a case series. *Lancet Neurol* 2010; 9(8): 776-85.
- McKinney RA. Excitatory amino acid involvement in dendritic spine formation, maintenance and remodelling. *J Physiol* 2010; 588(Pt 1): 107-16.
- Orlowski D, Bjarkam CR. A simple reproducible and time saving method of semi-automatic dendrite spine density estimation compared to manual spine counting. *J Neurosci Methods* 2012; 208(2): 128-33.
- Planaguma J, Leyboldt F, Mannara F, Gutierrez-Cuesta J, Martin-Garcia E, Aguilar E, *et al*. Human N-methyl D-aspartate receptor antibodies alter memory and behaviour in mice. *Brain* 2015; 138(Pt 1): 94-109.
- Zhou YD, Lee S, Jin Z, Wright M, Smith SE, Anderson MP. Arrested maturation of excitatory synapses in autosomal dominant lateral temporal lobe epilepsy. *Nat Med* 2009; 15(10): 1208-14.



Supplementary Figure 1: Immunoabsorption of patients' purified IgG with LGI1-expressing HEK293 cells Reactivity of patients' LGI1 IgG with rat brain (A), HEK293 cells that express LGI1 (B) and live cultures of neuron (C). Pre-absorption of patients' LGI1 IgG with HEK293 cells expressing LGI1 abolished the reactivity in all three conditions (D, E, F). In contrast, pre-absorption with HEK293 cells without LGI1 did not alter the reactivity in the three indicated conditions (G, H, I). Scale bar in G = 2 mm; Scale bar in H = 20 μm ; Scale bar in I = 50 μm .

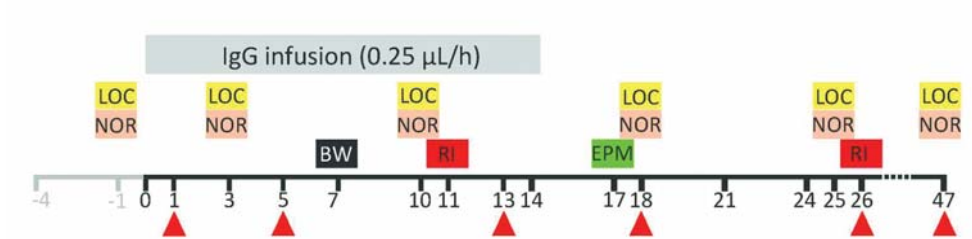
184x137mm (300 x 300 DPI)



Supplementary Figure 2: LGI1 IgG isolated from patients' serum does not react with brain of LGI1 null mice Purified LGI1 IgG from patients intensively reacts with hippocampus of wild type mice but it does not react with hippocampus of LGI1 null mice (tissue obtained as reported, (Lai et al., 2010)). Purified IgG from healthy participants (control) does not show reactivity with any of the brains. Scale bar = 200 μ m.

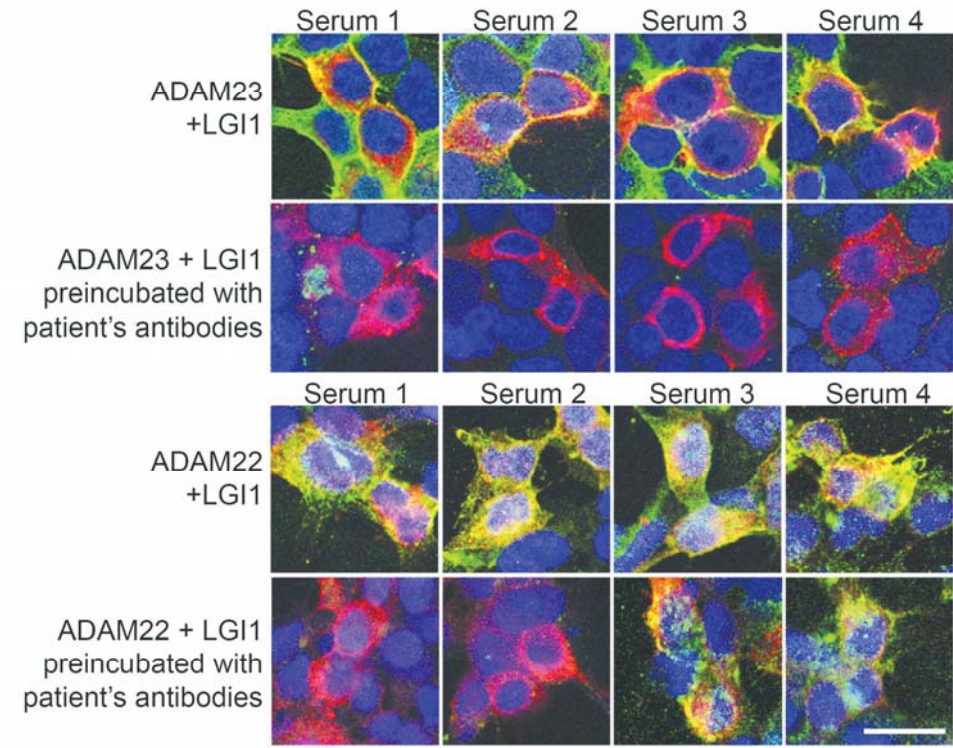
184x99mm (300 x 300 DPI)

Review



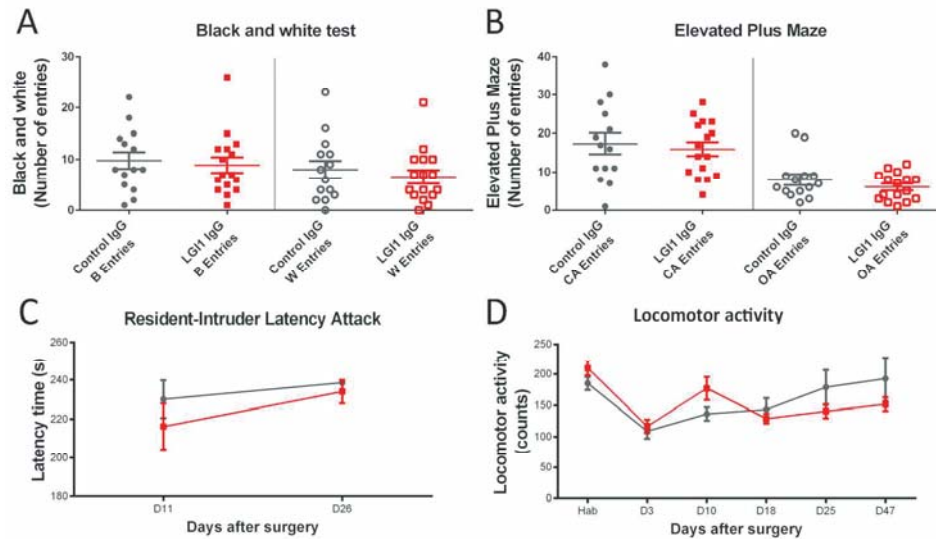
Supplementary Figure 3: Distribution of behavioral tests, period of infusion, and brain tissue studies At day 0, catheters and osmotic pumps were placed and bilateral ventricular infusion of patients' LGI1 IgG or control IgG started. Infusion lasted for 14 days. Memory (novel object recognition [NOR]), locomotor activity (LOC), anxiety (black and white test [BW] and elevated plus maze test [EPM]), and aggressiveness (resident intruder test [RI]) were assessed blinded to treatment at the indicated days. Animals were habituated for 1 to 4 days before surgery (baseline) to NOR and LOC. Red arrowheads indicate the days of sacrifice for studies of effects of antibodies in brain.

199x54mm (300 x 300 DPI)



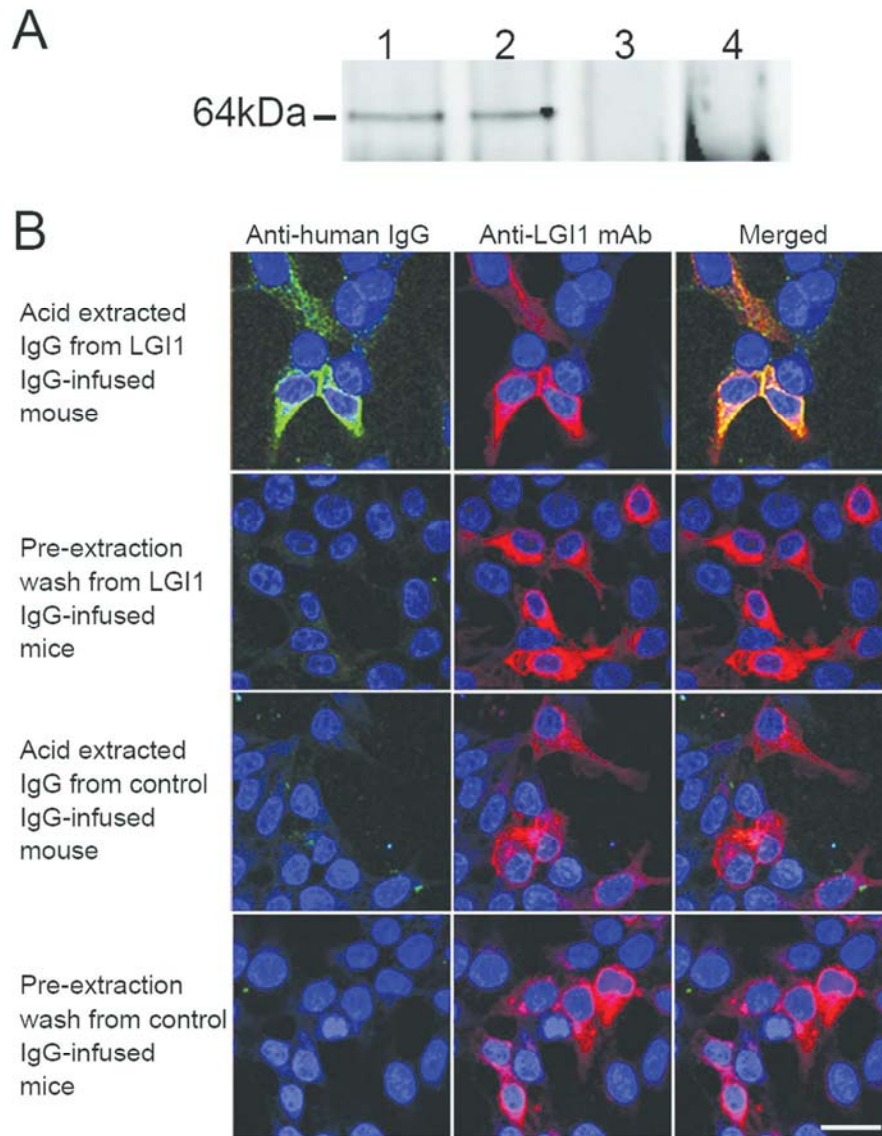
Supplementary Figure 4: Patients' LGI1 IgG blocks the binding of LGI1 to ADAM23 more frequently than to ADAM22 Sera from four additional representative patients show that all block the binding of LGI1 to ADAM23, but two of them (serum 3 and 4) do not block the binding of LGI1 to ADAM22. Scale bar = 20 μ m.

184x144mm (300 x 300 DPI)



Supplementary Figure 5: Tests of anxiety, aggression, and locomotor activity Tests of anxiety (black and white test, A, and elevated plus maze, B), aggression (resident intruder, C), and locomotor activity (D) did not show significant differences between mice infused with patients' LGI1 IgG and control (CT) IgG. B entries = black entries; W entries = white entries; CA entries = closed arm entries; OA = open arm entries. D = day of the experiment related to first day of IgG infusion; Hab = habituation.

199x112mm (300 x 300 DPI)



Supplementary Figure 6: Presence of patients' antibodies bound to LGI1 in brain of infused mice

In mice infused with patients' LGI1 IgG (A, lanes 1 and 2), but not in mice infused with control IgG (A, lanes 3 and 4), the extraction and precipitation of IgG from brain show that it is bound to LGI1 (64 kDa protein band in lanes 1 and 2). In another experiment, acid-extracted IgG from hippocampus of mice infused with patients' IgG shows the presence of LGI1 antibodies, which are demonstrated in a cell-based assay with HEK293 cells expressing LGI1 (first row in B). In contrast no LGI1 antibodies are detected in the tissue-wash before the acid extraction (second row) suggesting the acid-extracted IgG contained antibodies specifically bound to LGI1 in tissue. Similar experiments with samples obtained from mice infused with control IgG show absence of LGI1 antibodies (third and fourth rows). For all rows the expression of LGI1 in HEK293 cells was confirmed with a monoclonal rabbit antibody against LGI1 (1:1000, #ab30868, Abcam) showing the merged reactivities of the human and monoclonal antibodies. Scale bar = 20 μ m.

90x114mm (300 x 300 DPI)

6. DISCUSSION

Antibody-mediated encephalitis encompasses a novel category of severe but treatable neurological disorders that are directly mediated by autoantibodies against cell-surface proteins, ion channels, or neurotransmitter receptors. There are currently 16 such diseases identified; I discovered one of them (anti-GABA_AR encephalitis) and contributed to the discovery of another one (anti-neurexin-3 α encephalitis), both projects included as part of this thesis. The systematic approach I took to investigate these diseases and the integration of my findings to this approach are shown in **Figure 14**.

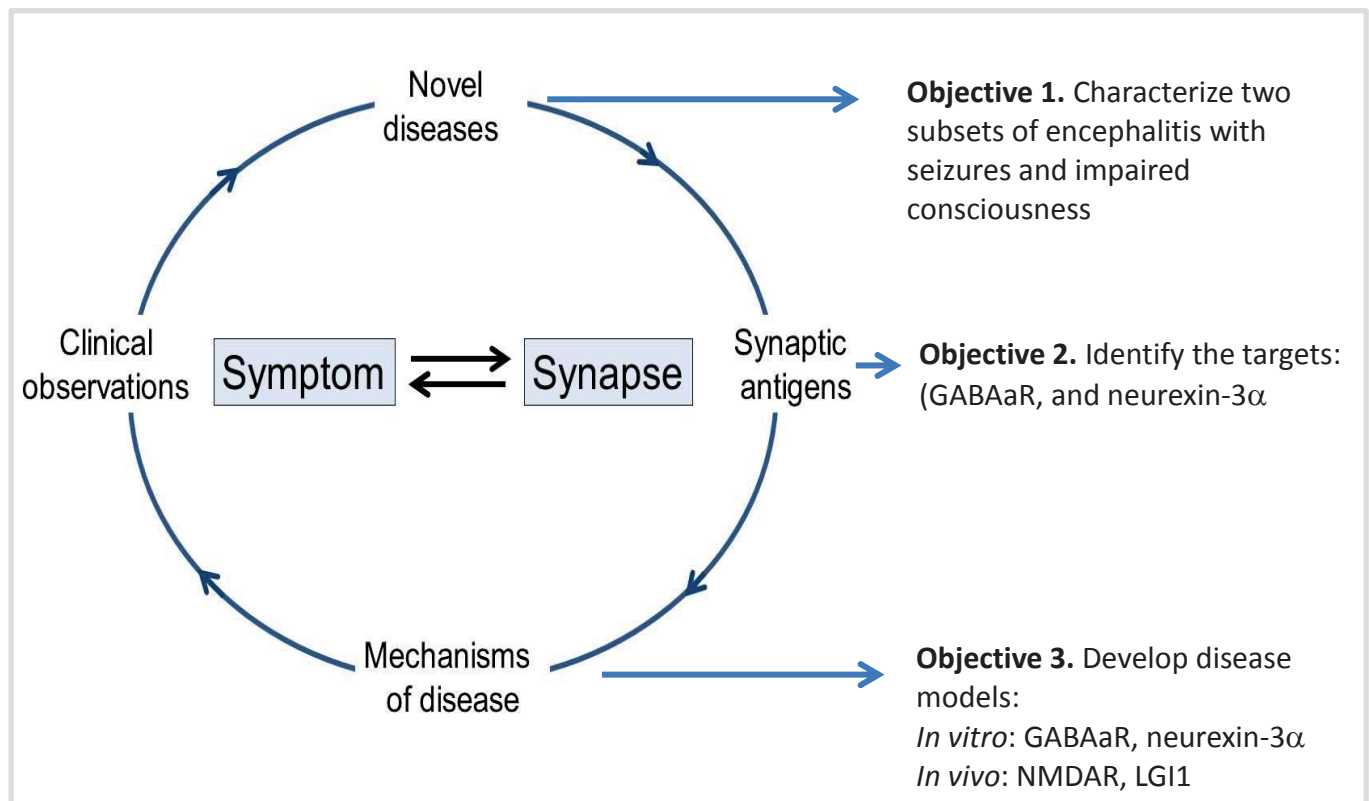


Figure 14. Translational research approach used in this thesis

The discovery of autoimmune encephalopathies is based on clinical observations; these lead to the identification of new neuronal cell-surface or synaptic antigens, which enable the development of diagnostic tests and identification of the mechanisms of disease. A better understanding of these mechanisms is important for the development of new treatment strategies and helping to navigate through the differential diagnosis, which in turn facilitates the identification of other diseases through refined clinical observations.

The **first objective (Paper 1 and 3)** of my thesis was to select groups of patients with encephalitis of unclear etiology but suspected to be autoimmune. Due to the large number of cases including serum, CSF and clinical information that Dr. Dalmau's lab receives as referral center for autoimmune encephalitides, I was able to screen hundreds of samples using brain tissue immunohistochemistry, live rat hippocampal neurons, and HEK293 cells transfected with a variety of known neuronal autoantigens. Out of all samples with positive neuronal reactivity

demonstrated with the first two techniques but negative for all known neuronal antigens, I was able to identify two groups of patients' samples that showed two novel and distinct novel patterns of brain reactivity.

These findings led me to the **Second objective (Paper 1 to 3)** of my thesis, which consisted in the precipitation of the target antigens and subsequent characterization of their identity using mass spectrometry (proteomics facility). The first antigen I characterized was the GABA_AR, and this led me to develop a specific HEK CBA to determine the presence of these antibodies in other patients. This test allowed me to confirm that all patients harboring antibodies with the same pattern of reactivity with rat brain had GABA_AR antibodies. As a result of these initial findings I participated in the identification of another autoantibody and surrogate antigen, neurexin-3 α ⁶⁹ which defines another group of autoimmune encephalitis. These studies resulted in the development of clinical diagnostic tests for patients with these disorders.

The presence of GABA_AR antibodies defines an autoimmune encephalitis characterized by prominent seizures or status epilepticus. These symptoms are usually refractory to antiepileptic medication, and may lead to death if not properly diagnosed or treated. However, prompt treatment with immunotherapy often results in clinical recovery. Similarly, patients with neurexin-3 α antibodies develop a form of encephalitis without a specific set of symptoms but almost always associated with seizures, confusion and decreased level of consciousness.

The GABA_ARs are pentamers that are composed of two α subunits, two β subunits, and one γ subunit; for each subunit there are multiple types that combine differently according to the location of the receptor, synaptic or extrasynaptic. I found that the antibodies of patients with anti-GABA_AR encephalitis are directed against the α 1 and β 3 subunits. Moreover, using cultured neurons I demonstrated that the antibodies alter the cell-surface dynamics of the GABA_AR causing a relocation of the synaptic receptors to extrasynaptic sites and supporting a direct pathogenic role of the antibodies. These effects may lead to hyperexcitability, which accounts for the epilepsy suffered by the patients, and a task for the future is to confirm in an animal model if the infusion of patients' antibodies lead to seizures. Indeed, in humans, mutations in the α 1 and β 3 subunits of the GABA_AR are associated with epileptic activity,^{169,170} which is in line with the symptoms of patients with anti-GABA_AR antibodies as well as the observed antibody-mediated decrease of GABA_AR I found in my experiments. These *in vitro* effects of patients' antibodies are reversible upon removal of the antibodies from the media, providing a possible explanation for the reversibility of patients' symptoms with immunotherapy (which eliminates the antibodies and antibody-producing cells).

After my original report of anti-GABA_AR encephalitis other investigators have reproduced similar findings.¹⁷¹ A study described antibodies against the β 3 subunit of the GABA_AR in two patients with cognitive impairment and multifocal brain MRI abnormalities. The application of patients' serum in cultures of rat hippocampal neurons produced a decrease of surface and synaptic GABA_ARs, and a decrease of miniature inhibitory postsynaptic currents (mIPSC) amplitude and frequency without affecting AMPAR-mediated miniature EPSCs. These findings also supported the pathogenicity of patients' antibodies, suggesting that they altered the levels

of synaptic GABA_AR, as I previously reported in **paper 1**. Interestingly, these two patients had an underlying thymoma that probably contributed to the development of the autoimmune response either by alteration of immune-regulatory mechanisms or by ectopic expression of GABA_AR. These hypotheses were not investigated by Ohkawa and colleagues but I subsequently tested it in a study of Simabukuro and colleagues,¹⁷² which I co-authored (see Chapter 6. **Annex**). In this study I demonstrated that the thymoma of a patient with autoimmune encephalitis and GABA_AR and LGI1 antibodies expressed both antigens (GABA_AR and LGI1).

More recently I participated in another study that expanded the number of patients with anti-GABA_AR encephalitis to 17 new cases¹⁷³ (**paper 2**). This study confirms that the encephalitis of these patients associates with prominent seizures and status epilepticus, and show that they have a characteristic brain MRI pattern of multifocal cortical-subcortical abnormalities. Moreover, given that a manuscript published by other investigators¹⁷⁴ suggested that the $\gamma 2$ subunit of the GABA_AR could also be a relevant disease-antigenic target, we investigated the clinical significance of $\gamma 2$ antibodies in 26 patients with anti-GABA_AR encephalitis. Our findings show that although all patients' antibodies recognized the $\alpha 1$ and/or $\beta 3$ subunits only 8/26 cases recognized the $\gamma 2$ subunit. Presence of these antibodies did not associate with any specific set of symptoms or distinctive clinical features (**paper 2**). These data established that in patients with anti-GABA_AR encephalitis the presence of antibodies against the $\gamma 2$ subunit does not add significant value to the diagnosis or prognosis of this disease.

The other autoantigen I isolated in a subgroup of patients with autoimmune encephalitis was neurexin-3 α (**paper 3**). This protein belongs to a family of synaptic cell-adhesion molecules and is involved in synapse formation and maturation. Neurexins are presynaptic proteins that link pre- and postsynaptic compartments, binding to neuroligins, cerebellins and leucine-rich repeat transmembrane neuronal proteins (LRRTMs), which mediate trans-synaptic signaling, and shape neural network properties by specifying synaptic functions. The three encoding genes (NRX1-3) produce a longer α - and a shorter β -neurexin isoforms using independent promoters. In mice, the combined knockout of all three α -neurexins is lethal at birth, possibly because of a strong impairment in neurotransmitter release.¹⁷⁵ In humans, mutations in the neurexin genes, such as NRX1 and NRX2, have been associated with schizophrenia and autism.¹⁷⁶ Specific ablation of neurexin-3 showed different pre- and postsynaptic functions in distinct brain regions. For example, in the hippocampus, extracellular sequences of presynaptic neurexin-3 mediate trans-synaptic regulation of postsynaptic AMPA receptors whereas in the olfactory bulb, intracellular sequences of neurexin-3 are selectively required for GABA release.¹⁷⁷

Using rat embryonic neurons in the stage of maturation and development of functional synaptic networks (e.g., DIV 1-14), we found that patients' antibodies caused a specific reduction of the levels of neurexin-3 α (without change of its postsynaptic ligand LRRTM2) as well as a decrease of the total number of synapses and the pre- and postsynaptic proteins Bassoon and Homer1. Bassoon is a synaptic protein highly expressed at the active zone where

it acts as a link between cytomatrix components and synaptic vesicle proteins.^{178,179} Homer1 is a protein of the postsynaptic density with a crucial role for the organization of PSD95.¹⁸⁰ Thus, the antibody-mediated decrease of neurexin-3 α affects synapse development and the recruitment of both pre- and postsynaptic scaffold proteins involved in the early stages of synaptogenesis. These findings are in line with studies showing that disruption of endogenous neurexin-neuroigin interaction by adding a recombinant neurexin reduces the number of presynaptic terminals and the number of inhibitory and excitatory synapses.^{181,182} Together, our findings suggest that patients' antibodies likely contributed to the pathogenesis of their disorder.

Overall, work of the manuscripts summarized above (**paper 1-3**) led to the identification of two novel autoimmune encephalitis and the corresponding antibodies and antigens, thus confirming the hypothesis that some encephalitis of unknown etiology are autoimmune.

After these studies, my next step was to demonstrate that autoantibodies from patients with autoimmune encephalitis are directly involved in patients' symptoms, thus addressing the **third objective (paper 4-6)**. For this, I first participated in the development of a mice model of NMDAR antibody mediated symptoms (the most frequent neuronal antibody-mediated encephalitis) (**paper 4 and 5**), and afterwards I applied the strategies and techniques learned from this disorder to better understand anti-LGI1 encephalitis (the second most common autoimmune encephalitis) and develop an animal model of this disease (**paper 6**).

Before developing the model of NMDAR antibody-mediated symptoms the only two models of CNS neuronal antibody-mediated symptoms included, stiff-person syndrome mediated by antibodies against amphiphysin,⁷⁶ and cerebellar ataxia mediated by antibodies against mGluR1.⁷⁴ None of these disorders associates with encephalitis and therefore our approach to develop NMDAR- antibody mediated symptoms was the first to attempt to model autoimmune encephalitis. There were four reasons that led to start the project of animal modeling of autoimmune encephalitis focusing specifically in anti-NMDAR encephalitis: First, it is the most common neuronal antibody-mediated encephalitis and therefore we had plenty of material (serum and CSF) to proceed with the studies of passive transfer of antibodies; Second, the syndrome of these patients is fascinating and provides a clinical picture that allows to determine how an antibody can affect memory and behavior; Third, the similarity between the syndrome and the models of genetic^{105,183} and pharmacologic^{184,185} reduction of NMDAR function strongly suggested that the NMDAR antibodies had a direct pathogenic effect on the receptors;⁸⁷ and Fourth, there was extensive experience using experiments with primary cultures of dissociated rat hippocampal neurons demonstrating that patients antibodies caused a reduction of the levels of synaptic and extrasynaptic NMDAR and a decrease of NMDAR-specific synaptic currents.^{58,59,106}

Given that patients with anti-NMDAR encephalitis always have higher titers of antibodies in CSF than in serum, and there is evidence of a long-lasting presence of these antibodies in the CSF, we designed the animal model using passive transfer of patients' antibodies into the ventricular system (as previously shown in Figure 13). For 14 days mini-osmotic pumps filled with patients' or control CSF and subcutaneously implanted in the back of mice (C57BL/6J),

infused continuously patients' antibodies, which from the ventricular system diffused to the brain parenchyma. During the 14-day infusion and afterwards until day 26, mice underwent the indicated memory and behavioral tests, and sets of animals were sacrificed at different time points in order to determine the presence of brain-bound antibodies and their effects on the NMDARs. As indicated in **paper 4**, this study provided four sets of experiments that satisfied the Witebsky's criteria for an antibody-mediated disease¹⁰⁷ including, 1) the development of symptoms in animals infused with patients' CSF, but not control CSF, 2) the demonstration that the infused antibodies reacted predominantly with brain regions with high density of NMDAR (e.g., hippocampus) and specifically recognized these receptors, 3) the identification of a selective decrease of density of total and synaptic NMDAR clusters and total NMDAR protein concentration without affecting PSD95, and the observation that these effects correlated with the concentration of brain-bound antibodies, and 4) the correlation noted between the intensity of the above-mentioned findings and time-course of patients' antibody infusion, as well as between the reversibility of symptoms and restoration of NMDAR levels after stopping the infusion of antibodies.

Overall, the groundbreaking findings of **paper 4** in the field of autoimmune encephalitis provided an unambiguous model that showed how a human autoantibody can cause memory and behavioral deficits through antibody-mediated internalization and synaptic depletion of NMDARs.

In 2012 Mikasova and colleagues,⁵⁹ using cultured neurons, reproduced the findings that patients' NMDAR antibodies caused internalization of these receptors, previously reported by Hughes et al.⁵⁸ In addition to these findings, they showed that patients' antibodies disrupted the cross-talk between NMDAR and ephrin B2 receptor (EphB2) and that activation of this receptor with its ligand (ephrin B2) antagonized the effects of patients' antibodies. Eph receptors are a family of receptor tyrosine-kinases that modulate LTP probably through their interaction with NMDAR and stabilization and clustering of this receptor in the postsynaptic membrane.^{186–189} Therefore, the observation using *in vitro* experiments, that activation of EphB2 antagonized the pathogenicity of patients' antibodies, led us to investigate whether similar favorable effects could be obtained in our recently developed mouse model. This hypothesis was important because in patients with anti-NMDAR encephalitis the process of recovery is long, probably as a result of the prolonged synthesis of antibodies by B cells or long-lived plasma cells present in the CNS¹⁹⁰ and the prominent alterations these antibodies cause in synaptic circuits. Therefore, any additional strategy that along with immunotherapy could abrogate the pathogenic effect of patients' antibodies would be potentially useful, leading to novel treatment approaches and potential therapeutic drugs.

Using the same experimental set up as that used in paper 4, we developed a model in which mice were infused with patients or control CSF, with or without soluble ephrin B2 ligand (**paper 5**). These studies reproduced our previous findings showing that mice infused with patients' CSF, but not control CSF, developed progressive memory and depressive-like behavior along

with deposits of NMDAR antibodies in the hippocampus. In addition, we observed a decrease of the density of cell-surface and synaptic NMDAR (as expected from our previous work) and also a decrease of levels of EphB2. These findings were accompanied by a marked impairment of long-term synaptic plasticity without altering short-term plasticity. Interestingly, the administration of ephrin-B2 antagonized the pathogenic effect of the antibodies in all the investigated paradigms, including memory, depressive-like behavior, density of cell-surface and synaptic NMDAR and EphB2, and substantially restored the long-term synaptic plasticity.

Overall, results from **paper 5** revealed a strategy beyond immunotherapy to antagonize patients' antibody effects. For example, in antibody-mediated disorders of the neuromuscular junction, such as myasthenia gravis or the Lambert-Eaton syndrome, the discovery of the pathophysiological underpinnings led to the development of drugs that antagonize the effects of the corresponding antibodies (e.g., anticholinesterases, 3,4-diaminopyridine).^{42,43} One envisions a similar strategy in anti-NMDAR and perhaps other autoimmune encephalitis, in which the use of immunotherapy along with small molecules crossing the blood-brain barrier and directly antagonizing the antibody effects could represent a future treatment approach.

Different from anti-NMDAR encephalitis and other autoantigens of limbic encephalitis, which are synaptic receptors or cell membrane proteins, LGI1 is a secreted neuronal protein that has several binding partners, possibly organizing a trans-synaptic complex that includes the pre-synaptic ADAM23 and Kv1.1 potassium channels, and the postsynaptic ADAM22 and AMPAR.^{136,191} A previous study examining the synaptic effects of patients' LGI1 antibodies showed that they disrupted the interaction of LGI1 with ADAM22 and reversibly reduced the postsynaptic clusters of AMPAR *in vitro* in rat hippocampal neurons.⁶⁰ The antibodies also altered the interaction of LGI1 with a soluble construct of ADAM23⁶⁰ but the effects on Kv1.1 potassium channels and plasticity, and whether patients' antibodies can impair memory in an animal model were not reported.

Having learned how to model in mice the symptoms of NMDAR encephalitis, I undertook the challenge to develop a model of LGI1 antibody-mediated symptoms examining the potential antibody-mediated alterations at both, the pre- and post-synaptic levels (Kv1.1 and AMPAR). Indeed, considering the interaction of LGI1 with both ADAM23 and ADAM22, I reasoned that patients' antibodies would have a downstream effect not only on AMPAR but also on the Kv1.1 potassium channels. Moreover, since anti-LGI1 encephalitis usually results in a treatable hippocampal syndrome with difficulty in forming new memories,^{110,112} I postulated that patients' antibodies would alter memory in a mouse model of cerebroventricular transfer of the antibodies.

In this study, which is currently under review, I did not have enough CSF from patients to perform all experiments, and therefore, I used IgG purified from patients' serum. I found that all patients' samples, but not controls prevented the binding of LGI1 to ADAM23, but only 60% to ADAM22. Using deletion constructs of LGI1 I found obligate binding of patients' antibodies

to the leucine rich repeat domain and less frequent binding to the epitempin domain (these domains are shown in Figure 10). Moreover, passive cerebroventricular transfer of patients' IgG antibodies to mice led to prolonged but reversible deficits in memory function. I then performed confocal analysis of hippocampal brain slices which showed a reduction of total and synaptic levels of Kv1.1 following the time course of animal memory deficits, with complete recovery 33 days after the end of the infusion. I noted that the reduction of AMPA receptors was present in a time-displaced manner following the loss of Kv1.1. In collaborative studies (Dr. C Geis from Jena, Germany, and M Radosevic from Dr. Dalmau's lab) we then used acute slice preparations of hippocampus to perform patch-clamp analysis from dentate gyrus granule cells; these studies revealed neuronal hyperexcitability with increased glutamatergic transmission and higher presynaptic release probability most likely induced by the reduced expression of Kv1.1. Analysis of synaptic plasticity by recording field potentials in the CA1 region of the hippocampus showed a severe impairment of long-term potentiation consistent with the memory deficits observed in the mice model, as well as in patients harboring these antibodies.

An important question raised by these findings is whether the LGI1 antibody-mediated increase of excitatory synaptic transmission is caused by alterations at pre- or post-synaptic level. At the synaptic level, findings in the genetic LGI1 deficient models as well as in our immune-mediated model make difficult to explain how reduced AMPAR function associates with epileptic seizures in patients with anti-LGI1 encephalitis. Homeostatic downregulation of postsynaptic AMPAR in response to an ongoing presynaptic hyperexcitability has been proposed but it remains speculative and is not yet supported by experimental evidence.¹²³ This hypothesis however, is in line with the observation that patients' LGI1 antibodies caused a reduction of Kv1.1 expression (from day 5 after onset of antibody infusion) that preceded the reduction of AMPAR clusters (from day 13) in the hippocampus of infused mice. It is known that presynaptic Kv1.1 potassium channel inactivation enhances release probability as a result of an increased and prolonged depolarization, increased Ca²⁺ influx, and subsequent potentiation of excitatory transmission.¹²⁰ Indeed, recent studies in slice cultures or acute slices of LGI1 knockout mice showed evidence for enhanced neuronal excitability, increased release of presynaptic glutamate, and enlarged excitatory synaptic drive.^{122,123}

Overall, my studies in **paper 6** using a model of passive-transfer of patients' LGI1 antibodies identified several underlying pathophysiological mechanisms that are in good agreement with previous observations in LGI1 deficient model systems. Our findings point towards an antibody-mediated disruption of LGI1-associated pathways that affect LGI1 signaling via pre- and postsynaptic mechanisms, resulting in synaptic hyperexcitability, decreased plasticity, and memory deficits.

7. CONCLUSIONS

General Conclusions

Among the many patients with encephalitis of unclear etiology, there are subgroups that are immune-mediated. The selection of patients with similar clinical features suspected to be immune-mediated is useful to identify new disorders associated with highly specific antibodies against neuronal cell-surface or synaptic antigens. Although the mechanisms that underlie the antibody effects are probably different for each antibody, my studies show they are usually pathogenic and likely contribute to patients' symptoms.

Specific Conclusions 1

- Anti-GABA_AR encephalitis is a new type of autoimmune encephalitis that affects children and adults, associates with prominent seizures and characteristic MRI abnormalities, and is treatable with immunotherapy. In some patients the immune response is triggered by the presence of a tumor.
- Anti-neurexin-3 α encephalitis is another form of autoimmune encephalitis that often occurs with seizures and is treatable with immunotherapy. No tumor association has been identified.

Specific Conclusions 2

- Immunoprecipitation of the target antigen of patients with anti-GABA_AR encephalitis demonstrated that the epitopes are mainly located in the α 1 and β 3 subunits, and less frequently in the γ 2 subunit. Whereas the antibodies against α 1 and β 3 subunits are disease relevant, the presence of additional antibodies to γ 2 does not modify the disease phenotype. Patients' GABA_AR antibodies cause a decrease in the total and synaptic levels of GABA_AR clusters, supporting their pathogenicity.
- Immunoprecipitation of the target antigen of patients with anti-neurexin-3 α encephalitis demonstrated that the target epitopes are specifically located in neurexin-3 α , but not in its post-synaptic ligand LRRTM2. Patients' antibodies cause a reduction of the total number of synapses and the pre/postsynaptic proteins bassoon/homer1, supporting their pathogenicity.
- Recombinant expression of the indicated subunits of the GABA_AR and neurexin-3 α in HEK293 cells, can be used as a test to diagnose patients with these autoimmune encephalitis.

Specific Conclusions 3

- The infusion of patients' NMDAR antibodies into the cerebroventricular system of mice, cause memory deficits, anhedonia, and depressive-like behavior. The infused antibodies specifically bind to brain NMDAR resulting in a highly specific reduction of the density of these receptors at synaptic and extrasynaptic levels. The behavioral and molecular effects caused by patients' antibodies are reversible upon stopping the infusion of antibodies. This model fulfills the Witebsky's criteria for antibody-mediated disease, and therefore the findings provide an animal model of antibody-mediated impairment of memory and behavior.
- The administration of ephrin-B2 antagonizes the pathogenic effects of patients' NMDAR antibodies in all the investigated paradigms, including memory, depressive-like behavior,

density of cell-surface and synaptic NMDAR and EphB2, and long-term synaptic plasticity. These findings reveal a strategy beyond immunotherapy to antagonize patients' antibody effects.

- The antibodies of patients with anti-LGI1 encephalitis abrogate the binding of the neuronal secreted LGI1 with the presynaptic ADAM23 and with the postsynaptic ADAM22.
- The cerebroventricular infusion of patients' LGI1 antibodies in mice cause protracted memory deficits, together with a decrease of presynaptic Kv1.1 potassium channels and post-synaptic AMPAR. The effects occur in association with an impairment of synaptic plasticity and an increase of neuronal excitability, which are in line with the models of genetic depletion of LGI1.

8. REFERENCES

- 1 Granerod J, Ambrose HE, Davies NWS, *et al.* Causes of encephalitis and differences in their clinical presentations in England: A multicentre, population-based prospective study. *Lancet Infect Dis* 2010; **10**: 835–44.
- 2 Venkatesan A, Tunkel AR, Bloch KC, *et al.* Case definitions, diagnostic algorithms, and priorities in encephalitis: Consensus statement of the international encephalitis consortium. *Clin Infect Dis* 2013; **57**: 1114–28.
- 3 Solomon T, Michael BD, Smith PE, *et al.* Management of suspected viral encephalitis in adults - Association of British Neurologists and British Infection Association National Guidelines. *J Infect* 2012; **64**: 347–73.
- 4 Ances B, Vitaliani R, Taylor RA, *et al.* Treatment-responsive limbic encephalitis identified by neuropil antibodies: MRI and PET correlates. *Brain* 2005; **128**: 1764–77.
- 5 Singh TD, Fugate JE, Rabinstein AA. The spectrum of acute encephalitis: causes, management, and predictors of outcome. *Neurology* 2015; **84**: 359–66.
- 6 Thakur KT, Motta M, Asemota AO, *et al.* Predictors of outcome in acute encephalitis. *Neurology* 2013; **81**: 793–800.
- 7 Byun JI, Lee ST, Jung KH, *et al.* Prevalence of antineuronal antibodies in patients with encephalopathy of unknown etiology: Data from a nationwide registry in Korea. *J Neuroimmunol* 2016; **293**: 34–8.
- 8 Tunkel AR, Glaser CA, Bloch KC, *et al.* The management of encephalitis: clinical practice guidelines by the Infectious Diseases Society of America. *Clin Infect Dis* 2008; **47**: 303–27.
- 9 Lancaster E. The Diagnosis and Treatment of Autoimmune Encephalitis. *J Clin Neurol* 2016; **12**: 1.
- 10 Leyppoldt F, Armangue T, Dalmau J. Autoimmune encephalopathies. *Ann N Y Acad Sci* 2015; **1338**: 94–114.
- 11 Chapman SJ, Hill AVS. Human genetic susceptibility to infectious disease. *Nat Rev Genet* 2012; **13**: 175–88.
- 12 Neilson DE, Adams MD, Orr CMD, *et al.* Infection-Triggered Familial or Recurrent Cases of Acute Necrotizing Encephalopathy Caused by Mutations in a Component of the Nuclear Pore, RANBP2. *Am J Hum Genet* 2009; **84**: 44–51.
- 13 Denier C, Balu L, Husson B, *et al.* Familial acute necrotizing encephalopathy due to mutation in the RANBP2 gene. *J Neurol Sci* 2014; **345**: 236–8.
- 14 Mørk N, Kofod-Olsen E, Sørensen KB, *et al.* Mutations in the TLR3 signaling pathway and beyond in adult patients with herpes simplex encephalitis. *Genes Immun* 2015; **16**: 552–66.
- 15 Zhang S-Y, Jouanguy E, Ugolini S, *et al.* TLR3 Deficiency in Patients with Herpes Simplex Encephalitis. *Science (80-)* 2007; **317**: 1522–7.
- 16 Guo Y, Audry M, Ciancanelli M, *et al.* Herpes simplex virus encephalitis in a patient with complete TLR3 deficiency: TLR3 is otherwise redundant in protective immunity. *J Exp Med* 2011; **208**: 2083–98.
- 17 Bigham AW, Buckingham KJ, Husain S, *et al.* Host genetic risk factors for West Nile virus infection and disease progression. *PLoS One* 2011; **6**: e24745.

- 18 Vora NM, Holman RC, Mehal JM, Steiner CA, Blanton J, Sejvar J. Burden of encephalitis-associated hospitalizations in the United States, 1998-2010. *Neurology* 2014; **82**: 443–51.
- 19 Dalmau J, Tüzün E, Wu H, *et al.* Paraneoplastic anti- N -methyl-D-aspartate receptor encephalitis associated with ovarian teratoma. *Ann Neurol* 2007; **61**: 25–36.
- 20 Dalmau J, Geis C, Graus F. Autoantibodies to Synaptic Receptors and Neuronal Cell Surface Proteins in Autoimmune Diseases of the Central Nervous System. *Physiol Rev* 2017; **97**: 839–87.
- 21 Darnell RB, Posner JB. Paraneoplastic Syndromes Involving the Nervous System. *N Engl J Med* 2003; **349**: 1543–54.
- 22 Darnell RB, Posner JB. Paraneoplastic Syndromes Affecting the Nervous System. *Semin Oncol* 2006; **33**: 270–98.
- 23 Rosenfeld MR, Dalmau JO. Paraneoplastic Disorders of the CNS and Autoimmune Synaptic Encephalitis. 2012; : 366–83.
- 24 Graus F, Titulaer MJ, Balu R, *et al.* A clinical approach to diagnosis of autoimmune encephalitis. *Lancet Neurol* 2016; **15**: 391–404.
- 25 Gresa-arribas N, Titulaer MJ, Torrents A, *et al.* Diagnosis and significance of antibody titers in anti-NMDA receptor encephalitis, a retrospective study. *Lancet Neurol* 2014; **13**: 167–77.
- 26 Drachman DB, Angus CW, Adams RN, Michelson JD, Hoffman GJ. Myasthenic Antibodies Cross-Link Acetylcholine Receptors to Accelerate Degradation. *N Engl J Med* 1978; **298**: 1116–22.
- 27 Drachman DB, Adams RN, Josifek LF, Self SG. Functional activities of autoantibodies to acetylcholine receptors and the clinical severity of myasthenia gravis. *N Engl J Med* 1982; **307**: 769–75.
- 28 Nagel A, Engel AG, Lang B, Newsom-Davis J, Fukuoka T. Lambert-eaton myasthenic syndrome IgG depletes presynaptic membrane active zone particles by antigenic modulation. *Ann Neurol* 1988; **24**: 552–8.
- 29 Waterman SA, Lang B, Newsom-Davis J. Effect of Lambert-Eaton myasthenic syndrome antibodies on autonomic neurons in the mouse. 1997; **42**: 147–56.
- 30 Dalmau J, Rosenfeld MR. Paraneoplastic syndromes of the CNS. *J Neurol* 2008; **257**: 327–40.
- 31 Tanaka K, Tanaka M, Igarashi S, Onodera O, Miyatake T, Tsuji S. Trial to establish an animal model of paraneoplastic cerebellar degeneration with anti-Yo antibody. *Clin Neurol Neurosurg* 1995; **97**: 101–5.
- 32 Bernal F, Graus F, Pifarré À, Saiz A, Benyahia B, Ribalta T. Immunohistochemical analysis of anti-Hu-associated paraneoplastic encephalomyelitis. *Acta Neuropathol* 2002; **103**: 509–15.
- 33 Bien CG, Vincent A, Barnett MH, *et al.* Immunopathology of autoantibody-associated encephalitides: Clues for pathogenesis. *Brain* 2012; **135**: 1622–38.
- 34 Blumenthal DT, Salzman KL, Digre KB, Jensen RL, Dunson WA, Dalmau J. Early pathologic findings and long-term improvement in anti-Ma2-associated encephalitis. *Neurology* 2006; **67**: 146–9.
- 35 Graus F, Vega F, Delattre JY, *et al.* Plasmapheresis and antineoplastic treatment in CNS paraneoplastic syndromes with antineuronal autoantibodies. *Neurology* 1992; **42**: 536–40.

- 36 Keime-Guibert F, Graus F, Fleury a, *et al.* Treatment of paraneoplastic neurological syndromes with antineuronal antibodies (Anti-Hu, anti-Yo) with a combination of immunoglobulins, cyclophosphamide, and methylprednisolone. *J Neurol Neurosurg Psychiatry* 2000; **68**: 479–82.
- 37 Rojas I, Graus F, Keime-Guibert F, *et al.* Long-term clinical outcome of paraneoplastic cerebellar degeneration and anti-Yo antibodies. *Neurology* 2000; **55**: 713–5.
- 38 Roberts WK, Deluca IJ, Thomas A, *et al.* Patients with lung cancer and paraneoplastic Hu syndrome harbor HuD-specific type 2 CD8+T cells. *J Clin Invest* 2009; **119**: 2042–51.
- 39 Santomasso BD, Roberts WK, Thomas A, *et al.* A T-cell receptor associated with naturally occurring human tumor immunity. *Proc Natl Acad Sci U S A* 2007; **104**: 19073–8.
- 40 Pellkofer H, Schubart AS, H??ftberger R, *et al.* Modelling paraneoplastic CNS disease: T-cells specific for the onconeural antigen PNMA1 mediate autoimmune encephalomyelitis in the rat. *Brain* 2004; **127**: 1822–30.
- 41 Musunuru K, Darnell RB. PARANEOPLASTIC NEUROLOGIC DISEASE ANTIGENS : RNA-Binding Proteins and Signaling Proteins in Neuronal Degeneration. *Annu Rev Neurosci* 2001; **24**: 239–62.
- 42 Drachman DB. Myasthenia gravis. *N Engl J Med* 1994; **330**: 1797–810.
- 43 Wirtz PW, Titulaer MJ, Gerven JM van, Verschuuren JJ. 3,4-diaminopyridine for the treatment of Lambert–Eaton myasthenic syndrome. *Expert Rev Clin Immunol* 2010; **6**: 867–74.
- 44 Ariño H, Gresa-Arribas N, Blanco Y, *et al.* Cerebellar Ataxia and Glutamic Acid Decarboxylase Antibodies: Immunologic Profile and Long-term Effect of Immunotherapy. *JAMA Neurol* 2014; **71**: 1009–16.
- 45 Dinkel K, Meinck H-M, Jury KM, Karges W, Richter W. Inhibition of γ -Aminobutyric Acid Synthesis by Glutamic Acid Decarboxylase Autoantibodies in Stiff-Man Syndrome. *Ann Neurol* 1998; **44**: 194–201.
- 46 Ishida K, Mitoma H, Song SY, *et al.* Selective suppression of cerebellar GABAergic transmission by an autoantibody to glutamic acid decarboxylase. *Ann Neurol* 1999; **46**: 263–7.
- 47 Mitoma H, Song SY, Ishida K, Yamakuni T, Kobayashi T, Mizusawa H. Presynaptic impairment of cerebellar inhibitory synapses by an autoantibody to glutamate decarboxylase. *J Neurol Sci* 2000; **175**: 40–4.
- 48 Gresa-Arribas N, Ariño H, Martínez-Hernández E, *et al.* Antibodies to inhibitory synaptic proteins in neurological syndromes associated with glutamic acid decarboxylase autoimmunity. *PLoS One* 2015; **10**: 1–14.
- 49 Dalmau J, Graus F. Antibody-Mediated Encephalitis. *N Engl J Med* 2018; **378**: 840–51.
- 50 Vincent A, Buckley C, Schott JM, *et al.* Potassium channel antibody-associated encephalopathy: A potentially immunotherapy-responsive form of limbic encephalitis. *Brain* 2004; **127**: 701–12.
- 51 Buckley C, Oger J, Clover L, *et al.* Potassium channel antibodies in two patients with reversible limbic encephalitis. *Ann Neurol* 2001; **50**: 73–8.
- 52 Vitaliani R, Mason W, Ances B, Zwerdling T, Jiang Z, Dalmau J. Paraneoplastic Encephalitis, Psychiatric Symptoms, and Hypoventilation in Ovarian Teratoma. *Ann Neurol* 2005; **58**: 594–604.
- 53 Boronat A, Gelfand JM, Gresa-arribas N, *et al.* Encephalitis and antibodies to DPPX, a subunit of

- Kv4.2 potassium channels. *Ann Neurol* 2013; **73**: 120–8.
- 54 Lai M, Huijbers MGM, Lancaster E, *et al.* Investigation of LGI1 as the antigen in limbic encephalitis previously attributed to potassium channels: a case series. *Lancet Neurol* 2010; **9**: 776–85.
- 55 Lancaster E, Huijbers MGM, Bar V, *et al.* Investigations of caspr2, an autoantigen of encephalitis and neuromyotonia. *Ann Neurol* 2011; **69**: 303–11.
- 56 Lancaster E, Lai M, Peng X, *et al.* Antibodies to the GABA(B) receptor in limbic encephalitis with seizures: case series and characterisation of the antigen. *Lancet Neurol* 2010; **9**: 67–76.
- 57 Dalmau J, Gleichman AJ, Hughes EG, *et al.* Anti-NMDA-receptor encephalitis: case series and analysis of the effects of antibodies. *Lancet Neurol* 2008; **7**: 1091–8.
- 58 Hughes EG, Peng X, Gleichman AJ, *et al.* Cellular and synaptic mechanisms of anti-NMDA receptor encephalitis. *J Neurosci* 2010; **30**: 5866–75.
- 59 Mikasova L, De Rossi P, Bouchet D, *et al.* Disrupted surface cross-talk between NMDA and Ephrin-B2 receptors in anti-NMDA encephalitis. *Brain* 2012; **135**: 1606–21.
- 60 Ohkawa T, Fukata Y, Yamasaki M, *et al.* Autoantibodies to epilepsy-related LGI1 in limbic encephalitis neutralize LGI1-ADAM22 interaction and reduce synaptic AMPA receptors. *J Neurosci* 2013; **33**: 18161–74.
- 61 Pinatel D, Hivert B, Boucraut J, *et al.* Inhibitory axons are targeted in hippocampal cell culture by anti-Caspr2 autoantibodies associated with limbic encephalitis. *Front Cell Neurosci* 2015; **9**: 265.
- 62 Carvajal-González A, Leite MI, Waters P, *et al.* Glycine receptor antibodies in PERM and related syndromes: Characteristics, clinical features and outcomes. *Brain* 2014; **137**: 2178–92.
- 63 Sabater L, Gaig C, Gelpi E, *et al.* A novel non-rapid-eye movement and rapid-eye-movement parasomnia with sleep breathing disorder associated with antibodies to IgLON5: a case series, characterisation of the antigen, and post-mortem study. *Lancet Neurol* 2014; **13**: 575–86.
- 64 Peng X, Hughes EG, Moscato EH, Parsons TD, Dalmau J, Balice-Gordon RJ. Cellular plasticity induced by anti- α -amino-3-hydroxy-5-methyl-4-isoxazolepropionic acid (AMPA) receptor encephalitis antibodies. *Ann Neurol* 2015; **77**: 381–98.
- 65 Hara M, Ariño H, Petit-Pedrol M, *et al.* DPPX antibody-associated encephalitis: Main syndrome and antibody effects. *Neurology* 2017; **88**: 1340–8.
- 66 Sinmaz N, Tea F, Pilli D, *et al.* Dopamine-2 receptor extracellular N-terminus regulates receptor surface availability and is the target of human pathogenic antibodies from children with movement and psychiatric disorders. *Acta Neuropathol Commun* 2016; **4**: 126.
- 67 Spatola M, Sabater L, Planaguma J, *et al.* Encephalitis with mGluR5 antibodies: Symptoms and antibody effects. *Neurology* 2018; **90**: e1964–72.
- 68 Petit-Pedrol M, Armangue T, Peng X, *et al.* Encephalitis with refractory seizures, status epilepticus, and antibodies to the GABAA receptor: a case series, characterisation of the antigen, and analysis of the effects of antibodies. *Lancet Neurol* 2014; **13**: 276–86.
- 69 Gresa-Arribas N, Planagumà J, Petit-Pedrol M, *et al.* Human neurexin-3 α antibodies associate with encephalitis and alter synapse development. *Neurology* 2016; **86**: 2235–42.
- 70 Pinto A, Gillard S, Moss F, *et al.* Human autoantibodies specific for the alpha1A calcium channel

- subunit reduce both P-type and Q-type calcium currents in cerebellar neurons. *Proc Natl Acad Sci U S A* 1998; **95**: 8328–33.
- 71 Liao YJ, Safa P, Chen Y, Sobel RA, Boyden ES, Tsien RW. Anti-Ca²⁺ channel antibody attenuates Ca²⁺ currents and mimics cerebellar ataxia in in Vivo. *PNAS* 2008; **105**: 2705–10.
- 72 Martín-García E, Mannara F, Gutiérrez-Cuesta J, *et al.* Intrathecal injection of P/Q type voltage-gated calcium channel antibodies from paraneoplastic cerebellar degeneration cause ataxia in mice. *J Neuroimmunol* 2013; **261**: 53–9.
- 73 Coesmans M, Sillevs Smitt PA, Linden DJ, *et al.* Mechanisms underlying cerebellar motor deficits due to mGluR1-autoantibodies. *Ann Neurol* 2003; **53**: 325–36.
- 74 Sillevs Smitt P, Kinoshita A, Leeuw B de, *et al.* Paraneoplastic cerebellar ataxia due to autoantibodies against a Glutamate receptor. *N Engl J Med* 2000; **342**: 21–7.
- 75 Werner C, Pauli M, Doose S, *et al.* Human autoantibodies to amphiphysin induce defective presynaptic vesicle dynamics and composition. *Brain* 2016; **139**: 365–79.
- 76 Sommer C, Weishaupt A, Brinkhoff J, *et al.* Paraneoplastic stiff-person syndrome: Passive transfer to rats by means of IgG antibodies to amphiphysin. *Lancet* 2005; **365**: 1406–11.
- 77 Gable MS, Sheriff H, Dalmau J, Tilley DH, Glaser CA. The frequency of autoimmune N-methyl-D-aspartate receptor encephalitis surpasses that of individual viral etiologies in young individuals enrolled in the california encephalitis project. *Clin Infect Dis* 2012; **54**: 899–904.
- 78 Pruss H, Dalmau J, Harms L, *et al.* Retrospective analysis of NMDA receptor antibodies in encephalitis of unknown origin. *Neurology* 2010; **75**: 1735–9.
- 79 Titulaer M, McCracken L, Gabilondo I. Treatment and prognostic factors for long-term outcome in patients with anti-NMDA receptor encephalitis: an observational cohort study. *Lancet Neurol* 2013; **12**: 157–65.
- 80 Armangue T, Titulaer MJ, Málaga I, *et al.* Pediatric anti-N-methyl-D-aspartate receptor encephalitis - Clinical analysis and novel findings in a series of 20 patients. *J Pediatr* 2013; **162**: 850–856.e2.
- 81 Titulaer MJ, Mccracken L, Gabilondo I, *et al.* Late-onset anti – NMDA receptor encephalitis. *Neurology* 2013; **81**: 1058–63.
- 82 Viacoz A, Desestret V, Ducray F, *et al.* Clinical specificities of adult male patients with NMDA receptor antibodies encephalitis. *Neurology* 2014; **82**: 556–63.
- 83 Florance NR, Davis RL, Lam C, *et al.* Anti-N-methyl-D-aspartate receptor (NMDAR) encephalitis in children and adolescents. *Ann Neurol* 2009; **66**: 11–8.
- 84 Schmitt SE, Pargeon K, Frechette ES, Hirsch LJ, Dalmau J, Friedman D. Extreme delta brush: a unique EEG pattern in adults with anti-NMDA receptor encephalitis. *Neurology* 2012; **79**: 1094–100.
- 85 Tüzün E, Zhou L, Baehring JM, Bannykh S, Rosenfeld MR, Dalmau J. Evidence for antibody-mediated pathogenesis in anti-NMDAR encephalitis associated with ovarian teratoma. *Acta Neuropathol* 2009; **118**: 737–43.
- 86 Irani SR, Bera K, Waters P, *et al.* N-methyl-D-aspartate antibody encephalitis: temporal progression of clinical and paraclinical observations in a predominantly non-paraneoplastic disorder of both sexes. *Brain* 2010; **133**: 1655–67.

- 87 Dalmau PJ, Lancaster E, Martinez-Hernandez E, Rosenfeld MR, Balice-Gordon R. Clinical experience and laboratory investigations in patients with anti-NMDAR encephalitis. *Lancet Neurol* 2011; **10**: 63–74.
- 88 Armangue T, Erro ME, Portilla- JC, Muñoz-cabello B, González-gutiérrez- L, González G. Autoimmune post – herpes simplex encephalitis of adults and teenagers. *Neurology* 2015; **85**: 1736–43.
- 89 Iizuka T, Sakai F, Ide T, *et al.* Anti-NMDA receptor encephalitis in Japan: long-term outcome without tumor removal. *Neurology* 2008; **70**: 504–11.
- 90 Mueller SH, Färber A, Prüss H, *et al.* Genetic predisposition in anti-LGI1 and anti-NMDA receptor encephalitis. *Ann Neurol* 2018; **83**: 863–9.
- 91 Granger AJ, Gray JA, Lu W, Nicoll RA. Genetic analysis of neuronal ionotropic glutamate receptor subunits. *J Physiol* 2011; **589**: 4095–101.
- 92 Malenka RC. Synaptic plasticity in the hippocampus: LTP and LTD. *Cell* 1994; **78**: 535–8.
- 93 Bliss TVP, Collingridge GL. A synaptic model of memory: long-term potentiation in the hippocampus. *Nature* 1993; **361**: 31–9.
- 94 Davis S, Butcher SP, Morris RG. The NMDA receptor antagonist D-2-amino-5-phosphonopentanoate (D-AP5) impairs spatial learning and LTP in vivo at intracerebral concentrations comparable to those that block LTP in vitro. *J Neurosci* 1992; **12**: 21–34.
- 95 Kapur S, Seeman P. NMDA receptor antagonists ketamine and PCP have direct effects on the dopamine D2 and serotonin 5-HT2 receptors—implications for models of schizophrenia. *Mol Psychiatry* 2002; **7**: 837–44.
- 96 Morris RGM, Anderson E, Lynch GS, Baudry M. Selective impairment of learning and blockade of long-term potentiation by an N-methyl-D-aspartate receptor antagonist, AP5. *Nature* 1986; **319**: 774–6.
- 97 Stringer JL, Greenfield LJ, Hackett JT, Guyenet PG. Blockade of long-term potentiation by phencyclidine and sigma opiates in the hippocampus in vivo and in vitro. *Brain Res* 1983; **280**: 127–38.
- 98 Luby ED, Cohen BD, Rosenbaum G, Gottlieb JS, Kelley R. Study of a new schizophrenomimetic drug; sernyl. *AMA Arch Neurol Psychiatry* 1959; **81**: 363–9.
- 99 Bailey K. Identification of a street drug as N-ethyl-1-phenylcyclohexylamine, a phencyclidine analog. *J Pharm Sci* 1978; **67**: 885–6.
- 100 Castellani S, Giannini AJ, Adams PM. Physostigmine and haloperidol treatment of acute phencyclidine intoxication. *Am J Psychiatry* 1982; **139**: 508–10.
- 101 Krystal JH, Karper LP, Seibyl JP, *et al.* Subanesthetic effects of the noncompetitive NMDA antagonist, ketamine, in humans. Psychotomimetic, perceptual, cognitive, and neuroendocrine responses. *Arch Gen Psychiatry* 1994; **51**: 199–214.
- 102 Weiner AL, Vieira L, McKay CA, Bayer MJ. Ketamine abusers presenting to the emergency department: a case series. *J Emerg Med* 2000; **18**: 447–51.
- 103 Forrest D, Yuzaki M, Soares HD, *et al.* Targeted disruption of NMDA receptor 1 gene abolishes NMDA response and results in neonatal death. *Neuron* 1994; **13**: 325–38.

- 104 Tsien JZ, Huerta PT, Tonegawa S. The essential role of hippocampal CA1 NMDA receptor-dependent synaptic plasticity in spatial memory. *Cell* 1996; **87**: 1327–38.
- 105 Mohn AR, Gainetdinov RR, Caron MG, Koller BH. Mice with reduced NMDA receptor expression display behaviors related to schizophrenia. *Cell* 1999; **98**: 427–36.
- 106 Moscato EH, Peng X, Jain A, Parsons TD, Dalmau J, Balice-Gordon RJ. Acute mechanisms underlying antibody effects in anti-N-methyl-D-aspartate receptor encephalitis. *Ann Neurol* 2014; **76**: 108–19.
- 107 Rose NR, Bona C. Defining criteria for autoimmune diseases (Witebsky's postulates revisited). *Immunol Today* 1993; **14**: 426–30.
- 108 Witebsky E, Rose NR, Terplan K, Paine JR, Egan RW. Chronic thyroiditis and autoimmunization. *J Am Med Assoc* 1957; **164**: 1439–47.
- 109 Irani SR, Alexander S, Waters P, *et al.* Antibodies to Kv1 potassium channel-complex proteins leucine-rich, glioma inactivated 1 protein and contactin-associated protein-2 in limbic encephalitis, Morvan's syndrome and acquired neuromyotonia. *Brain* 2010; **133**: 2734–48.
- 110 van Sonderen A, Thijs RD, Coenders EC, *et al.* Anti-LGI1 encephalitis: Clinical syndrome and long-term follow-up. *Neurology* 2016; **87**: 1449–56.
- 111 Iranzo A, Graus F, Clover L, *et al.* Rapid eye movement sleep behavior disorder and potassium channel antibody-associated limbic encephalitis. *Ann Neurol* 2006; **59**: 178–81.
- 112 Ariño H, Armangue T, Petit-pedrol M, *et al.* Anti-LGI1-associated cognitive impairment. *Neurology* 2016; **87**: 759–765.
- 113 Finke C, Prüss H, Heine J, *et al.* Evaluation of cognitive deficits and structural hippocampal damage in encephalitis with leucine-rich, glioma-inactivated 1 antibodies. *JAMA Neurol* 2017; **74**: 50–9.
- 114 Kim TJ, Lee ST, Moon J, *et al.* Anti-LGI1 encephalitis is associated with unique HLA subtypes. *Ann Neurol* 2017; **81**: 183–92.
- 115 van Sonderen A, Roelen DL, Stoop JA, *et al.* Anti-LGI1 encephalitis is strongly associated with HLA-DR7 and HLA-DRB4. *Ann Neurol* 2017; **81**: 193–8.
- 116 Zhou Y-D, Zhang D, Ozkaynak E, *et al.* Epilepsy Gene LGI1 Regulates Postnatal Developmental Remodeling of Retinogeniculate Synapses. *J Neurosci* 2012; **32**: 903–10.
- 117 Zhou Y-D, Lee S, Jin Z, Wright M, Smith SEP, Anderson MP. Arrested maturation of excitatory synapses in autosomal dominant lateral temporal lobe epilepsy. *Nat Med* 2009; **15**: 1208–14.
- 118 Caleo M. Epilepsy: synapses stuck in childhood. *Nat Med* 2009; **15**: 1126–7.
- 119 Owuor K, Harel NY, Englot DJ, Hisama F, Blumenfeld H, Strittmatter SM. LGI1-associated epilepsy through altered ADAM23-dependent neuronal morphology. *Mol Cell Neurosci* 2009; **42**: 448–57.
- 120 Geiger JRP, Jonas P. Dynamic Control of Presynaptic Ca²⁺ Inflow by Fast-Inactivating K⁺ Channels in Hippocampal Mossy Fiber Boutons. *Neuron* 2000; **28**: 927–39.
- 121 Schulte U, Thumfart JO, Klöcker N, *et al.* The epilepsy-linked Lgi1 protein assembles into presynaptic Kv1 channels and inhibits inactivation by KvB1. *Neuron* 2006; **49**: 697–706.
- 122 Boillot M, Lee C-Y, Allene C, Leguern E, Baulac S, Rouach N. LGI1 acts presynaptically to regulate excitatory synaptic transmission during early postnatal development. *Sci Rep* 2016; **6**: 21769.

- 123 Seagar M, Russier M, Caillard O, *et al.* LGI1 tunes intrinsic excitability by regulating the density of axonal Kv1 channels. *Proc Natl Acad Sci* 2017; **114**: 7719–24.
- 124 Henley JM, Wilkinson KA. AMPA receptor trafficking and the mechanisms underlying synaptic plasticity and cognitive aging. *Dialogues Clin Neurosci* 2013; **15**: 11–27.
- 125 Makino H, Malinow R. AMPA receptor incorporation into synapses during LTP: the role of lateral movement and exocytosis. *Neuron* 2009; **64**: 381–90.
- 126 Whitlock JR, Heynen AJ, Shuler MG, Bear MF. Learning induces long-term potentiation in the hippocampus. *Science* 2006; **313**: 1093–7.
- 127 Fukata Y, Adesnik H, Iwanaga T, *et al.* Epilepsy-related ligand/receptor complex LGI1 and ADAM22 regulate synaptic transmission. *Science (80-)* 2006; **313**: 1792–5.
- 128 Leonardi E, Adreazza S, Vanin S, *et al.* A computational model of the LGI1 protein suggests a common binding site for ADAM proteins. *PLoS One* 2011; **6**: e18142.
- 129 Kegel L, Aunin E, Meijer D, Bermingham JR. LGI Proteins in the Nervous System. *ASN Neuro* 2013; **5**: 167–81.
- 130 Yamagata A, Miyazaki Y, Yokoi N, *et al.* Structural basis of epilepsy-related ligand–receptor complex LGI1–ADAM22. *Nat Commun* 2018; **9**: 1546.
- 131 Sagane K, Ishihama Y, Sugimoto H. LGI1 and LGI4 bind to ADAM22, ADAM23 and ADAM11. *Int J Biol Sci* 2008; **4**: 387–96.
- 132 Sagane K, Hayakawa K, Kai J, *et al.* Ataxia and peripheral nerve hypomyelination in ADAM22-deficient mice. *BMC Neurosci* 2005; **6**: 33.
- 133 Irani SR, Pettingill P, Kleopa K a, *et al.* Morvan syndrome: clinical and serological observations in 29 cases. *Ann Neurol* 2012; **72**: 241–55.
- 134 Huijbers MG, Plomp JJ, van der Maarel SM, Verschuuren JJ. IgG4-mediated autoimmune diseases: A niche of antibody-mediated disorders. *Ann N Y Acad Sci* 2018; **1413**: 92–103.
- 135 Huijbers MG, Querol LA, Niks EH, *et al.* The expanding field of IgG4-mediated neurological autoimmune disorders. *Eur J Neurol* 2015; **22**: 1151–61.
- 136 Fukata Y, Lovero KL, Iwanaga T, *et al.* Disruption of LGI1-linked synaptic complex causes abnormal synaptic transmission and epilepsy. *Proc Natl Acad Sci U S A* 2010; **107**: 3799–804.
- 137 van Sonderen A, Petit-Pedrol M, Dalmau J, Titulaer MJ. The value of LGI1, Caspr2 and voltage-gated potassium channel antibodies in encephalitis. *Nat Rev Neurol* 2017; **13**: 290–301.
- 138 Lai M, Hughes EG, Peng X, *et al.* AMPA receptor antibodies in limbic encephalitis alter synaptic receptor location. *Ann Neurol* 2009; **65**: 424–34.
- 139 Höftberger R, van Sonderen A, Leypoldt F, *et al.* Encephalitis and AMPA receptor antibodies: Novel findings in a case series of 22 patients. *Neurology* 2015; **84**: 2403–12.
- 140 Shepherd JD, Huganir RL. The Cell Biology of Synaptic Plasticity: AMPA Receptor Trafficking. *Annu Rev Cell Dev Biol* 2007; **23**: 613–43.
- 141 Fukata Y, Tzingounis A V, Trinidad JC, *et al.* Molecular constituents of neuronal AMPA receptors. *J Cell Biol* 2005; **169**: 399–404.

- 142 Dong H, O'Brien RJ, Fung ET, Lanahan AA, Worley PF, Huganir RL. GRIP: a synaptic PDZ domain-containing protein that interacts with AMPA receptors. *Nature* 1997; **386**: 279–84.
- 143 Perez JL, Khatri L, Chang C, Srivastava S, Osten P, Ziff EB. PICK1 targets activated protein kinase Calpha to AMPA receptor clusters in spines of hippocampal neurons and reduces surface levels of the AMPA-type glutamate receptor subunit 2. *J Neurosci* 2001; **21**: 5417–28.
- 144 Meng Y, Zhang Y, Jia Z. Synaptic transmission and plasticity in the absence of AMPA glutamate receptor GluR2 and GluR3. *Neuron* 2003; **39**: 163–76.
- 145 Jia Z, Agopyan N, Miu P, *et al.* Enhanced LTP in mice deficient in the AMPA receptor GluR2. *Neuron* 1996; **17**: 945–56.
- 146 Gleichman AJ, Panzer JA, Baumann BH, Dalmau J, Lynch DR. Antigenic and mechanistic characterization of anti-AMPA receptor encephalitis. *Ann Clin Transl Neurol* 2014; **1**: 180–9.
- 147 Sonderen A Van, Ariño H, Petit-pedrol M, *et al.* The clinical spectrum of Caspr2 antibody – associated disease. *Neurology* 2016; **87**: 521–8.
- 148 Poliak S, Gollan L, Martinez R, *et al.* Caspr2, a new member of the Neurexin superfamily, is localized at the juxtaparanodes of myelinated axons and associates with K⁺ channels. *Neuron* 1999; **24**: 1037–47.
- 149 Traka M, Goutebroze L, Denisenko N, *et al.* Association of TAG-1 with Caspr2 is essential for the molecular organization of juxtaparanodal regions of myelinated fibers. *J Cell Biol* 2003; **162**: 1161–72.
- 150 Rodenas-Cuadrado P, Ho J, Vernes SC. Shining a light on CNTNAP2: complex functions to complex disorders. *Eur J Hum Genet* 2014; **22**: 171–8.
- 151 Pippucci T, Licchetta L, Baldassari S, *et al.* Epilepsy with auditory features: A heterogeneous clinico-molecular disease. *Neurol Genet* 2015; **1**: e5.
- 152 Peñagarikano O, Abrahams BS, Herman EI, *et al.* Absence of CNTNAP2 leads to epilepsy, neuronal migration abnormalities, and core autism-related deficits. *Cell* 2011; **147**: 235–46.
- 153 Olsen AL, Lai Y, Dalmau J, Scherer SS, Lancaster E. Caspr2 autoantibodies target multiple epitopes. *Neurol Neuroimmunol NeuroInflammation* 2015; **2**: 1–9.
- 154 Patterson KR, Dalmau J, Lancaster E. Mechanisms of Caspr2 antibodies in autoimmune encephalitis and neuromyotonia. *Ann Neurol* 2018; **83**: 40–51.
- 155 Titulaer MJ, Höftberger R, Iizuka T, *et al.* Overlapping demyelinating syndromes and anti-N-methyl-D-aspartate receptor encephalitis. *Ann Neurol* 2014; **75**: 411–28.
- 156 Pisani F, Mastrototaro M, Rossi A, *et al.* Identification of two major conformational aquaporin-4 epitopes for neuromyelitis optica autoantibody binding. *J Biol Chem* 2011; **286**: 9216–24.
- 157 Yu X, Green M, Gilden D, Lam C, Bautista K, Bennett JL. Identification of peptide targets in neuromyelitis optica. *J Neuroimmunol* 2011; **236**: 65–71.
- 158 Magana SM, Matiello M, Pittock SJ, *et al.* Posterior reversible encephalopathy syndrome in neuromyelitis optica spectrum disorders. *Neurology* 2009; **72**: 712–7.
- 159 Höftberger R, Sepulveda M, Armangue T, *et al.* Antibodies to MOG and AQP4 in adults with neuromyelitis optica and suspected limited forms of the disease. *Mult Scler* 2015; **21**: 866–74.

- 160 Di Pauli F, Mader S, Rostasy K, *et al.* Temporal dynamics of anti-MOG antibodies in CNS demyelinating diseases. *Clin Immunol* 2011; **138**: 247–54.
- 161 Kim S-M, Woodhall MR, Kim J-S, *et al.* Antibodies to MOG in adults with inflammatory demyelinating disease of the CNS. *Neurol Neuroimmunol neuroinflammation* 2015; **2**: e163.
- 162 Kinoshita M, Nakatsuji Y, Kimura T, *et al.* Anti-aquaporin-4 antibody induces astrocytic cytotoxicity in the absence of CNS antigen-specific T cells. *Biochem Biophys Res Commun* 2010; **394**: 205–10.
- 163 Hinson SR, Pittock SJ, Lucchinetti CF, *et al.* Pathogenic potential of IgG binding to water channel extracellular domain in neuromyelitis optica. *Neurology* 2007; **69**: 2221–31.
- 164 Hinson SR, Roemer SF, Lucchinetti CF, *et al.* Aquaporin-4-binding autoantibodies in patients with neuromyelitis optica impair glutamate transport by down-regulating EAAT2. *J Exp Med* 2008; **205**: 2473–81.
- 165 Vincent T, Saikali P, Cayrol R, *et al.* Functional consequences of neuromyelitis optica-IgG astrocyte interactions on blood-brain barrier permeability and granulocyte recruitment. *J Immunol* 2008; **181**: 5730–7.
- 166 Saadoun S, Waters P, Bell BA, Vincent A, Verkman AS, Papadopoulos MC. Intra-cerebral injection of neuromyelitis optica immunoglobulin G and human complement produces neuromyelitis optica lesions in mice. *Brain* 2010; **133**: 349–61.
- 167 Ramanathan S, Dale RC, Brilot F. Anti-MOG antibody: The history, clinical phenotype, and pathogenicity of a serum biomarker for demyelination. *Autoimmun Rev* 2016; **15**: 307–24.
- 168 Planagumà J, Leyboldt F, Mannara F, *et al.* Human N-methyl D-aspartate receptor antibodies alter memory and behaviour in mice. *Brain* 2015; **138**: 94–109.
- 169 Zhou C, Ding L, Deel ME, Ferrick EA, Emeson RB, Gallagher MJ. Altered Intrathalamic GABAA Neurotransmission in a Mouse Model of a Human Genetic Absence Epilepsy Syndrome. *Neurobiol Dis* 2015; **73**: 407–17.
- 170 Tanaka M, Olsen RW, Medina MT, *et al.* Hyperglycosylation and Reduced GABA Currents of Mutated GABRB3 Polypeptide in Remitting Childhood Absence Epilepsy. *Am J Hum Genet* 2008; **82**: 1249–61.
- 171 Ohkawa T, Satake S, Yokoi N, *et al.* Identification and characterization of GABA(A) receptor autoantibodies in autoimmune encephalitis. *J Neurosci* 2014; **34**: 8151–63.
- 172 Simabukuro MM, Petit-Pedrol M, Castro LH, *et al.* GABA_A receptor and LGI1 antibody encephalitis in a patient with thymoma. *Neurol - Neuroimmunol Neuroinflammation* 2015; **2**: e73.
- 173 Spatola M, Petit-Pedrol M, Simabukuro MM, *et al.* Investigations in GABA_A receptor antibody-associated encephalitis. *Neurology* 2017; **88**: 1012–20.
- 174 Pettingill P, Kramer HB, Coebergh JA, *et al.* Antibodies to GABA_A receptor α 1 and γ 2 subunits: Clinical and serologic characterization. *Neurology* 2015; **84**: 1233–41.
- 175 Missler M, Zhang W, Rohlmann A, *et al.* α -Neurexins couple Ca²⁺ channels to synaptic vesicle exocytosis. *Nature* 2003; **423**: 939–48.
- 176 Gauthier J, Siddiqui TJ, Huashan P, *et al.* Truncating mutations in NRXN2 and NRXN1 in autism spectrum disorders and schizophrenia. *Hum Genet* 2011; **130**: 563–73.

- 177 Aoto J, Földy C, Ilcus SMC, Tabuchi K, Südhof TC. Distinct circuit-dependent functions of presynaptic neurexin-3 at GABAergic and glutamatergic synapses. *Nat Neurosci* 2015; **18**: 997–1007.
- 178 Hayashi MK, Tang C, Verpelli C, *et al.* The Postsynaptic Density Proteins Homer and Shank Form a Polymeric Network Structure. *Cell* 2009; **137**: 159–71.
- 179 Südhof TC. The presynaptic active zone. *Neuron* 2012; **75**: 11–25.
- 180 Dieck S, Sanmartí-Vila L, Langnaese K, *et al.* Bassoon, a novel zinc-finger CAG/glutamine-repeat protein selectively localized at the active zone of presynaptic nerve terminals. *J Cell Biol* 1998; **142**: 499–509.
- 181 Scheiffele P, Fan J, Choih J, Fetter R, Serafini T. Neuroligin expressed in nonneuronal cells triggers presynaptic development in contacting axons. *Cell* 2000; **101**: 657–69.
- 182 Levinson JN, Chéry N, Huang K, *et al.* Neuroligins Mediate Excitatory and Inhibitory Synapse Formation. *J Biol Chem* 2005; **280**: 17312–9.
- 183 Belforte JE, Zsiros V, Sklar ER, *et al.* Postnatal NMDA receptor ablation in corticolimbic interneurons confers schizophrenia-like phenotypes. *Nat Neurosci* 2010; **13**: 76–83.
- 184 Jentsch J, Roth RH. The Neuropsychopharmacology of Phencyclidine From NMDA Receptor Hypofunction to the Dopamine Hypothesis of Schizophrenia. *Neuropsychopharmacology* 1999; **20**: 201–25.
- 185 Mouri A, Noda Y, Noda A, *et al.* Involvement of a Dysfunctional Dopamine-D1/N-Methyl-D-aspartate-NR1 and Ca²⁺/Calmodulin-Dependent Protein Kinase II Pathway in the Impairment of Latent Learning in a Model of Schizophrenia Induced by Phencyclidine. *Mol Pharmacol* 2007; **71**: 1598–609.
- 186 Henderson JT, Georgiou J, Jia Z, *et al.* The receptor tyrosine kinase EphB2 regulates NMDA-dependent synaptic function. *Neuron* 2001; **32**: 1041–56.
- 187 Kullander K, Klein R. Mechanisms and functions of eph and ephrin signalling. *Nat Rev Mol Cell Biol* 2002; **3**: 475–86.
- 188 Lisabeth EM, Falivelli G, Pasquale EB. Eph receptor signaling and ephrins. *Cold Spring Harb Perspect Biol* 2013; **5**: a009159.
- 189 Dalva MB, Takasu MA, Lin MZ, *et al.* EphB receptors interact with NMDA receptors and regulate excitatory synapse formation. *Cell* 2000; **103**: 945–56.
- 190 Martinez-Hernandez E, Horvath J, Shiloh-Malawsky Y, Sangha N, Martinez-Lage M, Dalmau J. Analysis of complement and plasma cells in the brain of patients with anti-NMDAR encephalitis. *Neurology* 2011; **77**: 589–93.
- 191 Sirerol-Piquer MS, Ayerdi-Izquierdo A, Morante-Redolat JM, *et al.* The epilepsy gene LGI1 encodes a secreted glycoprotein that binds to the cell surface. *Hum Mol Genet* 2006; **15**: 3436–45.

9. ANNEX

9.1. Other publications

- Hara M, Martinez-Hernandez E, Ariño H, Armangué T, Spatola M, **Petit-Pedrol M**, et al. Clinical and pathogenic significance of IgG, IgA, and IgM antibodies against the NMDA receptor. *Neurology*. 2018 Apr 17;90(16):e1386-e1394. (Article, Impact factor JCR 2016: 8.32 (D1))
- van Sonderen A, **Petit-Pedrol M**, Dalmau J, Titulaer MJ. The value of LGI1, Caspr2 and voltage-gated potassium channel antibodies in encephalitis. *Nat Rev Neurol*. 2017 May;13(5):290-301. (Review, Impact factor JCR 2016: 20.257 (D1))
- Ariño H, Armangué T, **Petit-Pedrol M**, Sabater L, et al. Anti-LGI1-associated cognitive impairment: Presentation and long-term outcome. *Neurology*. 2016 Aug 23;87(8):759-65. (Article, Impact factor JCR 2016: 8.32 (D1))
- van Sonderen A, Ariño H, **Petit-Pedrol M**, Leypoldt F, et al. The clinical spectrum of Caspr2 antibody-associated disease. *Neurology*. 2016 Aug 2;87(5):521-8. (Article, Impact factor JCR 2016: 8.32 (D1))
- Simabukuro MM, **Petit-Pedrol M**, Castro LH, Nitrini R, et al. GABAA receptor and LGI1 antibody encephalitis in a patient with thymoma. *Neurol Neuroimmunol Neuroinflamm*. 2015 Feb 12;2(2):e73. (Article, Impact factor JCR 2016: 8.166 (D1))
- Montojo MT, **Petit-Pedrol M**, Graus F, Dalmau J. Espectro clínico y valor diagnóstico de los anticuerpos contra el complejo proteico asociado a canales de potasio. *Neurologia*. 2014 Jan 29. pii: S0213-4853(13)00293-4. (Review, Impact factor JCR 2014 : 1.381 (Q4))
- Armangué T, **Petit-Pedrol M**, Dalmau J. Autoimmune Encephalitis in Children. *J Child Neurol*. 2012 November; 27(11): 1460–1469. IF:1.385 (Review, Impact factor JCR 2012 : 1.385 (Q3))
Monthly most read article from October 2012 until June 2014

9.2. Acknowledgments / Agraïments

D'alguna manera sento que ara és el moment de mirar enrere i valorar els anys dedicats al doctorat. Em sento afortunada d'haver-los passat treballant en allò que m'apassiona, que és fer recerca i que des de petita veia com el meu objectiu. Si bé, moltes són les persones ho han fet possible i m'han acompanyat en aquest camí i per les que només tinc paraules d'agraïment per haver confiat en mi.

En primer lloc, vull agrair a Josep Dalmau, el meu director de tesi, el meu mentor, haver-me iniciat en l'apassionant món de les encefalitis autoimmunitàries. Per la teva dedicació, criteri i rigurositat en tots i cadascun dels projectes. Ha sigut un privilegi comptar amb la teva guia.

Agrair també a Francesc Graus, tutor d'aquesta tesi, i a Albert Saiz per la seva disposició i col·laboració, per la seva visió clínica que dóna sentit a la nostra recerca.

I'd like to express my special appreciation to Myrna Rosenfeld for your kind help. For your contributions in papers and grants, and for making me see things from another point of view.

Obviament haig de donar les gràcies a totes les persones del lab, per fer-me sentir que aquesta és casa meva. Perquè m'heu fet créixer com a investigadora. Començant pels pilars del laboratori: l'Esther Aguilar, la Merche Alba i la Eva Caballero. Sense vosaltres res d'això hagués estat possible. He gaudit molt aprenent de vosaltres des del 'Bacalao al pil pil' fins al Summer HippoCampus.

En especial vull agrair a la Maria Rodés tota la dedicació i esforços que fa possible que tot funcioni, i per extensió, a Lindsey McCracken, for all your assistance from the other side of the ocean.

També, com no, a un equip de professionals, que saben que LGI1 és una molècula secretada. Gràcies per ser-hi, per discutir els projectes, les inquietuds i el que faci falta. A Jesús Planagumà per la seva sabiduria en *imaging* i per no tenir mai un no per resposta; a Francesco Mannara, el master of mice, per les excursions al PRBB i a Jena, per ensenyar-me amb paciència les cirurgies i els tests de comportament; a Marija Radoševik, per la teva gran aportació als projectes, però sobretot per ajudar-me a desxifrar l'electrofisiologia; a Lídia Sabater, per les confessions professionals i personals al final del dia; a Eugenia Martínez, per la seva manera tan didàctica de transmetre les coses, per saber dirigir amb tant de respecte; a Helena Ariño por tu pensamiento critico y creativo, por resolverme mis dudas clínicas; a Marianna Spatola, a quien empecé ayudando y has acabado ayudandome a mi. Gracias por tu optimismo; a Thais Armangué per ser una lluitadora; i a Marta Pedreño, por hacerme reir, por tener tanta confianza en mi, y por estar siempre dispuesta a ayudar. A Laurent Ladepeche por tus consejos profesionales. Y a Pablo Jercog, por tu disposición, por tu entusiasmo por la ciencia. Siempre tienes las palabras necesarias para hacer las cosas más fáciles.

A tots els que han passat pel lab (Romana Höftberger, Frank Leypoldt, Maarten Titulaer entre tants altres) que tant han enriquit el grup. A la Núria Gresa, la meva companya de congressos. Per tants experiments colze amb colze, per les purificacions de proteïnes amb el 3-way stop

cock. A Alfredo, el chilito, t'has fet estimar amb les teves rancheres. I a les noves incorporacions, Marta, Anna, Simone, Estibaliz i Victor, dir-vos que exprimiu al màxim aquest grup. En podeu aprendre tant!

Durant la tesi, he tingut la sort de treballar amb experts col·laboradors que han donat un valor afegit als projectes. I'd like to specially thank to Christian Geis, and your group members for a fruitful collaboration. For the scientific discussions that are always so needed. Agraïr a Xavier Gasull i David Soto la seva implicació en el projecte i les seves valuoses aportacions, així com a Rafael Maldonado i Melike Lakadamyali per haver-me obert les portes als seus laboratoris.

Vull donar les gràcies d'una manera especial als pacients, per cedir mostres i informació clínica, sense els quals cap d'aquests projectes hauria estat possible.

No puc deixar d'agrair a totes aquelles persones que m'han ajudat durant tots aquests anys fora del laboratori. Als meus amics de Sant Andreu, que sempre m'han fet costat. En especial a l'Aina i la Claudia, que durant anys heu sigut una mà a la que agafar-me (i per molt més).

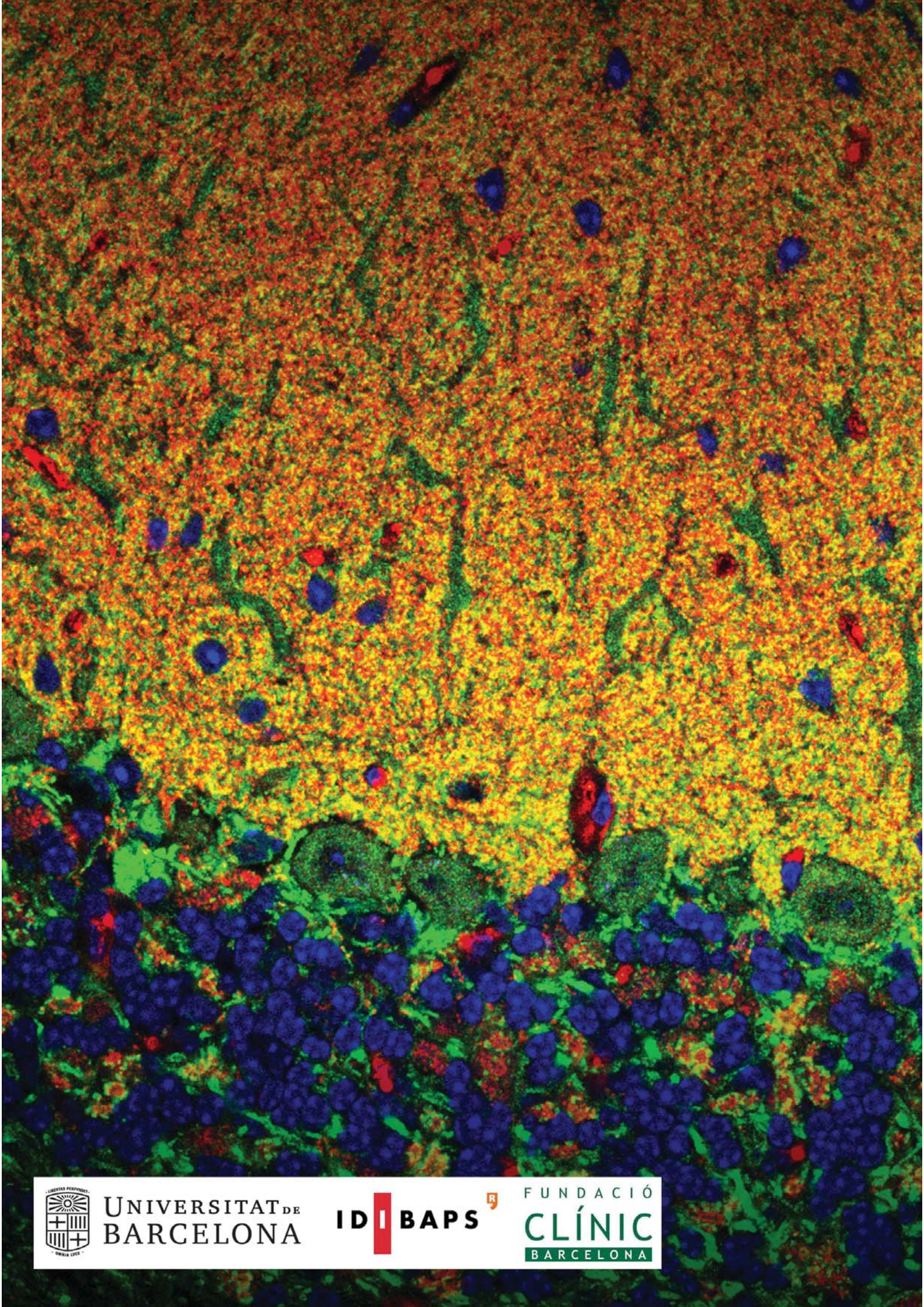
Als amics de Biologia, companys de fatigues, que sempre m'han animat a perseguir el meu somni. Els qui més heu entés les frustracions i les alegries del laboratori.

Als meus pares, Xavier i Anna, i a la meva germana Mireia, per ser el meu suport principal, pel vostre amor incondicional. Per haver-me donat la confiança i llibertat necessària, i per haver-me inculcat el valor de lluitar pels meus objectius. Tinc molta sort de tenir-vos.

A la iaia que, sense saber-ho, vas poder ser testimoni dels últims retocs de la tesi. M'hagués encantat ensenyar-te-la. M'has acompanyat durant tot aquest camí, sent un oasi on poder desconectar. Has sigut un exemple de tenacitat, de no rendir-te en allò que et proposaves.

A l'Albert, per ser el meu cheerleader incondicional, per empoderarme sempre, per treure el millor de mi. Per celebrar totes i cadascuna de les victòries al laboratori per petites que fossin.

Gràcies.



UNIVERSITAT DE
BARCELONA

ID **BAPS**



FUNDACIÓ
CLÍNIC
BARCELONA